Examining a new class of dual CDC7/CDK9 inhibitors, mechanisms of proliferation, and proliferation-based stratification in myeloma

Mark Robert Coyne

School of Medicine
and
National Centre for Biomedical Engineering Science, NUI Galway, Ireland

A thesis submitted to the National University of Ireland, Galway
for the degree of Doctor of Philosophy

August 2014

Supervisors: Prof. Corrado Santocanale and Prof. Michael O'Dwyer.

LIST OF FIGURES.

LIST OF TABLES.

Abbreviations

2N	Diploid
6-MP	6-mercaptopurine
6-thioguanine	6-TG
AACR	American Association for Cancer Research
ABC	ATP binding cassette transporters e.g. MDR1/p-glycoprotein
ACK	NH4Cl. KHCO3. Red cell lysis buffer.
AKT1	Ak mice that spontaneously developed thymomas: Protein kinase B (for merly Akt)
ALB	Albumin
ALDH	aldehyde dehydrogenase
ALL	Acute Lymphoblastic (or Lymphocytic) Leukaemia
ALT	Alanine Transaminase
AML	Acute Myeloid Leukaemia
AMY	Amylase
ANLN	anillin, actin binding protein
ANOVA	ANalysis Of VAriance
AP	alkaline phosphatase
AP-1	Activator protein-1
APOBEC3B	apolipoprotein B mRNA editing enzyme, catalytic polypeptide-like 3B
AraC	Cytosine arabinoside; cytarabine
ASCT	Autologous Stem Cell Transplant
ASF1	Anti-silencing factor 1
Asp	Aspartic Acid
ASPM	Asp (abnormal spindle) homolog, microcephaly associated
ATAD2	ATPase family, AAA domain containing 2
ATF1	Activating transcription factor 1
ATM	Ataxia-telangiectasia mutated
ATP	Adenosine triphosphate
ATR	ATM and Rad3-related
ATRA	all-trans-retinoic acid
AURKA	aurora kinase A
b-ME	Beta-mercaptoethanol
b2MG	beta 2 microglobulin
BAFF	B-cell activating factor
BAK1	BCL2-antagonist/killer 1; formerly Bak.
BAX	BCL2-associated X protein
BCL2L1	BCL2L1: BCL2-like 1; formerl Bcl-xL
BCL2L11	Bcl-2 interacting mediator of cell death:BCL2-like 11; formerly Bim.
BCL2	B-cell CLL/lymphoma 2
bFGF	basic fibroblast growth factor
BH3	Bcl-2 homology domain 3
BIM1	Binding to microtubules 1
BL	Burkitt lymphoma
BMA	B cell maturation antigen
BMI-1	BMI1 polycomb ring finger oncogene
Boc-D	BOC-Asp (OMe)-FMK- Caspase Inhibitor
bp	base pair
BRDF	BRCT and Dbf4 similar

BSA	Bovine Serum Albumin.
Bub1	Budding uninhibited by benzimidizole 1
BUB1	Budding uninhibited by benzimidazoles 1 homolog
BUB1B	Budding uninhibited by benzimidazoles 1 homolog beta
BUN	Urea
C-VAMP	Cyclophosphamide-Vincristine-Doxorubicin-Methlyrednisolone
C21orf45	chromosome 21 open reading frame 45
CA	Calcium
CAF-1	Chromatin assembly factor 1
CAM	Cell adhesion mediated
CASC5	cancer susceptibility candidate 5
CBF-1	C-promoter binding factor 1
CCNA2	Cyclin A2
CCNB1	Cyclin B1
CCNB2	Cyclin B2
CCNT1	Cyclin T1
CD8	Cluster of Differentiation 8
CDC45	Cell division cycle 45 homolog
CDC6	Cell Division Cycle 6
CDC7	Cell Division Cycle 7
CDK1	Cyclin Dependent Kinase 1
CDK4	Cyclin Dependent Kinase 4
CDK6	Cyclin Dependent Kinase 6
CDK9	Cyclin Dependent Kinase 9
CDKN2C	cyclin-dependent kinase inhibitor 2C (p18, inhibits CDK4)
CDKN3	cyclin-dependent kinase inhibitor 3
CDT1	Chromatin licensing and DNA replication factor 1
CENP	Centromere protein
CENPA	Centromere protein A; formerly CenH3.
CENPH	centromere protein H
CENPK	centromere protein K
CENPW	centromere protein W
CEP55	Centrosomal protein 55kDa
CHEK1	CHK1 checkpoint homolog (S. pombe)
CHEK2	CHK2 checkpoint homolog (S. pombe)
CHK1	Checkpoint kinase 1
CHK2	Checkpoint kinase 2
CI	Confidence Interval
CIn	Combination Index
CICD	Caspase independent cell death
CKD	Chronic Kidney Disease
CKDi	Cyclin Dependent Kinase inhibitor
CKS1B	CDC28 protein kinase regulatory subunit 1B
CKS2	CDC28 protein kinase regulatory subunit 2
CLSPN	Claspin
CLL	Chronic Lymphocytic Leukaemia
CLP-1	cardiac lineage protein-1
CMC	Carboxymethylcellulose
CMG	Cdc45, Mcm2-7 and GINS; Holohelicase
CNS	Central Nervous System

COSMIC	Catalogue of Smoatic Mutations in Cancer database
CR	Complete response
CRE	Creatinine
CRP	C-Reactive Protein
CSC	Cancer Stem Cell
CSL	CBF1, Suppressor of Hairless, Lag-1
CT	Computed Tomography
CTD	Carboxy-terminal repeat domain
CXCR4	C-X-C chemokine receptor type 4 (CD184; Fusin)
CyBorD	Cyclophosphamide-bortezomib-dexmethasone
CYCT1	Cyclin-T1; CCNT1
DAB	3,3'-diaminobenzidine
DBF4	Dumbbell forming unit 4
DCEP	Dexamethasone-Cyclophosphamide-Etoposide-Cisplatin
DD	Death domain
DDK	Dbf4 Dependent Kinase, Cdc7
DDR	DNA Damage Response
DEAB	Diethylaminobenzaldehyde
DEPDC1	DEP domain containing 1
DEPDC1B	DEP domain containing 1B
DFCI	Dana-Farber Cancer Institute
dH20	distilled water
DHFR	Dihydrofolate reductase
DHh	Desert Hedgehog
DISC	death-inducing signalling complex
DKK1	dickkopf1
DLBCL	Diffuse Large B-cell Lymphoma
DLL	Delta-like-ligand
Dm	Median Effect
DMEM	Dulbecco's Modified Eagle Medium
DNA	Deoxyribonucleic Acid
DNA-PK	DNA-dependent protein kinase
DR	Death receptor
DRF1	Dbf4-related protein: Now known as DBF4B
DRL	Death receptor ligand
DSB	Double Strand Break
dsDNA	double stranded DNA
DSIF	5,6-dichloro-1-b-D-ribofuranosylbenzimidazole sensitivity-inducing factor
DTL	Denticleless E3 ubiquitin protein ligase homolog
dTMP	thymidine monophosphate
DTT	dithiothreitol, PCR inhibitor
dUMP	deoxyuridine monophosphate
DYN1	Dynein 1
EA	Enrichment Analysis
EBI	European Bioinformatics Institute
ECM	Extracellular matrix
ECT2	epithelial cell transforming sequence 2 oncogene
EFS	Event-Free Survival
eGFR	Estimated Glomerular Filtration Rate
eIF2	Eukaryotic translation initiation factor 2

ELISA	Enzyme-linked immunosorbent assay
ELK1	ELK1, member of ETS oncogene family
EM-DR	Environmentally mediated drug resistance
EMBL	European Molecular Biology Laboratory
EORTC	European Organisation for Research and Treatment of Cancer
ER	Estrogen receptor
ERK	Extracellular signal-regulated kinases: Mitogen-activated protein kinase 1
Esp1	Extra spindle pole bodies 1
EZH2	enhancer of zeste homolog 2 (Drosophila)
FABP5	fatty acid binding protein 5 (psoriasis-associated)
FACT	Facilitates Chromatin Transcription
FAM72A /B/C/D	Family with sequence similarity 72, member A /B/C/D
FANCI	Fanconi anemia, complementation group I
FAS	Fas (TNF receptor superfamily, member 6). CD95.
FCP1	phosphatase
FdUTP	fluorodeoxyuridine monophosphate
FEAR	Cdc14 early anaphase release
FGFR3	Fibroblast growth factor receptor 3
FLIP	FADD like inducer of apoptosis
FUMP	5-fluorouridine monophosphate
G1	Gap 1
G2	Gap 2
GDF-15	Growth Differentiating Factor-15
GEMMs	Genetically Engineered Mouse Models
GEP	Gene Expression Profilling
GFP	Green Fluorescent Protein
GFR	Glomerular Filtration Rate
GGH	Gamma-glutamyl hydrolase (conjugase, folylpolygammaglutamyl hydro lase)
GINS1	GINS complex subunit 1 (Psf1 homolog)
GLI	Transcrition Regulators
GLI1	Glioma-associated oncogene family zinc finger 1:GLI family zinc finger 1
GLOB	Globulin
GLU	Glucose
GMNN	Geminin, DNA replication inhibitor
GO	Gene Ontology
gPI	Gene Expression based Proliferation Index
GSEA	Geneset Enrichment Analysis
GSK 3b	Glycogen synthase kinase 3b
H	Histone
Hb	Haemoglobin
HDACi	Histone Deacetylase Inhibitors
HELLS	helicase, lymphoid-specific
HES-1	Hairy/Enhancer of Split-1
HGF	hepatocyte growth factor
Hh	Hedgehog
HL	Hodgkin’s Lymphoma
HMCLs	Human Myeloma Cell Lines
HMGB2	High-mobility group box 2
HMMR	Hyaluronan-mediated motility receptor (RHAMM)

HRP	Horseradish peroxidase
HSD	Honestly significant difference
HSPs	heatshock proteins
HU	Hydroxyurea
IC50	Inhibition Concentration at 50%
ICN	Intracellular domain of Notch
IGF-1	Insulin-like Growth Factor
IgH	Immunglobulin Heavy Chain
IgL	Immunglobulin Light Chain
Ihh	Indian Hedgehog
IKKg	I-kB kinase g
IL-3	Interleukin-3
IL-6	Interleukin-6
IL-8	Interleukin-8
Il2rg	IL2 receptor gamma chain
IP3	Inositol-1, 4, 5-triphosphate
IP3R	Inositol-1, 4, 5-triphosphate receptor
IPA	Ingenuity Pathway Analysis
Ipl1	Increase in ploidy 1
ISS	International Staging System
Jak2	Janus kinase 2
JHMI	Johns Hopkins Medical Institutions
JNK	Jun N-terminal kinase
K+	Potassium
KAR9	Karyogamy 9
KIAA0101	KIAA0101
KIF11	Kinesin family member 11
KIF4A	Kinesin family member 4A
KIP2	Kinesin related protein 2
KSP	Kinesin Spindle Protein
LFA	Lymphocyte function-associated antigen
Lys	Lysine
M	Mitosis
MAD	Mitotic arrest deficient
MAD2L1	Mitotic arrest deficient-like 1
MAF	Musculoaponeurotic fibrosarcoma oncogene homolog
MAP	Mitogen Activated Protein
MAPK	Mitogen Activated Protein Kinase
MCB	MluI Cell cycle Box
MCC	Mitotic checkpoint complex
MCL1	Myeloid Cell Leukemia Factor-1
MCM	Minichromosome Maintenance Complex
MCM2	Minichromosome maintenance complex component 2
MCM4	Minichromosome maintenance complex component 4
MDRD	Modification of Diet in Renal Disease (Study where equation for GFR was devised)
MEF	Murine Embryonic Fibroblasts
MEF2	Myocyte enhancer factor 2
MELK	Maternal embryonic leucine zipper kinase
MEN	Mitotic exit network

MGUS	Monoclonal Gammopathy of Undetermined Significance
MIPIa	macrophage inflammatory protein 1a
MIT	Massachusetts Institute Technology
MK2	Mitogen-activated protein kinase-activated protein kinase 2: MAP kinase-activated protein kinase 2
MKK3	Mitogen-activated protein kinase kinase 3
MKK4	Mitogen-activated protein kinase kinase 4
MKK6	Mitogen-activated protein kinase kinase 6
MLF1IP	MLF1 interacting protein
MLN	Millennium
MM	Multiple Myeloma or myeloma.
MMRC	Multiple Myeloma Research Consortium
MMRF	Multiple Myeloma Research Foundation
MMS	Methyl Methane Sulfonate
MMS	methylmethanesulfonate
MMSET	WHSC1: multiple myeloma SET domain containing protein type III
MOMP	Mitochondrial Outer Membrane Permeabilisation
MP	Melphalan-prenisolone
MPS1	Multipolar spindle 1
MPT	Melphalan-prednisone-thalidomide
mq	milliq
MRD	Mediator of replication checkpoint 1
MRI	Magnetic Resonance Imaging
mSMART	Mayo Clinic Stratification for Myeloma and Risk Adapted Therapy
MTA	Material Transfer Agreement
MTD	Maximum tolerated dose
MTOC	Microtubule organising centres
MTX	Methotrexate
Mu	Murine/Mouse
MYC	Myelocytomatosis viral oncogene
MYO2	Myosin 2
N	Haploid
NA+	Sodium
NCAPG	non-SMC condensin I complex, subunit G
NCAPG2	non-SMC condensin II complex, subunit G2
NCBI	National Center for Biotechnology Information
NCI	National Cancer Institute
NCRI	National Cancer Registry of Ireland
NDC80	Kinetochore complex component homolog
NDC80	NDC80 homolog, kinetochore complex component (S. cerevisiae)
NEK2	NIMA (never in mitosis gene a)-related kinase 2
NELF	Negative Elongation Factor
NELF-E	Negative Elongation Factor-E
NFKB1	Nuclear factor kB; Formerly NFkB.
NHL	Non-Hodgkin’s Lymphoma
NJ	Neighbour Joining Method
NMS	Nerviano Medical Sciences
NOD	Non obese diabetic (mice)
NPC	Normal Plasma Cells
NSCLC	Non Small Cell Lung Cancer

NSG mice	NOD/SCID/Gamma mice or NOD.Cg-Prkdcscid Il2rgtm1Wjl/SzJ
NTPi	Nucleotide triphosphate inhibitors
NUF2	NDC80 kinetochore complex component, homolog
NUSAP1	Nucleolar and spindle associated protein 1
OIP5	Opa interacting protein 5
OPG	Osteoprotegerin
ORC	Origin Recognition Complex
OS	Overall Survival
P-TEFb	Positive Transcription Elongation Factor-b
PAF	polymerase II associated factor
pAKT1	phosphoAKT1
PARP1	Poly (ADP-ribose) polymerase 1; formerly PARP
PBK	PDZ binding kinase
PBS	Phosphate buffered Salt, also know as Hank's Solution.
PBS-T	Phosphate buffered Salt –Tween 20, percentage can vary.
PC	Plasma cell
PCLI	Plasma Cell Labeling Index
PCNA	Proliferating Cell Nuclear Antigen
PCR	Polymerase Chain Reaction
PD	Pfizer Drug
Pds1	Precocious dissociation of sisters
PET-CT	Positron emission tomography - computed tomography
PFS	Progression Free Survival
PHA	Pharmacia, now Pfizer
PHF19	PHD finger protein 19
PHOS	Phosphate
PI	Proliferation Index
PI3K	phosphatidylinositol 3-kinase
PIC	Pre-initation complex
PIM	Pim-1 oncogene (proviral integration site 1)
PK	Pharmacokinetic
PKC-d	Protein Kinase C - delta
PLIER	Probe Logarithmic Intensity Error Estimation
PLK1	Polo-like kinase 1
PLT	Platelet count
pMCM2	phosphoMcm2
pMK2	phosphoMK2
PMTX	Pemetrexed
pol	polymerasse
PP1/2A/4	Protein phosphatase 1/2A/4
PR	Partial response
PRC	Pre-replicative Complex
PRC1	protein regulator of cytokinesis 1
pre-RC	Pre-replicative Complex
PRR11	Proline rich 11
PT	Thalidomide-prednisone
Pt	Platinum
PTCH	Patched
PTEN	phosphatase and tensin homolog
PTTG1	pituitary tumor-transforming 1

PUMA	p53 upregulated mediator of apoptosis
qPCR	quantitative real-time RT-PCR
RACGAP1	Rac GTPase activating protein 1
RAD51AP1	RAD51 associated protein 1
RANKL	receptor activator of NFkB
RAS	Rat sarcoma: small GTPase superfamily; formerly Rb
RB1	Retinoblastoma protein
Rb	Rabbit
RC	Replicative Complex
RCT	Randomised Control Trial
Rd	Lenalidomide plus low-dose dexamethasone
RFP	Red Fluorescent Protein
RMA	Robust Multichip Analysis
RNA	Ribonucleic Acid
RNA Pol I	RNA polymerase I
RNA Pol II	RNA polymerase II
RNA Pol III	RNA polymerase III
RPB1	Larrgest subunit of RNA Pol II
RPMI	Roswell Park Memorial Institute
RRM2	Ribonucleotide reductase M2
RT-PCR	Reverse Transcriptase PCR
S	Synthesis
SAC	Spindle assembly checkpoint
SAHF	Senesence Associated Heterchromatic Foci
SB	SmithKiline Beecham, now GlaxoSmithKline
SCC1/3	sister chromatid cohesion 1 or 3
SCID	Severe combined immunodeficiency (mice)
SDF1a	stromal cell derived factor 1a
SDS	Sodium dodecyl sulfate
SDS-PAGE	Sodium dodecyl sulfate – Polyacrylamide Gel Electrophoresis.
Ser	Serine
SGOL2	shugoshin-like 2 (S. pombe)
SHCBP1	SHC SH2-domain binding protein 1
SHh	Sonic Hedgehog
siRNA	small interfering RNA (also know as short or silencing RNA)
SLBP	Stem loop binding protein
SMAC	Second mitochondrial activator of caspases; Diablo
SMC1	Structural maintenance of chromosomes 1
SMM	Smoldering Myeloma
SMO	Smoothened
SNP	Single Nucleotide Polymorphism
snRNA	small nuclear RNA
snRNP	small nuclear ribonnucleoprotein
SP	Side population
SPB	Spindle pole body
SPC25	SPC25, NDC80 kinetochore complex component, homolog (S. cerevisiae)
SPE	serum protein electrophoresis
SPOC	Spindle position checkpoint
SSB	Single Strand Break
ssDNA	single stranded DNA

SSU72	Serine 5 specific Phosphatase
STAT3	Signal transducer and activator of transcription 3
STMN1	stathmin 1
SUPT5H	Suppressor of Ty 5 homolog (S. ce
SVM	Support Vector Machine
SWOG	Southwest Oncology Group
synth	synthethic
TBIL	Total Bilirubin
TD	Thalidomide-dexamethasone
TdT	Terminal deoxynucleotidyl transferase
TF	Transcription Factor
Tgen	Translational Genomics Research Institute
Thr	Threonine
TIMP	thioinosine monophosphate
TM	Trade Mark
TMB	3, 3', 5, 5'-tetramethylbenzidine, substrate for HRP
TMEM97	transmembrane protein 97
TMPO	thymopoietin
TNF	Tumour necrosis factor
TNFR	Tumour necrosis factor receptor
TOP2A	Topoisomerase (DNA) II alpha
TP	Total Protein
TP53	Tumor protein p53
TPX2	TPX2, microtubule-associated, homolog (Xenopus laevis)
TRAIL	TNF – related apoptosis-inducing ligand
TRIP13	thyroid hormone receptor interactor 13
ts	Temperature sensitive mutants
TSA	trichostatin A
TT2	Total Therapy 2
TT3	Total Therapy 3
TTK	TTK protein kinase
TTP	Time to progression
TUNEL	Terminal deoxnucleotide transferase dUTP Nick End Labeling
TYMS	Thymidylate synthetase
Tyr	Tyrosine
U2	spliceosomal RNA
ub	ubiquitin
UBE2C	ubiquitin-conjugating enzyme E2C
UHRF1	ubiquitin-like with PHD and ring finger domains 1
UTP	Uracil Triphosphate
UV	Ultraviolet
V(D)J	Variable(Diverse)Joining as part of somatic recombination
VAD	Vincristine-adriamycin-dexamethasone
VCAM	Vascular cell adhesion molecule
VCD	Cyclophosphamide-bortezomib-dexmethasone
VD	bortezomib plus dexamethasone
VEGF	Vascular endothelial growth factor
VGPR	Very good partial response
VLA	Very late antigen
VMP	Bortezomib-melphalan-prednisone

VRd	Bortezomib-lenalidomide-dexamethasone
VTD	Bortezomib-thalidomide-dexamethasone
VTD-PACE	Bortezomib-Dexamethasone-Thalidomide Cisplatin-Doxorubicin-Cyclo phosphamide-Etoposide
WBC	White blood cell count
WEE1	WEE1 homolog (S. pombe)
WES	Whole Exome Sequencing
WGS	Whole Genome Sequencing
WHD	Winged Helix Domain
WHSC1	Wolf-Hirschhorn syndrome candidate 1
WNT	Wingless
XL	Exelexis
YFP	Yellow Fluorescent Protein
z-VAD	Benzyloxycarbonyl-Val-Ala-Asp (OMe) fluoromethylketone.
ZNF367	zinc finger protein 367
ZWILCH	Zwilch, kinetochore associated, homolog (Drosophila)
ZWINT	ZW10 interactor

Acknowledgements

I am forever grateful to my parents, Dolores and Robert S, whose support, love and guidance continues to inspire.

I acknowledge the patience, love and kindness of Mary. She has been a true pillar at my side, helping me to complete this work.

I also acknowledge my family, Lara, Derval and Bobby for their support and understanding throughout the duration of this thesis.

I thank my godmother and godfather, aunt and uncle, Maureen Keane and Padhraic Cannon for their encouragement, advise and support.

I acknowledge my supervisors Professor Michael O'Dwyer and Professor Corrado Santocanale who gave me this opportunity, which I can only can but build upon for the future.

I acknowledge my colleagues at the National Centre for Biomedical Engineering Science, at the National University of Ireland, Galway who helped tirelessly - Raffaella D'Auria, Dr Ania Kliszczak, Dr Alessandro Natoni, Dr Michael Rainey, Dr Laura Barkley and Gemma O'Brien.

I also take this opportunity to thank Molecular Medicine Ireland and the Higher Education Authority which under the Programme for Research in Third-Level Institutions Cycle 4, a European Regional Development fund has not only funded this work constituting my PhD but has changed the landscape of how to train and enrich Ireland's growing supply of Clinician-Scientists.

In addition, I would like to thank the European Haematology Association and the American So-

ciety of Hematology who supported my preliminary work through the award of a Research-Exchange Fellowship, affording me the tremendous opportunity of continuing my studies under the supervision of Prof Leif Bergsagel, Dr Marta Chesi, and Prof Bill Matsui at the Mayo Clinic Arizona and Johns Hopkins Medical Institutions respectively.

I take this opportunity to thank all my friends and colleagues at Mayo Clinic Arizona – Patrick Blackburn, Stephen Palmer, Victoria Garbitt, Dr Ric Valdez, Barbara Hale, Dr Esteban Braggio, Leslie Dixon, Dr Dan Riggs, Dr Ron Marler, Karla Stafford, Dr Naomi Gades, Dr Sangeetha Rajagopalan, Dr Travis Henry and last but by no means least Prof Leif Bergsagel and Dr Marta Chesi. I thank them for their boundless willingness to share their knowledge and considerable skills. I would like to thank Patrick Blackburn particularly, for all his help. I also wish to thank the broader Mayo Research Community, both at Scottsdale and Rochester that have deepened my understanding of B-cell biology, immunology, myeloma, bioinformatics and cancer molecular biology.

I also wish to thank all my friends and colleagues at Johns Hopkins – Dr Jasmin Agarwal, Quiji Wang, Dr Toshi Tanno, Vessi Penchev, Dr Akil Merchant, Dr Zeeshan Rasheed, Ross McMillan, Giselle Joseph, Yiting Lim, Marcy Omondi and Prof Bill Matsui. I also wish to acknowledge Dr Connie C. Talbot who helped immensely with furthering my bioinformatic skills.

Abstract

A key feature of progressive myeloma is a relative increase in proliferation. The DBF4-dependent kinase (DDK), cell division cycle 7 (CDC7), is an essential kinase for initiation of DNA replication. This thesis assesses the activity of the prototype CDC7 inhibitor PHA-767491 and its bioavailable related compound, NMS-354, in pre-clinical models of myeloma. Both such inhibitors are characterised as dual CDC7/CDK9 inhibitors.

The thesis finds first that PHA-767491 and NMS-354 demonstrate efficacy in pre-clinical cell-based myeloma and stem cell models. Secondly, CDC7/CDK9 inhibition is found to be additive to melphalan, bortezomib, and doxorubicin in myeloma cell lines. The combination of p38 MAPK and CDC7/CDK9 inhibitors is, unexpectedly, potently synergistic. CDC7/CDK9 inhibition activates MK2, a downstream target of the p38 MAPK pathway. However, thirdly, preliminary experiments did not reveal activity of NMS-354 in the Vk*MYC myeloma mouse models. Fourthly, DBF4 is found to be the main regulator of CDC7 in malignant and non-malignant plasma cells. DBF4 over-expression predicts an inferior overall survival and time to progression in newly diagnosed myeloma patients, but fails to reach independence from the gene-expression-based proliferation index on multivariate analysis. Dual staining with CD138, a plasma cell marker, and pMCM2 proves to be more predictive of plasma cell labeling index than the MIB index and gene expression-based proliferation indices. Finally, this thesis finds that the G2/M DNA damage checkpoint is the most important canonical pathway enriched in patients with a high proliferation index across TC myeloma groups.

Through the analysis of these various elements, this thesis examines the role of proliferation as a therapeutic strategy as well as a stratifier in myeloma, through examination of the DDK, CDC7.

CHAPTER 1: INTRODUCTION – LITERATURE REVIEW.

1.1. Myeloma

1.1.1. Introduction

Myeloma is an incurable clonal neoplasm originating in post-germinal B-cells, plasma cells. It has a well recognised clinical phenotype and its molecular characterisation has informed a number of new standards of care in myeloma treatment. This thesis examines the role of CDC7/CDK9 inhibition. The loss of replication initiation (CDC7 inhibition) and transcription elongation (CDK9 inhibition) presents a new treatment potential paradigm in myeloma. In addition, this work examines the importance of proliferation as a stratifier in myeloma as well as considering how best to target this relative but important change in myeloma cells.

1.1.2. Biology of Myeloma - Molecular Basis

Myeloma can be divided into two broad branches of hyperdiploid and non-hyperdiploid myeloma. These groups are classified through differences at both epigenetic and genetic levels. Non -hyperdiploid myeloma is characterised by recurrent non-random translocations involving the heavy and light chain loci leading to overexpression of the juxtaposed gene with the Ig light or heavy chain promoter. Juxtaposed genes, their frequency and location are described in Table 1.1.

Table 1.1

Locus	Oncogene product	Incidence
11q13	Cyclin D1	15-20%
6p21	Cyclin D3	5%
4p16.3	FGFR3/MMSET	12%
16q23	c-MAF	5-10%
8q24	c-MYC	<10%
6p25	MUM1/IRF4	5%
20q11	MAFB	5%
1q21	IRTA1/IRTA2	Rare
1q11		Rare
2p23	NMYC	Rare
3q21		Rare
9p13	PAX5	Rare
11q23	MLL1	Rare
12p13	Cyclin D2	Rare

Table 1.1. Recurrent non-random translocations in myeloma. Table indicating genetic locus, fusion onogene product and incidence. FGFR3 – fibroblast growth factor receptor 3; MUM1/IRF4 – multiple myeloma oncogene 1/interferon regulatory factor 4; IRTA – immune receptor translocation-associated gene; PAX5 – paired box gene 5; MLL1 – mixed lineage leukaemia 1.

Hyperdiploid myeloma is characterised by the occurrence of trisomies of all the odd chromosomes except for chromosome 11, chromosomes largely rich in ribosome-related genes.

It is generally accepted that the unifying event in myelomagenesis is direct or indirect deregulation of Cyclin D, an important mediator of cell cycle control, via non-random primary translocations involving the IgH/L loci (Bergsagel et al., 2005). In keeping with the low-proliferation index at diagnosis, deregulated Cyclin D alone is insufficient for transformation. Instead, transformation also requires further alteration in known oncogenic drivers (MYC, RAS, TP53) or aberrant coactivation and mutually exclusive pairing of S-phase acting kinases -CDK4-Cyclin D1 and CDK6-Cyclin D2- to occur (Bergsagel et al., 2005, Ely et al., 2005). This leads to a more proliferative and clinically resistant clone where the over-expression of numerous cell cycle and proliferation-related genes can be observed by gene-expression profile ([GEP] Zhan et al., 2006). Importantly, the patients stratified on the basis of this proliferation signature display the worst overall survival and time to progression (Zhan et al., 2006, Shaughnessy et al., 2007). High expression of myeloid cell leukemia-1 (MCL1), a potent anti-apoptotic BCL2 family member, and defects in the TP53 and MYC pathways are, furthermore, now known to be instrumental in inhibiting responsiveness to current and emerging myeloma therapeutics (Gertz et al., 2005, Wuilleme-Toumi et al., 2005).

The heterogeneity of myeloma in symptomatic progression, as well as the need for clinical treatment, its speed of progression, and clonal immunoglobulin idiotype all underline the heterogeneity in the underlying biology of myeloma. Investigation into the intrinsic genetics of myeloma has begun to outline the possible sources of such clinical heterogeneity. The development of this understanding will increase the clinican's ability at diagnosis to stratify a patient's individual prognosis, need for treatment, and the individual choice of treatment.

At diagnosis, myeloma is predominantly characterised by low proliferation, but with disease progression, it becomes relatively more proliferative, which is the central, and currently considered to be the most important (Hose et al., 2011), prognostic stratifier in myeloma.

1.1.3. Genomics

Genomics is increasing our understanding of myeloma. Bergsagel *et al* have used gene expression profiling (GEP) to identify recurrent translocations, specific trisomies, and expression of cyclin D genes to divide myeloma into 8 groups (Bergsagel et al., 2005). Shaughnessy *et al* have, further, created a 70-gene, as well as a subsequent 17-gene, poor-prognostic model using GEP, while the Intergroupe Francophone du Myéloma created a contrasting 15-gene model for similar risk stratification (Shaughnessy et al., 2007, Decaux et al., 2008). Carrasco *et al* have, moreover, provided a dataset of copy number variants from primary and myeloma cell lines creating another classification of poor prognostic risk (Carrasco et al., 2006). The datasets created by such activity provide a significant resource to complement molecular work. Other datasets can be expected as the technology matures and niche profiling develops further.

Next generation sequencing continues to evolve. Its speed, efficiency, costs and depth of sequence covered allow for the potential use of such powerful technology outside of the research area and into clinical practice, both at diagnosis and in management decisions. The next generation also implies a suite of 'sequence plus' solutions wherein the ability to perform simultaneous measurements of transcription, translation, or chromatin modifications are possible (mRNASeq, ChIPSeq etc).

There is much debate on whether exome sequencing (WES) should be used in preference to whole genome sequencing (WGS) in relation to the cancer genome. Non-coding sequence remain hugely important in transciprtion and epigenomic regulation in cancer biology. This was noted with Chapman *et al*'s paper who demonstrated the importance of BCL7A (Chapman et al., 2011). Whole genome sequencing utilises two main approaches – paired end and mate-pair sequencing.

In myeloma, there has being equal use of WGS and WES. Both Illumina and Life Technology platforms were used with a preference for Illumina. Peripheral blood was used predominantly as the normal tissue input to account for private single nucleotide polymorphisms. Chapman *et al*

excluded three samples due to the presence of low levels of circulating neoplastic plasma cells (Chapman et al., 2011).

Chapman *et al* reported a multicentre study of 38 myeloma genomes collated at The Broad Institute using both WES and WGS approaches (Chapman et al., 2011). The size is small but is still a good starting point. There is notable baseline heterogeneity in myeloma that was not accounted for in Chapman *et al* work, but which is clearly important as demonstrated by Walker *et al* (Walker et al., 2012). In any case, Chapman *et al* demonstrated known mutations in RAS and TP53 but, in addition, in up to 25% of cases, mutations in RNA processing and translation initiation – DIS3 and FAM46C – were detected. This makes biological sense when understanding the basic role of the plasma cell to secrete immunoglobulin. BRAF mutations are seen in 4% of myeloma patients. This was seen to be an activating mutation, G469A, that is shared with melanoma patients. Pathway enrichment studies demonstrated the dominance of NFKB1 and histone methylation (MMSET, HOXA9, KDM6A). Non-coding mutations clustered over BCL7A, a tumour suppressor gene. Walker *et al* found that RAS, DIS3, FAM46C, LRP1B, DNAH5, and WHSC1 were the most frequently mutated genes in their cohort of t(4;14) and t(11;14) myeloma (Walker et al., 2012). Mutational rates were higher in the t(4;14) group compared to the t(11;14) group. Transition and transversion rates was interestingly similar in both groups. It is important to note that this work illustrated the heterogeneity of myeloma. It showed that after initial non-random translocation, be it t(4;14) or t(11;14), each group follows a distinct pathway to evolving to symptomatic myeloma.

This technology can also be used to examine the evolution of clones over time. The pressures of selection illustrate how single nucleotide variants (SNVs) parallel clonal dominance patterns. Walker *et al* demonstrated that a single patient using single cell analyses had three different clones with only one shared mutation – ATM (Walker et al., 2012). One clone had mutations in four genes- ATM, FSIP2, CLTC and GLMN. The second clone had mutations in ATM and FSIP2 and the third clone had mutations in ATM, CLTC and GLMN. Such work will inform the drivers of myeloma but also the drivers of chemoresitance and thus tailored chemotherapy regimens. Egan *et*

al performed WGS on a t(4;14) patient at diagnosis, and at three different relapse events (Egan et al., 2012). 15 possible initiating events were identified. One of these possible initiating events was a mutation involving AFF1. AFF1 is implicated in altered methylation signatures in mice but is also, interestingly, involved in RNA pol II mediated transcription. RB1 mutation was shown at diagnosis, but biallelic deletion led to leukaemic transformation. This mirrored a similar finding with bialleleic deletion of TP53. ZKSCAN3 which modulates CCND2 was also mutated prior to leukaemic transformation. Again, some SNVs were present at diagnosis or second relapse, or at first relapse and leukaemic transformation suggesting a clonal variation over time.

Mulligan *et al* examined DNA collected from bortezomib trials for mutations with sequenom technology (Mulligan et al., 2014). New mutations in PDGFRA and JAK3 were identified. Although there are equal rates of NRAS and KRAS mutations in myeloma, NRAS mutations were associated with a significantly lower response rate to bortezomib, with shorter time to progression in bortezomib-treated patients (Mulligan et al., 2014).

In relation to GEP data, Hose *et al* have helpfully summarised all datasets currently available, and reported that the relative increase in proliferation is the most important measure that should be used for risk stratification in myeloma (Hose et al., 2011). In support of same, Dhodapkar *et al* demonstrated that only the GEP-proliferation (PR) subtype was predictive of progression in the largest MGUS observational study incorporating genomic techniques (Dhodapkar et al, 2014). This study supports the contention that examination of proliferation in the MGUS state is as important as in the active myeloma state.

However, to date there is no widely accepted measure of proliferation used in current stratification strategies. The other barrier to the introduction of such a measure is the question as to whether such a change would impact upon the existing management of the disease. However, with the advent of stricter budgets, cost-benefit analyses, and as, discussed later, mSMART, researchers are increasingly required to address the role of stratification (Dispenzieri et al., 2007, Kumar et al., 2009, Mikhael et al., 2013).

1.1.4. Microenvironment

The importance of the microenvironment has received significant attention in the myeloma field- emphasising the need to focus on the soil and not only the seed.

1.1.4.1. Microenvironment Niche

The bone marrow microenvironment niche includes haematopoietic and non-heamatopoietic cells. The supporting non-haematopoietic cells include bone marrow stromal cells, osteoclasts, endothelial cells and mesenchymal stem cell derivatives, including osteoclasts, adipocytes and chondrocytes. These cells interact with myeloma cells within the bone marrow hypoxic environment in turn eliciting autocrine and paracrine, direct and indirect, effects. The structural arrangement involves numerous extracellular matrix proteins including collagen, fibronectin, osteopontin and laminin. Noll *et al* have argued that the haematopoietic stem cell niche is a potential location for initiation of the myelomatous clone due to their similar dependence on certain pathways, adhesion proteins and cytokines (Noll et al., 2012). The stromal cell, however, is the best researched supporting cell in the myeloma microevironmental niche.

Haematopoietic cells have also a role in maintenance of normal plasma cell homoeostasis and ultimately the myeloma microenvironment. Macrophages, megakaryocytes, eosinophils, basophils and dendritic cells have demonstrated an important role (Winter et al., 2010, Rodriguez Gomez et al., 2010). When focusing on proliferation, recent attention has focused on the role of eosinophils in inducing proliferation in both neoplastic and non-neoplastic plasma cells, in mice and human cells (Chu et al., 2011, Wong et al., 2013, Wong et al., 2014)). This complements the known role of macrophages and dendritic cells (Kim et al., 2012, Kukreja et al., 2006).

This emphasises the individual role but discreet balance of haematopoietic and non-haematopoietic cells in myelomagenesis and maintenance of the microenvironment niche. The different adhesion proteins and cytokines secreted have been extensively studied in myeloma.

1.1.4.2. Cytokines

Numerous different factors - cytokines, chemokines - are secreted. They include interleukin-6 (IL-6), interleukin-3 (IL-3), insulin-like growth factor 1 (IGF-1), vascular endothelial growth factor (VEGF), B-cell activating factor (BAFF), basic fibroblast growth factor (bFGF), stromal cell derived factor 1a (SDF1a), macrophage inflammatory protein 1a (MIP1a), dickkopf1 (DKK1), heatshock proteins (HSPs) and tumour necrosis factor a (TNFa) (Hideshima et al., 2001, Podar et al., 2002, Mitsiades et al., 2002, Tai et al., 2006, Moreaux et al., 2004, Hideshima et al., 2002, Niida et al., 2004, Tian et al., 2003). Importantly, these secreted factors are further upregulated by myeloma cell adhesion to individual support cells.

Once these factors bind to the myeloma cell they stimulate signaling pathways that mediate survival (IL-6, HGF, IGF-1 affecting MCL1 and BCL2L1(Bcl-xL)), drug resistance, growth (IL-6, HGF, bFGF, and IGF-1), cell migration (SDF1A - CXCR4 interaction) but also osteoclastogenesis (IL-6, VEGF, receptor activator of NFKB1 ligand [RANKL], osteoprotegerin [OPG], MIP1a and IL-1b) and angiogenesis (IL-8 and VEGF) (Roodman et al., 2009, Jakob et al., 2006, Alsayed et al., 2006). Again, the major upregulated signal pathways involved within the myeloma cell include the extracellular signal-regulated kinase (ERK), Janus kinase 2 (Jak2)-signal transducer and activator of transcription 3 (STAT3), nuclear factor kB (NFKB1) and phosphatidylinositol 3-kinase (PI3K) pathways (Landowski et al., 2003, Hideshima et al., 2001). More recently, Tanno *et al* have demonstrated that growth differentiating factor 15 (GDF-15) is aberrantly secreted by bone marrow stromal cells in myeloma, potentiating self renewal and clonogenicity of myeloma cells (Tanno et al., 2013).

1.1.4.3. Adhesion proteins

Homotypic and heterotypic adhesion of tumour cells to either extracellular matrix (ECM) proteins or stromal cells are important in myeloma progression. After class switching in the lymph node, adhesion proteins (CD44, VLA-4, VLA-5, LFA-1, CD56, syndecan-1 and MPC-1) effect homing of the

myeloma cells to the bone marrow (Damiano et al., 1999, Damiano et al., 2000, Hazelhurst et al., 2000). Myeloma cells interact with stromal cells via VLA-4 binding to VCAM-1. ECM binding is mediated by CD138 or syndecan-1 binding to fibronectin. This interaction not only localises the myeloma cells to the bone marrow microenvironment but also stimulates cytokine secretion with downstream effects on defined intracellular pathways.

The development of plasma cell leukaemia is characterised by loss of expression of certain adhesion proteins (e.g. VLA-5, CD56 and CD138). Pavia *et al* examined the characteristics of circulating neoplastic plasma cells as compared with bone marrow neoplastic plasma cells in myeloma (Pavia et al., 2013). Circulating cells were characterised by downregulation of integrins (CD11a, CD11c, CD29, CD49d, CD49e), adhesion proteins (CD33, CD56, CD117, CD138) and activation molecules (CD28, CD38, CD81). This circulating population represented a subpopulation of bone marrow neoplastic cells. Circulating plasma cells were quiescent and more clonogenic than bone marrow myeloma cells when co-cultured with stromal cells. Interestingly, circulating disease seems to follow a circadian pattern of expression similar to CD34 expression (Pavia et al., 2013).

In addition, it is well described that myeloma cell lines resistant to melphalan and doxorubicin typically overexpress VLA-4 upregulating p27 mediating increased binding to fibronectin in cell lines. More recently, Jamaco *et al* have demonstrated that VCAM-1/VLA-4 through NFKB1 signalling in stromal and leukaemic cells induces chemoresistance (Jacamo et al., 2014).

The role of cytokines and adhesion proteins in survival has led to the creation of *in vivo* and *in vitro* model systems used in examining the potential efficacy of new anti-myeloma treatments in the pre-clinical assessment. Bortezomib, thalidomide and its derivatives target not only the myeloma cell but also the microenvironment.

1.1.5. Models of Disease

As myeloma is a heterogenous disease there is no one preclinical model system that adequately reflects the biology of the disease. This difficulty extends to the inability to predict efficacy of novel agents with an individual model.

There have been numerous workshop meetings seeking to agree a suitable algorithm for validation of novel therapeutics in myeloma. This has largely translated into the approach of the MMRC validation core. The advances in newer technologies with connectivity mapping programs have led to refinements of these algorithms. Dalton *et al* previously outlined four critical steps (Dalton, 2006):

1. Myeloma cell lines including those with acquired resistance to known anti-myeloma agents;
2. Myeloma microenvironment models – presence of survival cytokines, stromal cells, cell adhesion-mediated drug resistance (CAM-DR), environmentally mediated drug resistance (EM-DR);
3. Primary patient samples;
4. Multiple myeloma animal models.

1.1.5.1. Myeloma Cell Lines

By virtue of having more material to work with than with primary samples, makes myeloma cell lines the obvious starting place. The broad array of available cell lines capture the genetic diversity of myeloma – primary non-random translocations and RAS activating mutations. This now includes the long awaited hyperdiploid D1 cell line. Although these cell lines are broadly representative of myeloma patients, they have acquired, and continue to acquire, mutations not observed in myeloma patients – notably inactivating mutations of TP53. Moreover, the vast majority of cell lines are more proliferative than primary samples. Thus, therapeutics that target proliferation may demonstrate superior responses in cell lines than that which is observed directly in patients. This is nicely illustrated in the case of vincristine (Chesi et al., 2008). EBV positivity of cell lines is another finding not observed in patient samples. Stably transfected cell lines with a construct of interest (*cf.* MM1S-myrAKT1(myristoylated AKT1); MM1S-BCL2 (BCL2)) allows for closer examination of individual pathways of interest but the same cautions apply to these lines as to other myeloma lines (Mitsiades et al., 2002).

1.1.5.2. Myeloma Microenvironment Models

There are multiple variations of modeling the microenvironment in myeloma. The isolated use of known survival cytokines allows for the dissection of response to individual signals – IGF-1, IL-6 *etc.* The use of conditioned media or indeed direct adhesion of myeloma cells to stromal cells, usually HS-5 cell lines, allows for a broader assessment of response to more than one individual cytokine and in particular CAM-DR/EM-DR.

Dalton *et al* advocates two individual models – CAM-DR and EM-DR – for assessing drug resistance to novel compounds (Damiano et al., 1999, Damiano et al., 2000). In his work, he establishes CAM-DR with myeloma cells cultured on fibronectin-coated plates. Alternative plates with different coatings can also be used (Damiano et al., 1999). EM-DR was established with the HS-5 stromal cell line but can also be modified to include primary myeloma patient samples. Insertion of trans-well devices can look at soluble factors involved in a particular phenotype.

The choice of model used often reflects selectivity or lack of selectivity of the compound. This thesis examines the effect of individual cytokines, IL-6 and IGF-1, with and without serum. In addition the use of conditioned media as well as EM-DR model with a HS-5-GFP line are also examined.

1.1.5.3. Primary Patient Samples

Depending on the question posed the use of samples from relapsed refractory myeloma patients is the usual norm. Selection of the CD138 fraction to ensure cell viability assays are measuring effects on the myeloma cell. Other approaches are to examine the percentage of CD138 survival after treatments. This approach is dependent on cell viability assay using the Annexin V staining which generally require more cells.

1.1.5.4. Myeloma Mouse Models

There is an increasing number of mouse models used in myeloma research. These models can be divided essentially into four main broad model systems. These are summarised in Table 1.2.

Table 1.2

Model	Examples	Advantages	Disadvantages
Xenogenic transplants in immunodeficient mice	SCID NOD.SCID NOD.SCID.il2rg-	In vivo testing of HMCL therapy	Work poorly for early, intramedullary MM. Tissue localisation variable and aberrant. Microenvironment effects unclear/aberrant Immunocompetent host
Xenogenic transplants in humanised immunodeficient mice	SCID.hu SCID.rab SCID-synth-hu	Works for HMCL and MM Manipulate microenviroment	Challenging technology Chimeric microenvironment Immunocompromised host
Syngenic transplants of spontaneous tumours into immunocompetent mice	T2 or T33 MM tumours into C57/BL6 mice	Tumour homes to BM T33 an be grown as a cell line Can genetically manipulate cells	Genetic abnormalities unclear Doesn't reflect diversity of human MM
Genetically engineered mice	Vk*MYC tumours in MGUS prone C57/BL6 mice	Spontaneous Mimics biology of human myeloma De novo: early, intramedullary Transplanted: late, extramedullary Oncogenically similar to human myeloma	Genetic/phenotypic characterisation incomplete Unlikely to reflect diversity of myeloma Human MM subgroup correlation unknown; most likely TC1.

Table 1.2. Myeloma Mouse Models. Table listing the individual mouse models, working examples in the myeloma field and their individual group disadvantages and advantages. MM – Myeloma; HMCL – Human myeloma cell lines; SCID – Severe combined immunodeficiency; NOD – Non-obese diabetic; hu-human; rab-rabbit; synth-hu – synthethic human; Rg – Rag; TC1 – Myeloma Subgroup defined by recurrent Cyclin D1 translocation.

1.1.5.4.1. Xenogenic Transplantation

In this model, a variety of HMCLs were injected into single (Severe combined deficient [SCID]), double (Nonobese diabetic/ SCID mice [NOD/SCID]) or triple deficient (NOD/SCID/Il2rg-) mice. The myeloma group at the Dana-Farber Cancer Institute employs such a model under which NOD/SCID mice are injected with a stably transfected GFP construct in the HMCL, RPMI-8226/S. Mitsiades *et al* followed a cohort of 75 mice and detailed progressive disease similar to human symptomatic myeloma, with major involvement of the axial skeleton, but without significant spread to lungs, liver, spleen or kidney (Shultz et al., 2007, Mitsiades et al., 2003). Xenogenic transplants into particular strains of immunodeficient mice are useful for HMCLs and some extra-

medullary myeloma tumours, but rarely for intramedullary myeloma tumours. It is largely an *in vivo* assessment of efficacy against HMCLs. This model can be loosely extrapolated to studying microenvironmental effects of a particular study drug, but the fact that the mice are so immunocompromised extrapolates to a very different microenvironment found in human myeloma.

1.1.5.4.2. Xenogenic Humanised Transplantation

Xenogenic humanised transplantation is the use of mouse-human chimera to study human cells in mice (Ito et al., 2012b). In the myeloma field, this lead to the use of human fetal bones in the SCID-hu model. Due to the concerns in relation to fetal tissues, Yata *et al* developed a SCID-rab model utilising rabbit bone implanted subcutanesouly in unconditioned SCID mice (Yata and Yaccoby, 2004). This allowed the growth of CD138 expressing primary human myeloma cells. Such an environment is, an albeit imperfect, mimic of the tumour microenvironment, but is nonetheless better than cell lines based methods (Yata and Yaccoby, 2004).

The description of the SCID-synth-hu model appears to open the possibility of manipulating the microenvironment by co-injecting different combinations of human bone marrow cells with the synthetic bone matrix before injecting human tumour cells (Calimeri et al., 2011).

1.1.5.4.3. Syngenic Transplantation

A syngeneic transplant model involves a mouse myeloma cell line being injected into an immunocompetent host, usually C57/BL6. The Belgian myeloma group uses two different spontaneous C57/BL6 myeloma tumours, T2 and T33, that home to the bone marrow, and sometimes extramedullary sites, in immunocompetent mice. An example of this model is where Menu *et al* use 5T33MM mouse myeloma cells in validation of the novel CDK4/6 inhibitor PD0332991 (Menu et al., 2008).

The Vk*MYC transgenic mouse model for myeloma, discussed below, also has a syngenic corre-

late where Chesi *et al* have developed three mouse myeloma cell lines with different degrees of resistance to bortezomib (Chesi et al., 2008, Chesi et al., 2012). The Vk*MYC resistant cell line was injected into an immunocompetent C57/BL6 mouse and develops over a twelve week period, where a monoclonal paraprotein is detectable in the serum.

1.1.5.4.4. Genetically Engineered Mouse Models

There has been a recent growth in the ability of genetically engineered mouse models (GEMMs) to reflect disease states particularly at a stem cell level. Singh *et al* and Chen *et al*, for example, have shown the predictive nature of such approach in human clinical trials in NSCLC (Singh et al., 2010, Chen et al., 2012).

Chesi *et al* have, further, developed their Vk*MYC GEMM of myeloma in the C57/BL6 mouse strain that spontaneously develops MGUS, which is similar to the MGUS tumour that universally precedes myeloma in humans. In this model, during somatic hypermutation in the germinal centre of B cells, the immunocompetent C57/BL6 Vk*MYC model activates the MYC transgene, and develops myeloma in aged mice, a result that models the increased MYC expression in human myeloma compared with human MGUS. The slow growth of the myelomatous clone appears to reflect the biology of human myeloma faithfully, including bone marrow localisation and presumptive interaction with the microenvironment, low fraction of proliferating tumour cells, as well as secondary abnormalities such as bone disease and anaemia. Serum protein electrophoresis is used to detect the amount of tumour-specific monoclonal immunoglobulin. Therefore, it is possible to monitor the amount of tumour during the course of disease even when the tumour is dispersed at different intra- and extra-medullary locations.

Using the Vk*MYC GEMM of myeloma, Chesi *et al* have determined the effects of single drugs with both known and unknown clinical activity on myeloma tumours that have arisen spontaneously. Significantly, they found that four of six clinically effective drugs are active in this model.

Equally important is their finding that seven of eight clinically ineffective drugs are inactive in this model, even though many of these ineffective drugs have activity against HMCLs (Chesi et al., 2008). In addition, they provide evidence that the more aggressive disease that models end-stage drug-resistant myeloma responds only to combinations of drugs with single-agent activity against de novo Vk*MYC myeloma (Chesi et al., 2012).

Similar to the other GEMM models in NSCLC, the Vk*MYC GEMM model of myeloma is extremely promising for identifying both single agents and combinations of existing and new therapeutic agents that are more likely to be effective in clinical trials designed to investigate different disease stages. One caveat is that the myeloma tumours in Vk*MYC mice may not fully model some kinds of myeloma tumours (eg, tumours with t(4;14) translocations). However, unlike most of the other preclinical models used for myeloma (Table 1.2), these tumours appear to be localised in the appropriate microenvironment in immunocompetent hosts. Therefore, the Vk*MYC GEMM model also appears to be suitable for identifying therapies that target the interaction of tumour cells with the microenvironment and immunomodulatory therapies. Following from this, this model is now used increasingly by the MMRC in their pre-clinical validation drug screen to attempt to find new potential anti-myeloma drugs for future definitive treatments. This thesis utilises the Vk*MYC GEMM model in validation of the CDC7/CDK9 inhibitor.

1.1.6. Myeloma Stem Cells

Myeloma is characterised by neoplastic plasma cells, but it is unclear whether they represent the replicating component of the disease as they appear quiescent and terminally differentiated, as is the case in their normal counterparts (Bataille and Harousseau, 1997, Drewinko et al., 1981). Much of the work carried out in establishing a cancer stem cell (CSC) niche in myeloma comes from Matsui's laboratory at JHMI. Alternative explanations are proposed by a series of other independent investigators (Rasmussen et al., 2010, Yata and Yaccoby, 2004, Walker et al., 2013 and Chaidos et al., 2013). All things considered, CSC in myeloma is an evolving area of research, full of controversy and debate. Highly clonogenic CSC have been identified in several human malignan-

cies, including myeloma, and their combined resistance to chemotherapy and enhanced growth potential suggests that they may be responsible for disease relapse and progression (Matsui et al., 2008, Matsui et al., 2004). The ability to target the CSC niche is an area of active research in most cancers. In particular, groups have focused on the developmental pathways, including Wnt, Notch and Hh.

Matsui *et al* found that myeloma CSC best resemble memory cells ($CD138^{neg}CD19^{+}CD27^{+}$) that give rise to differentiated $CD138^{+}$ plasma cells that are relatively resistant to agents used to treat myeloma. CD138 can degrade rapidly after isolation. Alternative markers for malignant plasma cells are now increasingly used. These include CD269 (TNFRSF17/BCMA) and CD319 (SLAMF7/CS1) (Frigyesi et al., 2014).

Other groups have challenged the validity of a true stem cell in myeloma. The lack of RAS mutations in memory cells suggests that myeloma cells originate from precursor B-cells (Rasmussen et al., 2010). Walker *et al* using a sequencing approach demonstrates that in certain translocations, a D_H-J_H rearrangement would suggest that the origin of the myeloma clone is pregerminal B-cell and possibly at the pro-B cell progenitor cell level (Walker et al., 2013). Chaidos *et al* have demonstrated four distinct hierarchially organised phenotypically distinct populations defining myeloma (Chaidos et al., 2013). The pre-PC and PC characteristed by $CD19^{-}CD138^{-}$ and $CD19^{-}CD138^{+}$ retain an ability to convert phenotypically but also bidirectionally (Chaidos et al., 2013). Chen *et al* used the PKH26 dye to identify quiescent myeloma cells in the osteoblastic niche. Those that resided in the osteoblastic niche demonstrated enhanced stem-like properties (Chen et al., 2014). Equally, this may suggest that 'stemness' may in fact relate more to the ability of the cell to adapt to a state of resistance. Sigal *et al* has, for example, demonstrated that protein expression is a stochastic process that leads to phenotypic variation among cells, particularly demonstrated when cells are under pressure (Sigal et al., 2006). This accounts for non-genetic heterogeneity which could potentially lead to clonal evolution (Brock et al., 2009). This alternative view of 'stemness' is supported by Chaidos et al's work which illustrated that pre-PCs are up to 300 times more re-

sistant than their PC counterparts (Chaidos et al., 2013)

Matsui *et al* initially examined whether clonogenic myeloma cells could be identified in primary patient specimens and developed an *in vitro* method, similar to the human tumour cloning assay first described by Salmon and Hamburger (Hamburger and Salmon, 1977b, Hamburger and Salmon, 1977a), that allowed them to assess and quantify their clonogenic growth (Matsui et al., 2004). Using this system, Matsui *et al* studied the growth of cells that expressed CD138, that it is restricted to terminally differentiated plasma cells during normal lymphohematopoiesis, and which is absent on highly proliferative plasmablasts and B cells (Jego et al., 1999, Jego et al., 2001). Furthermore, CD138 is expressed on neoplastic plasma cells from virtually all patients with myeloma (Wijdenes et al., 1996).

Matsui *et al* found that fully differentiated $CD138^{+}$ plasma cells produced no tumour colonies (Matsui et al., 2008). Conversely, mononuclear cells isolated from bone marrow aspirates by density centrifugation, then depleted of $CD138^{+}$ plasma cells and $CD34^{+}$ cells (to eliminate normal hematopoietic progenitors that complicate clonogenic analyses), generated colonies consisting of clonal plasma cells by morphologic examination and the detection of CD138 expression and cytoplasmic Ig light chain restriction that matched the patient's monoclonal Ig (Matsui et al., 2008). This $CD138^{neg}$ cell fraction also formed colonies, in a dose-dependent manner, suggesting that colony formation was due to the proliferation of individual cells rather than cellular aggregation (Matsui et al., 2008). Furthermore, pooled myeloma colonies from the $CD138^{neg}$ cell fractions could be replated and continued to form colonies, suggesting that the self-renewal potential of myeloma progenitors was maintained in this culture system (Matsui et al., 2008). As a second assay of clonogenic myeloma growth, Matsui *et al* isolated $CD138^{+}$ and $CD138^{neg}$ cells from patients with myeloma and injected them into immunodeficient NOD/SCID mice. None of the animals injected with up to 5×10^{6} $CD138^{+}$ cells demonstrated evidence of engraftment after 16 weeks (Matsui et al., 2008). In contrast, $CD38^{bright}CD138^{+}$ human plasma cells, with the same Ig light

chain restriction, were found in the bone marrow of mice injected with $CD138^{neg}$ cells (Matsui et al., 2008). Importantly, this population was negative for CD45, which illustrates that normal human haematopoietic elements did not engraft.

The first challenge to the postulate that the $CD138^{neg}$ fraction characterised the myeloma clonogenic CSC came from work by Yata *et al*. Yata *et al*, argued that the tumourgenic potential of the clone depended more on the microenvironment. Moreover, their results suggest that $CD138^{+}$, but not $CD138^{neg}$, cells successfully engrafted in a hu-SCID model, which is contrary to Matsui's work (Yata and Yaccoby, 2004).

In other tumour systems, CSC appear to arise from normal self-renewing counterparts, such as haematopoietic stem cells in myeloid leukaemias and neural stem cells in brain tumours (Lapidot et al., 1994, Bonnet and Dick, 1997, Singh et al., 2003, Singh et al., 2004, Bedi et al., 1993, Hemmati et al., 2003). B cells are largely mature and lineage committed, but unlike myeloid and neural development in which cells progressively lose the capacity for self-renewal and long-term proliferation with differentiation, B cells appear to maintain self-renewal potential at several points during maturation and development. Self-renewal in this setting serves to foster the development of the fittest B cell clones and the highest degree of immunologic protection (Lanzavecchia and Sallusto, 2002). Self-renewal is also required by memory B cells to maintain life-long humoral immunity (Ahmed and Gray, 1996, Fearon et al., 2001, Dorner and Radbruch, 2005, McHeyzer-Williams and McHeyzer-Williams, 2005). Several studies have illustrated that myeloma is derived from a post-germinal B cell (Bakkus et al., 1994, Bakkus et al., 1995, Billadeau et al., 1993, Berenson et al., 1995, Kunkel et al., 1995, Vescio et al., 1995, Cao et al., 1995). Mindful of this, Matsui *et al* hypothesised that the myeloma CSC arose from memory B cells because of their inherent self-renewal potential. To prove this, $CD138^{neg}$ cells were further depleted with beads against pan-B cell (CD19, CD45), post-germinal center (CD20) and memory B cell (CD27) surface antigens. Loss of $CD19^{+}CD45^{+}CD20^{+}CD27^{+}$ limited subsequent clonogenic growth *in vitro* suggesting that

clonogenic myeloma cells are phenotypically identical to memory B cells.

The second challenge to Matsui's work came from Rasmussen *et al* and Chaidos *et al* (Rasmussen et al., 2010, Chaidos et al., 2013). Rasmussen *et al* examined the presence of the same genetic mutations in both memory B-cells and myeloma cells. Although defining primary, non-random translocations were present in both subsets, KRAS mutations were not present in memory B-cells, and thus most likely represent a clonal remnant that is only partially transformed, but which cannot repopulate the clonal transformed myeloma cells (Rasmussen et al., 2010). This work suggests a more naïve cell, that is, a pre-memory B-cell (Rasmussen et al., 2010). In addition, Chaidos *et al* have demonstrated four distinct hierarchially organised, phenotypically distinct, populations defining myeloma (Chaidos et al., 2013). The pre-PC and PC, characteristed by $CD19^{-}CD138^{-}$ and $CD19^{-}CD138^{+}$, retain an ability to convert phenotypically but also bidirectionally (Chaidos et al., 2013).

1.1.6.1. Stem cell characteristics that may mediate drug resistance

Normal adult stem cells exhibit resistance to many toxic agents, which is thought to be mediated by multiple cellular processes that include cellular quiescence and high expression of efflux transporters and intracellular detoxifying enzymes. Interestingly, these physiologic properties have formed the basis for distinct flow cytometric assays capable of enriching stem cells from normal tissues. Therefore, Matsui *et al* examined whether the myeloma CSC could be identified using these assays. Normal haematopoietic and neural stem cells express high levels of ATP binding cassette (ABC) transporters such as P-glycoprotein (MDR1) that actively export cytotoxic agents. Differential fluorescence of cells following incubation with the DNA binding dye Hoechst 33342 can produce the side population (SP) phenotype that has been found to highly enrich for normal stem cells (Goodell, 2002, Hirschmann-Jax et al., 2004, Kondo et al., 2004, Clayton et al., 2004). The SP phenotype is mediated by the export of Hoechst 33342 by the ABC transporter BCRP1 (ABCG2) and is thought to be indicative of high drug efflux capacity. Matsui *et al* stained two myeloma cell

lines, RPMI-8226-S and H929, with Hoechst 33342 and, similar to other studies reporting SP cells within human cell lines (Hirschmann-Jax et al., 2004, Kondo et al., 2004), Matsui *et al* detected small SP populations (0.4-1.2%) in each. The SP cells were also demonstrated to be $CD138^{neg}$ whereas non-SP cells are predominantly $CD138^{+}$.

Normal stem cells may also express relatively high levels of intracellular detoxifying enzyme activity such as aldehyde dehydrogenase (ALDH) (Kastan et al., 1990). One specific isoform of ALDH, retinaldehyde dehydrogenase (ALDHA1), that is required for the conversion of vitamin A to all-trans-retinoic acid (ATRA) is highly expressed in normal hematopoietic stem cells, presumably because of their large requirements for ATRA (Kastan et al., 1990). ALDH also mediates the intracellular neutralisation of cytotoxic chemotherapeutic agents such as cyclophosphamide and ifosfamide (Brodsky and Jones, 2005). Intracellular ALDH1 activity can be measured by flow cytometry (Jones et al., 1995). Matsui *et al* co-stained the human myeloma cell lines RPMI-8226-S and H929 with Aldefluor and anti-human CD138 antibodies and found that $CD138^{neg}$ cells expressed high ALDH activity. Normal hematopoietic stem cells are highly quiescent, (Morrison and Weissman, 1994, Goodell et al., 1996) and this property may also protect cells by limiting the activity of drugs that require transit through the cell-cycle for their effects or attenuating the expression of target proteins (Randall and Weissman, 1997, Venezia et al., 2004, Angstreich et al., 2005). Since normal memory B cells are quiescent in the absence of activating antigen (Bovia et al., 1998), Matsui *et al* examined the cell-cycle status of $CD138^{neg}$ and $CD138^{+}$ RPMI-8226-S and H929 cells following staining with propidium iodide. In each cell line, $CD138^{neg}$ cell lines were largely in G0/G1(98-99%) whereas $CD138^{+}$ cells were found to be actively cycling with only 72-77% in G0/G1.

1.1.6.2. Myeloma Stem Cell Drug Resistance

In order to determine whether myeloma plasma cells and CSC are biologically distinct and display unique drug sensitivities, Matsui *et al* studied the effects of four clinically utilised anti-myeloma agents on each cell population: dexamethasone (0.1 μM); the active metabolite of the standard

cytotoxic alkylator cyclophosphamide, 4-hydroperoxycyclophosphamide (4HC; 30 μg/ml); the thalidomide analogue lenalidomide (1 μM); and the proteosome inhibitor bortezomib (10 nM). The $CD138^{+}$ and $CD138^{neg}$ fraction of RPMI-8226-S and H929 myeloma cell lines was incubated with each agent for 72 hours, then washed free of drug and assessed for clonogenic potential by examining colony formation in methylcellulose. All four agents significantly inhibited $CD138^{+}$ plasma cells from each cell line, but had little effect on the clonogenic recovery of $CD138^{neg}$ cells. Similar results were demonstrated with primary cells and *in vivo* mouse work. Therefore, this suggests that myeloma CSC are biologically distinct from their mature plasma cell progeny and are relatively resistant to current anti-myeloma agents.

1.1.7. Clinical Features of Myeloma

Myeloma is characterised clinically by bone marrow plasmacytosis that can be symptomatic or non-symptomatic. This broad division determines not only the decision to treat, but also the very classification from pre-clinical to clinical stages that define myeloma. Myeloma is principally a gammopathy whereby the normal immunophysiological function of the plasma cell to secrete immunoglobulin, in response to a 'foreign' antigen, becomes pathological, in circumstances where oligoclonal, but ultimately monoclonal immunoglobulin, or the light chains thereof, are secreted in abundance.

Its clinical spectrum is wide. It extends from discrete secretion of the monoclonal immunoglobulin of varied idiotype without clinical pathological significance, an entity termed monoclonal gammopathy of undetermined significance (MGUS), to a smouldering state, which exhibits a further increase in plasmacytosis, until then asymptomatic, to symptomatic myeloma, and to, lastly, a terminal extramedullary leukaemic phase. It is now acknowledged that all myeloma has the potential to pass through these individual phases, although some may present at different stages, progress at variable speed and die before ultimate extramedullary extension occurs.

Symptomatic myeloma, necessitating treatment, implies that this clonal proliferation has lead to organ dysfunction and thus, clinical significance. Organ dysfunction is measured by the development of hypercalcaemia, renal insufficiency to renal failure, anaemia and bone disease with lytic destruction. The division is important to emphasise as among cancers early treatment, even when asymptomatic, usually confers a more favourable outcome; in myeloma such early treatment offers no survival benefit (Hjorth et al., 1993, Korde et al., 2011, Srivastava et al., 2013). However, this position may largely be due to the fact that treatments that target the true biology of individual myeloma have never been explored adequately in this cohort. Currently, a number of trials are underway assessing whether treatment during the MGUS phase alters overall survival or clinical progression. Both the Mayo Clinic group and the Spanish group have developed models for predicting the risk of MGUS progression. The Mayo group indicates 3 risk factors – non-IgG isotype, serum M- protein concentration >15 g/l, and an abnormal free light chain ratio. The Spanish group used a multiparametric flow cytometry to identify plasma cell populations associated with increased risk of progression. Turesson *et al* validated each individual model using a Swedish cohort of patients. Turesson *et al* validated the prediction of M-protein > 15 g/l and abnormal FLC ratio (Turesson et al., 2014). Interestingly, Turesson *et al* identified that immunoparesis is highly predictive of progression.

1.1.7.1. Epidemiology

Myeloma is the second most common haematological malignancy. It accounts for 1% of all cancers and approximately 10% of all haematological malignancies (Rajkumar, 2013, Rajkumar et al., 2011). In the US, over 20,000 new cases are diagnosed each year (Jemal et al., 2011, Siegel et al., 2012). The annual age adjusted incidence is 4/100,000 (Kyle et al., 2004). In Ireland, although the dataset is largely incomplete, the National Cancer Registry of Ireland (NCRI) describes 200-250 cases per year, accounting for approximately 1% of all cancers. This is higher than expected for a population of 4.5 million people. Myeloma is more common in men than in women and twice as common in patients of African descent than Caucasians (Landgren and Weiss, 2009). The median

age for onset is sixty-five (Kyle et al., 2003).

1.1.7.1.1. Risk of Progression to Myeloma

MGUS occurs in 3% of the population over the age of 50 years with a 1% risk of progression to symptomatic myeloma per year (Kyle et al., 2002, Kyle et al., 2006). Turesson *et al* demonstrated a 0.5% risk of progression using a Swedish cohort of patients (Turesson et al., 2014). Smouldering myeloma progresses to myeloma at a rate of approximately 10% per year over the first five years, 3% per year over the next five years and 1.5% per year thereafter (Kyle et al., 2003, Kumar et al., 2003). Approximately, 2% of patients have true non-secretory disease (Kyle et al., 2003).

1.1.7.2. Diagnosis

The diagnosis of myeloma requires two major findings: the presence of 10% bone marrow plasmacytosis or biopsy proven plasmacytoma; and evidence of a symptomatic state with end-organ damage (hypercalcaemia, renal insufficiency, anaemia or bone lesions) related to the plasma cell disorder (Kyle and Rajkumar, 2009).

It is recommended that, when myeloma is suspected, patients should be tested for the presence of a monoclonal protein (the M protein) using serum protein electrophoresis, serum immunofixation, and serum-free light chain assay (Katzmann et al., 2006). The bone marrow should be examined for recurrent non-random cytogenetic abnormalities with FISH for t(11,14), t(4;14), t(14;16), t(6;14) and t(14;20), hyperdiploidy (also termed trimsomies) and deletion of 17p (Kumar et al., 2009, Mikhael et al., 2013). Gene expression profiling (GEP), if available, has obvious prognositic value but with increased costs. Assessment for bone involvement was traditionally carried out by means of a skeletal survey, but low-dose whole body CT, PET-CT and MRI scans are increasingly used to provide added sensitivity and specificity. Moreover, serum carboxy-terminal collagen crosslinks are increasingly used to assess bone turnover and to determine the adequacy

of bisphosphonate therapy (Dizdar et al., 2007, Silvestris et al., 2007).

To assess treatment response, the serum M protein or measurable light chain ratio is measured monthly when on treatment, or every 3-4 months when off treatment. The International Myeloma Working Group uniform response criteria are used to evaluate response to therapy (Durie et al., 2006).

1.1.7.3. Risk Stratification

The role of risk stratification in myeloma is clearly both important and contentious. There has been considerable evolution in the understanding of its role since the description of the Durie-Salmon staging score (Durie and Salmon, 1975). The Durie-Salmon and the International Staging System are described in Table 1.3 (Greipp et al., 1993). Both provide prognostic information, but neither were designed to inform treatment choices.

Table 1.3

A

Stage	Criteria	Median OS (months)
I	Serum β2MG <3.5mg/L Serum Albumin ≥ 35g/L	62
II	Not I or III*	44
III	Serum β2MG ≥5.5mg/L	29

B

Stage	Criteria	Myeloma Cell Mass (Myeloma cells in billions/m²)*
I	*All of the following:* HB > 10g/dL Normal serum Ca^{2+} X-Ray - Normal or solitary plasmacytoma Low M-component IgG <5g/dL; IgA < 3g/dL Urinary light chain; < 4g/24º	600 billion
II	Neither I or III	600-1,200 billion
III	*I or more of the following:* Hb < 8.5g/dL Ca^{2+} > 12mg/dL Advanced lytic bone lesions High M-component IgG > 7g/dL; IgA > 5g/dL Urinary light chain > 12g/24º	> 1,200 billion
Subclass	A: Relatively normal renal function Cr < 2.0mg/dL B: Abnormal renal function Cr > 2.0mg/dL	

Table 1.3. Myeloma Clinical Prognostic Scores. A. International Staging System. **B.** The Durie and Salmon Staging System. *There are two categories for stage II: Serum β2MG < 3.5mg/ but serum albumin <35g/l; or serum β2MG 3.5 to <5.5mg/l irrespective of the serum albumin level. β2MG - β2-microglobulin; Ca^{2+} - serum calcium; M-component – monoclonal component; Cr – creatinine.

The Mayo Clinic mSMART score was devised to fill this void and create a score which directs treatment choice (Dispenzieri et al., 2007, Kumar et al., 2009, Mikhael et al., 2013). It attempts to rationalise treatment regimens based on individual risk stratification. There are three risk categories based largely on their cytogenetic or GEP analysis (Figure 1.1).

Figure 1.1

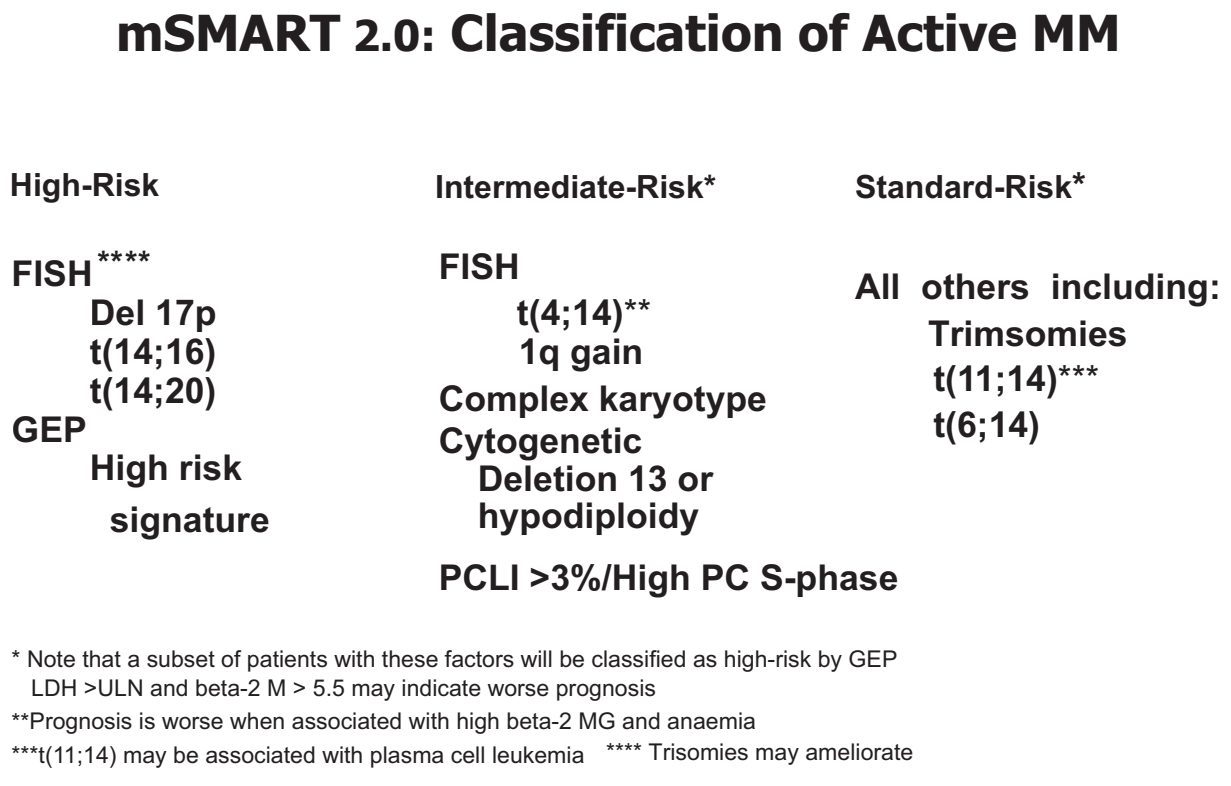

Figure 1.1. mSMART stratification of symptomatic myeloma. Flow diagram of what constitutes high, intermediate and low risk under the mSMART version 2 classification. mSMART - Mayo Clinic Stratification for Myeloma and Risk adapted therapy; FISH – Fluorescence in situ hybridization; GEP – Gene expression profiling; PCLI – Plasma cell labeling index; PC - Plasma cell.

Patients that harbour 17p deletion, t(14;16), t(14;20), or high risk GEP are considered "high risk". This translates into a median overall survival of fewer than 2-3 years despite tandem autologous stem cell transplations (ASCTs). Patients with t(4;14) translocation, chromosome 1q gain, karyotypic deletion 13(metaphase), complex karyotype or hypodiploidy are considered to have intermediate risk. However, patients with t(4;14) myeloma are a poor-risk sub-group in circumstances where there is an associated anaemia and the β2MG (> 5.5 SI Units) is raised. All other abnormalities are considered to be standard risk myeloma. Within the standard risk group it is important to note that t(11;14) can be associated with plasma cell leukaemia and that high LDH and β2MG indicate a poor prognosis. Standard risk is associated with an overall survival of 6-7 years. A high risk GEP takes precedence, and classifies the patient in the high-risk category. Likewise hyperdiploidy may ameliorate other high risk features but this is still debated (Dispenzieri et al., 2007, Kumar et al., 2009, Mikhael et al., 2013).

1.1.7.4. Myeloma Therapy

1.1.7.4.1. Current Therapy

1.1.7.4.1.1. Risk-Adapted Therapy

The mSMART, although contentious, attempts to provide a treatment algorithm based on the patients risk category and eligibility for ASCT. This is summarised in Figure 1.2 (Kumar et al., 2009, Mikhael et al., 2013).

Figure 1.2

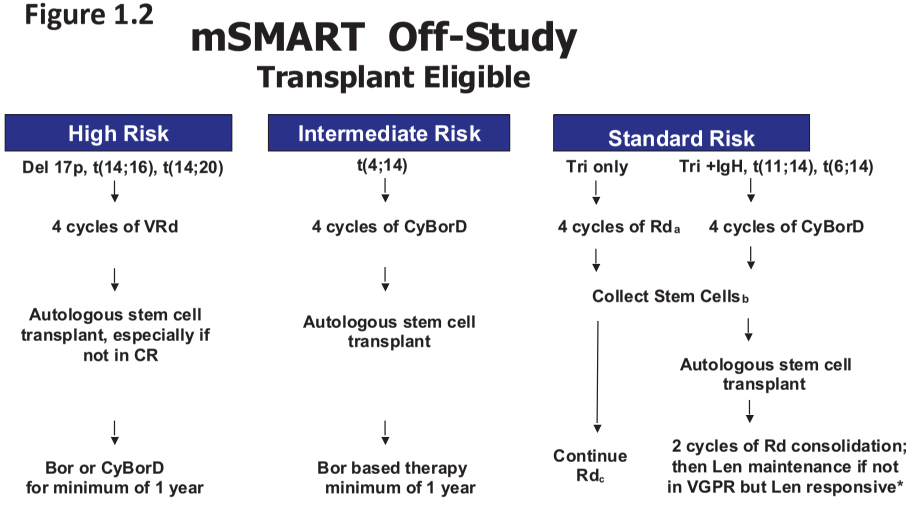

a Bortezomib containing regimens preferred in renal failure or if rapid response needed
b If age >65 or > 4 cycles of Rd Consider G-CSF plus cytoxan or plerixafor
c Continuing Rd is option for patients responding to Rd and with low toxicities; Dex is usually discontinued after first year *
*Consider risks and benefits; If used, consider limited duration 12-24 months

Dispenzieri et al. Mayo Clin Proc 2007;82:323-341; Kumar et al. Mayo Clin Proc 2009 84:1095-1110; Mikhael et al. Mayo Clin Proc 2013;88:360-376. v12.

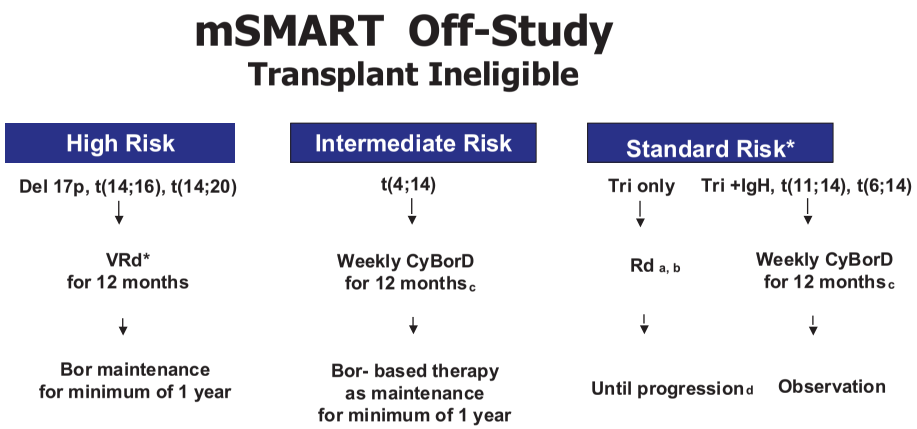

a In patients treated with Rd, continuing treatment is an option for patients responding well with low toxicities; Dex is usually discontinued after first year
b Bortezomib containing regimens preferred in renal failure or if rapid response needed
c CyBorD is considered a less toxic variation of VMP; VMP can be used as an alternative.
d Continuing Rd for patients responding to Rd and with low toxicities; Dex is usually discontinued after first year
*Clinical trials strongly recommended as the first option

Dispenzieri et al. Mayo Clin Proc 2007;82:323-341; Kumar et al. Mayo Clin Proc 2009 84:1095-1110; Mikhael et al. Mayo Clin Proc 2013;88:360-376. v9

Figure 1.2. mSMART treatment algorithm of symptomatic myeloma. Flow diagram of recommended off study treatment regimen depending on calculated risk and whether patient is transplant **A.** Eligible or **B.** Ineligible. mSMART - Mayo Clinic Stratification for Myeloma and Risk adapted therapy; VRd – Bortezomib (Velcade), Lenalidomide (Revlimid) and Dexamethasone; CyBorD – Cyclophosphamide, Bortezomib and dexamethasone; Rd - Lenalidomide (Revlimid) and Dexamethasone; Bor - Bortezomib; Len - Lenaldiomide; VGPR - Very Good Partial Response.

The debate concerning cure versus control, the need for a multi-drug strategy targeting complete response (CR), or a sequential disease control approach that emphasises quality of life as well as overall survival are at the core of treatment strategies and stratification. In standard risk patients, overall survival is similar regardless of whether CR is achieved.

1.1.7.4.1.2. Induction

1.1.7.4.1.2.1 Treatment Naïve

In the treatment naive category, induction usually involves two to four cycles of induction therapy before harvesting stem cells. The autologous stem cell transplant (ASCT) can be given upfront or reserved for first relapse.

The Mayo Clinic has adopted the following guidelines for treatment of transplant eligible patients outside of a clinical trial. Standard risk patients are treated with nonalkylator-based therapy such as lenalidomide plus low-dose dexamethasone (Rd) for four cycles followed by stem cell harvest. If the standard risk is defined only by hyperdiploidy Rd is continued. On the otherhand if defined by factors other than hyperdiploidy patients receive four cycles of Rd followed by stem cell transplant, followed by two cycles fo Rd consolidation and lenalidomide maintenance. Rd is superior to Thalidomide-dexamethasone (TD). Venous-thromboembolic prophylaxis is recommended when thalidomide and lenalidomide are used. Lenalidomide can alter the ability to mobilise stem cells so harvest is generally completed before the fifth cycle at the latest (Dispenzieri et al., 2007, Kumar et al., 2009, Mikhael et al., 2013).

Intermediate and high-risk patients are treated with a bortezomib based induction followed by ASCT and then bortezomib-based maintenance. Harousseau *et al* compared bortezomib plus dexamethasone (VD) versus vincristine-adriamycin-dexamethasone (VAD) as pre-transplant in-

duction therapy (Harousseau et al., 2010). The VD cohort received a very good partial response of 38% compared with 15% achieved by VAD. PFS and OS did not show statistical difference. Three drug combinations cyclophosphamide-bortezomib-dexmethasone (CyBorD or VCD), bortezomib-thalidomide-dexamethasone (VTD) and bortezomib-lenalidomide-dexamethasone (VRd) have shown better response rates and PFS compared to TD (Cavo et al., 2010) as well as VD (Moreau et al., 2011). There is an ongoing trial comparing VRd to Rd. Preliminary studies suggest the CyBorD has similar activity to VRd. CyBord is generally well tolerated and less expensive than VRd. There is currently no data on whether these combinations are better in terms of OS than Rd. Moreover, there have been no comparisons in terms of the quality of life attendant upon the individual combinations. Bortezomib combinations appear to overcome the historically poorer prognosis associated with t(4;14) translocation. This development was accounted for in the most recent version of the mSMART 2.0 score (Version 12). The Mayo Clinic also uses CyBorD for intermediate risk for four cycles followed by ASCT then a bortezomib-based regimen for a minimum of a year (formerly at least two years). The use of the 'at least'principle is in people with del 17 or TP53 mutation. In general, therapy is never stopped as far as it is tolerated due to high rate of relapse when the TP53 mutation is present. For high-risk patients, Mayo Clinic uses VRd but further prospective data from the EVOLUTION trial may suggest CyBorD to an accepted alternative (Kumar S, 2010b). Preliminary results are reflected in the version 12 of mSMART2.0 which suggests a preference for CyBorD maintenance for a minimum of a year. To reduce toxicity, bortezomib is given weekly subcutaneously and dexamethasone 40mg once a week (Moreau et al., 2011).

Standard, intermediate and high-risk patients that are not suitable for ASCT have this step omitted. In addition, melphalan used in combination are also well tolerated as seen with the two Intergroupe Francophone Myelome trials illustrated superiority of melphalan-prednisone-thalidomide (MPT) to thalidomide-prednisone (PT) (Facon et al., 2007, Hulin et al., 2009, Wijermans et al., 2010, Waage et al., 2010, Palumbo et al., 2006). San Miguel *et al* demonstrated, in a large phase III trial, improved OS of bortezomib-melphalan-prednisone (VMP) compared to melphalan-

prenisolone (MP) (San Miguel et al., 2008). Jacobus *et al* examined Rd in patients aged over 70 years who were ineligibile for ASCT and demonstrated a three year OS of 70% comparable to MPT and VMP (Jacobus S, 2010). Interestingly, in a similar patient cohort, Palaumbo *et al* did not demonstrate superiority of melphalan-prednisolone-lenaldiomide to MP alone (Palumbo A, 2009). E1A06 an ECOG RCT is currently comparing MPR to MPT. In the elderly cohort the GEM2005 trial seems to suggest the need for an akylator where VMP is superior to VTD but this is an interim finding (Mateos et al., 2014).

1.1.7.4.1.3. Autologous Stem Cell Transplantation

The role of ASCT is another contentious area in myeloma, as much of the evidence relating to this modality predates the now commonly used immunomodulatory and bortezomib based regimens. The median OS is increased by one year with ASCT (Attal et al., 1996, Child et al., 2003, Blade J, 2003, Kumar et al., 2003, Vesole, 2003). There are three RCTs demonstrating that OS is similar whether ASCT is carried out early (immediately after four cycles of induction chemotherapy) or delayed (at time of relapse as salvage therapy) (Fermand et al., 1998, Facon T, 1996, Barlogie B, 2003). The PETHEMA myeloma group demonstrated no benefit of ASCT in patients responding to induction therapy (Blade J, 2003). This suggests that the benefit of ASCT may be within the small population that is refractory to induction therapy. There are conflicting results on the benefit of tandem or double ASCT is myeloma. In many centres, tandem ASCT is reserved to patients who fail to achieve VGPR with the first ASCT. This constitutes a minority of patients and, in general, the preference is to treat patients with maintenance therapy rather than tandem ASCT.

1.1.7.4.1.4. Post Transplant Therapy

Post Transplant Therapy includes the periods previously termed maintenance and consolidation. Thalidomide has only shown modest progression free survival (PFS) and overall survival (OS) benefit in two RCTs (Attal et al., 2012, McCarthy PL, 2010). The use of the second-generation immu-

nomodulatory drug, lenalidomide, post ASCT has shown better PFS, but benefits in terms of OS are yet to be demonstrated (Attal et al., 2012, McCarthy PL, 2010). The increased incidence of solid malignancy in the lenalidomide maintenance group has sobered its use outside of clinical trials. The HOVON-65/GMMG-HD4 illustrated that bortezomib administered every other week post-transplant produced better OS than thalidomide maintenance (Sonneveld P, 2010). It is increasingly recognised that bortezomib maintenance in the intermediate and high-risk patient categories, particularly the TP53 mutation cohort, is important, but the data supporting this continues to be awaited. Equally, lenalidomide maintence is used outside of the high-risk cohort which does not achieve VGPR. In the most recent version of mSMART2.0 (Version 12), bortezomib maintenance is recommended for at least a year in both intermediate and high-risk transplant ineligible patient cohorts. In the transplant eligible cohort, bortezomib is recommended for a minimum of a year for the intermediate-risk cohort whilst CyBorD maintenance is instead recommended for the high-risk cohort (Dispenzieri et al., 2007, Kumar et al., 2009, Mikhael et al., 2013).

1.1.7.4.1.5. Relapsed Refractory Symptomatic Myeloma

The choice of regimen in relapsed refractory symptomatic myeloma largely depends on prior therapy and the timing of the relapse, but also on the clinical nature of the relapse *i.e.*, whether it is indolent or aggressive. In relapses occurring six months after stopping therapy, salvage with the initial regimen is a valid option. In an indolent relapse, Rd, VD or with combinations with alkylators are valid options. In a more aggressive situation, a combination of active agents is advised. The remission duration in relapse refractory myeloma decreases with each regimen (Kumar et al., 2004). The OS and PFS in the relapsed refractory setting to both lenaldomide and bortezomib are poor with median times of 9 and 5 months respectively (Kumar S, 2010a). In the refractory group two, but generally three-group, combinations are used. Rechallenging with a similar cocktail to that provided at induction or modification of the cocktail to exclude the main induction agent are commonly used mechanisms. Orlowski *et al* demonstrated the effectiveness of liposomal doxorubicin in combination with bortezomib (Orlowski et al., 2007). Unfortunately, however, the

pegylated liposomal preparation is no longer available.

When patients are doubly refractory to immunomodulatory and bortezomib based therapy, outside of a clinical trial, the use of high dose regimens constitutes the mainstay of therapy. This includes DCEP (Dexamethasone-Cyclophosphamide-Etoposide-Cisplatin), C-VAMP (Cyclophosphamide-Vincristine-Doxorubicin-Methlyrednisolone), VDT-PACE (Bortezomib-Dexamethasone-Thalidomide Cisplatin-Doxorubicin-Cyclophosphamide-Etoposide). These high dose regimens have not been compared in radomised control trials and thus, estimates of PFS and OS, and indeed, efficacy are lacking.

1.1.7.4.2. Novel Therapy in Myeloma

Despite the use of high-dose chemotherapy in combination with ASCT and the recent introduction of immunomodulatory agents as well as proteasome inhibitors, myeloma has a poor overall outcome. At best only 40% of patients achieve a CR, and almost all patients eventually relapse and die of their disease. The remission duration in relapse refractory myeloma decreases with each regimen employed. The emergence of carfilzomib, pomalidomide, HDAC inhibitor classes including vorinostat and pabinostat as well as mononclonal antibodies including darantumumab and elotuzumab, however, show promise in the relapsed refractory setting.

1.1.7.4.2.1. New Proteasome Inhibitors

There is a number of trials that have tested the efficacy and safety of carfilzomib in a variety of patient populations. Carfilzomib is the first epoxyketone tested in myeloma. This structural class also includes oprozomib; its structural analog that is orally bioavailable (ONX-0912, formerly, PR-047). This structural class only inhibits the chymotryptic-like subunit of the proteasome. In the 003 (bortezomib refractory), 004 (bortezomib naïve), and 006 (in combination with lenalidomide or dexamethasone) trials, there is clear evidence of activity of carfilzomib either as single agent or in combination (Vij et al., 2012a and b, Niesvizky et al., 2013, Jagannath et al., 2012, Siegel

et al., 2012b). Even in patients who are heavily pretreated the median duration of response and time to progression is very favourable. This suggests that carfilzomib has the potential to be an active drug and may in certain situations, overcome bortezomib resistance. The adverse profile, in particular peripheral neuropathy, is a rare event in the phase II trials – Grade II 9.6% and Grade III 1.4% (004 trial). In the relapse cohort, a large proportion were bortezomib naïve of those who were evaluated. The response is independent of age, cytogenetics, and prior therapy; no patient in the 004 trial had to have the therapy discontinued due to peripheral neuropathy. Carfilzomib in combination with lenalidomide and dexamethasone (CRd) demonstrates a response rate of 76.9% with a median progression-free survival of 15.4 months (Wang et al., 2013). The overall benefit in terms of survival is the subject of the ASPIRE trial. The question arises as to whether it will reach superiority over VRD. Answering this will require a head to head comparison but already the side effect profile is balanced in favour of the CRd combination. The use of higher doeses (56mg/m^2; standard dose 20mg/m^2) of carfilzomib demonstrated increased efficacy (Lendvai et al., 2014). Ixazomib (MLN-9708) is from the same structural class as bortezomib, the bononate peptide family. Ixazomib therefore, inhibits both the caspase-like and the chymotryptic-like subunit of the proteasome. It is another second-generation inhibitor currently in development (Kumar S, 2012). Ixazomib causes less peripheral neuropathy than bortezomib but also has the advantage of being an oral therapy. Richardson *et al* reported that 15% of relapsed refractory myeloma patients (n = 60) in a phase 1 trial of twice weekly ixazomib achieved a partial response or better (Richardson et al., 2014). The weekly dosing of ixazomib demonstrated a similar response rate to the twice-weekly dosing (Kumar et al., 2014).

There are a number of trials evaluating ixazomib in combination with lenalidomide and dexamethasone in the relapsed disease setting as well as in the newly diagnosed setting. Preliminary results suggest very significant activity with a different adverse profile to that which had been seen with bortezomib. Mirizomib (NPI-0052) is an intravenous proteasomal inhibitor similar to carfilzomib and bortezomib, however its molecular structure and spectrum of activity are

different and represent a third structural class of proteasomal inhibitors: the salinosporamides (Richardson P, 2011). Unlike carfilzomib and oprozomib (inhibits chymotriptic-like subunit only), bortezomib and ixazomib (inhibits both chymotrypsin-like and caspase-like subunit), mirizomib inhibits all three of the catalytic proteasomal subunits as opposed to just the chymotryptic-like subunit. A third proteasomal inhibitor is the oral form of carfilzomib, oprozomib (ONX-0912) that has a similar pharmacokinetic profile to carfilzomib and is currently been tested in phase I clinical trials. It is also important to note that carfilzomib, oprozomib and mirizomib, unlike bortezomib and ixazomib, inhibit the proteasome irreversibily.

1.1.7.4.2.2. New Immunomodulatory Drugs

Pomalidomide is a third generation immunomodulatory drug. It has the advantage of being more potent, with an adverse events profile more similar to lenalidomide rather than thalidomide. Early data from Lacey *et al* demonstrated an overall response rate of 49% in the 2mg and 43% in the 4mg cohort (Lacy et al., 2009). The most striking finding was that pomalidomide was able to overcome lenalidomide and bortezomib resistance, giving it an important role as we start to develop regimens for the patient cohort which is dual refractory to both lenalidomide and bortezomib. Richardson *et al* demonstrated a phase I/II study with pomalidomide alone or pomalidomide plus dexamethasone among relapsed refractory myeloma patients. In this trial the single agent response rate was only 13%, but when dexamethasone was added in this refractory patient population, the response rate jumped to 34% (Richardson et al., 2013b). It is important to put these numbers in perspective in that, regardless of which of the trials are examined in the context of pomalidomide in a doubly refractory patient population, it appears that the response rate is roughly 30% and some of these responses can in fact be quite durable. The most common adverse event was myelosuppression and with dose modification this can be managed in a safe way. Pomalidomide has been tested in combination with a number of other agents - clarithromycin and dexamethasone (Mark et al., 2012), carfilzomib and dexamethasone (Shah et al., 2012a), doxurubicin and dexamethasone (Hilger et al., 2013), bortezomib and dexamethasone (Richard-

son et al., 2013a), cyclophosphamide and dexamethasone (Baz et al., 2012) and cyclophosphamide and dexamethasone (Larocca et al., 2013). The dose used in these combination was 4mg on days 1-21 of a 28 day cycle.

1.1.7.4.2.3. Histone Deacetylase Inhibitors

There are a number of histone deacetylase inhibitors (HDACi) currently being trialled in relapsed refractory myeloma - vorinostat, panobinostat, givinostat, quisinostat and romidepsin. A novel HDAC-6-specific inhibitor, rocilinostat (ACY-1215), is also under investigation. Vorinostat and panobinostat in combination with lenalidomide and dexamethasone appears to be the most active combination that can be given in a relatively safe way. The overall response rate demonstrated is 53%. Even more exciting is the work combining HDACi with proteasome inhibitors. This has evolved from pre-clinical work at the DFCI suggesting that HDACi block aggresome function with subsequent inhibition of autophagy. It is postulated that autophagy is the major mode of resistance in patients who have undergone proteasome inhibition. Data combining vorinostat, panobinostat with the third HDACi romidepsin, with bortezomib among a group of bortezomib refractory patients again suggest a response rate of approximately 30%. This has given rise to a number of randomised phase III trials.

The first of these phase III trials was the VANTAGE trial which was presented by Dimopopulus *et al* at ASH 2012 (Dimopoulos et al., 2011). This trial involves 637 patients with relapsed and refractory disease randomised to receive either bortezomib and vorinostat or single agent bortezomib. It appears that the group which received the combination of bortezomib and vorinostat did have a longer duration of remission compared to bortezomib plus placebo. It is important to note that there was no difference in OS and there was a statistically significant, albeit small, improvement in PFS (7.6 versus 6.8 months), favouring the group that received bortezomib in combination with vorinostat compared to the group that received bortezomib alone. There were, however, more adverse effects noted in the combination arm, comprising largely haematological and gastrointestinal toxicities. Some of those adverse effects limit the long-term clinical utility of these data as

the improvement in PFS was relatively short. Again, it is interesting to postulate that with different doses and different scheduling, vorinostat in combination could potentially be a very active agent and provide a more durable duration of response.

The PANORAMA 2 study is a trial of panobinostat plus bortezomib and dexamethasone in relapsed and bortezomib refractory patients (Richardson P, 2012, 2013). The overall response rate was approximately 29%. There was grade III/IV thrombocytopaenia but, in general, there was very little peripheral neuropathy and most of the cytopaenias were manageable with dose interruption or subsequent dose modification. More recently PANORAMA 2, has demonstrated the ability of panobinostat to restore bortezomib sensistivity (Richardson et al., 2013). These trials illustrate the activity of this class of compound and its potential ability to overcome resistance. Dosing schedules are very important for administering these drugs in combination with bortezomib. The current dosing schedules indicate that the dose of vorinostat is possibly too high and it is important to consider how to alter this in order to deliver this combination more effectively.

Rocilinostat (ACY-1215), the HDAC-6-specific inhibitor, demonstrated no efficacy as monotherapy. It is currently being trialled in combination with bortezomib and lenalidomide (Raje et al., 2013).

1.1.7.4.2.4. Monoclonal Antibodies

There are various monoclonal antibodies against cell surface markers under clinical study in myeloma. They target proteins such as CD138 (*cf.* mBT062-DM4), key marker for myeloma cells, CD56 (*cf.* Lorvotuzumab, IMGN901-huN901-DM1), CD38 (*cf.* Daratumumab, HuMax-CD38, Ab005, SAR650984), CS1 (*cf.* HuKuc63, Elotuzumab), BAFFR (*cf.* Tabalumab, TACI-IG), FGFR3 (*cf.* Dasatinib), FGF (*cf.* TKI258), BMA (*cf.* J6MO-mcMMAF), CD40 (*cf.* Dacetuzumab, SGN-40, Lucatumumab), Il-6 (*cf.* Siltuximab, CNTO328, Altixumab), and IGF-1 (*cf.* CP-571, EM164). The use of disease specific protein allows for the use of adoptive cell therapy (*cf.* CD44v6, Bivatuzumab). The two leading monoclonal antibodies in myeloma at advanced stages of development are elotuzumab

and daratumumab. Most have been combined with lenalidomide and dexamethasone (Elotuzumab, Lorvotuzumab and Dacetuzumab) (Lonial et al., 2012, Richardson et al., 2012, Berdeja et al., 2012, Agura et al., 2009) as well as bortezomib and dexamethasone (Elotuzumab, Tabalumab and Siltuximab) (Jakubowiak et al., 2012a, Raje et al., 2012b, Rossi et al., 2008). Daratumumab has attracted increased attention as it appears to have efficacy as monotherapy.

1.1.7.4.2.4.1. Elotuzumab

Elotuzumab is a humanised monoclonal anti-CS1 antibody. CS-1 is an antigen that is largely restricted to plasma cells; it promotes cell adhesion and has an effect on clonogenic growth, tumourgenicity, and perhaps signalling via the c-MAF mediated interactions with the bone marrow stromal cells. The effect of elotuzumab in combination with bortezomib and or lenalidomide has been studied. Jakubowiac *et al*, for example, demonstrated that the combination of bortezomib and elotuzumab achieved an overall response rate of 48% among the 27 evaluable patients with a median time to progression of 9.4 months in this combination (Jakubowiak et al., 2012a). Most intriguing is the data regarding the combination of elotuzumab with lenalidomide and low dose dexameathasone (Lonial et al., 2012). The phase II data suggest a high overall response rate of approximately 92%, with adverse effects largely related to antibody infusion. There were no additional adverse effects that would be expected with lenaldomide or dexamethasone alone. This trial is being followed up in two large phase III trials evaluating lenalidomide and dexamethasone with elotuzumab verus elotuzumab in newly diagnosed patients.

1.1.7.4.2.4.2. Daratumumab

Daratumumab is a humanised monoclonal antibody targeted against CD38. This agent, unlike elotuzumab, has single agent activity even in the relapsed refractory myeloma. It is tolerated quite well with a favourable safety profile. Overall response rate in the expanded cohort of the phase II trial was 30-35%. In those who received greater than 4mg the response rate was 67%, with PR up to 40%. These results are highly promising in a cohort with a median of six previous

treatments. There are ongoing studies building on its single agent activity combing it with other anti-myeloma agents – bortezomib, and lenalidomide – D-RVD, a four drug combination.

1.1.7.4.2.4.3. Bivatuzumab

Recently, Casucci *et al* demonstrated pre-clinical efficacy using cell adoptive therapy in myeloma. Bivatuzumab is a monoclonal antibody to a splice variant of CD44 linked to T cell signalling domains from CD28 and CD3 zeta (Casucci et al., 2013). What is interesting with this approach is that a suicide gene, iCasp9, was added to the viral vector which allowed rapid clearance of gene engineered T-cells. This allowed for off-target monocytopaenia to fully resolve in animal models.

1.1.7.4.3. Targeting Proliferation

Traditionally, drugs which target replication do so either by interfering with molecules required for DNA polymerization, or activating the DNA damage response (DDR). These are commonly used in cancer therapy but equally in infectious disease when treating viruses. In myeloma, in the pre-novel therapy era, there have being many combinations of replication targeting or what was termed 'cell-cycle specific' chemotherapy. DNA template damaging drugs, namely alkylating agents (melphalan and cyclophosphamide), have been the most successful 'anti-replication' drugs used in the infancy of anti-myeloma therapies. Melphalan in combination with prednisolone (MP) was the gold standard in myeloma treatment in the 1970s and 1980s with a three year OS 42%.

The difficulty in assessing the efficacy of the majority of these combinations is that the sample size is quite small, often with fewer than 20 patients and the trials are, in general, not randomised and, at best, observational studies. Bergsagel *et al* used a 'rolling' approach that if no patient in the 11 patient cohort had a response- this had a 90% probability that the drug had a response rate less than 20%, if at all (Bergsagel et al., 1962). As discussed earlier, with development of refractoriness to both bortezomib and IMiDs, high dose treatment combinations are becoming

increasingly used when patients are ineligible for clinical trials, however there is little data supporting their use in such situations.

Nucleotide Triphosphate inhibitors (Anti-folates [methotrexate and pemetrexed], pyrimidine anti-metabolites [5-flurouracil, capecitabine and hydroxyurea] and purine anti-metabolites [6-mercaptopurine, 6-thioguanine and hydroxyurea]) illustrates no real activity in myeloma. Alberts *et al* reviewed cytarabine, HU, 6-MP, and vincristine treatment in 12 patients with a PR to non cell cycle specific chemotherapy (Alberts et al., 1977). Only vincristine (6/8 patients) was shown to induce further reduction in bone marrow plasma cell burden. No response was noted in 33 refractory myeloma patients treated with 6-thioguanine (Edelstein et al., 1990). Methotrexate is used in intrathecal regimens where myeloma spreads to the CNS, but is not used as systemic treatment in myeloma. Pemetrexed illustrated pre-clinical promise in cell lines but has not reached the clinic (Ramirez et al., 2007).

Chain elongation inhibitors cytarabine (AraC or cytosine arabinoside) and gemcitabine characterise this group, though it also includes anti-virals such as acyclovir, its derivatives, and foscarnet. As indicated with Alberts *et al*, AraC failed to demonstrate an anti-myeloma effect. In a small cohort of patients refractory to VAD, ESHAP, combining etoposide, methylprednisolone, cytarabine and cisplatin, demonstrated a response rate of 67% (D'Sa et al., 2004). Barlogie *et al* in a small cohort of patients refractory MP, high dose melphalan and VAD demonstrated responses to EDAP (etoposide, cisplatin, cytarabine and dexamethasone) with a 40% response rate and median OS of 4.5 months (Barlogie et al., 1989). Moreover, the same group used EDAP as part of total therapy 1 (TT1) during cycle 5 of induction. Gemcitabine in combination with cisplatin in the relapsed refractory setting demonstrated a median OS of 13 months. Gemcitabine was also tested in combination with paclitaxel (Gazitt et al., 2006). In this combination, one patient had a CR with 3 patients achieving a PR. The SWOG-9803 trial recruited 29 patients for single agent gemcitabine with no major clinical response demonstrated (Weick et al., 2002).

DNA polymerase inhibitors such as the anti-viral foscarnet and aphidicolin have not been trialled in myeloma patients.

DNA template damaging drugs block replication fork progression with three main lesions - DNA adducts, DNA strand breaks and DNA-protein crosslinks. DNA alkylating agents includes nitrogen mustard derivatives (melphalan, chlorambucil and cyclophosphamide) but also methylmethane-sulfonate, MMS, the platinum derivatives (Pt – Cisplatin, Oxaliplatin, and Carboplatin), and DNA cleaving agents (bleomycin and neocarcinostatin).

Melphalan and cyclophosphamide continue to have an important role in stem cell mobilisation, transplant conditioning, novel combination therapy but, increasingly, in high dose therapy for relapsed refractory myeloma. Cisplatin is used in total therapy 2 and 3 as part of DCEP. It is also used as a salvage treatment in refractory myeloma as part of DCEP and DT-PACE, as previously mentioned. In myeloma, bleomycin has been trialled in combination, but has demonstrated no real effect, albeit in small sized trials (Bennett et al., 1978, Bonnet et al., 1982, Bonnet et al., 1984). TOP1 inhibitors include the camptothecin derivatives – topotecan and irinotecan. Topotecan was used in combination with melphalan and cyclophosphamide in small non-randomised cohorts achieved a CR of 12% in the relapse refractory cohort. TOP2 inhibitors include the anthracyclines and etoposide. Again, TOP2 inhibition forms part of high-dose treatments that are increasingly used in the relapsed refractory setting. Idarubicin was examined extensively in myeloma not only as a treatment used in induction, stem cell mobilisation, transplant conditioning, but also in the relapse refractory myeloma patients (Fenk et al., 2005). Its role as an oral alternative was quite attractive; that said, it has more myelotoxicity. Low dose idarubicin was historically investigated in combination with cyclophosphamide and dexamethasone (CID) with MP resistant myeloma (Glasmacher et al., 1997, Glasmacher et al., 2004, Kashyap et al., 1999). High dose idarubicin in combination with cyclophosphamide and melphalan demonstrated increased toxicity with a

treatment mortality of 20% versus 0% in the standard group arm. Idarubicin has been previously used as an oral alternative to the traditional VAD regimen with similar efficacy (Heyll et al., 1997). Z-Dex (idarubicin in combination to dexamethasone) demonstrated similar efficacy to other mobilisation regimens (Cook et al., 1997). More recently, idarubicin has been used in combination with bortezomib and melphalan (VIM) in relapsed refractory myeloma. In addition, the German group is evaluating its effect in a cohort with similar characteristics in combination with thalidomide and cyclophosphamide (T-CID).

Bendamustine combines an alkylator structure with a purine analog ring. Its activity in combination with bortezomib, thalidomide and lenalidomide in relapsed refractory myeloma demonstrate modest response rates with at best PR achieved.

Melphalan-flufenamide, a novel prodrug of melphalan, may prove efficacious in myeloma. Peptidases over-expressed in myeloma cells may allow for higher plasma cell levels of melphalan with possibly more anti-myeloma effect (Chauhan et al., 2013).

TH302 is another alkylator activated in a hypoxic niche of the bone marrow microenvironment. It is currently under investigation in combination with dexamethasone (Chobrial et al., 2013).

1.1.7.4.3.1. Cyclin Dependent Kinase Inhibitors

This is an ever-growing group of small molecular inhibitors with varying specifities to individual CDKs. They can be further categorised to those that are ATP or non-ATP competitive inhibitors. These include flavopiridol (pan-CDK inhibitor), selicilib [roscovitine, CY202 (CDK2/7/9)], SNS-032 [BMS-387032 (CDK2/7/9 inhibitor)], PD0332991 [Seleciclib, (CDK4/6 inhibitor)], Dinaciclib (CDK 1/2/5/9 inhibitor) and many others.

Gojo *et al* demonstrated pre-clinical efficacy of flavopiridol in myeloma (Gojo et al., 2002). Inter-

estingly, Dispenzieri *et al* evaluated its efficiacy in a phase II trial. The trial stopped recruiting as there was no major response noted in the first 18 patients. It is important to note that 7 patients had a PCLI > 1% despite demonstrating no response (Dispenzieri et al., 2006).

Mac Callum *et al* and Raje *et al* demonstrated pre-clincial efficacy with Roscovitine (MacCallum et al., 2005, Raje et al., 2005). Indisulam (E7070) has not been reviewed in the myeloma setting. In phase I trials SNS-032 demonstrated greater efficacy in CLL relative to myeloma (Tong et al., 2010)

CDK5 inhibition was identified as one of the top bortezomib-sensitising mechanisms in high-throughput RNAi screening (Zhu et al., 2011). Kumar et al in a phase 1/2 trial of dinaciclib demonstrated some single agent activity and may synergise with bortezomib (Kumar et al., 2012).

1.1.7.4.3.2. Other pathways

AKT1 inhibiton is another promising target and is currently being studied in phase III clinical trials. Perifosine has been combined with bortezomib and lenaldiomide with reasonable PR achived in 32% and 50% respectively (Richardson et al., 2011 and Jakubowiak et al., 2012). Afuresertib (GSK211083) is a novel AKT1 inhibitor with a monotherapy effect (Spencer et al., 2011, Spencer et al., 2014). The trial included six myeloma patients where three patients had a partial response and the other three had a minimal resonse (Spencer et al., 2014)

KSP or kinesin spindle protein inhibitors further offer exciting possibilities for research as well as important new options for patients. In addition, targeting the process of ubiquitylation is a promising possibility. ARRY-520 is a KSP inhibitor in phase I/II trials. At ASH 2012 ARRY-520 demonstrated response rates of between 20-30% in a double refractory patient population with the most common sides effect being myelosuppression (Shah et al., 2012). A small molecule inhibitor, b-AP-15, of two deubiquitylating enzymes, USP14 and UCHL5 has demonstrated activity in myeloma models (Tian et al., 2014). USP14 and UCHL5 are differentially expressed in neoplastic plasma cells relative to normal plasma cells.

In conclusion, when one reflects upon and reviews the compounds that have shown the most benefit in myeloma, it is apparent these involve two classes: the DNA alkylators and TOP2 inhibitors. It is equally important to ask why other targets have been less successful, particularly those that traditionally target DNA replication? It is also interesting to note that alkylators and TOP2 inhbitors also have effects on transcription which may be more important in the plasma cell setting. Mindful of this, this thesis will explore the targetting of these two processes synchronously, both replication and transcription, with the dual CDC7/CDK9 inhibitor.

1.2. CDC7

CDC7 (Hsk1; CDC7L1; HsCDC7; huCDC7; MGC117361; MGC126237; MGC12623) Cell division cycle 7, S cervisiae, homolog-like 1 maps to chromosome 1p22. It encodes a serine-threonine kinase conserved across species (Faul et al., 1999, Jiang et al., 1999, Landis and Tower, 1999).

Work in this niche area spans over the past four decades. Initial work in yeast inspired work in other models leading to cDNA isolation from HeLa cells (Hartwell, 1973, Jiang and Hunter, 1997). From this base, the basic protein domains and motifs were deciphered. In addition to the usual 11 subdomains found in serine-threonine kinases it contains two additional kinase inserts in mammalian CDC7 whereas there are three found in the canonical kinase domain in yeast Cdc7p (Figure 1.3.A). This difference was highlighted when the crystal structure of CDC7 was described in 2012 (Hughes et al., 2012).

1.2.1. CDC7 Regulation

CDC7 has two known regulatory subunits, DBF4 (ASK; CHIF; DBF4A; ZDBF1) and DBF4B (Drf1; ASKL1; chifb; ZDBF1B; FLJ13087; MGC15009) which have cyclical activity mirroring CDC7 activity across the different cell cycle transition points (Montagnoli et al., 2002). In lower eukaryotes CDC7 levels remain constant, however, it is increasingly being observed that, in human cells, they peak at the G2/M transit point. Logically, CDC7 action depends on the binding of its individual regulators. There is an emerging evidence implicating members of the PLK1 family of Polo-like kinases in positively regulating the G2/M transition, events in anaphase, mitotic exit, cytokinesis but also in reductional segregation of chromosomes in meiosis I. It remains possible that DBF4 may regulate PLK1 to prevent premature activation of events in mitosis before completion of DNA replication (Visintin et al., 2003, Hu et al., 2001, Bork et al., 1997, Koonin et al., 1996). The increase in CDC7 at G2M may also indicate a release from DBF4 in order for DBF4 to interact with PLK1.

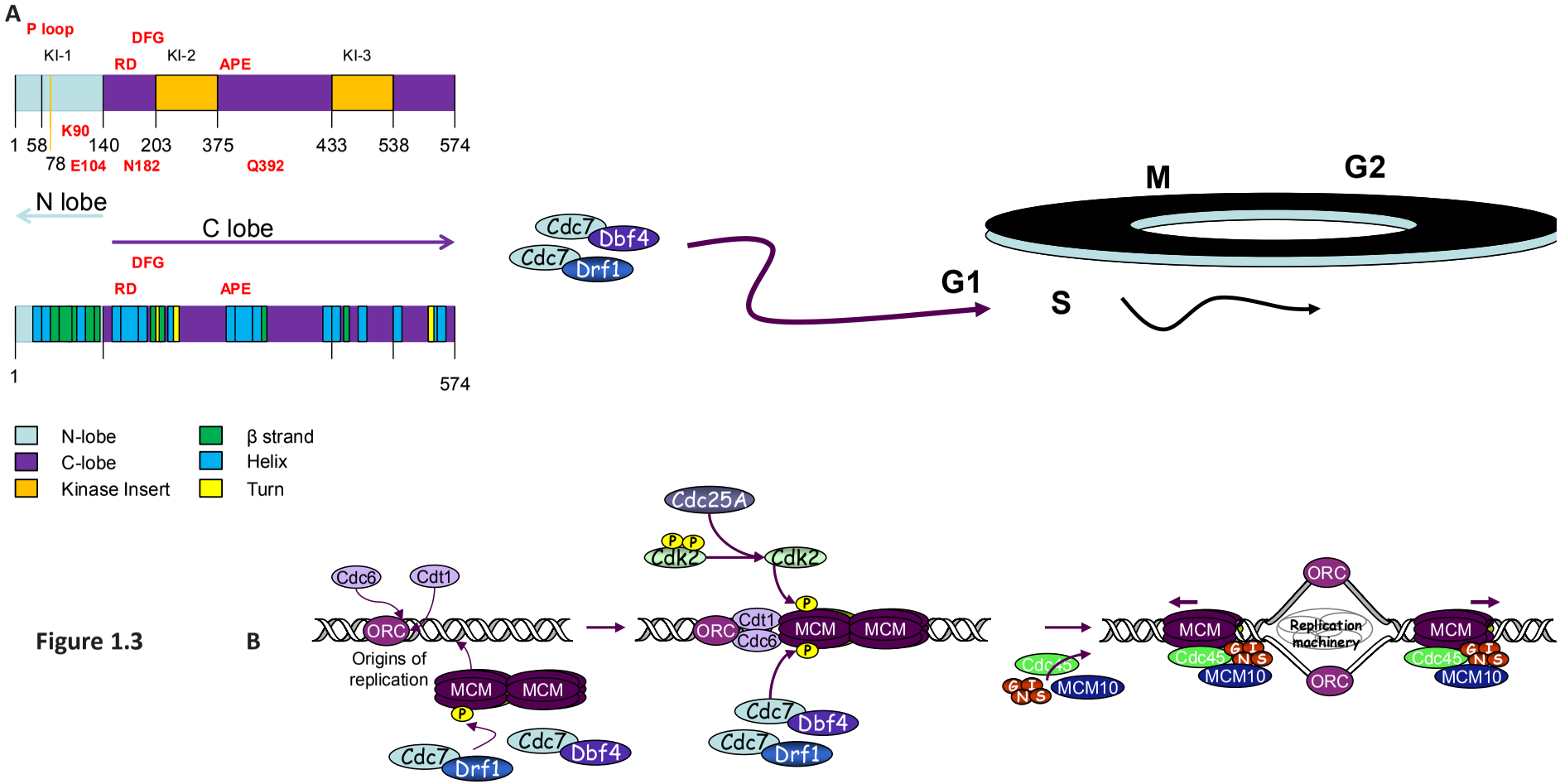

Figure 1.3

Mitosis-Early G1
-Pre-replicative complex assembly
-Cdc7 kinase activity

G1-S transition
-Increased Cdk activity
-Cdc7 kinase activity

Active replication forks

Figure 1.3. Schematic of CDC7 structure and its role in initiation of replication. A. CDC Structure. Conserved domains of CDC7 with N (sky-blue) and C (purple) lobe and Kinase Inserts (KI; orange) 2 and 3. Yeast ortholog also contain KI1 not seen in mammalian CDC7. Secondary structure is indicated with alpha helix (blue), turn (yellow) and beta strands (green). Highlighted in red are the conserved catalytic loop containing the RD signature motif. DFG and APE motif containing the activation segment are highlighted in red. B. Initiation of Replication. Pre-replicative complex is formed at the origin. Loading the holohelicase after DDK phosphorylation of MCM. DDK in partnership with CDK2 triggers the loading of GINS and CDC45 driving the formation of active replication forks. Adapted from schema by Dr Michael Rainey.

1.2.2. CDC7 Function

The essential function of CDC7 in eukaryotic cell cycle progression was first identified by Hartwell *et al* who discovered that *CDC7* inactivation prevented cells from initiating S-phase in S. cerevisiae (Culotti and Hartwell, 1971; YEAST). *Cdc7* was unique in this screen of mutants in that protein synthesis was not required after Cdc7p activity for the completion of S-phase (Hartwell et al., 1973;YEAST). The identification of a temperature-sensitive allele of *DBF4* defective in S-phase initiation eventually led to the hypothesis that Dbf4p and Cdc7p may function in a common pathway to control the start of replication (Johnston and Thomas, 1982;YEAST). Interestingly, Dbf4p was also identified in a screen for high-copy suppressors of *cdc7* (*ts*) (Kitada et al., 1992;YEAST). Cdc7p was subsequently found to encode a serine/threonine protein kinase whose activity is controlled by cyclical expression of the kinase regulatory subunit Dbf4p (Hollingsworth and Sclafani, 1990, Oshiro et al., 1999, Patterson et al., 1986;YEAST). It has also been shown that activity of Cdc7p depends on the direct binding and activation of the Dbf4p regulatory subunit (Yoon and Campbell, 1991, Yoon et al., 1993; YEAST). Together, these studies strongly suggested that Cdc7p and Dbf4p function in concert to regulate passage through the G1/S transition (Figure 1.3.B). Deletion of *DBF4* or *CDC7* is lethal, but cdc7Δ and dbf4Δ cells can be rescued by the bob1-1 mutation in *MCM5*, a component of the eukaryotic replicative helicase (Hardy et al., 1997;YEAST).

Homologs of *CDC7* and *DBF4* were not identified in other species until the discovery of hsk1+, an essential gene required for the initiation of S phase in fission yeast (Masai et al., 1995; SCHPO). Like *CDC7*, hsk1+ encodes a 507 amino acid protein comprising the catalytic subunit of Cdc7. Following the identification of hsk1+, putative Cdc7 homologs from additional species, including humans, were identified (Jiang and Hunter, 1997, Kim et al., 1998). Budding yeast *DBF4* encodes a 704 amino acid protein with three motifs (N-terminal, Middle & C-terminal) with homology across species (Masai et al., 2000;SCHPO). All homologs share highest sequence similarity within the M-motif, while the N and C-terminal regions show the highest degree of sequence divergence (Masai et al., 2000; SCHPO). Activator of S-phase kinase (ASK), DBF4, the human homolog of

Dbf4p, was identified in a 2-hybrid screen and encodes the 695 amino acid regulatory subunit of Cdc7p (Kumagai et al., 1999). Although ASK shares the three common regions (N, M & C) of sequence similarity, the C-terminal half of the protein is less well conserved.

Detailed mutational analyses of budding and fission yeast *DBF4*/dfp1+ identified regions essential for Cdc7p activity and binding to the origin recognition complex (ORC) (Gabrielse et al., 2006; SCHPO). In Dfp1, the individual M and C-motifs were sufficient to bind and partially activate fission yeast Hsk1, while intervening sequences were replaceable for kinase binding and activation (Ogino et al., 2001;SCHPO). These results suggested that activation of Cdc7p/Hsk1 might occur through bipartite binding to the Dbf4p/Dfp1 regulatory subunit. Similarly, the budding yeast Dbf4p C-terminal zinc-finger motif stimulated Cdc7p binding and catalytic activity, but was not essential for cell growth (mutants exhibit a slow S-phase) in the presence of an intact M-motif (Harkins et al., 2009). Mutations within region N in Dbf4p/dfp1+ were found to confer general sensitivity to DNA damaging agents, but had little to no effect on growth under normal conditions (Gabrielse et al., 2006, Ogino et al., 2001;SCHPO). These results suggest a possible role for the DBF4 N-terminus in regulating cellular responses to stress.

Hughes *et al* have demonstrated that the DBF4 C-motif is sufficient to support the CDC7 kinase acitivity by binding to the N-terminal region of CDC7. DBF4s M-motif is simply used to support the C-terminal region of CDC7 (Hughes et al., 2012). Additional regulation may be present as the kinase insert 2 is largely deleted in the construct used by Hughes *et al* (Hughes et al., 2012; Figure 1.3.A).

The DBF4 N-terminus was originally described as having similarity to BRCT repeat sequences (Masai and Arai, 2000). Identified in the human gene BRCA1, BRCT domains are primarily found in DNA damage-response proteins (Bork et al., 1997, Koonin et al., 1996). Crystallisation of the BRCA1 tandem BRCT repeat identified the domain as a phosphopeptide-binding module (Clap-

perton et al., 2004). The c-terminal region of the BRCT sequence is conserved in DBF4 homologs naming this sequence the BRDF (BRCT and Dbf4 similar) motif (Gabrielse et al., 2006).

However, crystallisation of this domain by Guarne *et al* suggests that it nonetheless adopts a canonical BRCT-fold (Gabrielse et al., 2006, Matthews et al., 2009). The function of the DBF4 BRCT domain is unknown and proteins that interact exclusively with the BRCT domain have not been identified. Dbf4p is a target of Rad53-dependent (CHK2 homolog) checkpoint phosphorylation in response to replication stress; this regulation requires an intact Dbf4p N-terminus (Gabrielse et al., 2006, Weinreich and Stillman, 1999; YEAST). In addition, Cds1/Rad53 kinase activation is severely perturbed in hsk1-89 cells and the hsk1-89 mutation is synthetically lethal with the checkpoint protein Rad3/Mec1 (ATR homolog in yeast) suggesting functional overlap between CDC7-DBF4 and the DNA damage response pathway (Takeda et al., 2001;SCHPO). A possible function of the Dbf4 BRCT domain is to interact with phosphorylated Rad53 (CHK2 homolog) FHA domain. Molecular modeling of the crystallised BRCT domain raises this possibility, but biochemical evidence for this is lacking (Matthews et al., 2009). Masai *et al* proposed that human CDC7-DBF4 interacts with components of stalled replication forks and may be required for replication restart in response to replication stress (Matsumoto et al., 2005).

1.2.3. Expression and Regulation of CDC7 subunits during the Cell Cycle

CDC7 catalytic activity is regulated by cyclical expression of DBF4 throughout the cell cycle (Jackson et al., 1993). In contrast to its regulatory subunit, Cdc7 protein levels remain relatively constant during the yeast cell cycle (Jackson et al., 1993;YEAST). Mammalian CDC7 activity is positively regulated by serum stimulation and E2F transcription factor activity (Kim et al., 1998). Dbf4 protein levels remain low throughout G1 and increase at the transition into S-phase and decrease at the end of mitosis (Jackson et al., 1993;YEAST). DBF4 promoter elements suggest that its transcription is under control of the Mlul cell-cycle box (MCB) transcriptional element, however the observed protein oscillation within cells appears to be regulated at the level of protein stability

(Wu and Lee, 2002;HUMAN). Dbf4p contains two putative "RXXL" destruction boxes within the protein N- terminus suggesting a role for APC-Cdc20 in regulating Dbf4p destruction. Mutation of the N-terminal destruction box can stabilise Dbf4p (Ferreira et al., 2000; YEAST). In addition, inactivation or mutation of genes encoding APC subunits stabilises DBF4 protein, however the precise regulation of DBF4 destruction remains enigmatic (Weinreich and Stillman, 1999, Cheng et al., 1999). APC activity is regulated by the specificity components, CDC20 and CDH1/FZR1, which become active at the metaphase-to-anaphase transition and during mitotic exit respectively (Zachariae and Nasmyth, 1999). The contribution each subunit plays in targeting DBF4 for destruction is currently unclear; however, persistent expression of Dbf4p in mitotic exit mutants (cdc5-1, dbf2-1 and cdc14-1) at non-permissive temperature, tends to provide evidence against the argument that Cdc20p is the exclusive regulator and suggests that Dbf4p levels persist late into mitosis, long after completion of S-phase (Weinreich and Stillman, 1999, Cheng et al., 1999; YEAST).

The method of DBF4 regulation is unclear. CDK phosphorylates DBF4 during the normal cell cycle (Ubersax et al., 2003). A serine within the N-terminal DBF4 D-box ("RSPL") matches a consensus CDK phosphorylation site and is phosphorylated *in vivo* after treatment with MMS. It is possible that CDK actively inhibits DBF4 destruction prior to mitotic exit when the CDC20 APC is active. CDC14 dephosphorylation of CDK sites raises the possibility that CDC14 may antagonise CDK phosphorylation of DBF4 and allows the APC access to the DBF4 destruction box late in mitosis.

1.2.3.1. S-phase Initiation

While we now have a relatively developed understanding of the role of CDK in replication initiation, the precise biochemical role for CDC7 at origins is less clear. What is apparent is that localisation of CDC7 to origins is critical for the timely and accurate firing of replication origins throughout S-phase. Diffley *et al* demonstrated by a one-hybrid assay that Dbf4p interacts with origins, and that this genetic interaction is dependent on the origin recognition complex ORC (Diffley et al., 1995; YEAST). Additionally, studies in Xenopus indicate that Cdc7 associates with the pre-RC at origins and this association is dependent on Dbf4 (Jares et al., 2004; Xenopus). The pre-

RC proteins ORC2, ORC3, MCM2 and MCM4 all interact with DBF4 suggesting a model whereby DBF4 targets CDC7 to sites of pre-RC binding (Kneissl et al., 2003; MOUSE/YEAST). The DDK can phosphorylate multiple proteins at the origin including several MCM subunits, CDC45 and polymerase alpha (Nougarede et al., 2000, Weinreich and Stillman, 1999, Kihara et al., 2000). Mapping of DDK phosphorylation sites on MCM proteins and the identification of the bob1-1 (mcm5, P83L) bypass suppressor of cdc7D and dbf4D cells led to the hypothesis that the DDK activates the MCM replicative helicase (Hardy et al., 1997, Sato et al., 1997, Masai et al., 2000). It is thought that phosphorylation of MCM proteins by CDC7 likely leads to a conformational shift in the helicase complex, initiating origin unwinding and DNA replication (Zou and Stillman, 2000). Other evidence suggests a model whereby CDC7 phosphorylation of MCM N-termini may trigger MCM double hexamer dissociation and DNA unwinding (Remus et al., 2009). MCM2 phosphorylation by CDC7 is an essential step in origin firing, in particular, specifically at Ser40 and Ser53 residues (Cho et al., 2006).

The mechanism whereby cells regulate the timing of origin firing throughout S-phase and delay the activity of the DDK on late origins in response to cellular stress remains to be established. Recent evidence indicates that an initiating phosphorylation event by a CDC7-independent kinase primes the pre-RC MCM2-7 complex for phosphorylation by the DDK, suggesting a model in which the spatial and temporal regulation of the DDK activity on origins might be controlled (Francis et al., 2009).

1.2.3.2. Meiosis

CDC7s role in meiotic DNA recombination still needs validation in higher eurkaryotes. Matos *et al* evaluated the role of Cdc7p in meiotic chromosome segregation in the yeast model system (Matos et al., 2008; YEAST). Matos *et al* demonstrated that Cdc7p activity connects the pre-meiotic S phase, homologous recombination and monopolar attachment (Matos et al., 2008; YEAST). Its major role lies at the initiation of recombination where it promotes double strand

breaks and recruitment of an essential complex, monopolin for homologous seggregation to the kinetochore, the site of attachment of microtubules to centromeric DNA. Monopolin is localised to the kinetochore with the help of Cdc5p (PLK1), a pololike kinase, a familiar DDK partner. Thus, in lower eukaryotes, Cdc7p both initiates DNA replication and allows meiotic cells to undergo reductional homologous chromosomal segregation in the first division of meiosis, Meiosis I (Matos et al., 2008; YEAST).

1.2.3.3. Replication Stress

It is clear that tumour cells upregulate CDC7 in response to replication stress. Inhibition of CDC7 in cells undergoing such stress demonstrates synergistic killing with hydroxyurea and etoposide DNA targetting drugs (Tenca et al., 2007). CDC7 seems to have an active role in the repair pathway, ATR-CHK1, via its involvement with CLSPN at checkpoint induction (Kim et al., 2008, Rainey et al., 2014). The tumour suppressor TP53 is a key target of the DNA damage checkpoint in mammalian cells and transcriptionally activates key proteins involved in cell cycle arrest and apoptosis (Levine, 1997).

Depletion of CDC7 also suggests a TP53-dependent replication checkpoint in cancer cells. Some cells that are depleted of CDC7 are susceptible to DNA damage during replication and require TP53 to maintain cell viability and avoid apoptosis (Tenca et al., 2007, Montagnoli et al., 2004). Bonte *et al*'s work also supports a link between TP53 and CDC7 expression in maintaining cell viability in stressed cells. There, Bonte *et al* demonstrated a correlation between TP53 loss and increased CDC7-DBF4 expression (Bonte et al., 2008). These studies suggest functional interplay between the DDK and TP53 in maintaining cancer cell viability in the presence of genome stress. The discovery in yeast that mutations within Dbf4p N region confer sensitivity to DNA damaging agents and eliminate Rad53-dependent (CHK2 homolog) checkpoint phosphorylation on Dbf4p, raise the possibility that the Dbf4 N-terminus may regulate cellular responses to DNA damage. The well-established role for CHK2 involvement in human cancers and identification of somatic mutations of CHK2 in human breast cancer patients suggests this research could have important

implications for our understanding of cell biology and human disease (Allinen et al., 2001, Ingvarsson et al., 2002).

1.2.4. Targeting CDC7

CDC7 depletion by small interfering RNA causes numerous tumour cell lines to enter apoptosis in a TP53-independent manner, while simply arresting cell cycle progression in normal untransformed cells (Montagnoli et al., 2004). Furthermore, CDC7 depletion, in contrast to replication fork blockade, does not cause a sustained activation of the DDR, which is a common feature of resistance to chemotherapeutics that target replication elongation (Montagnoli et al., 2004). These characteristics led to the development of small molecule Cdc7 inhibitors.

1.2.4.1. Prototype Compounds

PHA-767491 is the prototype CDC7 inhibitor and has been characterised and shown to have activity in many preclinical cancer models (Montagnoli et al., 2008). As well as inhibiting CDC7, this compound also potently inhibits CDK9 (Montagnoli et al., 2008). This cross reactivity can be considered beneficial in the treatment of a number of haematological cancers. CDK9 will be discussed in detail below but, in essence, it phosphorylates RNA polymerase II (RNA pol II) and effects the rate of transcription, thus inhibition leads to depletion in the pool of proteins with short half-lives (Hampsey and Reinberg, 1999, Sharma et al., 2006). Among these proteins, the anti-apoptotic protein BCL2 family member, MCL1, has a critical survival role in most malignant B-cells (Gojo et al., 2002, Sharma et al., 2006, Derenne et al., 2002, Beroukhim et al., 2010). CDC7s fundamental role in initiation of replication has enticed several international groups and also Pharma to develop different small molecule inhibitors to CDC7, launching a new novel drug class. As CDC7 phosphorylation occurs at specific sites on MCM2, this provides a specific marker for pharmacodynamic assessment, a novel nuance of pharmacogenomics (Montagnoli et al., 2006). Traditional DNA targeting drugs lead to *ds*DNA breaks, creating a stalled pool of *ss*DNA, a known player in most DNA repair processes (Dimitrova and Gilbert, 2000). The consequence is activation of the checkpoint repair pathways – ATM/ATR , CHK1/2, DNA-PK (Zhou and Elledge, 2000).

Apoptosis induced by CDC7 inhibition is independent of TP53 status in tumour cell lines, whereas non transformed human dermal fibroblasts escape apoptosis by means of TP53 activation (Montagnoli et al., 2004). This was confimed in a different manner where CDC7 silencing induced apoptosis independent of TP53 status (Bonte et al., 2008). Further confirmation is illustrated by the plenary studies on mice, where CDC7 conditional silencing allowed the design of a mouse cross with complementary TP53 silencing. This complementary silencing of CDC7 and TP53 rescued the lethality of the CDC7 depletion alone, illustrating apoptosis in these 'normal' cells is mediated in a TP53 dependent manner which is different to the manner executed in neoplastic cells (Kim et al., 2002).

1.2.4.2. CDC7 Prototype Inhibitor - PHA-767491

Montagnoli *et al* describe the cellular and *in vivo* effects of the prototype CDC7 inhibitor, PHA-767491 (Montagnoli et al., 2008). Its initial characterisation studies described it as a dual CDC7/CDK9 inhibitor. This prototype compound is the only compound to date which unambiguously demonstrates inhibition of origin firing. This was examined through the use of the technique of DNA combing (Herrick and Bensimon, 1999, Herrick et al., 2002). Here, labelled DNA is extracted and its fibres uniformly stretched across glass slides. Specific labelling allows for subsequent calculation of the average inter-origin distance, speed of fork replication, ultimately illustrating inhibition of origin firing. Cell proliferation was largely inhibited in a panel of 61 human cell lines and had anti-tumour activity in leukaemic, colonic, ovarian and breast xenograft cancer models. These findings fuelled the rapid development of rival compounds. NMS-354 is a daughter of PHA-767491 which is available orally and has a more satisfactory pharmacodynamical profile than its parent prototype compound. It has similar widespread anti-neoplastic activity.

XL-413 is the next most developed compound. It lacks peer reviewed publication of its data but its lauching poster at the EORTC-NCI-AACR joint symposium illustrates similar cellular and xenograft anti-neoplastic activity (Robertson, 2008). Initial characterisation studies show cross activity against the PIM1 kinase. In preliminary data, described in this poster, XL-413 attenuates induc-

tion of DDR signalling in response to etoposide. Hughes *et al* demonstrated that XL-413 is a more selective kinase inhibitor than PHA-767491 when assessed in across a panel of 77 human kinases (Hughes et al., 2012).

The rationale behind decisions to develop the remaining compounds for clinical use remains somewhat unclear (Shafer et al., 2008, Zhao et al., 2008). The Memorial Sloan Kettering compound CKI-7 again lacks peer review literature but its launching poster at the Modern Drug Discovery and Development Summit, along with a further appearance at the American Society of Haematology Annual Meeting, describes a naturally occurring compound, independent of ATP binding. This is quite exciting but again requires validation. The fact that it shows good preclinical activity in both cellular and xenograft models of leukaemia in a nanomolar range may serve to support its independence of ATP binding.

1.2.5. CDC7 Potential Role as a Biomarker of Proliferation

Markers of proliferation have been readily used for prognostically stratifying various cancer states defining several proliferation indices (Stoeber et al., 2001). The markers used depend on the technique and tissues used. Immunohistochemically, two nuclear antigens, Ki67 (MK167/MIB index) and Proliferating Cell Nuclear Antigen (PCNA) have assumed roles as cell proliferation biomarkers (Holt et al., 1997, Neoptolemos et al., 1995, Gimotty et al., 2005, Gimotty et al., 2004). Increased expression of CDC7, its regulators and its functional effects on the licensing replicative machinery all support their roles as potential biomarkers. The MCM proteins have been most investigated in this area (Stoeber et al., 2001, Musahl et al., 1998, Madine et al., 2000, Gonzalez et al., 2005). Table 1.4 summarises previous studies.

Table 1.4

Biomarker	Evaluation	Reference
MCM2-7		Semple et al, Gonzalez et al,
	Breast	Reena et al.
	Bowel	Nishihara et al, Tokuyasu et al, Guzinska et al, Burger et al, Huang et al.
	Cervical	Siddiqui et al, Beccati et al, Shi et al, Shroyer et al.
	Ovarian	Kulkarni et al, Gakiopoulou et al.
	Bladder	Burger et al.
	CLL	Obermann et al.
	NHL	Obermann et al.
	Lung	Yang et al, Hashimoto et al.
	Head & Neck	Chatrath et al, Szelacowska et al.
	Thryoid	Cho Mar et al.
	Prostate	Ananthanarayanan et al.
	Kidney	Dudderidge et al.
Cdt1		Semple et al, Gonzalez et al.
Cdc6		Semple et al, Gonzalez et al.
	Cervical	Murphy et al.
	Brain	Ohta et al.

Table 1.4. Replication proteins used as biomarkers. Table includes replication protien and tissue evaluated in with accompanying reference.

In addition, immunohistochemical staining on primary tumours have illustrated direct detection of CDC7 and its regulator DBF4 relative to normal tissue counterparts (Bonte et al., 2008). Equally, antibodies to MCM2 phosphorylation site ser40/41, specific to CDC7 activity can be adapted for use in multiple techniques as a surrogate of CDC7 activity (Montagnoli et al., 2008).

The question of proliferation in myeloma is something of a paradox, and unraveling its complexity presents challenges. Although, comparatively speaking myeloma is not proliferative, the relative increase in proliferation is the most important and critical prognostic risk factor known to date. To this end CDC7, and in particular its regulators and specific target, are examined in myeloma datasets in this thesis. In addition, as CDC7 phosphorylation is a more specific measurement of active replication, present during S, G2, and M but absent in G0 and G1. Its role as a measure of proliferation in myeloma is assessed in this thesis in a cohort of myeloma patients comparing PCLI, gPI and MIB index.

1.3. CDK9

Grana *et al* first identified CDK9 in a cDNA screen intended to isolate new members of the CDK1 family (Grana et al., 1994). It was named PITARLE based on the characteristic Pro-Ile-Thr-Ala-Leu-Arg-Glu motif. Unlike other CDC2 family members, it was unable to phosphorylate histone H1 but retained a 'retinoblastoma protein kinase'-like phenotype. CDK9 and its regulatory partner cyclin T1 (CCNT1) were previously termed the Positive Transcription Elongation Factor b (P-TEFb). Its interaction with CCNT1 was first noted in *Drosphilia* and the HIV transcription apparatus (Peng et al., 1998, Wei et al., 1998). CDK9 is the catalytic subunit in P-TEFb, while CDK9/CCNT1 is the dominant P-TEFb complex in most cell types. However, other forms of P-TEFb have been reported to be involved in the regulation of transcription in specialised physiological events (Giacinti et al., 2006, Giacinti et al., 2008).

CDK9 and CCNT1 are constitutively expressed throughout the cell cycle, maintaining a constant kinase activity (Garriga et al., 1996, Grana et al., 1994). Once the p-TEFb complex with its cyclin partner CycT1 (CCNT1) was isolated from *Drosphillia* its function became clearer (Peng et al., 1998, Wei et al., 1998;DROME). In *Drosphillia*, Marshall *et al* successfully purified P-TEFb and noted its role in transcription elongation rather than initiation. In addition, loss of the CTD abolished transcription or productive elongation (Marshall and Price, 1995, Marshall et al., 1996;DROME). The same laboratory went on to describe the individual CDK9 isoforms, CDK9 [(42kDa); CDK9(42)] and CDK9 [(55kDa);CDK9(55)], that differ in 117 residues at the N-terminus (Shore et al., 2003). CDK9(42) is localised in the nucleoplasm whereas CDK9(55) is found in the nucleolus (Liu and Herrmann, 2005).

An interesting switch occurs in monocyte differentiation. CDK9(55) increases in preference to CDK9(42). The opposite is seen in lymphocytes with a gradual loss of CDK9(55) and increase in CDK9(42) with lymphocyte activation (Liu and Herrmann, 2005). Plasma cells with a post-germinal cell origin would expect to have a predominance of CDK9(42). There is still little known about

the functional differences of CDK9(55) and CDK9(42) but their relative abundance, differential localisation would suggest differential roles. Liu *et al* have demonstrated that CDK9(55) binds to Ku70 indicating a possible role in repair of DSB (Liu et al., 2010). In this work shRNA depletion of CDK9 (55) protein induces increased DSBs and eventual apoptosis (Liu et al., 2010). Conversely, overexpression of a CDK9(55) variant that is resistant to shRNA knockdown rescued the phenotype. CDK9 also interacts with other cyclins, cyclin T2a, cyclin T2b and cyclin K (Fu et al., 1999, Peng et al., 1998). For simplicity, unless otherwise stated 'CDK9' will imply CDK9/CCNT1.

The carboxy-terminal domain (CTD) is unique to RNA Pol II. The CTD consists of multiple repeats of the heptapeptide sequence YSPTSPS. The number of this repeat, $[YSPTSPS]_n$, varies among species, the largest repeat seen in humans: yeast - $[YSPTSPS]_{26}$, *C. elegans* - $[YSPTSPS]_{32}$, *Drosophila* - $[YSPTSPS]_{45}$, and humans $[YSPTSPS]_{52}$. The number of repeats is important for RNA Pol II function, but so is the phosphorylation at Ser-2 and Ser-5 within the Y**S**PT**S**PS heptapeptide repeat. A loss of function substitution of Ser-2 or Ser-5 within the Y**S**PT**S**PS heptapeptide repeat is uniformly lethal (West and Corden, 1995).

Christmann *et al* demonstrated that the CTD is only phosphorylated with transcription elongation not at initiation (Laybourn and Dahmus, 1989, Christmann and Dahmus, 1981). It is now established that the CDK7 acts at Ser5 whereas CDK9 acts at Ser2 occurring at transcription initiation and elongation respectively. CDK7 phosphorylation at Ser5 of RNA pol II primes RNA pol II for elongation, but its progression is inhibited by two negative elongation factors, *i.e.* 5,6-dichloro-1-b-D-ribofuranosylbenzimidazole sensitivity-inducing factor (DSIF) and negative elongation factor (NELF). This negative regulation facilitates proper capping of pre-mRNA. CDK9 phosphorylates the Spt5 subunit of DSIF (Ivanov et al., 2000) and the RD subunit of NELF (Fujinaga et al., 2004) removing the negative elongation block. In addition, CDK9 phosphorylates RNA Pol II CTD at Ser-2 allowing transcriptional elongation to proceed from abortive to productive elongation. Bai *et al* arrived at similar findings with the *tif1-/- moonshine* mutant where elongation was res-

cued with loss of function of DSIF (Bai et al., 2013). Guenther *et al* performed a genome wide screen and found that most genes thought to be transcriptionally inactive are in fact halted post-initiation and pre-elongation. It is interesting to note that these genes encoding 'stemness' are halted at pre-elongation and thus require CDK9 for differentiation (Guenther et al., 2007).

1.3.1. Regulation of CDK9

Like other CDKs, CDK9 is regulated by CDKis with an individual twist. A small nuclear RNA, 7SK sn-RNA, discovered in 1976, is an important regulator of CDK9 (He et al., 2008, Jeronimo et al., 2007, Krueger et al., 2008, Peterlin and Price, 2006, Zhou and Yik, 2006). It is transcribed by RNA Pol III (Egloff et al., 2006, Murphy et al., 1987, Peterlin and Price, 2006, Zieve et al., 1977). 7SK snRNP sequesters CDK9 away from the DNA template preventing transcription (Nguyen et al., 2001, Yang et al., 2001). Interestingly, in a reconstituted system 7SK is necessary, but not sufficient, to inhibit the kinase activity of CDK9 (Chen et al., 2004), indicating that other factor(s) may be involved in the inhibition of CDK9.

HEXIM1 is one potential factor discovered through affinity purification of the inactive CDK9 complex. HEXIM1 is a nuclear protein originally identified as a hexamethylene bisacetamide (HMBA)-inducible protein in human vascular smooth muscle cells (Ouchida et al., 2003). HMBA is a hybrid bipolar compound used to induce cell differentiation (Marks et al., 1994). HEXIM1 requires 7SK to inhibit CDK9 as shown in in vitro kinase assays (Michels et al., 2003, Yik et al., 2003). In addition to HEXIM1, its homolog HEXIM2, and two other proteins, PIP7S/LARP7 and BCDIN3, are now known to stabilise 7SK snRNP. Jeronimo *et al* demonstrated all predicted and actual interactors with the CDK9 complex (Jeronimo et al., 2007).

It is still uncertain how CDK9 is recruited to RNA pol II-dependent transcribed genes. Moreover, the roles of individual transcription factors such as CIITA (Kanazawa et al., 2000), NFKB1 (Barboric et al., 2001), MYC (Eberhardy and Farnham, 2001), STAT3 (Giraud et al., 2004), the androgen receptor (Lee et al., 2001a), and the aryl hydrocarbon receptor (Tian et al., 2003) in recruiting

CDK9 to their respective promoter targets seem to lend credence to the argument that gene-specific recruitment is involved. However, this contention does not fit with the work discussed earlier, which supports CDK9 as important in global RNA pol II transcription (Chao and Price, 2001, Shim et al., 2002). The bromodomain protein, BRD4, is a potential candidate that recruits CDK9 to different promoters. Jang *et al* demonstrated an interaction of the BRD4 bromodomain with the major portion of active CDK9 by affinity purification of BRD4-associated proteins (Jang et al., 2005). BRD4 is a ubiquitously expressed nuclear protein that belongs to the conserved BET protein family (Shang et al., 2004), whose members contain two tandem bromodomains and a single extra terminal domain (Jeanmougin et al., 1997). NMR spectroscopy revealed the ability of bromodomains to bind acetylated histones and thus potentially modulating chromatin (Zeng and Zhou, 2002). Indeed, Dey *et al* illustrated the ability of MCAP, BRD4's murine homolog, to bind to euchromatin during the G2/M transition (Dey et al., 2000), possibly suggesting a role in epigenetic memory (Dey et al., 2000, Nishiyama et al., 2006). Moreover, Dey *et al* demonstrated by photobleaching that BRD4 binds in a dynamic fashion to histone H3 and H4 depending on the acetylation signature (Dey et al., 2000, Dey 2003). Jang *et al* categorically demonstrated that BRD4 recruits uninhibited CDK9 to RNA pol II and, thus, increases or decreases transcription depending on the level of BRD4 present (Jang et al., 2005, Yang et al., 2005).

1.3.2. CDK9 Function

Historically, studies relating to the role of CDK9 in transcription have generally focused on isolated single genes (MYC, HSP90 etc.), but CDK9 is believed to be a general transcription elongation factor. This is supported by the work of Chao *et al* whereby flavopiridol, a pan-CDK inhibitor, was shown to inhibit phosphorylation of RNA Pol II CTD at Ser 2, but, more importantly, when using a nuclear run-on assay a widespread block of RNA pol II transcription was demonstrated (Chao and Price, 2001). Consistent with this result, CDK9 knockdown in *C. elegans* embryos demonstrated loss of phosphorylation of Ser2 of RNA Pol II CTD and expression of early embryonic genes (Shim et al., 2002). However, CDK9 is not involved in transcription of class II genes which include intron-

less histone H2B, U2 snRNA and GAPDH genes (He et al., 2006, Medlin et al., 2005).

1.3.2.1. mRNA processing

Co-transcriptional events are defined by processes occurring simultaneously with transcription or, indeed, prior to termination of transcription (Neugebauer, 2002). There is a broad body of literature supporting such occurrences, spanning examinations of processes involved in mRNA maturation such as capping (Schott and Hoyt, 1998 1998), base deamination, splicing (Tennyson 1995), polyadenylation (Fong and Bentley, 2001) and even degradation. Most of these co-transcriptional events happen during transcription elongation and require hyperphosphorylation of the heptapeptide of RNA pol II at Ser2 and Ser5.

1.3.2.2. Cell growth and differentiation

The balance of 7SK snRNP/HEXIM1 or BRD4 bound CDK9 complex depends on the cell type and physiological conditions but equally upon the need for cellular growth and differentiation. In HeLa cells under normal growth conditions, about half of nuclear CDK9 is sequestered into the 7SK snRNP, whereas the other half binds to BRD4 (Zhou and Yik, 2006). The 7SK snRNP pool can be called upon in times of stress in a global response to increased transcriptional needs (Nguyen et al., 2001b, Yang et al., 2001). Treatment with actinomycin D, (5,6-dichIor-1-b-D-ribofuranosylbenzimidazole) DRB, uv and staurosporine leads to increased BRD4-CDK9 complex formation with reduction in the HEXIM1/7SK snRNP-CDK9 pool (Michels et al., 2004, Michels et al., 2003, Nguyen et al., 2001b, Yang et al., 2005, Yik et al., 2003). In cellular differentiation the equilibrium shift is in preference to the 7SK snRNP pool (He et al., 2006). Interestingly, the relative level of 7SK snRNP pool to the BRD4 pool correlates with the degree of differentiation or growth of the cell in question (He et al., 2006).

The role of AKT1 in releasing active CDK9 from HEIXM1/7SK snRNP was demonstrated in viral transcription and differentiation. AKT1 phosphorylates HEIXM1 at Thr270 and Ser278 allowing CDK9 to activatate RNA pol II at Ser2 (Chen et al., 2008). In addition, the sequential action of

PP2B (protein phosphatase 2B) and PP1A (protein phosphatase la) with Ca^{2+} release facilitates CDK9 release with dephosphorylation of CDK9 phospho-Thr186 located in its T-loop (Contreras et al., 2007).

1.3.3. Targeting CDK9

There are a number of pan-kinase inhibitors that also target CDK9. Flavopiridol is one such pan-kinase inhibitors that has already been studied in myeloma (Gojo et al., 2002, Dispenzieri et al., 2006).

CDKI-71 is a CDK9 inhibitor but, similar to other emerging compounds, it is not fully selective and has potential effects on CDK2. Liu *et al* have demonstrated efficacy in large range of cell lines including solid malignancies, CLL primary cells but also lung embryonic fibroblasts. No animal work was completed in this study (Liu et al., 2012).

EXEL-8647 and EXEL-3700 are two compounds under development with Exelixis. EXEL-3700 has underwent animal work with the MDA-MD-231T xenograft model demonstrating exciting potential (Heuer, 2008).

In myeloma, the BET domain inhibitor, JQ1, showed promise in targeting MYC mediated transcription. It is interesting to note that JQ1 is largely a BRD4 inhibitor and thus directly effects RNA pol II dependent transcription due to lack of active CDK9 complex recruitment (Bai et al., 2013, Delmore et al., 2011). Chaidos *et al* demonstrated pre-clinical efficacy of I-BET151 and I-BET762. I-BET151 induces transcriptional repression of MYC and MYC-dependent networks by blocking recruitment of p-TEFB to chromatin (Chaidos et al., 2014). This block was dependent on BRD2-4. Interestingly, HEXIMI upregulation was BRD2-4 independent (Chaidos et al., 2014).

1.4. Aims

DNA replication and transcription are two highly regulated processes essential for life. It is not surprising that both systems can be manipulated by cancer for its own gain. In myeloma, the relative increase in proliferation predicts an inferior overall survival across all myeloma groups. The fact that a measure of proliferation is not uniformly part of any prognostic score is puzzling. This thesis addresses these two aspects of myeloma, seeking to fulfil the following three main aims.

The first aim of this thesis is to examine whether the DDK, CDC7, can be used as a measure of proliferation in myeloma.

The second aim of this thesis is to establish pathways associated with proliferation in order to inform the selection of potential treatments in myeloma, based on *in silico* connectivity mapping.

The third aim of this thesis is to establish whether CDC7/CDK9 inhibition is a potential mechanism for the treatment of myeloma.

To achieve these aims, the thesis examines four key questions:

1) Does CDC7 expression or expression of its regulators DBF4 or DBF4B predict an inferior event free survival (EFS) and overall survival (OS) independent of other conventional prognostic scores?

2) Can a surrogate of CDC7/DBF4 expression, pMCM2, be used in stratifying myeloma with high proliferation and poor overall prognosis and survival?

3) Can genes associated with proliferation in myeloma across TC groups be used to predict known drugs that may target these pathways, by means of connectivity mapping?

4) Can CDC7/CDK9 inhibition be positively validated across myeloma pre-clinical myeloma models?

CHAPTER 2: MATERIAL AND METHODS.

2.1. Tissue culture techniques.

2.1.1. Cell Culture

Myeloma cell lines KMS-18, OCI-My5, and U266, were kindly provided by Dr Marta Chesi, Prof P. Leif Bergsagel and Dr Keith Stewart (Mayo Clinic Arizona). RPMI-8226-LR5 (Melphalan resistant) and RPMI-8226-Dox 40 (Doxorubicin resistant) were kindly provided by Prof William Dalton (Moffitt Cancer Center). Dexamethasone-sensitive (MM.1S) and Dexamethasone – resistant (MM.1R) were kindly provided by Dr Steven Rosen (Northwestern University). All lines were cultured in RPMI 1640 media (Sigma-Aldrich) supplemented with 10% fetal bovine serum[(FBS);Sigma-Aldrich], 2 mM L-glutamine (Sigma-Aldrich), 50 U/ml penicillin(Sigma-Aldrich), and 50 μg/ml streptomycin (Sigma-Aldrich). Drug-resistant cell lines were cultured with doxorubicin, melphalan or dexamethasone to confirm their lack of drug sensitivity.

All cell lines were maintained in a state of logarithmic growth at 37°C in humidified air with 5% CO_2.

2.1.2. Ethical issues

Myeloma patient samples were obtained with informed consent. This was carried out with local governing Ethics Committee approval (National University of Ireland, Galway and Johns Hopkins Medical Institutes' Institutional Review Board) in accordance with the Declaration of Helsinki.

2.1.3. Microenvironment Models

2.1.3.1. Models

Three models were utilised. Single individual addition of known stimulation factors (IL-6 and IGF-1), stromal co-culture and conditioned media were employed. Stromal co-culture experiments utilised the HS-5 human stromal cell line developed from human bone marrow (American Type Culture Collection [ATCC]).

HS-5 was transduced with second generation lentivirus containing a pGIPZ construct expressing

green fluorescent protein [(GFP) Openbiosystems]. This allowed HS-5 cells to be identified easily. Purity was assessed using flow cytometric analysis for percentage anti-CD138 positivity.

Conditioned media was obtained from 48 hour old media of 80% confluent (pre-confluent) HS-5 cells. The MM1S, myeloma cell line was used for these experiments. This allowed a sensitive (bortezomib) and resistant (dexamethasone) control to be used thoughout these experiments, being based on previously published work (Bisping et al., 2009).

2.1.3.2. Starvation

Cells were plated as normal, incubated for 24 hours before being removed from culture media, washed with, and then cultured in, serum-free RPMI media (2 mM L-glutamine, 50 U/ml penicillin and 50 μg/ml streptomycin) for 24 hours.

2.1.3.3. Stimulation

Cells were stimulated by the addition of IL-6 (10 ng/ml) and IGF-1 (50 ng/ml). Stromal stimulation was achieved by incubating myeloma cells with HS-5 GFP cells, allowing direct contact for seven hours, before removal and replating prior to drug treatment. Conditioned media was supplemented at 20% v/v RPMI media. Viability was read at 12 – 24 hours post-stimulation as below.

2.1.4. Cell Viability

2.1.4.1. Cell TitreGlo

Cells were seeded in triplicate at a density of 5,000 and 10,000 cells in 100 μl in 96 well plates, treated with the relevant single or combination drug(s) and analysed 48 - 72 hours post-treatment with a cell viability assay: Cell TitreGlo (Promega). This assay is a luciferase based luminescence assay which quantifies the amount of ATP in cells which is directly proportionate to the amount of viable cells present.

2.1.4.2. Colony Forming Assay - Clonogenicity

Clonogenic growth was assessed by plating 1000 cells/ml for cell lines in 1 ml 1.2% methylcellulose, 30% BSA, 10^{-4} M 2-mercaptoethanol and 2 mM L-glutamine. Primary cells were plated at 100,000 cells/ml in Methocult® (H4230 Methylcellulose Medium; Stem Cell Technologies) containing 10% lymphocyte conditioned media. Samples were plated in duplicate for cell lines and quadruplicate for primary cells onto 35mm^2 tissue culture dishes. Colonies for more than 40 cells were scored at seven days for cell lines and 14 – 21 days for myeloma colonies from clinical samples. Self-renewal was assessed through serial replating. This was accomplished by washing plates three times with culture media and re-suspending cells in the original volume of methylcellulose as described above.

2.1.5. Plasma Cell Labeling Index

The Plasma Cell Labeling Index (PCLI) was performed by incubating bone marrow plasma cells with 10 µM BrdU for 1 hour. Cells were fixed with BD CytoFix buffer and permeabilised with BD Cytoperm buffer as per insert guidelines (BD Pharmingen). Plasma cells were identified by intracytoplasmic immunofluorescence using anti-k or anti-l light-chain antibodies bound to fluorscein. The percentage of myeloma cells in S-phase was determined using an anti-bromodeoxyuridine monoclonal antibody (BU-1) and a rhodamine-labelled goat anti-mouse antibody employing a double fluorescent technique (BD Pharmingen). The percentage was translated into a low, intermediate, high and very high PCLI as follows:

0= 0.0-0.2% – low

1= 0.3-0.99% – intermediate

2= 1.0 – 3.0% – high

3= >3.0% – very high

This test was developed and its performance characteristics determined by Laboratory Medicine and Pathology, Mayo Clinic, Rochester MN, USA. It has not been cleared or approved by the US FDA.

2.1.6. Cell Purification

Bone marrow mononuclear cells were separated using Ficoll-Hipaque density sedimentation, and plasma cells were purified (>95%, CD138+) by positive selection with anti-CD138 MACS Micro-beads (Miltenyl). For stem cell studies, the CD138- subset was further depleted of normal haematopoietic progenitors using CD34 antibodies (Miltenyi Biotec).

2.1.7. Analyses

2.1.7.1. IC50 Calcuation

IC_{50} (Median effect [D_m]) was calculated both with the Chou-Talalay based median-effect equation and a non-linear regression four parametric logistic graph-fitting approach (slope, IC_{50}, upper and lower value normalisation) using Compusyn (Compusyn Inc)(Chou, 2008) and GraphPad Prism (GraphPad Software Inc) respectively.

2.1.7.2. Combination Indices Calculation

The combination between PHA-767491 and other anti-myeloma agents (doxorubicin, melphalan, and bortezomib) was analysed with Compusyn software (Compusyn Inc). The combination between PHA-767491 and SB202190 and SB203580 was also analysed with Compusyn software (Compusyn Inc). Data from cell viability assays were expressed as a fraction of cells affected by the dose (Fa) in the drug-treated cells compared with untreated cells (control). This program is based on the Chou-Talalay method according to the following equation: $CIn = (D)_1/(Dx)_1 + (D)_1(D)_2/(Dx)_1(Dx)_2$ where $(D)_1$ and $(D)_2$ are the doses of drug 1 and drug 2 that have the same

x effect when used alone and CIn, is the combination index. CIn < 1.0 indicates synergism: CIn = 1 indicates an additive effect and CIn > 1.0 corresponds to an antagonistic effect (Chou, 2008). Myeloma cells were treated for 48 hours with combinations of PHA-767491 and other drugs at either a constant ratio or non-constant ratio combination design, and cell viability assays were completed as described above.

2.2. Molecular Cell Biology.

2.2.1. Chemicals

PHA-767491 (10 mM; Nerviano Medical Sciences (Montagnoli et al., 2008)), NMS-354 (10 mM; Nerviano Medical Sciences), SB202190 (10 mM; Sigma-Aldrich) and SB203580 (10 mM; Sigma-Aldrich) were dissolved in dimethyl sulfoxide [(DMSO); Sigma-Aldrich] and stored at -20^{o}C, then thawed and diluted in media for cell culture experiments. Bortezomib (500 μM; OrthoBiotech) was dissolved in dH20 stored and used in the same way. Doxorubicin (10 mM;Sigma-Aldrich), Melphalan (3.3 mM; Sigma-Aldrich) and Dexamethasone (500 μM; Sigma-Aldrich) were prepared as previously described. For animal work a suspension of NMS-354 was made freshly in 0.5% carboxymethylcelullose [(CMC); Sigma-Aldrich], every day at the desired concentration, usually 20 mg/kg.

Recombinant human insulin-like growth factor-1 (IGF-1; 100 μg/ml;R&D) and interleukin-6 (IL-6; 10 μg/ml;R&D) were diluted in dH_20 [0.1% w/v bovine serum albumin (BSA)]

2.2.2. Antibodies

Antibodies against MCL1, total caspase 3, cleaved caspase-3 (Asp175), PARP, caspase 8, caspase 9, pAKT1(Thr308), p38, pp38(Thr180/Tyr182), pMK2(Thr334) and AKT1 were purchased from Cell Signalling. Antibodies against MCM2 were raised against the N terminus of human MCM2 protein in collaboration with Pocono Rabbit Farm and Laboratory Inc. (Canadensis, PA, US). CDC7 dependent phosphorylation of MCM2 at ser40 was detected using pMCM2ser40/41 as previously

described (Montagnoli et al., 2006). Antibodies against RNA pol II and pSer2 RNA pol II were purchased from Covance Research Products.

2.2.3. Immunoblotting

For mechanistic studies 5 x 10^6 myeloma cells were cultured with 5 μM PHA-767491 and harvested at one, three, six, nine, and twelve hours. Washed cells were lysed using lysis buffer - 1% sodium dodecyl sulfate (SDS) or TGN buffer [Tris (pH 8.0), 150 mmol/l NaCl, 1.0% Tween 20, 10% glycerol, 1 mmol/l phenylmethylsulfonyl fluoride (PMSF), 5 μg/ml aprotinin, 5 μg/ml leupeptin, 75 mmol/l NaF, 20 mmol/l ß-glycerolphosphate, 0.4 mmol/l sodium vanadate, and 1 mmol/l DTT]. Cell lysates were subjected to SDS-polyacrylamide gel electrophoresis (SDS-PAGE), transferred to acrylamide membrane and immunoblotted with relevant antibodies.

2.2.4. Gene Expression Analysis

2.2.4.1. RNA isolation

RNA was isolated with RNeasy kit (Qiagen) according to the manufacter's guidelines. Prior to extraction, pellets were stored at -80°C. Briefly, the cell pellet was lysed and subsequently homogenised with shredding spin column (QiaShredder, Qiagen), membranes were bound to columns, washed and finally, RNA was eluted with Rnase free H_20. Concentrations were quantified using the nanodrop (Nanodrop 2000C, ThermoScientific), recording concentration, 260/280 ratio for quality analysis and 260/230 ratio for contamination. Having both ratios approaching 2 indicate good quality RNA extraction with no overt contamination.

2.2.4.2. cDNA

cDNA was synthesised using SuperScript (Invitrogen) according to the manufacturer's guidelines. Reverse transcriptions were performed using either random nonamer primers for read-through analysis and oligod(T_{23})VN (New England Biolab) for polyadenylation analysis. Oligod(T_{23})VN is termed an achored oligo-dT primer which forces the primer to anneal to the start of the polyA

tail, thereby preventing priming at internal sites in the polyA tail (Nam et al., 2002).

One microgram of total RNA was mixed with 2 µl random nonamer (15 µM, Sigma-Aldrich) or oligo-dT (50 µM) primers (New England Biolab), 1 µl dNTPs (10 mM, Promega), and brought to a volume of 12 µl in RNAse-free water. Samples were heated at 65 °C for five minutes and placed on ice. A total volume of 5 µl containing 4 µl 5X first strand buffer, 2 µl 0.1 M DTT, 1 µl (40 U/ µ L) RNAse inhibitor (RNase OUT) (Invitrogen), and 1 µl (200 U) Superscript II reverse transcriptase (Invitrogen) was added to each sample and incubated at 42 °C for 50 minutes. Finally, the reverse transcriptase was inactivated by heating at 70 °C for 15 minutes.

2.2.4.3. qPCR

One µl of each cDNA sample was used for quantitative real-time PCR analysis in a final volume of 15 µl. Real-time PCR analysis was performed using the iQ SYBR Green Supermix (BioRad) with the primers listed in Table 2.1.

Table 2.1

Name	Sequence
36B4 F	GATTGGCTACCCAACTGTTG
36B4 R	CAGGGGCAGCAGCCACAAA
HIST1H2BD Total F	ACGATGCCTGAACCTACCAA
HIST1H2BD Total R	AGCCTTAGTCACCGCCTTCT
HIST1H2BD PolyA F	CCAACTCA TCCTGGTTTGCT
HIST1H2BD PolyA R	TCCCCTCGGTAACCTTCTTT

Table 2.1. RT-PCR Primers. Table summary of forward (F) and reverse (R) primers used.

SYBR Green, which unlike EtBr recognises only dsDNA, has very low fluorescence in the absence of dsDNA and very high fluorescence in the presence of double stranded DNA. A two-step protocol (10 min at 95 °C; followed by 40 cycles of: 95 °C for 15 seconds and 60 °C for 1 minute) followed by a melting curve analysis was used for each primer pair and performed on an I-Cycler

Real-Time PCR System (BioRad).

qPCR analysis was quantified using the D-DCt method. Fold change was calculated as $E^{D\text{-}DCt}$, where E stands for primary efficiency. Polyadenylated HIST1H2BD were analysed by oligo-dT primed reverse transcription followed by quantitative real-time PCR analysis using primers that lie in the first exon of the respective gene. All qPCRs were normalised to 36B4 prior to additional normalisation and statistical analyses. 36B4 is an mRNAs for RPLP0 (ribosomal protein, large, P0). This is also known as P0, L10E, RPPO, PRLP0, 60S acidic ribosomal protein P0, ribosomal protein L10, Arbp or acidic ribosomal phosphoprotein P0. It was used by Pirngruber *et al* in similar work deciphering the functional role of CDK9 and used to offset the interplay of RNA pol II, fulfilling a suitable standard control (Pirngruber et al., 2009a, Pirngruber et al., 2009b).

2.3. Flow Cytometry and Immunohistochemistry.

2.3.1. DNA content

1 x 10^6 myeloma cells at desired time points were fixed with ice-cold 70% v/v ethanol-PBS whilst the re-suspended pellet was vortexed continuously. Cells were fixed for 24 hours at +4^{o}C, subsequently washed with PBS, incubated for 15 minutes with 500 µl propidium iodide/RNAase Staining Buffer (BD Bioscience), and analysed using a FACSCanto flow cytometer (BD Bioscienes).

2.3.2. Annexin V staining

3.5 x 10^5 cells from selected time points were aliquoted for Annexin V staining. Cell pellets were re-suspended in 50 µl of Annexin V incubation buffer (10 mM HEPES/NaOH, pH 7.4, 140 mM NaCl, 2.5 mM $CaCl_2$) containing 6 µl of annexin V-fluorescein isothiocyanate (IQ Corp.) for 15 minutes on ice. The reaction was stopped by adding 300 µl of fresh incubation buffer, and the samples were analysed immediately using a FACSCanto flow cytometer (BD Biosciences). Results were ex-

pressed as percentage of Annexin V-positive cells.

2.3.3. Aldefluor staining

Aldefluor staining was completed according to manufacturer's guidelines (Stem Cell Technologies). Samples are divided in two, with and without diethylaminobenzaldehyde (DEAB). Samples were re-suspended in aldefluor buffer (25 μM Verapamil, 0.2% BSA, 2 mM EDTA in PBS), containing aldefluor reagent and incubated at 37°C for 30-60 minutes, vortexing every five minutes to ensure aldefluor reagent doesn't settle at the bottom. Samples were then pelleted and re-suspended in aldefluor buffer and analysed immediately using a FACSCanto or Aria (BD Biosciences) or further stained with a surface marker and incubated in the dark for the required incubation at +4°C. Percentage of stem cells (low side scatter and high FL1) are obtained by using the paired DEAB control to gate the required area.

2.3.4. Single Intracellular antibody staining

Cells were fixed with 100 μl of 2% paraformaldehyde (Sigma-Aldrich) for 30 minutes in the dark. This was washed with 1 ml PBS and re-suspended in 100 μl PBS. Cells can be stored at +4°C overnight. Once ready to analyse, cells were washed with 1% BSA/PBS. The cells were subsequently permeabilised with 1% BSA/0.5% Saponin. The relevant antibodies e.g. BAK1 and BAX and isotype controls were added (1 μg/sample) and incubated for one hour on ice. These were once again washed with 1 ml 1% BSA/PBS. If the antibodies were not conjugated to a flurophore, the cells were once again re-suspended in the permeabilisation buffer (1% BSA/0.5% saponin) and incubated with species-specific secondary fluorophore for 30 minutes in the dark at +4°C. They were then washed two further times in PBS and re-suspended in PBS prior to analysis with the FACS Canto flow cytometer (BD Biosciences).

2.3.5. Dual pSer40/41MCM2/ALDH staining

In this method, the cells were fixed with 70% methanol/PBS and stored overnight at -20°C. The samples were then pelleted and washed with the dual staining incubation buffer (1% FBS in PBS). The cells were permeabilised with 0.25% TritonX-100/PBS and blocked with 10% FBS/PBS. Primary antibodies were incubated at 1:50-1:100 for one to two hours, washed, and further incubated with relevant secondary antibodies (anti-mouse-Cy5 and anti-rabbit-AlexaFluor488, both 1:1000) for thirty minutes, washed twice and subsequently analysed by flow cytometry.

2.3.6. Immunohistochemistry

For this method, tissues were fixed in 10% buffered formalin for 24 hours at room temperature. Enough fixative was used to ensure that the tissues were fully covered - covering between 5-10 times the tissue volume. Tissues were then trimmed into appropriate size and shape and placed in embedding cassettes.

Paraffin embedding was performed by an automated machine (for a total of 16 hours) at the Mayo Clinic Immunohistochemisty Core employing the procedure that follows: 70% Ethanol, two changes, 1 hour each: 80% Ethanol, one change, 1 hour: 95% Ethanol, one change, 1 hour: 100% Ethanol, three changes, 1.5 hour each. This was followed by Xylene three changes, 1.5 hour each and finally embedded in paraffin wax (58-60 °C), two changes, 2 hours each, embedding tissues into paraffin blocks.

Paraffin blocks were trimmed as necessary and cut at 5 μm. The 5 μm paraffin ribbons are placed in water bath at about 40-45 ºC and subsequently mounted and baked onto the slides.

To confer specificity, all tissue specimens were dual stained with an antibody to the relevant protein of interest and additionally to the myeloma cell surface protein syndecan-1/CD138. This dual staining method involves the combination of the individual chromophores together on one slide

without the presence of a background contrast stain. The method used throughout the investigations carried out for the purposes of this thesis was the Heat Induced Epitope Retrieval method. Briefly, this involves deparaffinising slides with Citrosol (Thermo-Fisher), dehydrated with 100% ethanol and hydrated with tap water. The antigen was retrieved by boiling in a 1 mM EDTA solution over 15 minutes. Once cool, the first staining was started with the lightest of the chormophores, alkaline phosphatase (AP), and the least abundant antigen e.g. pMCM2/MK167(Ki67). Here, the slides were blocked first with Milk-TBS-T for 20 minutes and subsequently washed with H_20. The primary AP-conjugated antibody was incubated overnight with the most dilute workable concentration. Both the long incubation and dilute concentration confer increased specificity and, as a result, better images.

The following day the AP-secondary antibody IgG species-specific was incubated for 45 minutes after washing off the primary antibody. The chromogen was developed using the AP specific reaction buffer NBT-BCIP [10 μl stock (Roche) into 500 μl of Tris 0.1 M pH=9.5, NaCl 0.1 M, $MgCl_2$ 0.05 M]. This reaction can be quite slow and to increase the efficiency of the reaction, the incubation was carried out over a beaker of hot H_2O (the higher the temperature, the more efficient the reaction). The reaction was stopped by washing thoroughly in H_2O. To prepare for the second chromogen, the slides were brought to the boil in the same EDTA solution used originally for retrieving the antigen. The Biotin-HRP chromogen was used for the second antigen staining. Again, as with AP, the slides were blocked with a suitable blocking agent, in this case with avidin first, and biotin second (DAKO). After washing with TBS-T, the slides were incubated with the primary biotin-conjugated antibody overnight. The next day, the slides were washed and blocked with H_2O_2. After washing, the slides were incubated with a Biotin-secondary IgG and species-specific for 45 minutes, washed and further incubated with Avidin-HRP. This multi-layer approach intensifies the signal. After further washing, the slides were developed with the chromogen DAB. Once adequate colour was achieved, the reaction was halted by immersion in H_2O. The slides were glycerol-gelatin mounted.

All immunohistochemisty slides were analysed using an Olympus BX41 microscope. Q-Color3 camera and its software Q-capture (Olympus) were used for picture acquisition and analysis.

2.4. Bioinformatics.

2.4.1. Gene Expression Profiling

2.4.1.1. Human Genomic Data Sets

There are a number of different GEP data sets relating to the field of myeloma, which are publically available. These are summarised in Table 2.2.

Table 2.2

		HMCL	MMC	sMM	MGUS	BMPC
E-MTAB-81	U133 A+B	20	65	0	7	7
	U133 + 2.0	20	168	0	5	7
GSE2658	U133 + 2.0		345	0		
GSE6477	U133 A	44	101	0	22	15
GSE5900	U133 + 2.0	0	0	12	44	22

Table 2.2. Human Myeloma Gene Expression Profile Datasets. Tabular summary of datasets.

Their use, however, is limited by the public availablity of the clinical parameters relating to the individual data sets. These data sets are hosted at two major international respositories: NCBI Geo Datasets (GeoDatasets); and the EMBL European Bioinformatics Institute (EBI).

More recently, The Multiple Myeloma Genomics Portal (MMGP) was developed as a genomics portal relating singularly to the field of myeloma research (MMGP). The MMGP is part of the Multiple Myeloma Genomics Initiative, a collaboration of The Multiple Myeloma Research Consortium (MMRC), The Broad Institute of MIT and Harvard, and the Translational Genomics Re-

search Institute (TGen). Funding is provided for this initiative by the Multiple Myeloma Research Foundation (MMRF). The development of the portal and data curation is performed by the portal team of the Broad Institute and Dana Farber Cancer Center.

The MMGP provides access to and indeed, some limited analysis of, the MMGP portal data sets. These include the MMRC funded reference aCGH, gene expression, RNA-sequence (RNA-Seq) data and additional public multiple myeloma datasets. Its integral relationship with The Broad Institute at MIT/Harvard ensures that new data analysis tools, as they become available, are integrated with existing data at the MMGP.

The UAMS precedent dataset relating to patients undergoing TT2 and TT3 has two different entries in the NCBI Geo Datasets repository - GSE2658, and GSE24080. GSE24080 has clinical parameters attached to the source raw dataset without any additional MTA or legal contraints for future publication.

2.4.1.2. GSE24080/GSE2658 Dataset

This myeloma data set was contributed by the Myeloma Institute for Research and Therapy at the University of Arkansas for Medical Sciences (UAMS, Little Rock, AR, USA). Gene expression profiling of highly purified bone marrow plasma cells was performed in newly diagnosed patients with myeloma. The training set consisted of 340 cases enrolled on total therapy 2 (TT2) and the validation set comprised 214 patients enrolled in total therapy 3 (TT3). Plasma cells were enriched by anti-CD138 immunomagnetic bead selection of mononuclear cell fractions of bone marrow aspirates in a central laboratory. All samples applied to the microarray contained more than 85% plasma cells as determined by 2-color flow cytometry (CD38+ and CD45-/dim) performed after selection. The microarray platform utilised was the Affymetrix Human Genome U133 Plus 2.0 Array (HG-U133_Plus_2).

Dichotomised overall survival (OS) and event-free survival (EFS) were determined based on a two-year milestone cutoff. A gene expression model of high-risk myeloma was developed and validated by the data provider and later on validated in three additional independent data sets (Zhan et al., 2007, GSE24080, Zhan et al., 2006, Hanamura et al., 2006).

2.4.1.3. GSE26863[GSE26760 (GEP) and GSE26849 (aCGH)] Datasets

This myeloma dataset was contributed by the MMRC and comprises a reference collection for myeloma genomics (MMRC, Norwalk, CT, USA). It contains individual datasets for gene expression profiling [GSE26760 (GEP)], array comparative genomic hybridisation [GSE26849 (aCGH)] and RNA-Seq. The collection contains purified myeloma cells of newly diagnosed and relapsed patients with myeloma. The initial 100 GEP collected were known locally as the Mayo 100.

Again, plasma cells were enriched by anti-CD138 immunomagnetic bead selection of mononuclear cell fractions of bone marrow aspirates in a central laboratory (Mayo Clinic, Arizona).

The microarray platform utilised for GEP was the Affymetrix Human Genome U133 Plus 2.0 Array (HG-U133_Plus_2). The microarray platform used for aCGH was the Agilent-014693 Human Genome CGH Microarray 244A. Datasets and sequencing datasets are referenced here (GSE26863, GSE26849, GSE26760, Chapman et al., 2011).

2.4.1.4. General Design

The Broad Institute summarises the general algorithm of GEP using a functional genomics pipeline. This describes the following:

Experimental Design

-

Data acquisition

(microarray design)

-

Data pre-processing

(scaling/normalisation/filtering)

-

Data analysis/Hypothesis generation

-Supervised

-Unsupervised

-

Validation/Annotation

-EA – GO/GSEA

-*In silico* testing

--Cross validation/Train/Test

-*In vitro* testing

With this pipeline in mind each individual data set can be examined from raw .CEL or .CHP files and processed through the acquisition and preprocessing segments of the pipeline. In general, raw .CEL files are available from the NCBI –Geodatasets and EMBL-EBI repositories and require such processing. This processing will be covered in the next subsection.

2.4.1.5. Dataset Processing

All of the GEP-based data sets used in this thesis are from Affymetrix microarray platforms (HG-U133_Plus_2). A number of methods were used to extract Affymetrix signal, all of which aimed to complete three key processes: to correct for background noise; to normalise; and to summarise. There are a number of popular methods employed for this purpose, notably MAS5, RMA, GC-RMA and PLIER. Moreover a number of software interfaces exist which allow the researcher to

extract, pre-process, analyse and visualise in the same software platform, particularly Partek, GenePattern, GeneSpring GX, R *etc*. Some of these programs work best on processed data, such as Spotfire and Workbench. This work uses MAS5 and RMA at different stages depending on the output used in the individual calculation involved.

2.4.1.6. UAMS and MMRC Datasets

2.4.1.6.1. UAMS

One dataset was created, as discussed above. QC analysis indicated 2 potential outliers. These 2 outliers were excluded from the study. This left 557 GEP arrays for renormalisation and summarisation.

2.4.1.6.2. MMRC

Two datasets were created. The first was the 239 individual patients with paired CGH and GEP arrays. The second was the entire post-QC GEP dataset of 309 GEP arrays that includes the seven sequential samples and the GEP samples that do not have a paired CGH array for any number of reasons plus 17 independent runs of the SUHRR at 2 μg.

Summarisation was done on each batch as single runs on a Mac Pro workstation with two dual core Xeon microprocessors and 8Gb of ram using either Windows XP SP2 (32bit) or Mac OSX 10.5 Leopard.

2.4.1.7. Summarisations

a. MAS5 chip by chip summarisation was performed in Expression Console V1.1 using default parameters. The raw results file contains the complete output that includes the signal values, present/marginal/absent cells, and the detection p-value.

-UAMS_MAS5_Raw.txt

-MMRC_Pairs_MAS5_Raw.txt

-MMRC_All_MAS5_Raw.txt

Sequential exports produced individual files with the signal values and detection values.

-UAMS_MAS5_Signal_Matrix.txt

-MMRC_Pairs_MAS5_Signal_Matrix.txt

-MMRC_Pairs_MAS5_Detection_Matrix.txt

-MMRC_All_MAS5_Signal_Matrix.txt

-MMRC_All_MAS5_Detection_Matrix.txt

It is important to note that MAS5 is a single chip summarisation and is not variance stabilised.

To normalise the distribution of signal intensities the raw MAS5 signals were log2 transformed in Excel 2007 as follows:

-UAMS_MAS5log2_Signal_Matrix.txt

-MMRC_Pairs_MAS5log2_Signal_Matrix.txt

-MMRC_All_MAS5log2_Signal_Matrix.txt

b. RMA summarisations were performed in Affymetrix Power Tools (APT1.10.2) at Mayo Clinic and Partek GS (V6.5) at JHMI using default parameters. Both runs were performed in a single iteration.

APT and Partek were chosen for these summarisations as these are significantly faster than the identical methods in R with the bioconductor Affy package.

The primary raw outputs from APT are:

-UAMS_RMA_Raw_Output.txt

-MMRC_Pairs_RMA_Raw_Output.txt

-MMRC_All_RMA_Raw_Output.txt

The primary outputs were curated in Excel 2007 to generate signal matrix tables:

-UAMS_RMA_Signal_Matrix.txt

-MMRC_Pairs_RMA_Signal_Matrix.txt

-MMRC_All_RMA_Signal_Matrix.txt

It is also important to state that MAS5 is a per-chip summarisation; it should not be used in most cases but was included here to allow for the rapid assessment of each samples TC classification, Proliferation Indices, UAMS indices, and other historic MAS5 based indices. In this work, MAS5 was used for calculation of these traditional indices but for other calculations, in particular the work evaluation the drivers of proliferation, RMA was used.

In addition, it is important to note that RMA is a multi-chip summarisation but is variance stabilised. The signal values for RMA are log2 transformed.

2.4.1.8. Probe IDs

CDC7(CDC7) and DBF4(DBF4A) expression is derived from information related to the probe 204510_at and 204244_s_at respectively. There are four probes for DRF4B(Drf1/DBF4B), namely, 238757_at, 1555378_at, 238508_at and 206661_at. In murine 430 2.0 affymetrix arrays, the probesets used for CDC7 and DBF4A was 1426021_a_at and 1417269_at respectively. Other individual probeset IDs can be obtained from NetAffx Analysis Centre (NetAffx).

2.4.1.9. Calculations

2.4.1.9.1. Gene Expression based Proliferation Index

There are a number of GEP based PI (gPI) in the literature with good correlation between indices (Hose et al., 2011). The Mayo Clinic utilises the gPI published by Zhou *et al* and was calculated using the normalised value of 12 genes that are associated with proliferation [TOP2A (201292_at),

TYMS (202589_at), TK1 (202338_at), MK167 (212021_s_at), KIAA0101 (202503_s_at), GINS1 (206102_at), UBE2C (202954_at), KIF11 (204444_at), ZWINT (204026_s_at), CKS1B (201897_s_at), TRIP13 (204033_at), CCNB1 (214710_at)]. The three main gPI and their probeset IDs are summarised in Table 2.3.

This along with other frequent calculations can be completed quickly with the Perl command:-

```
grep -f ProbeList.txt Dataset.txt > Output(e.g PI).txt
```

2.4.1.9.2. Proliferation Index

PI was calculated using the normalised value of the 12 genes as stated above scaled to the maximum value among 22 plasma cell samples form 32 healthy donors (defined as PI = 1), 414 newly diagnosed myeloma, and 45 myeloma lines. The normalised subgroup PI was shown the relative alteration to NPC by adjusting NPC PI as 1. Poor risk PI score was noted on log2MAS5 normalised data set as greater than 13.6 (Zhan et al., 2006).

2.4.1.9.3. DBF4 Poor Risk Score

Poor and normal risk cut off for DBF4 expression was established using a similar approach to the PI cutoff, employing the scaling of normalised expression of DBF4 in the same sample set using normal plasma cells, myeloma samples, and HMCLs. Poor risk DBF4 score was defined as greater than 10.36.

2.4.1.9.4. TC Classification

The TC classification was calculated using the MAS5 dataset using the method published by Chng et al (Bergsagel et al., 2005). Bergsagel et al described eight TC classes (Bergsagel et al., 2005). These eight TC classes are based on the RNA expression of 8 genes (CCND1, CCND2, CCND3, FGFR3, MMSET, MAF, ITGB7 and CX3CR1). Briefly, the relative expression level was a fraction of

Table 2.3

A

Probeset ID	Gene
202589_at	TYMS
202338_at	TK1
214710_s_at	CCNB1
212021_s_at	MKI67
202503_s_at	KIAA0101
206102_at	GINS1
201292_at	TOP2A
202954_at	UBE2C
204026_s_at	ZWINT
204444_at	KIF11
201897_s_at	CKS1B
204033_at	TRIP13

B

Probeset ID	Gene
201292_at	TOP2A
202095_s_at	BIRC5
202705_at	CCNB2
204641_at	NEK2
225521_at	ANAPC7
204092_s_at	AURKA
209642_at	BUB1
203213_at	CDC2
218542_at	C10orf3
219918_s_at	ASPM
223381_at	CDCA1

C

Probeset ID	Gene
219918_s_at	ASPM
204092_s_at	AURKA
209464_at	AURKB
202095_s_at	BIRC5
204531_s_at	BRCA1
209642_at	BUB1
203755_at	BUB1B
203418_at	CCNA2
214710_s_at	CCNB1
202705_at	CCNB2
203213_at	CDC2
202870_s_at	CDC20
205167_s_at	CDC25C
203967_at	CDC6
221520_s_at	CDCA8
209714_s_at	CDKN3
218542_at	CEP55
205394_at	CHEK1
201897_s_at	CKS1B
204170_s_at	CKS2
203764_at	DLG7
38158_at	ESPL1
206102_at	GINS1
204318_s_at	GTSE1
213008_at	KIAA1794
204444_at	KIF11
219306_at	KIF15
218755_at	KIF20A
209408_at	KIF2C
204162_at	KNTC2
203362_s_at	MAD2L1
220651_s_at	MCM10
201930_at	MCM6
212021_s_at	MKI67
212789_at	NCAPD3
218662_s_at	NCAPG
219588_s_at	NCAPG2
204641_at	NEK2
221923_s_at	NPM1
201202_at	PCNA
200886_s_at	PGAM1
204887_s_at	PLK4
203554_x_at	PTTG1
222077_s_at	RACGAP1
204240_s_at	SMC2
203145_at	SPAG5
205339_at	STIL
210052_s_at	TPX2
202954_at	UBE2C
204026_s_at	ZWINT

Table 2.3. Gene-Expression based Proliferation Indices. Tabular summary of A. TC, B. UAMS and C. German based gPI. Table includes individual genes included with individual probesets. gPI – Gene expression Proliferation Index. TC – Mayo Clinic gPI. UAMS – University of Arkansas Medical School.

the highest signal (1.0) for the individual 8 genes in the patient samples analysed. Cut-offs for individual genes were as follows – FGFR3 > 0.3(TC1), MMSET > 0.1 (TC2), CCND3 > 0.5 (TC3), MAF < 0.1 (TC4), ITGB7 > 0.18 (TC5), CX3CR1 > 0.02 (TC5), MAF > 0.27 (TC5), CCND1 > 0.25 (TC6), CCND1 > 0.024 and CCND2 < 0.09 (TC 7), CCND2 > 0.09 and CCND1 <0.024 (TC8), CCND2 < 0.07 (TC9).

2.4.1.9.5. Other calculations

ISS score, CKD stage and the UAMS 70-gene poor-risk signature were calculated as previously described (Greipp et al., 2005, Shaughnessy et al., 2007).

The ISS as demonstrated in table 1.3 is defined by the patients' serum beta2-microglobulin (β2MG) and serum albumin (Greipp et al., 2005). ISS stage I is defined by a β2MG < 3.5 mg/l with an albumin > 35 g/l. ISS stage III is defined by β2MG > 5.5 mg/l. ISS stage II is defined not ISS I or III.

Chronic kidney disease (CKD) stages are defined by the individual patients estimated GFR calculated by the Modification of Diet in Renal Disease (MDRD) study equation which utilises four variables: body-surface area, race, gender and age. CKD 1 is defined as a GFR > 90; CKD 2 is defined as a GFR between 60-89; CKD3 is defined as a GFR between 30-59; CKD 4 is defined as GFR 15-29; CKD5 is defined as < 15. Units used are ml/min/1.73m^2.

The 70-gene poor risk signature was defined by a discriminant score greater than 1.5 whereas a good risk score was defined by a discriminant score of less than 1.5. The discriminant score was calculated as follows. Discriminant score = 200638_s_at x 0.283 - 1557277_a_at x 0.296 x 200850_s_at x 0.208 + 201897_s_at x 0.314 x 202729_s_at x 0.287 + 203432_at x 0.251 + 204016_at x 0.193 + 205235_s_at x 0.269 + 206364_at x 0.375 + 206513_at x 0.158 + 211576_s_at x 0.316 + 213607_at x 0.232 - 213628_at x 0.251 - 218924_s_at x 0.230 - 219918_s_at x 0.402 + 220789_s_at x 0.191 + 242488_at x 0.148 (where the variables represent the Affymetrix value for the particular probe). The additional modification of scaling the score to a range of 0 to 100 to assist in interpretation. This scaling is done using the equation [original GEP70 + 1.6] * 20 = scaled GEP70.

2.4.1.10. Statistical Analyses

Taking account of the availablilty of clinical parameters the UAMS data set, GSE24080 was utilised in further statistical survival analysis. The other major dataset, the MMRC data set, GSE26760, was equally interrogated but survival analysis was not completed as clinical data is still not available.

The ANOVA and Tukey-Kramer HSD (honestly significant difference) correction were used for significance of unsupervised differential expression between different symptomatic stages of myeloma (Kramer, 1956). This test is an exact alpha-level test if the sample sizes are the same and conservative if the sample sizes are different (Hayter, 1984). Each multiple comparison test begins with a comparison circle plot, which is a visual representation of group mean comparisons. Circles for means that are significantly different either do not intersect, or intersect slightly, so that the outside angle of intersection is less than 90 degrees. If the circles intersect by an angle greater than 90 degrees, or if they are nested, the means are not significanlty different. The Mantel-Cox-Log-Rank test was used to calculate significant differences for survival and the Fisher-Exact Test was used to determine statistical significant independence from conventional prognostic markers. The Pairwise method was used for multivariate correlations. This generates a correlation matrix of correlation coefficients that summarises the strenght of the linear relationships between each pair of response variables. The two-tailed confidence interval (CI) was determined with a confidence coefficient of 95% with an α-value of 0.05. The JNP 9.0 (SAS, Carry NC, USA) advanced statistical program was used for individual statistical calculations.

2.4.1.11. Gene Expresssion Analysis Tools

There are a number of tools available for interrogation of genomic data.

Expression Console™ is a software application that enables probe set summarisation and initial data quality examination for Affymetrix expression arrays. Expression Console software takes probe cell intensity files (*.CEL) and creates probe-level summarisation files (*.CHP) using the selected algorithm workflow. The algorithms offered include MAS5 Statistical algorithm, Probe

Logarithmic Intensity Error Estimation (PLIER), Robust Multichip Analysis (RMA). Probe level summarisation files can then be further analysed using software applications from Affymetrix GeneChip Compatible partners to identify differentially expressed genes (GeneChip).

Expression Console™ software supports probe set summarisation and CHP file generation for 3' expression (e.g., GeneChip® Human Genome U133 Plus 2.0 Array), gene-level (e.g., GeneChip® Human Gene 1.0 ST array) and exon-level arrays (e.g., GeneChip® Human Exon 1.0 ST Array).

GenePattern is a powerful integrative genomic analysis platform that supports tool interoperability and reproducible *in silico* analyses. It provides access to more than 180 tools for GEP, proteomics, SNP analysis, flow cytometry, RNA-seq analysis, and common data processing tasks. It is hosted at The Broad Institute at MIT/Harvard. A web-based interface provides easy access to these tools and allows the creation of multi-step analysis pipelines. The advantage of such an approach is that pipelines can be saved for future analysis and data can be run on the local GenePattern server via the ePortal. GenePattern was used in this thesis for display options of summarised results from other platforms, in particular relating to mouse data (GenePattern).

GeneSpring is another platform. This thesis utilises two different versions GX10 and GX 7 (GeneSpring GX 7/10 (Agilent Technologies, Santa Clara, CA, USA)). Both programs although manufactured by Agilent operate quite different.

Oncomine is an internet-based application that integrates and unifies high-throughput oncogenomic profiling data so that target expression across a large volume of cancer types can be assessed online.

It is based on the original Oncomine product provided by the University of Michigan. It remains under a free license for non-commercial users pursuing non-commercial purposes. It can be used

for a quick evaluation of any potential hypothesis governing a particular data set. Most published data sets are available through the public repositories, but additional Pharma-based data sets are available through this web-based resource (Oncomine).

Partek GS (Partek Inc., St Louis, MI, USA) was used for filtering, summarising and differential expression analysis. It can easily import raw *.CEL files or *. CHP created with Expression Console™ software. The RMA algorithm was used for hypothesis not involving the MAS5 calculated indices.

Spotfire (TIBCO Spotfire, Göteberg, Sweden) is another integrated platform that allows manipulation of bioinformatics data. It was used to prepare data for loading into IPA by using Spotfire's venning function limiting differential genes with absolute fold change and p-value. Spotfire also has a direct output to GO remotely.

Agilent Genomic Workbench (Agilent Technologies, Santa Clara, CA, USA) integrates aCGH, expression analysis within the one program. It is similar to Partek an GenePattern but its display function for aCGH is superior.

2.4.2. Pathway and Functional Analysis Tools

2.4.2.1. Gene Ontology

The Gene Ontology project provides an ontology of defined terms representing gene product properties. The ontology covers three domains: **cellular component**, the parts of a cell or its extracellular environment; **molecular function**, the elemental activities of a gene product at the molecular level, such as binding or catalysis; and **biological process**, operations or sets of molecular events with a defined beginning and end, pertinent to the functioning of integrated living units: cells, tissues, organs, and organisms.

For example, the gene product CDC7 can be described by the molecular function term S-phase ki-

nase, the biological process terms cell proliferation and the cellular component terms nucleotide binding, purine nucleotide and ATP binding.

The GO ontology is structured as a directed acyclic graph, and each term has defined relationships to one or more other terms in the same domain, and sometimes to other domains. The GO vocabulary is designed to be species-neutral, and includes terms applicable to prokaryotes and eukaryotes, single and multicellular organisms (GO). Most pathway programs feed into GO server for GO analysis (*cf.* Gene-MANIA, go-perl, go-moose, GenePattern, Spotfire, IPA, Partek etc). In this thesis, Spotfire, IPA and Partek were used for this purpose for ease of analysis. In particular, GO was used in addition to IPA to analyse the potential drivers of the proliferative phenotype of myeloma using the GSE24080 data set as described under the IPA section of the methods detailed below.

2.4.2.2. Ingenuity Pathway Analysis (IPA)

IPA (Redwood City, CA, USA) is a pathway analysis tool quite different to GO analysis. IPA is best described as an integrative genomics data analysis tool to evaluate the pathway, driver or cause of differential processes. Data can be loaded from a variety of experimental platforms. In this thesis, such software was used to analyse the potential drivers of the proliferative phenotype of myeloma. The GEO dataset GSE24080 was used to explore these drivers. The dataset was first transformed with a RMA algorithm, then filtered, based on the individual patient's TC class. Within each TC class, patients were further categorised based on their gene expression proliferation index (gPI) as either high or low. Differentially expressed genes between those with a high proliferation index and low proliferation index were calculated. The intersection of the set of genes differentially expressed, with a p-value <0.05 and absolute two-fold change, were obtained and analysed further to examine the pathways driving proliferation using tools for pathway analysis and gene ontology (Ingenuity).

2.4.3. Connectivity Mapping

2.4.3.1 Cmap

The Broad Institute hosts a gene-expression based connectivity map called the Cmap. The Cmap utilises the gene expression prolife obtained from four different cell lines:HL60, MCF7, PC3 and SKMEL5, treated with 10 µM for 6 and 12 hours with 164 wide ranging bioactive compounds not limited to known anti-cancer agents. It uses the Kolmogorov-Smirnov statistic used for Gene Set Enrichment Analysis as opposed to hierarchical clustering when interrogating for shared patterns or maps with a signature of interest.

Hypotheses are generated by searching for multiple independent instances of the same perturbagen, or group of functionally or structurally similar perturbagens, with consistently high (positive or negative) connectivity.

CHAPTER 3:

Examining the role of the DBF4 Dependent Kinase, CDC7 in proliferation-based stratification of myeloma.

INTRODUCTION:

The use of genomics is increasing our understanding of myeloma. Multiple prognostic scores and, more recently, stratification for individual treatment algorithms were created as result of such research (Bergsagel et al., 2005, Shaughnessy et al., 2007, Decaux et al., 2008, Dispenzieri et al., 2007, Kumar et al., 2009, and Mikhael et al., 2013). The datasets resulting from this activity provide a significant resource to complement molecular work. Since myeloma at diagnosis is characterised by a low proliferation index that increases with relapse (Witzig et al., 1999, Steensma et al., 2001) correlating with an adverse prognosis (Boccadoro, et al., 1984 and Greipp et al., 1993, Steensma et al., 2001), this thesis examines if CDC7, or its regulators DBF4 and DBF4B, are differentially expressed in normal plasma cells versus different 'stages' of myeloma.

RESULTS:

3.1. Expression of CDC7 and its regulators in myeloma gene expression datasets.

CDC7 and its regulator, DBF4 but not its alternative regulator, DBF4B are expressed in neoplastic and non-neoplastic plasma cells

GSE24080, a publicly available dataset, was used to examine whether myeloma cells express CDC7 or its regulators DBF4 or DBF4B. This dataset comprises the transcription profiles of 560 newly diagnosed myeloma patients treated at the UAMS with total therapy 2 and 3 depending on enrolment dates. It also contains expression data of myeloma cell lines (HMCLs), normal plasma cells (NPCs), smouldering myeloma (SMM) and monoclonal gammopathy of undetermined significance (MGUS).

Five groups were constructed to represent the clinical and genetic evolution of myeloma; from NPC; MGUS; SMM; symptomatic myeloma (MM); and extramedullary myeloma best represented by HMCLs. GSE24080 was mined for expression of CDC7 and its regulators DBF4, and DBF4B (Figure 3.1).

Figure 3.1

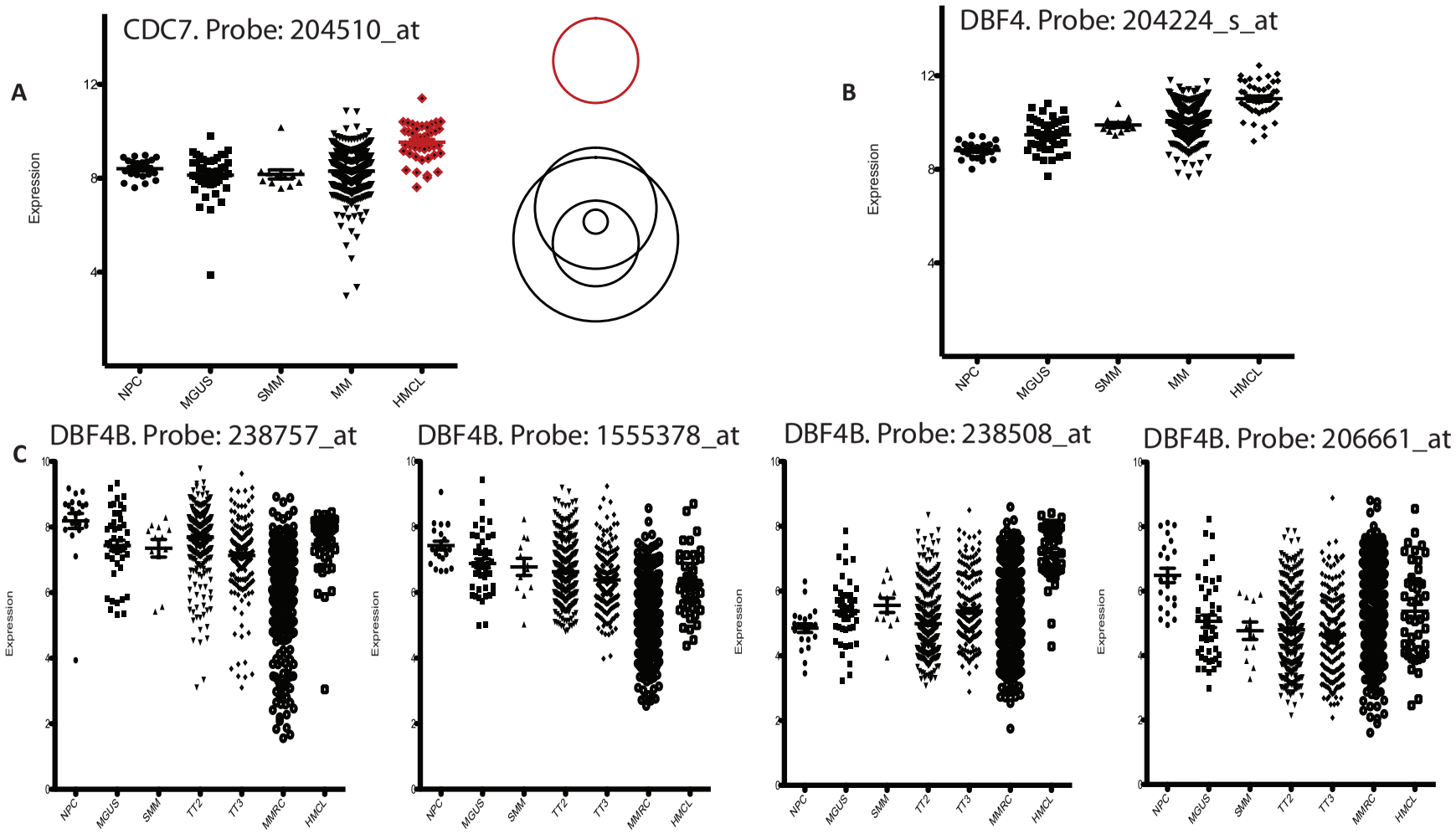

[**Figure 3.1. Expression of A. CDC7 B. DBF4 and C. DBF4B** as determined by gene expression profiling in normal bone marrow plasma cells (NPC), monoclonal gammopathy of undetermined significance cells (MGUS), smoldering myeloma cells (SMM), myeloma (MM) cells and myeloma cell line (HMCL) cells. Data is represented in a columnar dot blot where each dot represents a patients expression of the indicated gene. In A. and B. the columns from left to right are NPC, SMM, MM, HMCLs. In C. the columns from left to right are NPC, SMM, TT2, TT3, and HMCLs. TT2 and TT3 indicate MM group divided into those that went on to receive total-therapy 2 and total therapy 3 respectively. MMRC indicates Multiple Myeloma Research Consortium dataset. In relation to the CDC7 (A.) plot, the Tukey-Kramer plot is indicated adjacent with differently coloured circles. Each individual circle represents individual groups – NPC, MGUS, SMM, MM and HMCLs. Circles that do not intersect indicate significantly different means. $P < 0.05$.]

In the first instance, there was expression of CDC7 and DBF4 but not DBF4B across plasma cell groups. DBF4B was not expressed in any of the 4 probesets used (238757_at, 1555378_at, 238508_at and 206661_at: Figure 3.1.C). This suggests a preferential CDC7 regulator in plasma cell biology.

DBF4 is differentially expressed in an increasing 'step-wise' manner across clinical groupings of asymptomatic and symptomatic myeloma in a statistically significant manner

Using the same dataset and clinical cohorts as above, mean expression across individual groups were analysed for differential expression between groups and statistical significance using a ANOVA statistic with a Tukey-Kramer correction (Figure 3.1.A and 3.2).

Figure 3.2

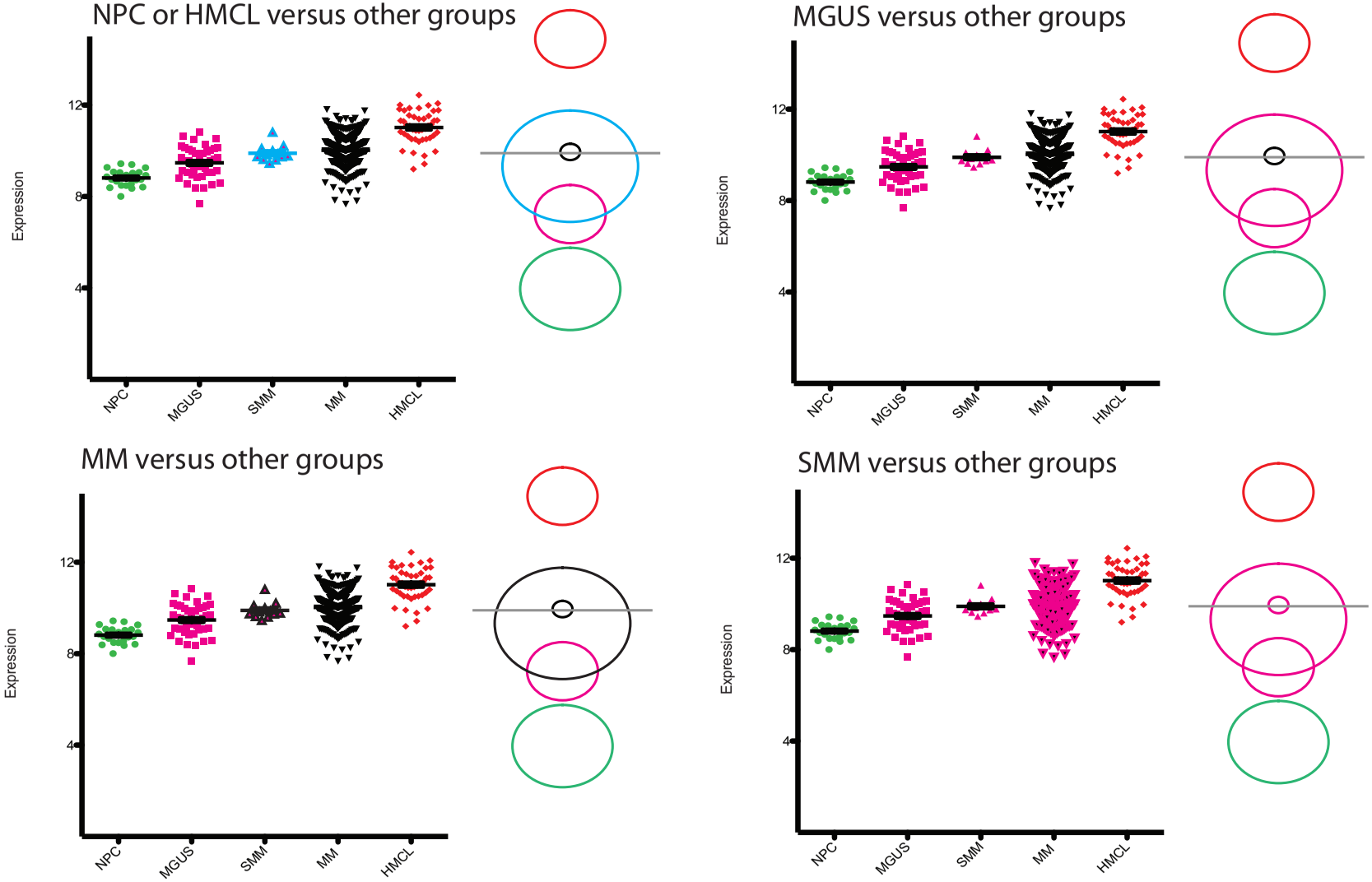

Figure 3.2. Expression of DBF4. Determined by gene expression profiling in normal bone marrow plasma cells (NPC), monoclonal gammopathy of undetermined significance cells (MGUS), smoldering myeloma cells (SMM), myeloma (MM) cells and myeloma cell line (HMCL) cells. Data is represented in a columnar dot blot where each dot represents a patients expression of *DBF4*. The columns from left to right are NPC, SMM, MM, HMCLs. Tukey-Kramer plots are indicated adjacent with differently coloured circles. Each individual circle represents individual groups corresponding to the different colours – NPC, MGUS, SMM, MM and HMCLs. Circles that do not intersect indicate significantly different means. $P < 0.05$.

Differential expression was noted in both CDC7 and DBF4 probesets. In relation to CDC7, the mean expression was statistically different only between the NPC and HMCLs grouping, illustrated in Figure 3.1.A. and accompanying Tukey-Kramer plot. The Tukey-Kramer circle plots are a visual demonstration of the comparison of group means. There was no significant differential CDC7 expression between other groups, as demonstrated by intersecting Tukey-Kramer plots.

Interestingly, in relation to DBF4 expression, there was a statistically significant differential mean expression between multiple groups. NPC and HMCL had significantly different mean DBF4 expression relative to all other groups (Figure 3.2). MGUS had significantly different mean DBF4 expression relative to NPCs, MM, and HMCLs. SMM had significantly different mean DBF4 expression relative to NPCs and HMCLs but was not significantly different to MGUS or MM. Lastly, MM had significantly different mean DBF4 expression relative to HMCLs, MGUS and NPCs but not to SMM as noted already.

The intersection of Tukey-Kramer circle plots suggests a close relationship of individual groups. SMM is related both to MGUS and MM, whereas MGUS itself is only closely related to SMM, and not MM.

DBF4 is therefore differentially expressed in an increasing 'step-wise' manner across clinical groupings of asymptomatic and symptomatic myeloma in a statistically significant manner.

Normal DBF4 copy number despite increased mean expression across groups

The MMRC genomics portal hosted at The Broad Institute was accessed to evaluate for copy number change at the CDC7 and DBF4 genomic loci. The MMRC aCGH dataset was utilised for this purpose.

Figure 3.3

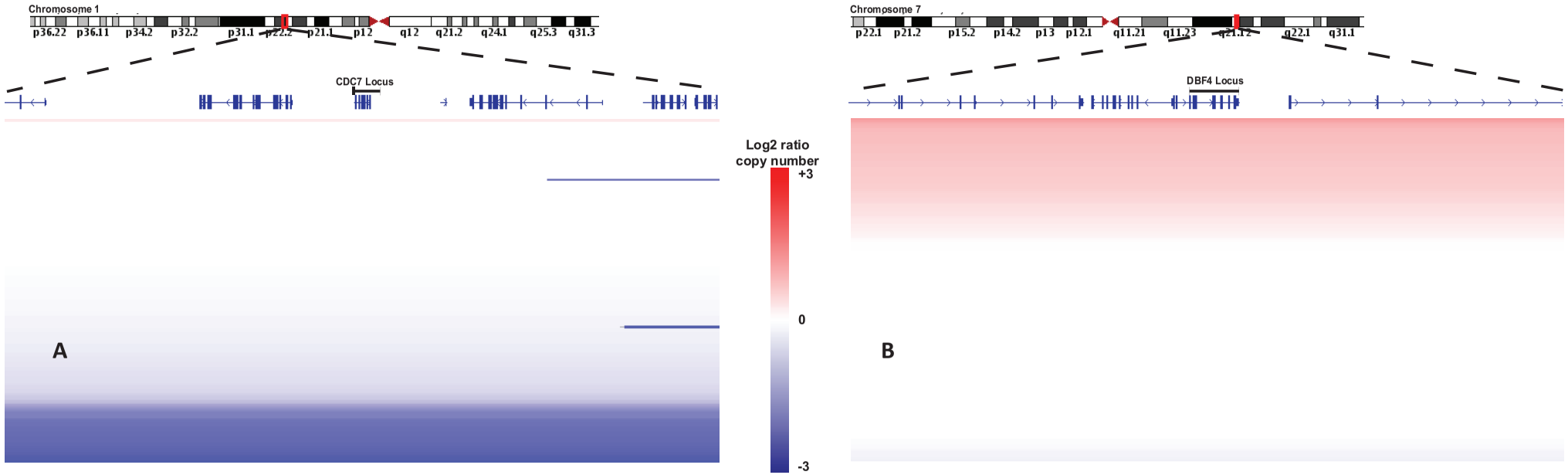

Figure 3.3. A copy number heatmap of A. CDC7 and B. DBF4 loci and flanking regions in a set of 170 publically available myeloma aCGH samples. Rows indicate individual patient samples.

A copy number heatmap of CDC7 and DBF4 loci and flanking regions in a set of 170 publically available myeloma aCGH samples is demonstrated in Figure 3.3, indicating no focal loss or gain at either loci.

Although DBF4 mean expression is increased across clinical myeloma groupings, there is no change in copy number at a gene level.

Overexpression of DBF4 predicts an inferior survival

The UAMS cohort, GSE24080, consisting of 560 newly diagnosed myeloma patients undergoing total therapy 2 or 3 paired with autologous transplantation, was utilised to evaluate for prognostic impact of differential expression of DBF4. High-risk and low-risk DBF4 expression thresholds were established using percentile log ranking. The Mantel-Cox-Log-Rank test was used to calculate significant differences for survival analyses. Multivariate correlation analysis was completed using the pairwise method.

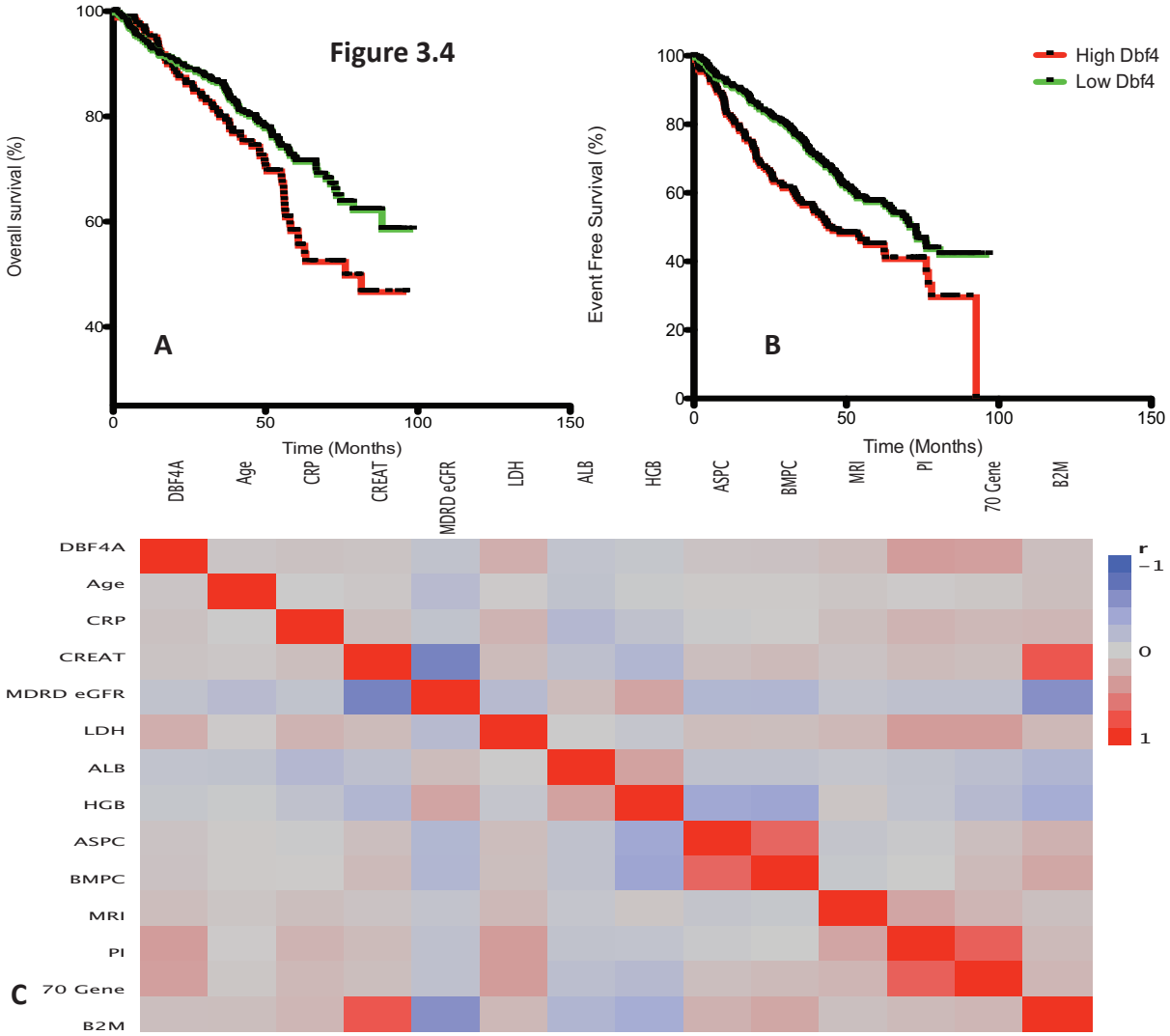

Figure 3.4. Prognostic value of DBF4 expression. Overexpression of DBF4 predicts an inferior survival. Prognostic relevance of DBF4 expression in the UAMS cohort n=557 treated with

total therapy and autologous stem cell transplantation. **A.** Overall survival. **B.** Event-free survival (EFS). High-risk DBF4 expression confers both poor OS and EFS. C. Correlation of clinical stratifiers and DBF4 expression in a correlation heatmap matrix. Both matrices allow multiple relationships of variables to be observed simultaneously. The two variables being compared at any one time are those directly adjacent to each other on the diagonal. Each variable represented in each diagonal point is indicated by the overlying column title. Correlations are displayed among variables on a scale from red (+1) to blue (-1).

Presence of high-risk DBF4 expression was an adverse prognostic factor in terms of event free survival (EFS) and overall survival (OS) in this dataset (Figure 3.4).

Multivariate analysis was performed on DBF4 high-risk expression with other know prognostic factors and important clinical parameters in myeloma: age; LDH; CRP; creatinine; MDRD eGFR; albumin; haemoglobin; percentage plasma cells on aspirate and trephine; number of lytic lesions on MRI imaging; PI; 70 gene poor prognostic UAMS score; and β2MG. The correlation heatmap of these individual parameters is illustrated in Figure 3.4.C.

DBF4 high-risk expression is positively correlated with parameters that are used clinically as surrogate measurements of replication, namely LDH, PI score and 70 gene prognostic score (r values [CI]: 0.37 [0.29 – 0.44] and 0.36[0.28 – 0.42] respectively). As a comparison, PI and the 70 gene score show a higher correlation with each other (r values [CI]: 0.72 [0.68 – 0.76]).

Overexpression of DBF4 therefore predicts an inferior survival.

DBF4 overexpression is not an independent prognostic predictor

The UAMS cohort, GSE24080, consisting of 560 newly diagnosed myeloma patients undergoing total therapy 2 or 3 paired with autologous transplantation, was again utilised to evaluate for prognostic impact of high-risk DBF4 expression. The Fisher Exact Test was used to establish independence.

As mentioned in chapter 2, symptomatic myeloma is indicated by presence of hypercalcaemia, renal impairment, anaemia or lytic bone disease. In terms of prognostic measurements, the international staging score is still in use. This is based on albumin and β2MG blood concentration. Other factors have not been shown to improve prognostic modelling in myeloma. In any

case, these individual factors were compared with the DBF4 high-risk expression score. These factors included LDH, CRP, cyogenetic abnormalities and number of lytic lesions found by diagnostic MR imaging. CRP is an indirect measure of IL-6 activity and LDH an indirect measure of proliferation.

Using the Fisher Exact Test, DBF4 expression was not shown to be independent to the known prognostic scores of PI (Prob> χ^2: p value - 0.0001), 70 gene score (Prob> χ^2: p value - 0.0001), the International Staging System (ISS) (Prob> χ^2: p value - 0.0004), β2MG (Prob> χ^2: p value - 0.0088), LDH (Prob> χ^2: p value - 0.0001) and cytogenetic abnormalities (Prob> χ^2: p value - 0.0229). DBF4 was independent of albumin concentration (Prob> χ^2: p value - 0.1136), age (Prob> χ^2: p value - 0.23), CRP concentration (Prob> χ^2: p value - 0.3547), number of MRI lytic lesions (Prob> χ^2: p value - 0.129), gender (Prob> χ^2: p value - 0.9885), and renal impairment (Prob> χ^2: p value - 0.2669).

DBF4 overexpression is therefore not an independent prognostic predictor.

3.2. Utilising CDC7 activity as a biomarker of proliferation in myeloma.

Many replication proteins are overexpressed in transformed or cancer cell lines when compared to normal cells, which render them potentially important biomarkers for routine clinical applications in cancer diagnosis and prognosis. Among them, Ki-67 (MK167 or MIB) proliferative index has been widely used as a tumour cell proliferation marker. In myeloma, plasma cell labelling index (PCLI), gene-expression based proliferation indices (gPI) and LDH have been used sporadically as surrogate measures of proliferation but, thus far, do not form part of any accepted prognostic score. The Mayo Clinic has moved to incorporate measures of proliferation into their risk-treatment stratification mSMART score but this is not used uniformly across the world.

As CDC7 phosphorylation of MCM2 is a more specific measurement of active replication than MIB index, its role as a measure of proliferation in myeloma is assessed in this section in a cohort of myeloma patients comparing PCLI, gPI and MIB index.

pMCM2/CD138 dual staining correlates strongly with both PCLI, gPI and MIB index

High-risk myeloma is represented best by a relative increase of proliferation index from 0.2% up to 1-3%. This is demonstrated with the old, time-consuming, technique of labelling plasma cells with BrdU – Plasma cell labelling index (PCLI). A newer, more expensive, method is a calculation based on GEP is the gene expression proliferation index (gPI).

Although DBF4 is not an independent predictor of poor risk myeloma, we tested if a surrogate staining, phosphorylation of MCM2, a direct measure of active CDC7-DBF4, could be used to predict high-risk myeloma with a proliferative phenotype. Moreover, pMCM2 staining compared to MIB index, Ki67, and gPI in predicting PCLI was also examined.

In a cohort of 70 patients, PCLI and gPI were compared with pMCM2 and Ki67 dual CD138 staining to look specifically at proliferation within the plasma cell population (Figure 3.6). The percentage cut off between groups in the dual stained cohorts: low; intermediate; high; and very high proliferation index were recorded as per the published PCLI index. Low was indicated by 0 - 0.2% dual positive cells. Intermediate was indicated by 0.3 - 0.99% dual positive cells. High was indicated by 1.0 - 3.0% dual positive cells. Very high was indicated by greater than 3% dual positive cells. Each patient had 400 cells scored, 100 from four different parts

of the same slide. Once scored and risk applied to each patient as measured by each assay, multivariate correlation analysis was completed using the pairwise method.

Figure 3.5

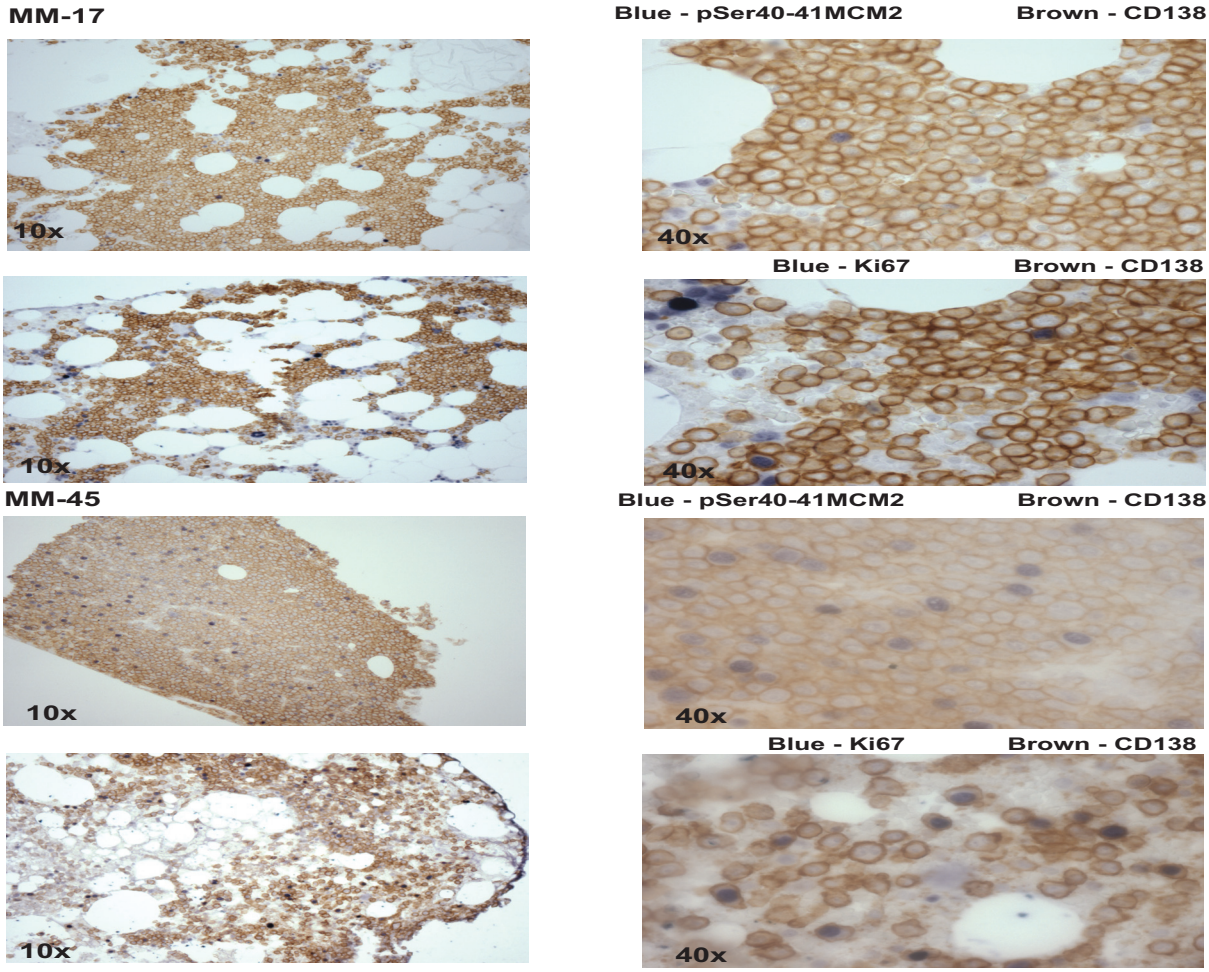

Figure 3.5. pMCM2/CD138 and Ki67/CD138 dual staining in myeloma. Two patients MM-14 and MM-45 dual stained with CD138, a plasma cell marker and two different markers of proliferation, pMCM2 and Ki67. Brown staining relates to CD138 staining whereas blue staining relates to Ki67 and pMCM2 staining as indicated in the respective photograph.

Figure 3.6

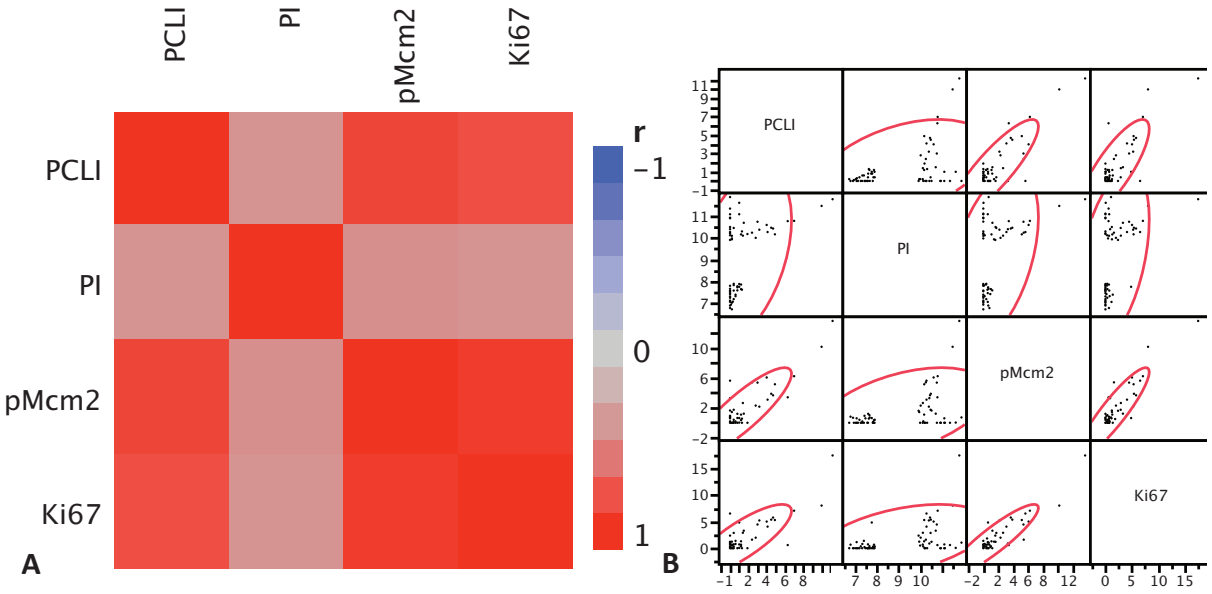

Figure 3.6. pMCM2/CD138 dual staining correlates with both PCLI, gPI and MIB index. Correlation of individual measures of proliferation displayed as **A.** Correlation heatmap matrix and **B.** Scatterplot matrix. Both matrices allow multiple relationships of variables to be observed simultaneously. The two variables being compared at any one time are those directly adjacent to each other on the diagonal of the matrix. Each variable represented in each diagonal point is indicated by the overlying column title. Correlations are displayed among variables on a scale from red (+1) to blue (-1). Each scatterplot shows the relationship between a pair of variables, a bivariate graph. PCLI = plasma cell labelling index, gPI = genomic proliferation index, MIB = Ki67 index.

A similar correlation of gPI with PCLI to that previously reported (r value [CI]: 0.43[0.21-0.61]) was observed (Hose et al., 2011). Both Ki67 and pMCM2 staining showed a stronger correlation with PCLI than with gPI and PCLI (r value [CI]: 0.81 [0.71-0.88] and 0.86 [0.78 – 0.91] respectively) (Figure 3.6). It was found that pMCM2/CD138 dual staining correlates strongly with both PCLI, gPI and MIB index.

Dual staining with CD138/pMCM2 best predicts PCLI proliferation index

To assess the ability of the pMCM2/Ki67/gPI to predict a PCLI with high proliferation accurately, the receiver operating characteristic (ROC) analysis was preformed.

Figure 3.7

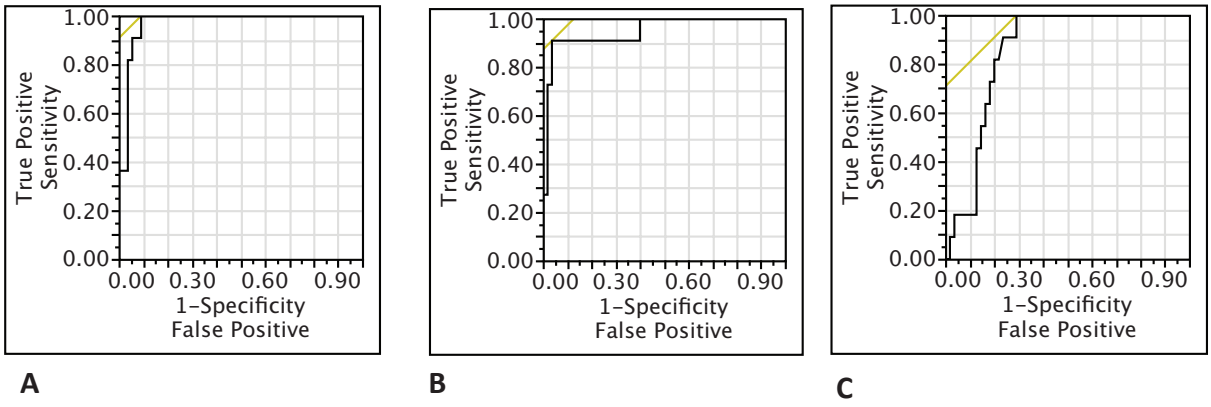

Figure 3.7. pMCM2/CD138 dual staining best predicts PCLI. ROC analysis was used to predict PCLI using **A.** pMCM2/CD138 staining **B.** Ki67/CD138 staining and **C.** gPI. PCLI = plasma cell labelling index, gPI = genomic proliferation index, MIB = Ki67 index.

The pMCM2/CD138 dual-stained material had the greatest accuracy in predicting a high PCLI with an area under the curve (AUC) of 0.97 (Figure 3.7). This compares to an AUC of 0.94 and 0.85 for Ki67/CD138 and gPI respectively. An AUC of > 0.90 implies greatest accuracy while those with > 0.80 - 0.90 have moderate predictive ability.

Dual staining with CD138/pMCM2 was found to best predict PCLI proliferation index.

3.3. Evaluating genes associated with proliferation in myeloma.

Direct or indirect deregulation of Cyclin D is a unifying event in myelomagenesis but the driver of the subsequent proliferative phenotype remains unknown (Bergsagel et al., 2005). Individual groups have proposed the role of TP53, IL-6 and MYC (Bergsagel et al., 2005). If this is a discrete mechanism in all myeloma remains unclear. The importance of establishing the driver or the characteristics of evolution to a proliferative phenotype is clearly important. It underlines the need to explore strategies to treat relapsed refractory myeloma with a proliferative phenotype, an ever-increasing cohort of myeloma patients which have such dismal outcome. In this section, genes associated with the proliferation phenotype are isolated. These genes are subsequently interrogated by pathway analysis to ascertain pathways associated with the proliferation phenotype. Finally, the geneset is further interrogated using connectivity mapping hosted at The Broad Institute, for novel compounds to target this proliferative signature.

90 genes are associated with the proliferation phenotype in myeloma

The UAMS GEO dataset, GSE24080, was used to evaluate genes associated with proliferation in myeloma. In order to examine this, the dataset was broken into individual TC classes defined by their recurrent non-random **t**ranslocations and **c**yclin D expression. Within each TC class, patients were further categorised based on their gPI as either high or low as described by Zhou *et al* (Zhou et al., 2001). There are eight TC classes as described by Bergsagel *et al* and illustrated in Table 3.1 (Bergsagel, 2005). The TC class described by recurrent translocations involving 4p16 can be further broken down into those that are FGFR3 positive or negative. It is now widely accepted that the recurrent translocation universally involves WHSCI/MMSET rather than FGFR3. Equally, the MAF group can be further divided into those with a recurrent rearrangement with MAF (16q23) or MafB (20q11).

Table 3.1

TC	TC group	Recurrent Translocation	Cyclin Dysregulated	Gene(s) at breakpoint
1	4p16 FGFR3+	4p16	D2	FGFR3+/MMSET
2	4p16 FGFR3-	4p16	D2	MMSET
3	6p21	6p21	D3	CCND3
4	mafB	20q11	D2	MAFB
5	maf	16q23	D2	MAF
6	11q13	11q13	D1	CCND1
7	D1	none	D1	none
8	D1+D2	none	D1 +D2	none
9	D2	none	D2	none

Table 3.1. Myeloma TC Classes. Summary of each individual TC group. Groups 1-9. Indicates group name, recurrent translocation, D Cyclin that is overexpressed, and genes at the translocation breakpoint.

The dataset was first transformed with a RMA algorithm using Partek (Partek Inc.). The individual gPI label was calculated based on MAS5 extracted data.

Differentially expressed genes between those with a high proliferation index and low proliferation index were calculated using Spotfire (TIBCO Spotfire), and are represented with their individual volcano plots (Figure 3.8.A). Genes that were differentially expressed with an absolute 2-fold change and p-value < 0.05 were selected (Figure 3.8.B). The intersection of all TC groups was calculated.

Figure 3.8

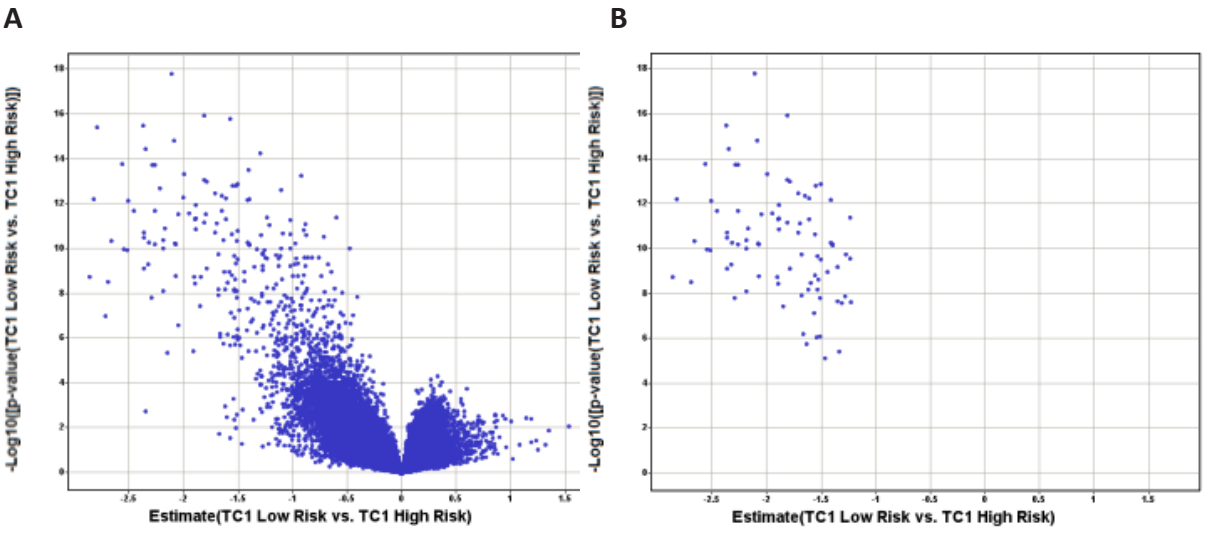

P< 0.05. Absolute 2 fold change

Figure 3.8. Differential Expression between High and Low-Risk Proliferation Index within TC class. GSE24080 was transformed, and normalised with RMA and filtered based on individual TC class. Differential expression between high and low proliferation index groups was calculated for all TC classes. TC1 is displayed **A**. Output data was further filtered to illustrate dif-

ferentially expressed genes with an absolute 2-fold change and p-value <0.05 **B.** across each TC group.

The intersection of all TC groups isolated 90 genes (Appendix II). The top genes were RRM2, NUF2, CENPA, NDC80, CDK1, CEP55, TOP2A, PBK, ASPM, BUB1, BUB1B, SCHBP1, PRR11, RACGAP1, ATAD2, MAD2L1, NUSAP1, TYMS, NEK2, DTL, PBK, TTK, ZWINT, GINS1 and CCNB1. These 90 genes are enriched in those with a high proliferative index relative to those with a low proliferation index regardless of TC group involved.

This work suggests that there are 90 genes are associated with the proliferation phenotype in myeloma.

The G2/M DNA damage checkpoint regulation is the most significantly enriched canonical pathway associated with the proliferation phenotype in myeloma

To evaluate potential pathways associated with the proliferation phenotype in myeloma, the 90 genes (IPA uses the term molecules) were analysed further using tools for pathway analysis (Ingenuity Pathway Analysis [IPA]) and gene ontology directly from Spotfire (TIBCO Spotfire).

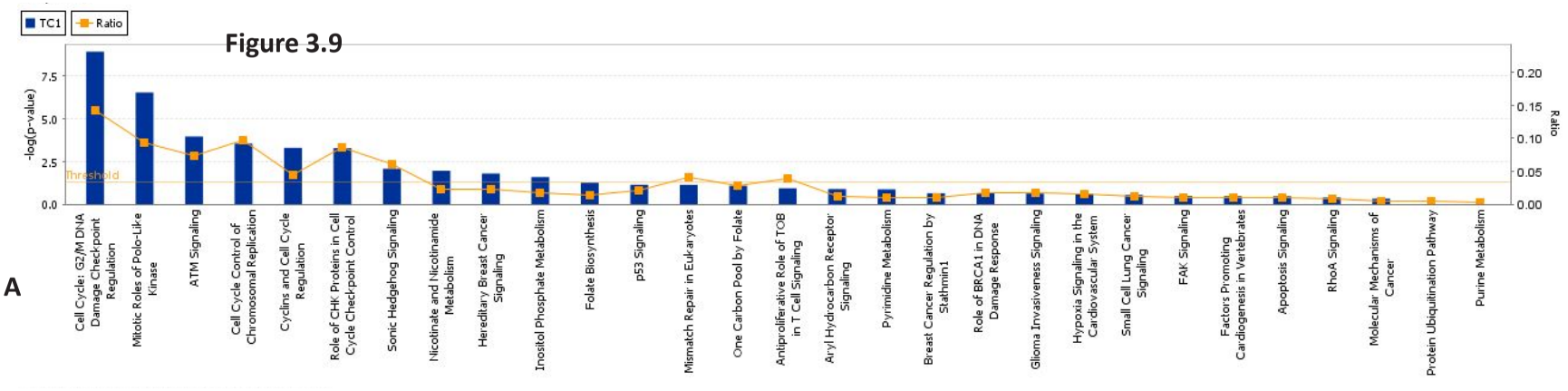

A

	P-Value	Ratio
Cell Cycle: G2M DNA Damage Checkpoint Regulation	1.18×10^{-9}	7/49 [0.143]
Mitotic Roles of Polo-like Kinases	2.89×10^{-7}	6/64 [0.094]
ATM Signaling	1.1×10^{-4}	4/54 [0.074]
Cell Cycle Control of Chromosomal Replication	2.84×10^{-4}	3/31 [0.097]
Cyclins and Cell Cyclin Regulation	5.02×10^{-4}	4/89 [0.045]

B

Figure 3.9. Canonical Pathways involved in the Proliferative Phenotype in Myeloma. A. Canonical pathways listed with reducing ratio. The genes of intersection were analysed and modeled through the use of Ingenuity Pathways Analysis. The IPA Canonical Pathways analysis identified the pathways from the ingenuity Pathways Analysis library of canonical pathways that were most significant in the intersection dataset. The significance of the association between the dataset and the canonical pathway was measured based on a ratio of the number of differentially expressed transcripts from the dataset that map to the pathway divided by the total number of molecules that exist in the canonical pathway. Significant canonical pathways are listed in order of significance bases on this ratio. The individual pathways are listed in **B.** Top 5. The full list is displayed in the appendix. Each table lists the individual canonical pathways, p-value of significance, ratio and molecules derived from the intersection list that enriches in each individual pathway

Interestingly, the top seven canonical pathways with highly significant p-values and IPA ratios isolated were G2/M DNA damage checkpoint regulation, mitotic role of polo-like kinases, ATM signalling, cell cycle control of chromosomal replication, cyclins and cell cycle regulation, CHK proteins in cell cycle checkpoint control and interestingly sonic hedgehog signalling (Figure 3.9; A. and C.).

The G2/M DNA damage checkpoint regulation was found to be the most significantly enriched canonical pathway associated with the proliferation phenotype in myeloma.

The networks associated with the proliferative phenotype in myeloma

The dataset was analysed with the IPA and GO network algorithm. This algorithm creates the most likely network, based on individual molecules in the dataset, which in turn is based on known relationships, and which is curated and hosted, by IPA in their knowledge database. The genes connected in a network may or may not be biologically relevant. In this analysis, the molecules comprise the intersecting geneset compiled form differentially expressed genes across TC groups.

Figure 3.10

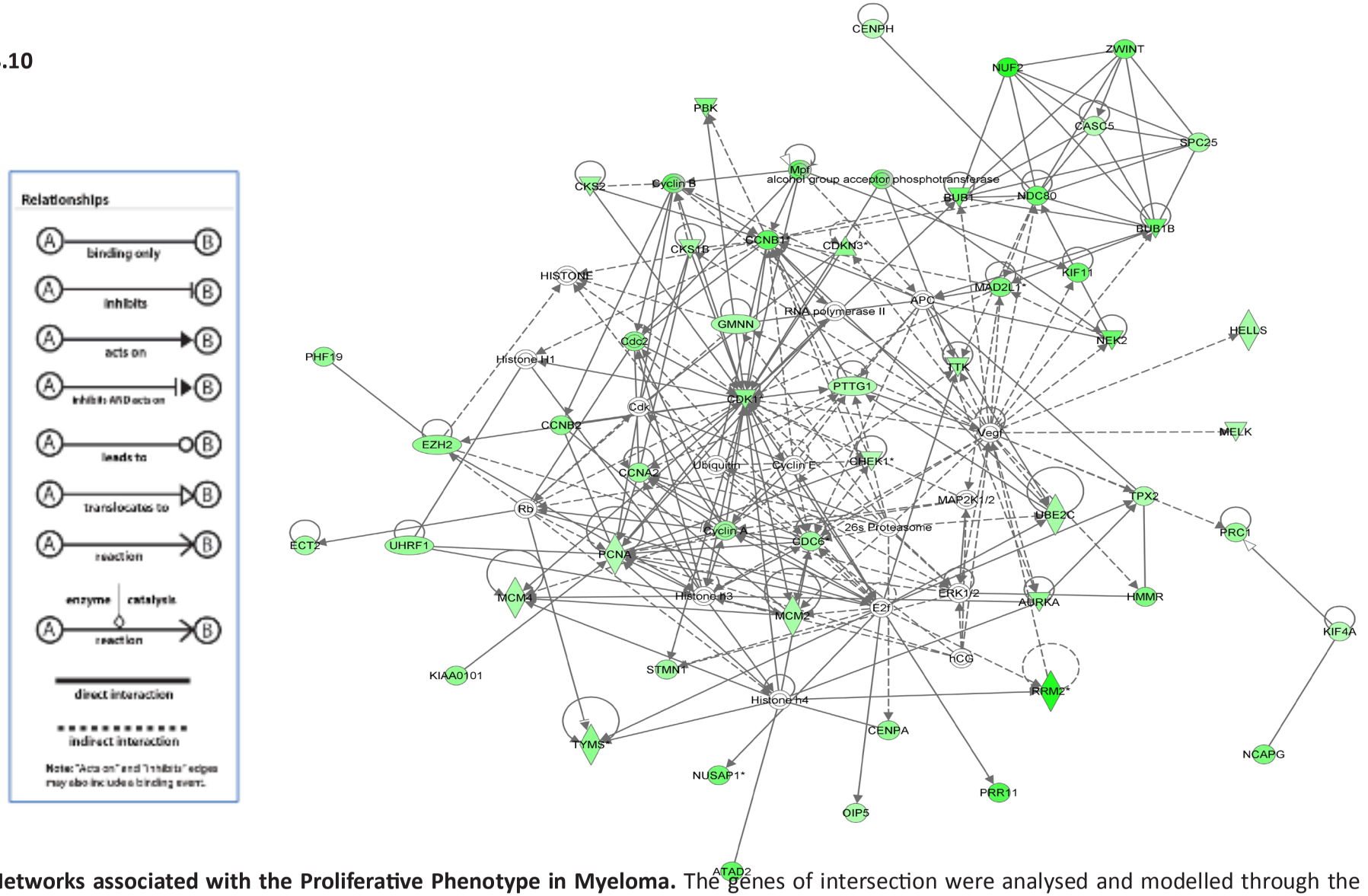

Figure 3.10. Networks associated with the Proliferative Phenotype in Myeloma. The genes of intersection were analysed and modelled through the use of Ingenuity Pathways Analysis as per Figure 3.9. The IPA network analysis identified the most significant network from the ingenuity Pathways Analysis library of networks that were most significant in the intersection dataset. Individual relationships between genes are indicated in the adjacent table. Green colour indicates high expression of the particular gene in patients with a high proliferation index relative to those without.

Two dominant networks were identified as illustrated in Figure 3.10. The first network highlights Histone, Histone H1, Rb, 26s proteasome, RNA polymerase II, APC, VEGF, MAP2K1/2, E2F and ERK1/2. The second network highlights TP53, MYC, IL-6, CCND2, CDKN2A and HNF4A. It is interesting to note the direct interaction of p38 with MYC, TP53, and indirect interaction with Il-6, p16 and TOP2. Again, this demonstrates known offenders in myelomagenesis.

GO confirmed that the intersection genes had seven dominant processes: cell proliferation; chromatin assembly; chromosome condensation; CENPA containing nucleosomes; histone exchange; and positive regulation of chromosome segregation.

This *in silico* analysis suggest that there are two dominant networks associated with the proliferative phenotype in myeloma.

Connectivity mapping suggests a number of potential therapeutics for myeloma patients with a high proliferation index

The Cmap is a useful resource that can be used in drug discovery (Lamb et al, 2006, Lamb et al., 2007). It utilises the gene expression prolife obtained from four different cell lines: HL60, MCF7, PC3 and SKMEL5, treated with 10 μM for 6 and 12 hours with 164 wide ranging bioactive compounds not limited to known anti-cancer agents. It uses the Kolmogorov-Smirnov statistic used for Gene-Set Enrichment Analysis, as opposed to hierarchical clustering, when interrogating for shared patterns or maps with a signature of interest. With this in mind, the gene signature (Appendix II) derived from differentially expressed genes from those with and without a high proliferation index was interrogated against the Broad Institute connectivity map.

Table 3.2

A

10 Perturbagens							
rank	cmap name	mean	n	enrichment	p	specificity	percent non-null
1	vorinostat	-0.248	12	-0.687	0	0.1062	50
2	sirolimus	0.256	44	0.439	0	0.1024	50
3	LY-294002	0.25	61	0.324	0	0.2819	57
4	resveratrol	0.533	9	0.673	0.00014	0.1078	77
5	puromycin	0.703	4	0.888	0.00016	0.0787	100
6	trifluoperazine	0.392	16	0.51	0.00022	0.1827	68
7	prochlorperazine	0.433	16	0.501	0.00028	0.1456	75
8	etacrynic acid	0.617	3	0.938	0.00038	0	100
9	etoposide	0.675	4	0.867	0.0004	0.0513	100
10	clioquinol	0.58	5	0.819	0.00042	0.0209	100

B

50 Perturbagens							
rank	cmap name	mean	n	enrichment	p	specificity	percent non-null
1	sirolimus	0.268	44	0.465	0	0.0843	52
2	MS-275	0.799	2	0.995	0.00002	0.0173	100
3	bepridil	0.657	4	0.937	0.00002	0	100
4	resveratrol	0.557	9	0.714	0.00004	0.0882	77
5	prenylamine	0.631	4	0.9	0.0001	0.0197	100
6	prochlorperazine	0.479	16	0.541	0.0001	0.1019	81
7	trifluoperazine	0.432	16	0.534	0.0001	0.1442	68
8	thioridazine	0.414	20	0.468	0.00016	0.3014	70
9	fluphenazine	0.393	18	0.489	0.0002	0.114	66
10	captopril	-0.462	5	-0.843	0.00026	0	80

Table 3.2. Cmap predicted drugs potentially targeting the proliferative cohort. Summary of drugs identified using **A.** 10 **B.** 50 perturbagens. This table displays a summary of top 10 ranked drugs (cmap name) with accompanying arithmetic mean of the connectivity score, n, the number of instances, a measure of the enrichment of those instances in the order list of all instances, a permutation p value (p) for the enrichment score, specificity of that enrichment and the non null percentage. Instance is the basic unit of data in Cmap. It represents the probeset. Perturbagen represents the inputted upregulated and downregulated gene signature. The non-null percentage is defined as the percentage of all instances in a set of instances that share the majority non-null category of connectivity score. P value is an estimate of likelihood that the enrichment of a set of instances in the list of all instances in a given result would be observed by chance. This value is determined empirically by computing the enrichment of one hundred thousand sets of instances selected at random from the set of all instances in the result. n is n instances for calculation of Kolmogorov-Smirnov statistic. Specificity provides an estimate of the uniqueness of the connectivity between a set of instances and a signature of interest based upon the behaviours of that set of instances in a large number of results produced from a collection of diverse signatures.

This revealed a number of potential drugs (Table 3.2), which may target this cohort of patients with the worst OS and TTP. Included in the top ten drugs were HDACi, MS-275, mTOR inhibitors, sirolimus, Ca^{2+} channel blockers, bepridil, and a number of atypical anti-psychotics.

DISCUSSION:

Stratification of Myeloma using surrogate measures of proliferation.

DBF4 expression

The DBF4-dependent kinase CDC7 is an essential kinase involved primarily in the initiation of DNA replication. Previous studies have shown that CDC7 and DBF4 are overexpressed in cell lines relative to their normal tissue (Hess et al., 1998, Bonte et al., 2008). The UAMS dataset illustrated that both CDC7 and DBF4 are expressed in myeloma patients. DBF4B (formerly Drf1) which encodes DBF4B is not expressed, which suggests that DBF4 is the primary regulator of CDC7 in plasma cells. The dataset was further filtered into five groups illustrating that CDC7 mean expression was only significantly different between HMCLs and NPCs. The mean DBF4 expression was significantly different across multiple groups, paralleling, in a step-wise manner, the clonal evolution of myeloma to clinically significant symptomatic myeloma.

DBF4 expression was not localised to any of the seven UAMS groups identified by Zhan et al through unsupervised hierarchical clustering (Zhan et al., 2006). There was increased relative expression within the proliferative group, but, importantly, within the hyperdiploid group and the low bone disease group also. The proliferative group is associated with a poorer prognosis whereas the hyperdiploid and low bone disease groups predicts a good prognosis. There was no copy number change in the DBF4 genetic locus suggesting that DBF4 overexpression is not associated with a gain or loss of function mutation.

A striking feature is that DBF4 overexpression is an adverse prognostic factor predicting worse OS and PFS. It is not surprising that DBF4 overexpression correlates best with LDH, PI and UAMS poor prognostic score. However, DBF4 overexpression did not reach independence relative to other myeloma stratifiers i.e. Proliferation Index, 70-gene poor risk signature or International Staging System. Taken together, this means that although DBF4 overexpression confers and predicts a poor prognosis, it is not independent to other surrogate known measures of proliferation.

Surrogate measures of Proliferation

Although myeloma is considered one entity, it has significant heterogeneity, both at a genetic but equally at a clinical level, with varied clinical outcome. Stratification is critical to match novel treatments with the group likely to obtain maximum benefit and thus advance care pathways in myeloma. The Plasma Cell Labeling (PCLI) and gene expression Proliferation Index (gPI) have already been shown to be an independent predictor of time to progression and overall survival. This relative increase in proliferation is now seen as the most important predictor of inferior prognosis in myeloma yet it is not universally assessed at diagnosis. PCLI is a cumbersome technique and is only used in a handful of centres around the world. Moreover, gPI is expensive and also not used universally. Immunohistochemisty, on the other hand, is routinely available in histopathology labs. Moreover, trephine-based indices serve to include patchy infiltrates of malignant plasma cells that may be missed on aspirate-based indices. In addition, due to the large size of plasma cells, it is not uncommon for the aspirate not to reflect the true clinical burden in an individual patient.

Phosphorylation of MCM2 is a specific measure of CDC7 activity, present in cells during S, G2 and M but absent in G0 and G1 phase of the cell cycle (Montagnoli et al., 2008, Vanotti et al., 2008). The MIB index highlights cells during G1, S, G2 and M phase of the cell cycle. Thus, CDC7 is more specific for active replication. An antibody raised to phospho-Ser40/41 MCM2 (pMCM2) is a specific measure of CDC7 activity. Dual staining with CD138 allowed for plasma cells to be identifed with ease. The gold standard in measuring proliferation in myeloma is the PCLI. CD138/pMCM2 dual staining predicted PCLI with greatest accuracy. This was closely followed by dual CD138/Ki67 staining. The MIB index is used commonly in haematopathology in relation to evaluating high grade lymphomas. PCLI had a similar correlation to gPI, as has been previously published. Taken together, this would suggest that dual staining is better than gPI at predicting the proliferative

myeloma phenotype defined by PCLIs. As the MIB index is more routinely used, the extension of its use as part of a new stratification system in myeloma provides interesting possibilities for further exploration. An alternative would be to use PET/CT imaging using the standardised uptake value (SUV) as measure of proliferation. Low dose irradiation would make the technique more acceptable in terms of radiation exposure. This would combine the need to document lytic bone disease but in addition the advantage of possibly documenting proliferation.

Genes Associated with Proliferation

Hose *et al* demonstrated that proliferation is a central independent prognostic factor in myeloma (Hose et al., 2011). The UAMS proliferative subgroup of myeloma defined by a proliferation GEP confers the worst overall survival and time to progression despite novel therapy. Steensma *et al* demonstrated previously that PCLI predicts early disease progression and death (Steensma et al., 2001). However, the genes association with proliferation and indeed the potential driver behind proliferation has not being clearly defined. The importance of establishing these genes or the characteristics of evolution to a proliferative phenotype is clearly important. It underlines the need to successfully target relapsed refractory myeloma with a proliferative phenotype, an ever-increasing cohort of myeloma patients with such dismal outcome.

This thesis employed a novel design to attempt to answer these questions. It is important to note that this large dataset comprises 560 newly diagnosed patients with myeloma prior to receiving any anti-myeloma treatment. This removes biases that may be associated with therapy driven clonal selection that is now well described in myeloma. Separating myeloma into their distinct TC class excludes dominating differences associated with known recurrent non-random translocations. Separation also allows the complete evaluation of which set of genes is expressed differently between those with a proliferation and a non-proliferation phenotype within each group. The intersection of these individual TC class differences revealed 90 shared genes, providing an output for evaluating myeloma as a complete entity.

The pathway analysis revealed some puzzling observations, however. The top three pathways identified are involved primarily in regulation of repair rather than replication. It is a paradox that pathways associated with arresting a cell from further replication would characterise the top three pathways enriched in the proliferative phenotype. Taken individually, the G2/M accompanied by ATM would imply a DDR secondary to DSBs.

Gorgoulis *et al* in a plenary paper evaluated pre-cancerous and cancerous lesions for the occurrence of activation of the DDR (Gorgoulis et al., 2005). They demonstrated that replication stress leading to DSBs with subsequent genomic instability was an essential pathway taken in the evolution of human pre-cancerous lesions. Gorgoulis *et al* also illustrated that this occurred more readily at fragile sites which are the natural genomic weak points to replication stress (Gorgoulis et al., 2005). However, its role associated with proliferative tumour phenotypes has not been described. The paradox is partially resolved by four distinct possibilities – adaptation, recovery, mitotic escape or indeed, presence of a negligent G2/M checkpoint. Adaptation is where there is overriding of a checkpoint, despite persistence of DNA damage, whereas complete repair of damage or indeed repair to below a threshold that activates the DDR with re-entry into the cell cycle is called recovery. In order to demonstrate checkpoint adaptation, one needs to demonstrate an arrest signal, an arrest and a persistence of the arrest signal despite re-entry into the cell cycle (Bartek and Lukas, 2007).

Toczyski *et al* have demonstrated three key players involved in adaption in yeast (Toczyski et al., 1997). Adaptation-defective mutants at G2/M were characterised as CDC5[(cdc5-ad); Polo-like kinase (Plk)] and CKB2 [(ckb2)subunits of casein kinase II] mutants. Adaptation was rescued with deletion of RAD9. Later work illustrated the importance of Ptc2 and Ptc3 (PP2C-like phosphatases) and the Srs2 helicase (Pellicioli, Toczyski et al., 1997, Pellicioli et al., 2001). Moreover, Yoo et al also demonstrated that Plk in Xenopus inactivates Claspin after a prolonged interphase ar-

rest allowing entry into mitosis despite persistent damage in what was termed a mitotic-escape (Yoo et al., 2004). Taken together, this finding fits quite nicely with the third canonical pathway identified by pathway analysis – mitotic control of polo-like kinases.

In myeloma, aCGH data illustrates categorically that there is widespread persistence of damage across the myeloma genome in a shredding or 'chromotripsis' manner. It is difficult to illustrate an arrest phenotype in primary cells. The literature suggests that malignant plasma cells are arrested in G0, like their non-malignant plasma cell counterparts. Even leaving this aside, this work reveals some highly interesting findings and gives rise to some intriguing possibilities. One possibility suggests that proliferation in myeloma is preceded by failure of the DDR in myeloma to repair DSBs. This has obvious implications for the next cycle of replication which may lead to further genomic instability in an already 'genomically-sick' myeloma clone. The role of AID in B-cell development with both somatic hypermutation and class switching is well established and cannot be ignored. Moreover, the evolving description of chromotripsis, i.e. a single 'cataclysmic' event leading to shredding of the genome, may reveal a potential role of AID induced chromotripsis in myeloma (Stephens et al., 2011). The potential product is a clone with DSB that are not repaired, such that the cell succumbs to adaption or mitotic escape represented clinically as myeloma with a proliferation phenotype. Equally, this work would suggest that myeloma with a proliferative phenotype is significantly associated with G2/M DNA damage response checkpoint, possibly attempting to repair DSBs. Future work may wish to investigate whether this translates to an actual arrest pattern or not.

Using network analysis, this work also confirms the importance of Cyclin D but, in addition, emphasises the influence of three main pillars driving these canonical pathways in myeloma – TP53, IL-6, and MYC. It is also interesting to consider the potential of the p38 MAPK in supporting this proliferative phenotype both directly and indirectly. It may also provide a potential explanation for the potent synergism observed between p38 MAPK inhibitors and CDC7/CDK9 inhibitors.

Connectivity Mapping - Prediction of Suitable Targets of Proliferation

Using connectivity mapping at the Broad Institute, the compounds known to target this particular proliferative signature illustrates some tantalising possibilities. Lamb *et al* demonstrated the potential of connectivity mapping (Cmap) as a means for drug discovery (Lamb et al., 2006, Lamb et al., 2007). It is important to emphasise that this is at best a hypothesis-generating tool that requires biological confirmation. That considered, it nonetheless highlights a number of compounds that have already attracted some attention in the myeloma world – HDACi, Ca^{2+} - channel blockers and mTOR inhibitors. Unfortunately, the CDC7 inhibitor is not included in the reference compounds. It would be clearly of importance in future studies to note what category of compounds it groups with but in addition if it is a potential '*in silico*' treatment for myeloma patients with a high proliferation index.

In conclusion, the proliferative phenotype in myeloma is associated with a gene expression signature pointing towards a problem with the G2/M checkpoint. Cmap predicts a number of potential new drugs that may be potential active against myeloma patients with a high proliferation index but require pre-clinical validation.

CHAPTER 4:

Investigating the hypothesis that the DBF4 Dependent Kinase (DDK), CDC7 is a targetable kinase in myeloma.

INTRODUCTION:

To fulfil this aim, this thesis examined the effects of CDC7 inhibition in six different pre-clinical contexts; these will be discussed in separate sections. To do so, the thesis will use the model proposed by Dalton *et al*, which is now part of the validation core of the MMRC (Dalton et al., 2006). CDC7 inhibition was achieved using the prototype small molecule inhibitor, PHA-767491 and a related bioavailable compound, NMS-354 (Montagnoli et al., 2008 and Menichincheri et al., 2010). Both small molecules were designed as CDC7 inhibitors but they also inhibit CDK9 and are therefore best considered as dual CDC7/CDK9 inhibitors.

Section 4.1 examines the activity of CDC7/CDK9 inhibition in myeloma cell lines and primary myeloma patient samples. In addition, it determines whether inhibition of both kinases is achieved in myeloma cells. It further examines whether there is an effect on the cell-cycle and whether apoptotic machinery are induced or not.

Section 4.2 builds on the preceding section and examines the effect of CDC7/CDK9 inhibition in a number of models of the myeloma microenvironment. This thesis utilises six well-published models - direct exogenous IL-6 and IGF-1 treatments (Klein et al., 1995, Anderson and Lust, 1999, Ogawa et al., 2000, Mitsiades et al., 2004) in serum starved and serum replete conditions; co-culture with bone marrow stromal cells; and lastly, culture with conditioned media (Damiano et al., 1999, Dalton et al., 2004, Bisping et al., 2009).

Section 4.3 examines the effects of CDC7/CDK9 inhibition on the stem cell niche. It examines the effects on clonogenicity, self-renewal, and the myeloma stem cell phenotype (Matsui et al., 2008, Matsui et al., 2004).

Section 4.4 examines the role of CDC7/CDK9 inhibition in combinations with drugs traditionally used as part of anti-myeloma treatment strategies using the Chou-Talalay methodology (Chou, 2008).

Section 4.5 evaluates and explores a particularly novel combination of CDC7/CDK9 inhibition and p38 MAP kinase inhibition in myeloma cells.

Section 4.6 builds on preceding work to evaluate the effects of CDC7/CDK9 inhibition *in vivo* using the de-novo transgenic Vk*MYC myeloma mouse model (Chesi et al., 2008).

RESULTS:

4.1. Examining CDC7/CDK9 inhibition in myeloma cells.

The relative increase in proliferation in myeloma cells is now seen as the worst predictor of overall survival and time to progression. This is so, despite the introduction of novel agents including proteasome inhibitors and immunomodulating treatments (Steensma et al., 2001, Hose et al., 2011, Dhodapkar et al., 2014). The myeloma kinome has been interrogated using a variety of approaches, but these have unanimously failed to examine or include CDC7 (Claudio et al., 2007, Tiedemann et al., 2009). As CDC7 is critical for initiation of replication, this thesis examines whether its inhibition demonstrates efficacy in a number of myeloma pre-clinical models.

The activity of PHA-767491 and NMS-354 as a single agent in myeloma cell lines

In order to assess the capability of a CDC7/CDK9 inhibitor to affect cell division and survival of myeloma cells, a panel of human myeloma cell lines was challenged with the prototype CDC7/CDK9 inhibitor, PHA-767491 and its related bioavailable compound, NMS-354. This panel of myeloma cell lines represents, broadly, the spectrum of primary non-random translocations, which define myeloma, and also contains TP53 mutants.

The viability of myeloma cells treated with CDC7/CDK9 inhibitors was assessed by CellTitre Glo, an ATP-based cell viability assay, 72 hours after drug treatment. Statistical comparison of TP53 mutant versus wild-type was completed using the student t-test. Correlation was calculated using bivariate analysis with least squares regression. IC_{50} represents the concentration of the drug that induces 50% drop in viability as assessed by CellTitre Glo using non-linear four parametric logistic graph-fitting approach (slope, IC_{50}, upper and lower value normalisation).

Figure 4.1

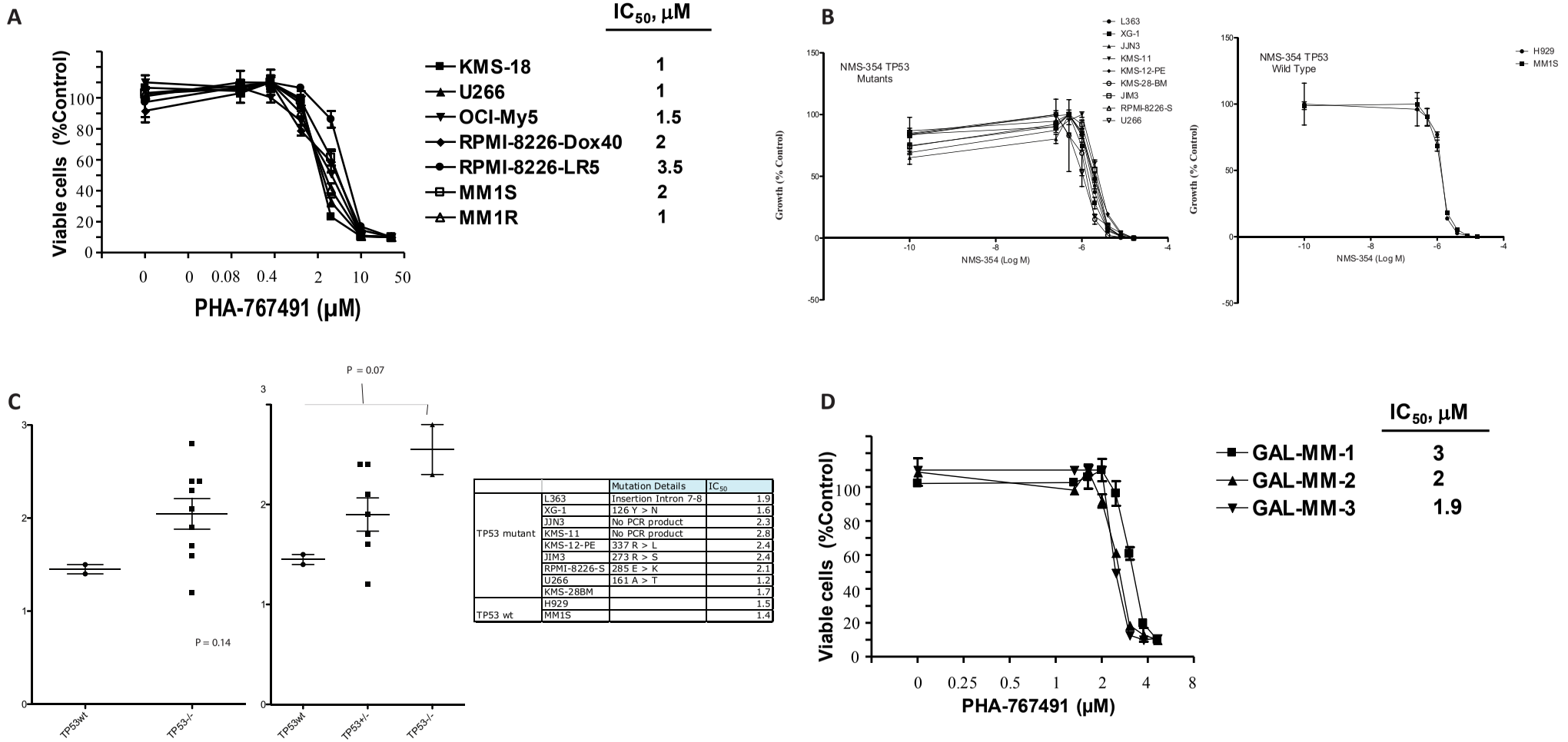

		Mutation Details	IC_{50}
TP53 mutant	L363	Insertion Intron 7-8	1.9
	XG-1	126 Y > N	1.6
	JJN3	No PCR product	2.3
	KMS-11	No PCR product	2.8
	KMS-12-PE	337 R > L	2.4
	JIM3	273 R > S	2.4
	RPMI-8226-S	285 E > K	2.1
	U266	161 A > T	1.2
	KMS-28BM		1.7
TP53 wt	H929		1.5
	MM1S		1.4

Figure 4.1. Anti-myeloma activity of PHA-767491 and NMS-354. Activity of **A.** PHA-767491 **B.** NMS-354 against both drug-sensitive and drug-resistant myeloma cell lines, including the dexamethasone-resistant MM.1R, doxorubicin-resistant RPMI-8226/Dox40 and melphalan-resistant RPMI-8226/LR5 cells. **C.** Comparision of activity of NMS-354 in TP53 mutant and non-mutant myeloma cell lines. Tabular summary adjacent to scatterplots. **D.** Activity of PHA-767491 against primary myeloma tumour cells isolated from patients resistant to conventional or investigational therapies (including conventional or high-dose chemotherapy, thalidomide, lenalidomide and bortezomib). Cell viability was examined by CellTitre Glo 72 hours after drug treatment. For each sample, bars represent percent survival (mean ±SD) of drug-treated cells of at least three independent experiments.

Cell viability was inhibited at low micromolar levels of PHA-767491 in all cell lines with an average and median IC_{50} value of 2.25 µM and 2 µM respectively (Figure 4.1.A). Importantly, PHA-767491 is equally active in myeloma cell lines resistant to conventional agents including cell lines such as MM1R (dexamethasone), RPMI-8226-Dox40 (doxorubicin) and RPMI-8226-LR5 (melphalan) (Figure 4.1.A). In addition, its bioavailable related compound, NMS-354 illustrates similar efficacy but with significantly more potency (Figure 4.1.B). It is important to note that, although there were few cell lines that were wild-type TP53, there was no significant difference in mean IC_{50} of mutant versus wild-type TP53 cell lines (Figure 4.1.C). Moreover, there was no correlation of gene expression proliferation index (gPI) and IC_{50} of cell lines ($r = 0.01$).

Overall, these experiments demonstrate that PHA-767491 and NMS-354 treatment is equally active in myeloma cells lines, even those with known resistance to dexamethasone, doxorubicin, and melphalan. Mutation of TP53 does not confer resistance to either compound, although the number of lines with wild type TP53 status is small. NMS-354 shows similar efficacy to PHA-767491 but with increased potency.

PHA-767491 induces cytotoxicity in primary myeloma cells extracted from patients refractory to conventional and novel anti-myeloma agents.

The efficacy of PHA-767491 on $CD138^{+}$ purified primary tumour cells from three myeloma patients who have relapsed after conventional or high-dose cytotoxic chemotherapy as well as novel therapeutics such as immunomodulatory thalidomide derivatives or the proteasome inhibitor bortezomib was then tested (Table 4.1). The three patients sampled also represent a cohort with poor prognostic features (baseline cytogenetics, mSMART 1.0, ISS score and clinical progression to standard and novel therapeutics).

Table 4.1

Primary Sample	Cytogenetics	ISS	mSMART	Prior Rx
GAL-MM-1	Tetraploid, 13q-	Stage 3	High Risk	MPT/V/R/D
GAL-MM-2	Clonal Evolution. t(11;14)	Stage 3	High Risk	VMPT/ASCT
GAL-MM-3	t(4;14)	Stage 3	High Risk	VRD/ASCT

Table 4.1. Clinical characteristics of primary myeloma samples. Table listing relevant cytogenetic abnormality, International Staging Score (ISS), mSMART score, and prior treatments received by the individual patients. mSMART - Mayo Clinic Stratification for Myeloma and Risk adapted therapy. MPT - Melphalan, Prednisolone and Thalidomide. V - bortezomib (Velcade). R- lenalidomide (Revlimid), D - Dexamethasone. ASCT - Autologous Stem cell therapy. mSMART score is version 1.0.

As indicated in the Figure 4.1, cell viability was examined by CellTitre Glo, an ATP-based cell viability, 72 hours after drug treatment.

Recognising the sample number was small, it was nonetheless found that PHA-767491 was capable of reducing the viability of these primary myeloma cells with an average and median IC_{50} value of 2.3 µM and 2 µM, respectively (Figure 4.1.D). These results indicate that PHA-767491 induces cytotoxicity in myeloma cell lines as well as primary myeloma cells, even in those patients clinically resistant to conventional and novel therapeutics.

PHA-767491 causes a transient accumulation of cells traversing the S-phase of the cell cycle followed by apoptosis

To characterise the effect of PHA-767491 on the cell cycle of myeloma cells, KMS-18 was treated with either dimethyl sulfoxide (DMSO) or 5 µM PHA-767491 in a time course experiment. KMS-18 is a myeloma cell line that carries the translocation t(4;14), associated with poor clinical prognosis and which affects the expression of multiple genes associated with proliferation (Brito et al., 2009). Samples were taken, and the percentage of cells in different phases of the cell cycle was assessed by measuring the DNA content of each cell by flow cytometry.

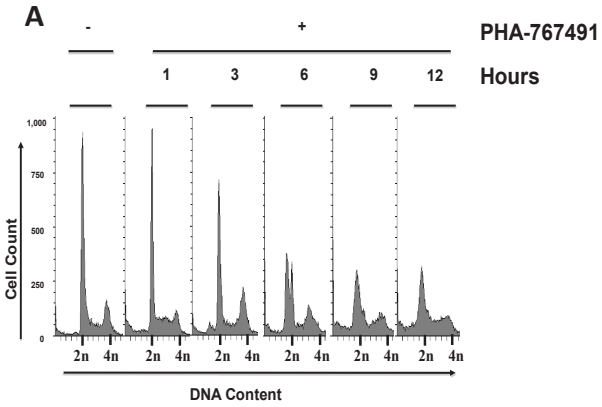

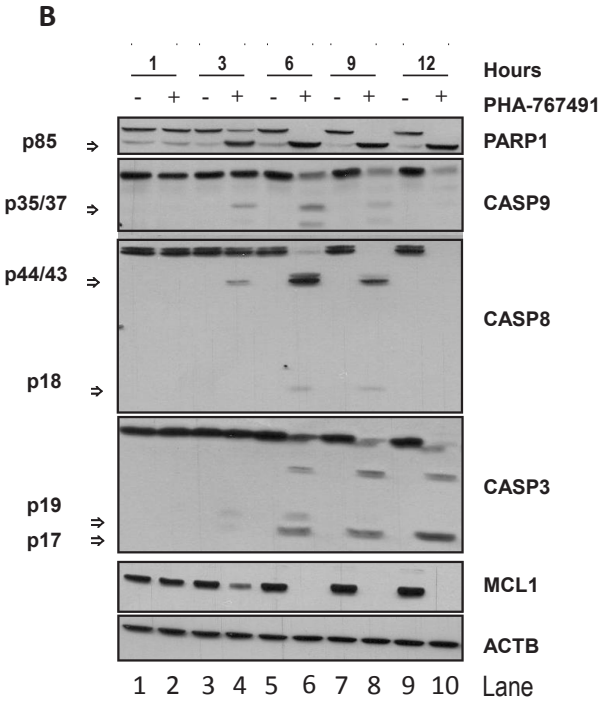

Figure 4.2

C

	Cell Cycle Phase, % Total Events			
Time, hour.	Sub-G1	G1	S	G2M
Control	10	52	21	16
1	15	46	28	11
3	14	38	21	27
6	41	22	25	12
9	49	15	23	13
12	50	14	24	12

Figure 4.2. PHA-767491 causes transient accumulation of myeloma cells with S and G2 DNA

content, MCL1 downregulation and apoptosis. KMS-18 myeloma cells were incubated with 5 µM PHA-767491 for the indicated time. **A.** Cells were fixed, stained with propidium iodide and analysed by flow cytometry for cell cycle profile. **B.** Protein extracts were prepared and analysed by immunoblotting for markers of apoptosis using the indicated antibodies. Arrows indicate individual caspase cleavage fragments. **C.** Table summary of % cell cycle phase of results illustrated in Figure 4.2.A.

After one hour of treatment, there was an increase in the number of cells with an S-phase DNA content, while after three hours the fraction of cells with either fully or almost fully replicated DNA content was 27% compared with 16% in control cells. At later times, a massive and progressive accumulation of cells with less than 2N DNA content was observed (Figure 4.2.A. and C). These results are consistent with the finding that KMS-18 myeloma cells, like other cancer cell types and unlike primary fibroblasts (Montagnoli et al., 2004, Montagnoli et al., 2008), are unable to restrain entry into an abortive S-phase caused by CDC7 inhibition and thus unable to survive PHA-767491 treatment.

The apoptotic machinery is involved in the response of myeloma cells to PHA-767491. MCL1 is possibly the key factor regulating the overall levels of apoptotic cell death observed in myeloma cells in response to the pharmacological inhibition of CDC7/CDK9.

To investigate the mechanism of cytotoxicity in myeloma cells triggered by pharmacological CDC7/CDK9 inhibition, protein samples prepared from the same KMS-18 cells were analysed by immunoblotting with a range of antibodies using a candidate approach. MCL1 is an anti-apoptotic protein critical for survival in myeloma cells and most malignant B-cells (Wuilleme-Toumi et al., 2005, Gojo et al., 2002, Derenne et al., 2002, Beroukhim et al., 2010).

MCL1 showed a potent, time-dependent, reduction within three hours of treatment with PHA-767491 (Figure 4.2.B; Lane 4, 6, 8, 10). Moreover, the kinetics of activation of the initiator caspases 8 and 9 as well as the executioner caspase 3 and cleavage of its substrate PARP1 correlated with the downregulation of MCL1 (Figure 4.2.B).

Altogether, these results indicate that the apoptotic machinery is involved in the response of myeloma cells to PHA-767491 and suggest that MCL1 is possibly the key factor regulating the overall levels of apoptotic cell death observed in myeloma cells.

PHA-767491 induced apoptosis involves BAX/BAK1 activation.

PHA-767491 induces downregulation of MCL1. BAX and BAK1 are the gateway proteins to the mitochondrial, intrinsic, apoptosis pathway, ultimately inducing apoptosis via mitochondrial outer membrane permeabilisation (MOMP). The binding of BCL2 proteins to BAX and BAK1 differs depending on the protein involved. MCL1 binds better to BAK1, but MCL1 can also effectively block BAX mediated apoptosis. The effect of PHA-767491 on BAX and BAK1 oligomerisation were assessed.

KMS-18 myeloma cells were pre-incubated with 50 µM Boc-D, a pan-caspase inhibitor, for one hour prior to treating the same cells with 5 µM PHA-767491 for six hours. Additional controls of no treatment and individual PHA-767491 and Boc-D treatments were synchronously processed. PARP1 cleavage was also examined to illustrate that Boc-D is functioning in the experiment.

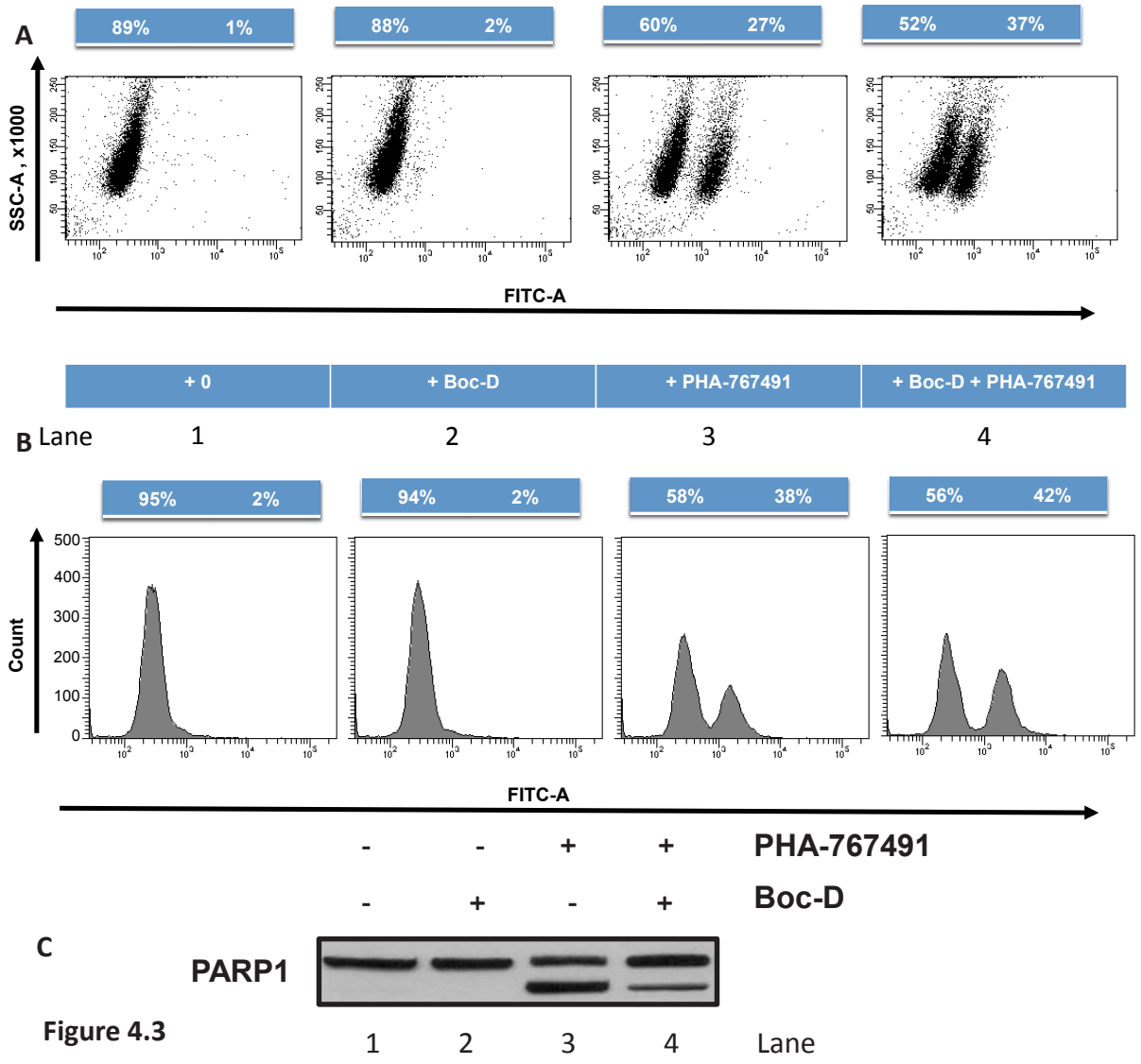

Figure 4.3

Figure 4.3. BAK1 and BAX are activated. KMS-18 myeloma cells were incubated with 5 µM

PHA-767491 for six hours. In Boc-D treated samples, samples were pre-treated with 50 µM Boc-D for one hour. Cells were fixed, permeabilised and incubated with antibodies for **A.** BAK1 and **B.** BAX. **C.** Protein extracts were prepared and analysed by immunoblotting for PARP1 (PARP) cleavage in order to demonstrate and control for Boc-D activity. Boc-D indicates BOC-Asp (OMe)-FMK - Caspase Inhibitor.

This revealed that both BAK1 and BAX are activated, with similar levels of activation [(27% (BAX) versus 38% (BAK1)) Figure 4.3 A3 and B3]. Both BAK1 and BAX activation are not inhibited by Boc-D, the pan-caspase inhibitor (Figure 4.3 A4 and B4). There is reduction of PARP1 cleavage indicating that apoptosis is inhibited in Boc-D treated samples. Although the initiator CASP8 is also cleaved, it is clear that CDC7/CDK9 inhibition induces activation of mitochondrial gateway proteins BAK1 and BAX indicating that PHA-767491 acts also through the intrinsic apoptosis pathway.

PHA-767491 induced apoptosis involves activation of BAX and BAK1, the gateway mitochondrial proteins.

PHA-767491 potently inhibits biomarkers of CDC7 and CDK9 activity.

The reduction of Ser40MCM2 phosphorylation is a sensitive pharmaco-dynamic marker of CDC7 inhibition (Montagnoli et al., 2008, Vanotti et al., 2008). KMS-18 myeloma cells were again treated with 5 µM PHA-767491 in a time course and processed for immunoblotting, using specific antibodies recognising either total MCM2 protein or the CDC7 dependent phosphorylated species of MCM2.

To assess the inhibition of CDK9 by PHA-767491, cellular levels of phosphorylation of the carboxy-terminal repeat domain (CTD) of RNA pol II at serine 2 were measured (Hampsey and Reinberg, 1999).

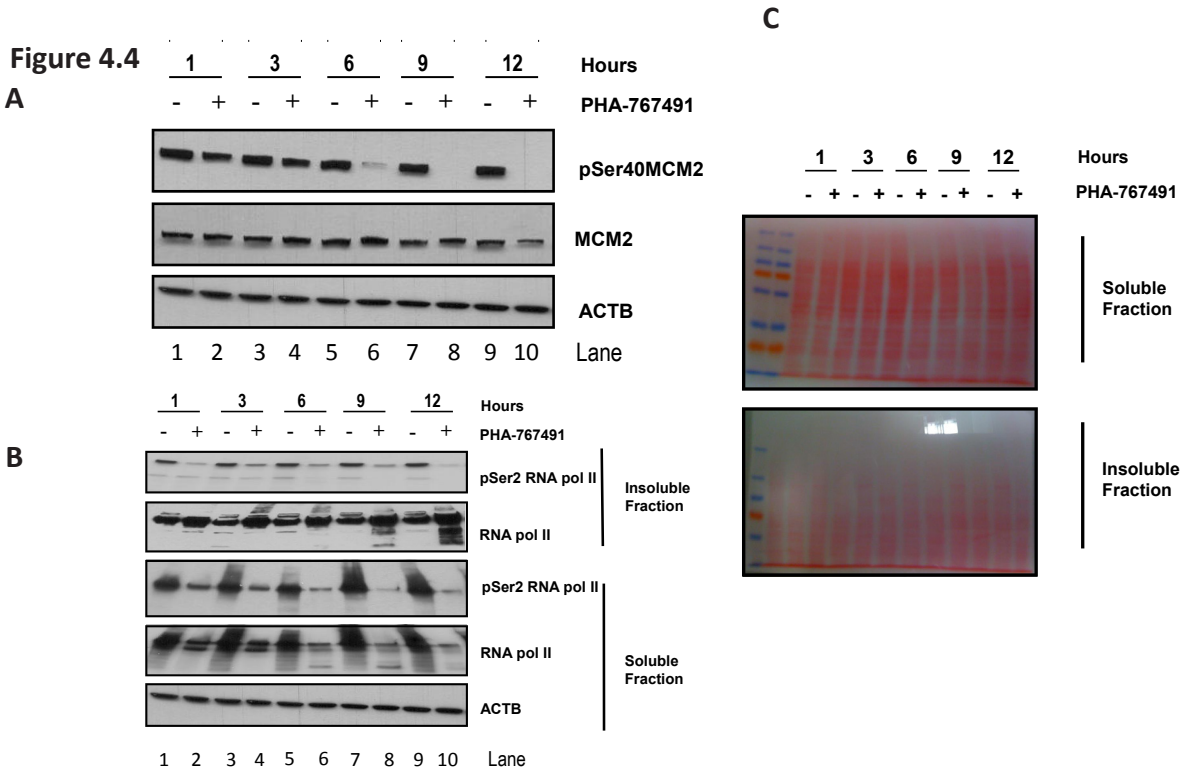

Figure 4.4. PHA-767491 inhibits CDC7 and CDK9 kinases. KMS-18 myeloma cells were incubated with or without 5 μM PHA-767491 for the indicated time. Protein extracts were prepared and analysed by immunoblotting for **A.** levels of MCM2 phosphorylation at serine 40, a specific biomarker of CDC7 activity **B.** levels of RNA polymerase II phosphorylation at serine 2, a specific biomarker of CDK9 activity. This analysis isolated a soluble and insoluble chromatin-enriched fraction. Levels of total MCM2 and β-actin were included as controls. **C.** Loading control for the insoluble fraction.

Consistent with direct inhibition of CDC7 kinase by PHA-767491, it was observed that MCM2 phosphorylation at serine 40 was reduced as early as one hour post-treatment, with a progressive and complete loss at later time points (Figure 4.4.A; Lane 2, 4, 6, 8, 10).

Upon treatment with PHA-767491, levels of pSer2 RNA pol II decreased with kinetics that closely mirrors that of pSer40MCM2 (Figure 4.4.B). Moreover, by biochemical fractionation of the extract into a soluble protein fraction and an insoluble chromatin-enriched fraction, it was observed that RNA pol II accumulates in the insoluble fraction, suggesting that the dynamics of transcription complexes could be affected (Figure 4.4.B and Figure 4.4.C). Taken together, this indicates that PHA-767491 inhibits both CDC7 and CDK9 activity, thereby directly affecting DNA replication and possibly RNA polymerase II - dependent transcription in myeloma cells.

4.2. Examining CDC7/CDK9 inhibition in myeloma models of the microenvironment.

Given the major role that microenvironmental signals play in drug resistance (Dalton et al., 2004, Hideshima et al., 2001), several experimental models have been developed with the goal of mimicking the interactions of myeloma cells with the microenvironment. Such models include the addition of exogenous survival signals, such as IL-6 (Klein et al., 1995, Anderson and Lust, 1999) and IGF-1 (Ogawa et al., 2000, Mitsiades et al., 2004) or co-culture with bone marrow stromal cells (Cell adhesion mediated – drug resistance, CAM-DR and environmentally mediated – drug resistance, EM-DR) (Dalton et al., 2004). These models attempt to recreate the paracrine, autocrine and receptor mediated effects on myeloma cell proliferation and drug resistance.

IL-6 and IGF-1

The ability to supplement serum rich media with specific factors allows for the assessment of chemoresistance induced by such factors in the context of multiple active proliferation and survival pathways. Serum deprivation followed by addition of a single exogenous factor allows the contribution of such a factor to be assessed independently from other mitogenic and survival factors.

It was, therefore, decided to examine whether the addition of IL-6 and IGF-1 could overcome the cytotoxic effects of PHA-767491 in both the presence and absence of serum. Two sets of controls were used. It has been published previously that supplementation with IL-6 offered some protection from treatment with bortezomib and dexamethasone (Mitsiades et al., 2004 and Bisping et al., 2009). In addition, IGF-1 and IL-6 induces AKT1 signalling with phosphorylation of AKT1 at threonine 308.

Figure 4.5

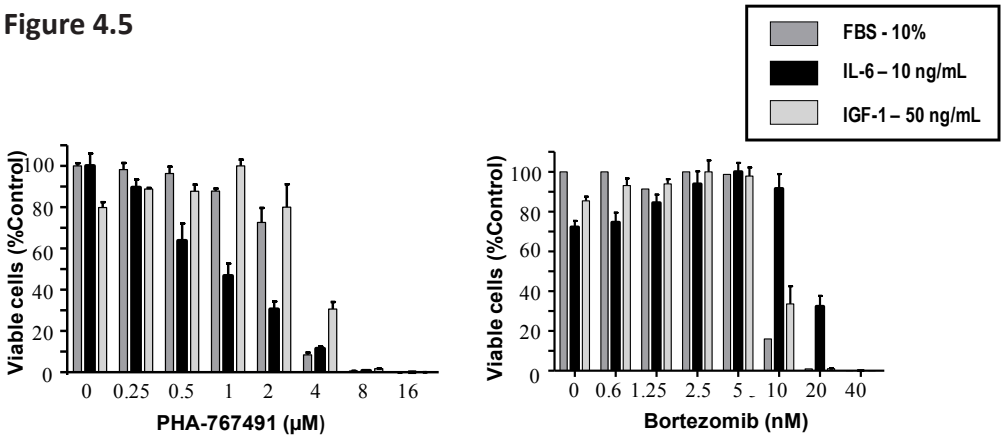

Figure 4.5. PHA-767491 inhibits viability of MM1S cells in the presence of IL-6 and IGF-1. MM1S cells were cultured in normal serum conditions (dark grey bars) or with the additional presence of 10 ng/ml IL-6 (black bars) and 50 ng/ml IGF-1 (light grey bars). Cells were challenged with the indicated concentration of PHA-767491 and cell viability was examined by CellTitre Glo 24 hours after drug treatment. For each sample, bars represent percent survival (mean ± SD) of drug-treated cells.

Figure 4.6

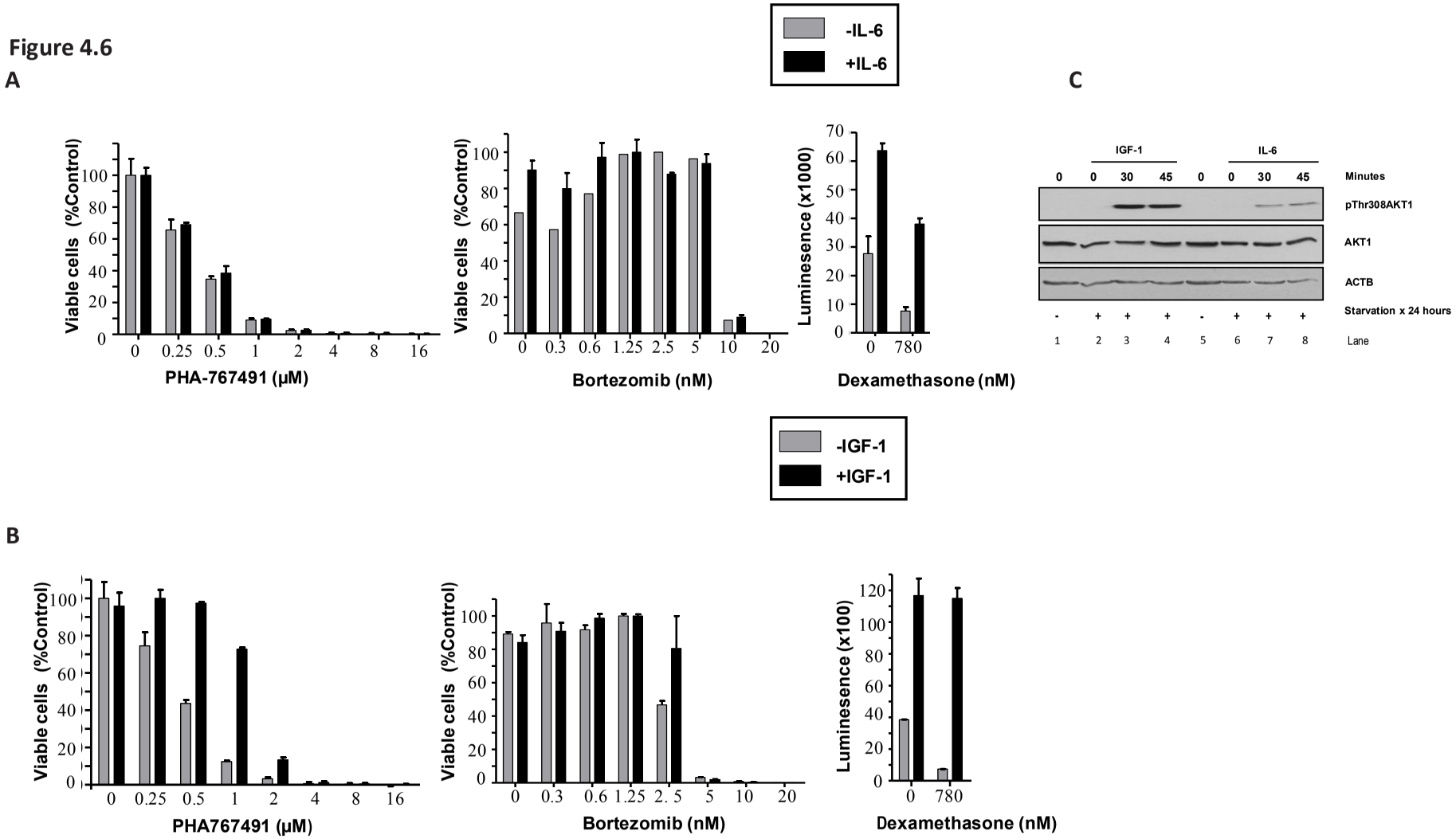

Figure 4.6. PHA-767491 inhibits viability of MM1S cells in the presence of IL-6 and IGF-1 under serum starvation conditions. A. After growing MM1S cells for 24 hours in serum-free media, cells were cultured further in the presence (black bars) or absence (dark grey bars) of 10 ng/ml IL-6 and **B.** presence (black bars) or absence (dark grey bars) of 50 ng/ml IGF-1. In both cases myeloma cells were challenged with the indicated concentration of drugs for 24 hours and viability was assessed. For each sample, bars represent percent survival (mean ± SD) of drug treated cells. **C.** IGF-1 and IL-6 induce AKT1 signaling. Serum starved MM1S cells were cultured in presence of 10 ng/ml IL-6 and 50 ng/ml IGF-1 for 30 and 45 minutes. Protein extracts were prepared and analysed by immunoblotting for a marker of AKT1 signaling (pThr308). Total AKT1 and β-actin were included as loading controls.

Interestingly, the cytotoxic activity of PHA-767491 did not decrease when MM1S myeloma cells were grown in the presence of 10 ng/ml IL-6 in normal serum conditions (Figure 4.5); if anything PHA-767491 appears to be slightly more active upon IL-6 stimulation.

In contrast, when grown in the presence of 50 ng/ml IGF-1, the IC50 of PHA-767491 increased from 2.5 µM to 3.5 µM (Figure 4.5), while the potency of bortezomib was not affected.

When myeloma cells were challenged in the absence of serum, PHA-767491 was significantly more potent compared with normal serum conditions (IC50 0.4 µM versus 2 µM), indicating that some as yet unidentified serum component can provide protection (Figure 4.6). Under these serum-free conditions, addition of IL-6 did not protect against PHA-767491 or bortezomib (Figure 4.6.A), while IGF-1 increased PHA-767491 IC50 from 500 nM to 1 µM.

Cell-adhesion Mediated Resistance

As the bone marrow microenvironment has been shown to confer drug resistance in myeloma cells, the effect of PHA-767491 on myeloma growth after stromal stimulation with HS-5-GFP cells was assessed.

MM1S cells were either mock treated or stimulated with HS-5-GFP cells for 7 hours of direct contact, removed and replated prior to drug treatment to look for evidence of cell-adhesion mediated resistance (CAM). PHA-767491 was cytotoxic to HS-5-GFP as this was a transformed line. To examine the individual effect on myeloma cells, myeloma cells were removed as indicated. The presence of only myeloma cells and not HS-5-GFP was assessed by flow cytometry staining for CD138 expression.

Figure 4.7

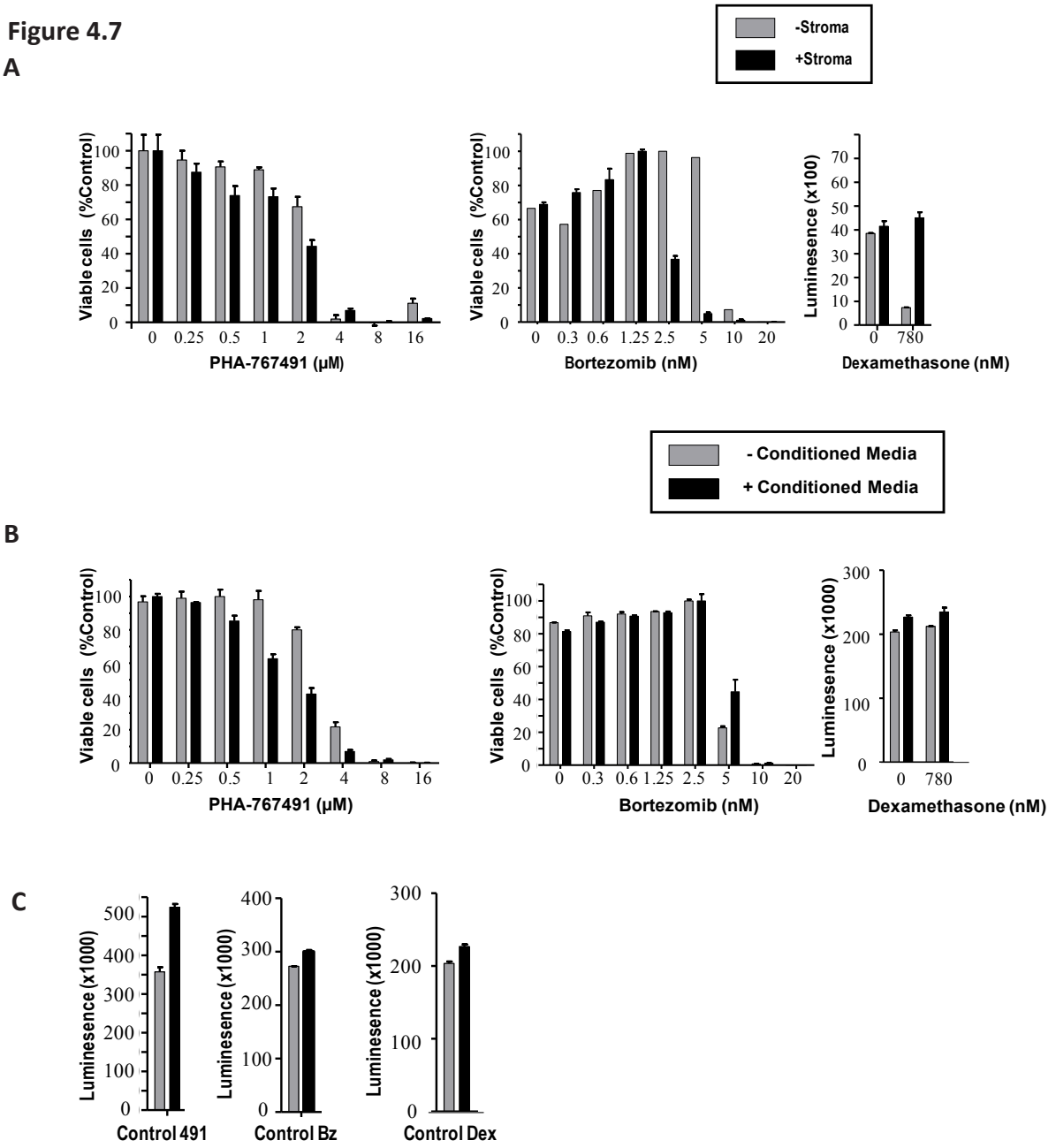

Figure 4.7. PHA-767491 inhibits viability of MM1S cells in the presence of HS-5-GFP stromal cells, and conditioned media of HS-5-GFP stromal cells. A. MM1S cells were cultured in normal serum conditions (dark grey bars) or with after HS-5 receptor priming for 7 hours (black bars). **B.** MM1S were cultured in normal serum conditions (dark grey bars) or with 20% 48 hour-old HS-5 conditioned media (black bars). In both cases myeloma cells were challenged with the indicated concentration of drugs for 24 hours and the viability assessed. For each sample, bars represent percent survival (mean ± SD) of drug-treated cells. **C.** MM1S control cells treated with vehicle culture (dark grey bars) or with 20% 48 hour-old HS-5 conditioned media (black bars). Y-axis Luminescence x 1000.

HS-5-GFP cells did not confer any CAM resistance to PHA-767491, however they protected cells from dexamethasone (Figure 4.7.A).

Conditioned Media

To account for stromal-derived survival factors other than direct adhesion, MM1S were cultured with 20% conditioned media derived from 48 hour pre-confluent HS-5-GFP cells.

Under these conditions, the addition of conditioned media stimulated cellular metabolism evidenced by an increase ATP production (Figure 4.7.C). However, the potency of PHA-767491 in inducing cytotoxicity was not altered (Figure 4.7.B). Similar results were obtained with bortezomib and dexamethasone (Figure 4.7.B).

Overall, these experiments indicate that IL-6 treatment, direct contact with stroma, or culturing in conditioned media does not alter the anti-proliferative effects of PHA-767491, however IGF-1 confers a moderate resistance to PHA-767491.

4.3. Examining CDC7/CDK9 inhibition in the myeloma stem cell niche.

Cancer stem cells (CSC) were originally identified in human acute myeloid leukaemia two decades ago (Lapidot et al., 1994). This was followed by CSC being described in an increasing number of human cancers, including colon, pancreas, and head and neck carcinomas (O'Brien et al., 2007, Ricci-Vitani et al., 2007, Li et al., 2007 and Prince et al., 2007). The self-renewal and long-term growth potential of CSC suggest they are ultimately responsible for disease relapse and progression. The Matsui lab originally isolated and characterised clonogenic cells within myeloma cell lines and primary clinical specimens, finding them to resemble memory B cells ($CD138^{neg}CD19^{+}CD27^{+}$), that give rise to differentiated $CD138^{+}$ plasma cells and are relatively resistant to agents used to treat myeloma (Matsui et al., 2004, Matsui et al., 2008). Alternative interpretations are increasingly proposed by other investigators, with the introduction of newer synonyms such as tumour initiating cells, states of resistance and concepts of self-renewal (Rasmussen et al., 2010, Yata and Yaccoby, 2004, Walker et al., 2013, Chaidos et al., 2013). However, there remains a population of residual cells that adopt a state of 'resistance', requiring definitive treatment algorithms (Sigal et al., 2006). Therefore, novel therapies such as CDC7/CDK9 inhibitors may inhibit myeloma stem or tumour initiating cells and improve long-term clinical outcomes.

CDC7/CDK9 inhibition blocks clonogenic growth and self-renewal in myeloma cell lines

Clonogenic growth, as measured by the colony formation assay, has been traditionally used as one of the first tests to assess an effect on the stem cell niche. Self-renewal is the ability of a clone to repopulate, a key aspect of stemness. Both clonogenic growth and self-renewal assays were used by Matsui *et al* in experiments characterising the myeloma stem cell population (Matsui et al., 2008, Matsui et al., 2004). To assess the ability of the CDC7/CDK9 inhibitor to affect clonogenic growth and potentially the myeloma stem cell population, myeloma cell lines were incubated with each drug for 72 hours, then washed free of drug and the clonogenic potential was assessed by examining colony formation in methylcellulose.

Clonogenic growth was established by plating 1000 cells/ml in 1.2% methylcellulose supplemented with BSA, 2-mercaptoethanol and L-glutamine. U266, H929 and RPMI-8226-S have

all being characterised and published as having a clonogenic fraction. U266 and H929 have shown to have an active Hh pathway which is a critical pathway in stem cell survival whereas RPMI-8226-S is inactive. Samples were plated in duplicate onto 35mm^2 tissue culture dishes. Colonies with more than 40 cells were scored at seven days. Self-renewal was assessed through serial plating. This was accomplished by washing plates three times with culture media and re-suspending cells in the original volume of methylcellulose as described earlier.

Figure 4.8

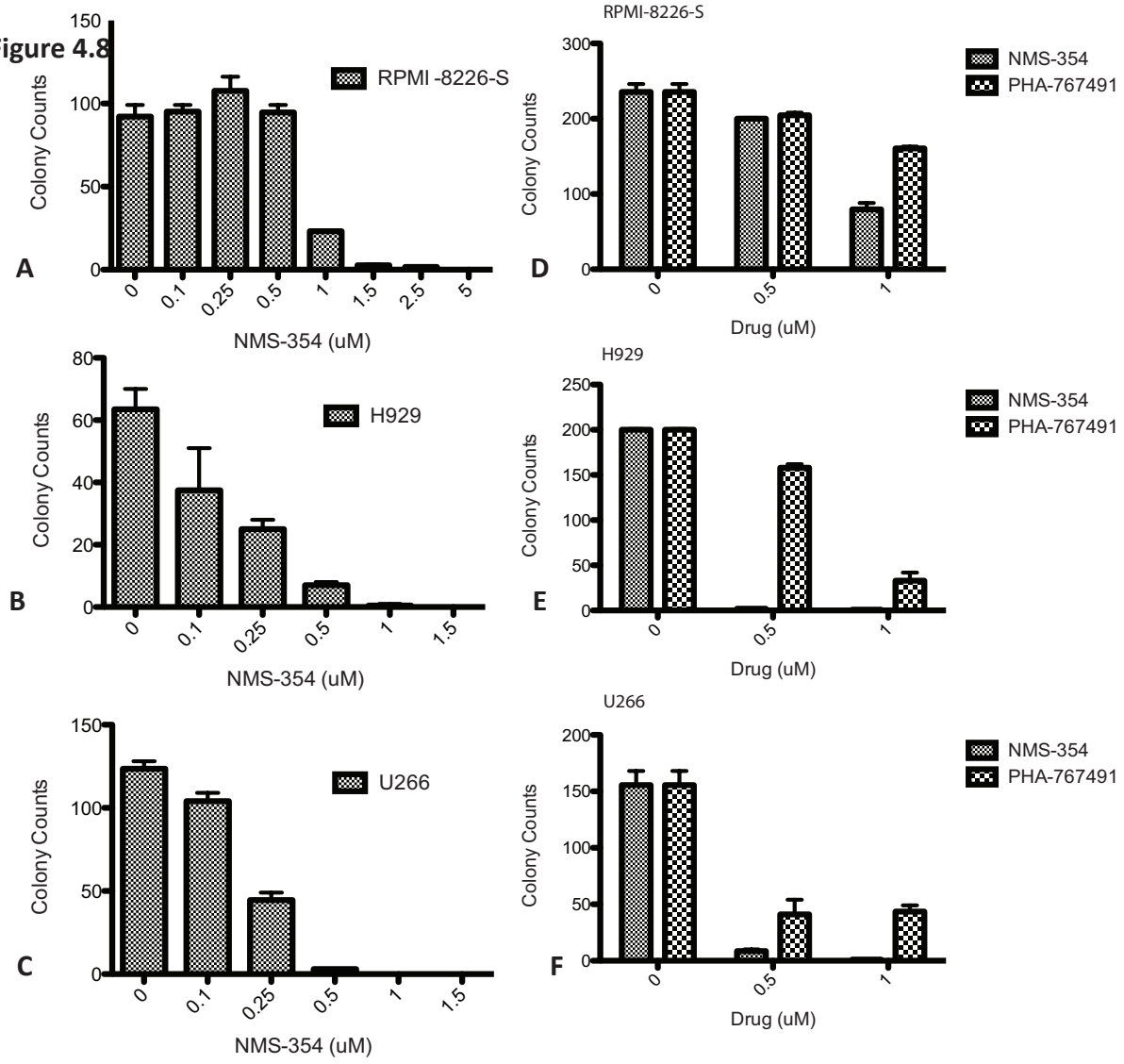

Figure 4.8. Clonogenic recovery of myeloma cell lines. A. RPMI-8226-S, **B.** H929, **C.** U266 post 72 hour treatment with **A-F.** NMS-354 or **D-F.** PHA-767491. Values represent the mean of four experiments.

PHA-767491 and NMS-354 both inhibited clonogenic growth significantly compared with vehicle control in all lines (Figure 4.8). U266, H929 were more sensitive than RPMI-8226-S (Figure 4.8.A-C). NMS-354 had a more potent effect than PHA-767491 (Figure 4.8.D-F). Both drugs showed a more potent effect than that described earlier by the cell viability assay. The loss of clonogenic growth potential could result from a direct toxic effect but there was no

significant increase in the apoptosis of cells treated with either agent at this concentration 0.5 µM, detected by Annexin V/PI staining (Figure 4.9.A-C).

Self-renewal was assessed by the serial plating technique of the colony forming assay. RMPI-S, H929, and U266 myeloma cells were incubated with NMS-354 for 72 hours, then washed free of drug and plated with a density of 1000 cells/ml in duplicate. Once scored at seven days, the same cells were plated with the density relative to the vehicle control which was plated at 1000 cells/ml. Cells underwent two serial or consecutive replating rounds. This is a measure of self-renewal.

Figure 4.9

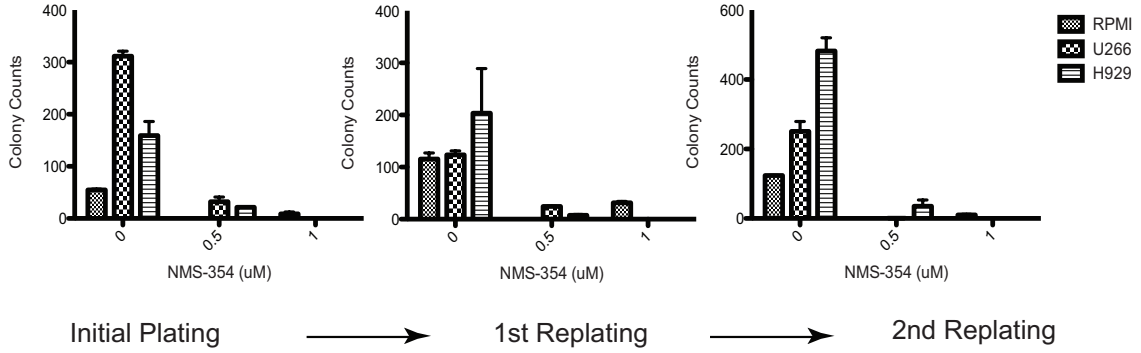

Figure 4.9. Measurement of self-renewal. Clonogenic expansion of RPMI-8226-S, U266 and H929 cells during serial replating after initial NMS-354 treatment at stated dose for 72 hours followed by wash out. Results are the mean SEM of 3 separate experiments for each cell lines and represent the fold clonogenic expansion expressed as a ratio of number of colonies scored compared to the previous plating. SEM = Standard Error of the mean.

All three lines illustrated a block in self-renewal capacity with NMS-354 (Figure 4.9).

CDC7/CDK9 inhibition therefore blocks clonogenic growth and self-renewal in myeloma cell lines.

CDC7/CDK9 inhibition blocks clonogenic growth and self-renewal in primary myeloma cells

The myeloma stem cell is most similar to a pre-memory B-cell, consisting largely of a CD138 negative clone. Mononuclear cells were isolated from the bone marrow aspirates of three patients by density centrifugation then depleted of $CD138^+$ plasma cells and $CD34^+$ cells (to eliminate normal hematopoietic progenitors that complicate clonogenic analyses). Cells were incubated in quadruplicate for 72 hours with 0.5 µM or 1 µM of NMS-354 or vehicle alone and

assessed for inhibition of clonogenic growth. The third patient was incubated with 0.75 μM.

Figure 4.10

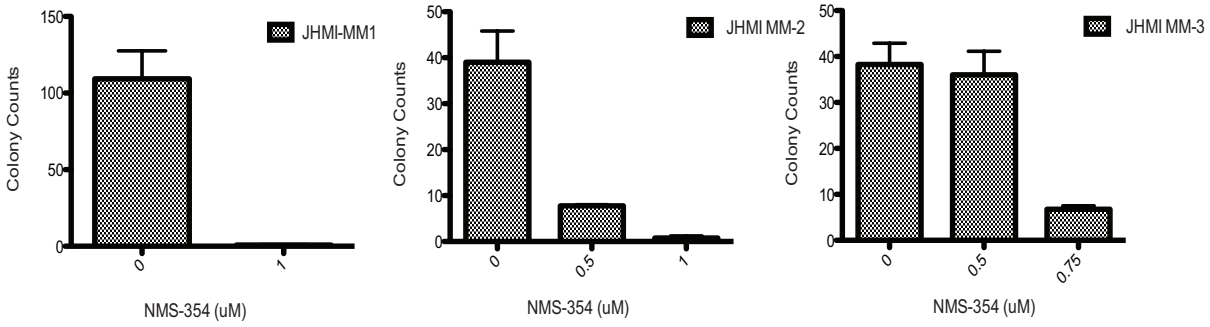

Figure 4.10. Clonogenic recovery of primary myeloma cells. Relative colony formation of CD-138^{neg}CD34^{neg} BM mononuclear cells isolated from three patients with myeloma, treated with NMS-354 at stated doses for 72 hours followed by wash out. Plated in quadruplicate.

All three samples showed similar levels of inhibition of clonogenic growth to that shown for myeloma cell lines (Figure 4.10).

CDC7/CDK9 inhibition was found to block clonogenic growth and self-renewal in primary myeloma cells.

NMS-354 discordantly enriches the putative myeloma stem cell pool

To further explore the effect of NMS-354 on clonogenic growth and self-renewal, H929 myeloma cells were examined for effects on two central characteristics of the myeloma stem cell. The myeloma stem cell has high ALDH activity like most stem cells, but in addition does not express CD138 (Matsui et al., 2008, Matsui et al., 2004).

Figure 4.11

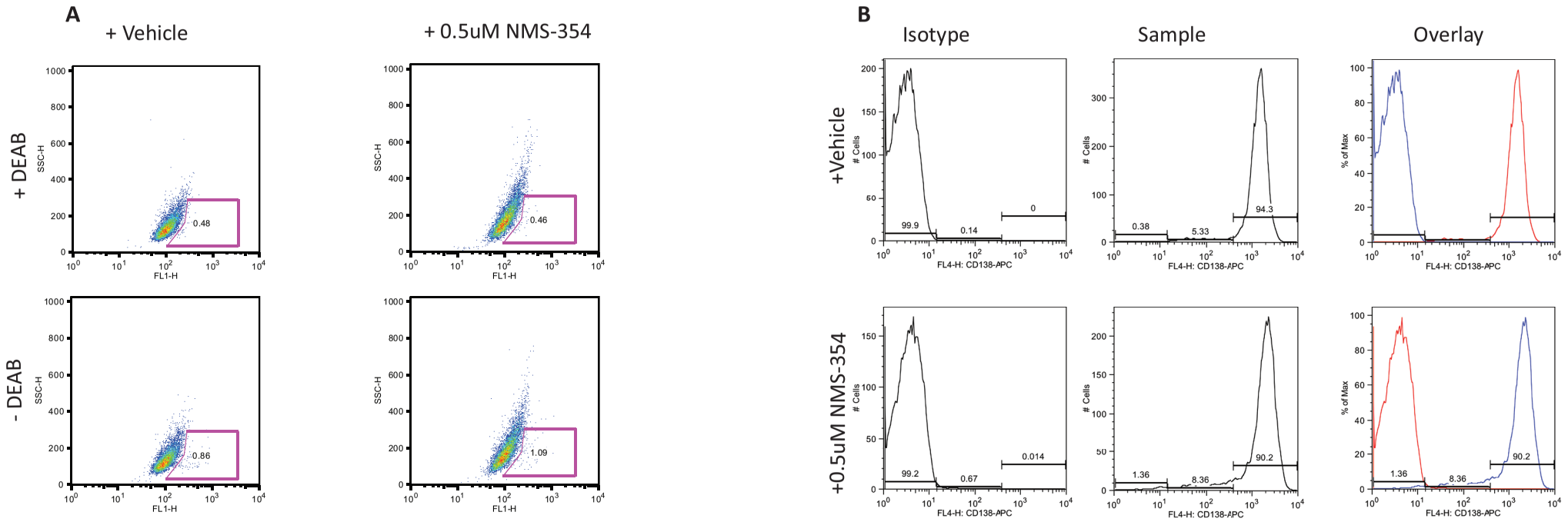

Figure 4.11. NMS-354 potentially enriches the myeloma stem cell pool. H929 cells were treated for 72 hours with 0.5µM NMS-354 and evaluated for **A.** Aldefluor staining and **B.** CD138 expression by flow cytometry. Percentage of stem cells (low side scatter and high FL1) are obtained by using the paired DEAB control to gate the required area. This % is indicated in the purple boxed area. DEAB = diethylaminobenzaldehyde.

Interestingly, there was an increase in both $CD138^{neg}$ cells and cells with high ALDH activity (Figure 4.11). To complement the effect demonstrated with the clonogenic assay, the population of $CD138^{neg}$ with high ALDH staining should be expected to be reduced. Alternatively, this suggests an increase in the myeloma stem cell pool, without differentiation, at 72 hours.

Figure 4.12

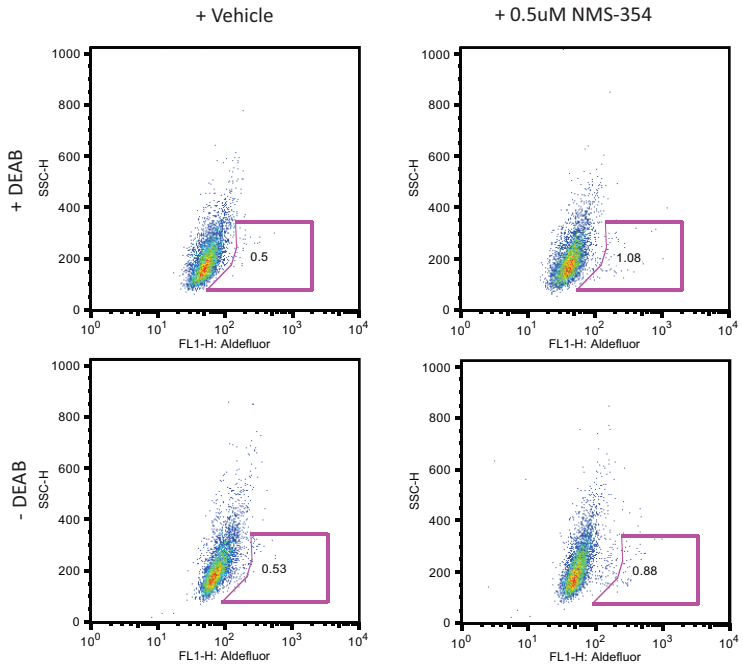

Figure 4.12. NMS-354 enriches the myeloma stem cell pool. H929 cells, as per Figure 4.11, were treated for 72 hours with 0.5 µM NMS-354, washed and plated, were examined 7 days post wash out for Aldefluor staining by flow cytometry. Percentage of stem cells (low side scatter and high FL1) are obtained by using the paired DEAB control to gate the required area. This % is indicated in the purple boxed area. DEAB = diethylaminobenzaldehyde.

To examine if an effect occurred later than that captured at 72 hours, a delayed time point at 7 days post drug washout was completed. ALDH positive cells were once again increased in the NMS-354 treated cells compared to vehicle control (Figure 4.12).

This finding is discordant. NMS-354 enriches the putative myeloma stem cell pool. Instead of a reduction in the stem cell population there is an increase in the stem cell population which can only be rationalised by a direct effect on cell differentiation.

CDK9 inhibition, but not CDC7 inhibition, is important in clonogenic and self-renewal block

PHA-767491 and NMS-354 are dual CDC7 and CDK9 inhibitors. It is hard to separate their individual function. To determine which loss of activity was involved in the block of cell differentiation, surrogate measures of CDC7 and CDK9 function were completed on H929 cells post NMS-354 treatment.

As outlined previously, in section 4.1, the reduction of Ser40 MCM2 phosphorylation is a sensitive pharmaco-dynamic marker of CDC7 inhibition. Equally ALDH activity traditionally measured using Aldefluor reagent is proportional to the amount of ALDH in the cell. Using a dual-staining technique, H929 cells incubated for 72 hours with NMS-354, washed out, were fixed and examined by flow cytometry for changes in phosphorylation of MCM2 and ALDH compared with vehicle control.

CDK9 controls replication-dependent histone 3' end mRNA processing. Replication-dependent histone mRNAs are not usually polyadenylated, but instead end in a conserved stem-loop structure (Pirngruber et al., 2009a, Pirngruber et al., 2009b). With knockdown of CDK9, increased replication-dependent histone mRNA polyadenylation occurs (Pirngruber et al., 2009a, Pirngruber et al., 2009b). To address the inhibition of CDK9 by NMS-354, the level of HIST1H2BD polyadenylation in NMS-354 treated cells compared with vehicle control was examined.

Figure 4.13

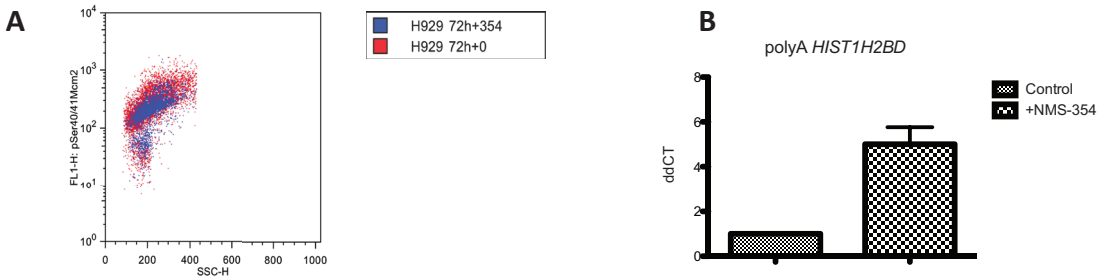

Figure 4.13. CDK9 inhibition but not CDC7 inhibition is important in clonogenic and self-renewal block. H929 cells were treated with 0.5 µM NMS-354 and analysed for **A.** pMCM2 by flow cytometry and **B.** expression of polyadenylated HIST1H2BD by oligo-dT-primed quantitative reverse transcriptase PCR for target inhibition. Gene expression was normalised to an unregulated gene, RPLP0, and the control condition, and is represented as relative mRNA expression; mean value ±SD, n=3.

Despite an increase in ALDH compared with the control, there was no difference in phos-

phorylation, indicating that CDC7 was not inhibited at the incubation dose (Figure 4.13. A). NMS-354 treatment increased polyadenylation of the HIST1H2BD gene approximately 5-fold, consistent with CDK9 inhibition (Figure 4.13.B).

CDK9 inhibition, but not CDC7 inhibition, is therefore important in clonogenic and self-renewal block.

4.4. Examining CDC7/CDK9 inhibition in combination with melphalan, bortezomib, and doxorubicin.

The success of drug combinations has been demonstrated across many cancers but its clear success was most notably captured in the treatment of paediatric acute lymphoblastic leukaemia. The major goal of combination regimens is to attack the clonal process from multiple survival pathways or processes, thus ultimately reducing resistance and preventing clonal escape. Even allowing for current combinations strategies, most myeloma patients relapse and become refractory to current treatment algorithms. Egan *et al* and Walker *et al* have illustrated the effects of certain treatments on genomic evolution within the myeloma clone over time (Egan et al., 2013, Walker et al., 2013).

The combination index (CIn) method of Chou-Talalay is based on the multiple drug effect equation derived from the median-effect principle of the mass-action law. It provides quantitative determination for synergism (CIn <1), additive effect (CIn = 1) and antagonism (CIn > 1. It takes into account both the potency (the Dm value) and the shape of the dose–effect curve (the m value) of each drug alone and their combination. This thesis utilised the Chou-Talalay methodology to assess efficacy of different combinations with the CDC7/CDK9 inhibitor.

PHA-767491 shows an additive effect with melphalan, bortezomib and doxorubicin

In order to test the potential of a CDC7/CDK9 dual inhibitor in combination with standards of care, MM1S myeloma cells were treated with PHA-767491 together with either melphalan, bortezomib, or doxorubicin. Combination experiments were performed by treating cells with each drug in a constant and non-constant combination ratio. After incubation, cell viability was assessed and data was then analysed with the Chou-Talalay median-dose-effect formula. Combination index (CIn) for each experimental combination point was calculated (Chou, 2008).

Combinations were performed simultaneously as well as sequentially.

Figure 4.14

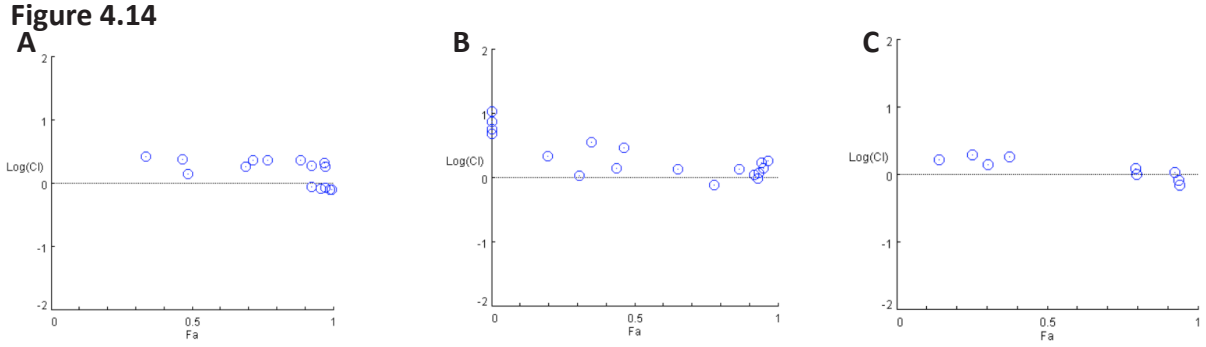

D

PHA-767491 (μM)

Melphalan (μM)

Fa	0	1	2	4	8	16
0	0	0.18	0.39	0.89	0.98	0.98
2	0.49	0.49	0.33	0.92	0.99	0.98
4	0.73	0.47	0.69	0.96	0.99	0.99
8	0.86	0.72	0.77	0.97	0.99	0.99
16	0.95	0.88	0.92	0.99	0.99	0.99
32	0.99	0.97	0.97	0.99	0.99	0.99

CI	0	1	2	4	8	16
0						
2		1.4	2.7	0.9		
4		2.4	1.8	0.8		
8		2.4	2.3	0.9		
16		2.3	1.9	0.8		
32		1.8	2.1	0.8		

E

PHA-767491 (μM)

Doxorubicin (nM)

Fa	0	1	2	4	8	16
0	1	0.76	0.69	0.15	0.04	0.03
31	1.08	0.86	0.73	0.17	0.04	0.04
63	1.1	0.85	0.48	0.15	0.04	0.04
125	0.44	0.41	0.46	0.11	0.03	0.04
250	0.1	0.19	0.2	0.05	0.02	0.03
500	0.04	0.1	0.08	0.03	0.02	0.02

CI	0	1	2	4	8	16
0						
31		1.4	2.5	0.8	0.8	1.5
63		1.9	1.6	0.9	0.9	1.6
125		1.3	2	0.7	1.1	1.8
250		1.2	1.4	1	1.4	2.1
500		1.5	1.5	1.7	2.1	2.8

F

PHA-767491 (μM)

Bortezomib (nM)

Fa	0	1	2	4	8	16
0	0	0.2	0.3	0.8	0.95	0.95
1.3	-0	0.14	0.25	0.8	0.95	0.95
2.5	0.23	0.3	0.37	0.79	0.96	0.96
5	0.94	0.94	0.94	0.92	0.97	0.96
10	0.99	0.99	0.99	0.99	0.99	0.99
20	0.99	0.99	0.99	0.99	0.99	1

CI	0	1	2	4	8	16
0						
1.3		1.8	2	1	0.8	1.5
2.5		1.6	2	1.3	0.8	1.5
5		0.7	0.8	1	1	1.8
10		0.8	0.8	0.9	1	1.3
20		1.6	1.6	1.7	1.8	2

Figure 4.14. Combination Analysis of PHA-767491 using Chou-Talalay Median-Effect Equation. MM1S cells were treated with PHA-767491 and in combination with **A.** Melphalan **B.** Doxorubicin **C.** Bortezomib in a non-constant ratio in a simultaneous fashion. Cell viability was examined by CellTitre Glo 48 hours after drug treatment. Combination Indices (blue circles) were calculated and plotted in relation to the fraction of cells affected (Fa) at any given experimental point. Raw Data is tabulated in **D**, **E** and **F**. The raw data reported in D relates to graph A, E to graph B, and F to graph C.

Figure 4.15

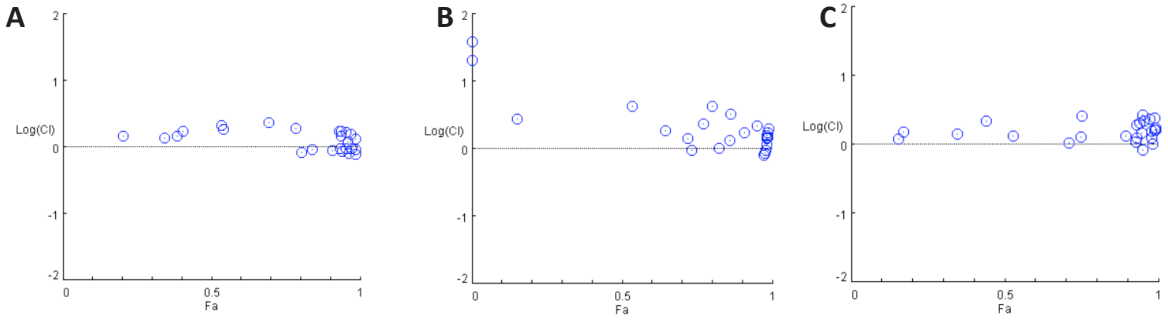

D

PHA-767491 (μM)

Melphalan (μM)

Fa	0	1	2	4	8	16
0	0	-0	0.17	0.77	0.95	0.95
1.3	0.05	0.16	0.17	0.71	0.93	0.93
2.5	0.4	0.34	0.53	0.75	0.93	0.94
5	0.95	0.44	0.95	0.9	0.95	0.95
10	0.98	0.75	0.98	0.98	0.98	0.97
20	0.99	0.95	0.99	0.99	0.99	0.99

CI	0	1	2	4	8	16
0						
1.3		1.2	1.5	1	1	1.9
2.5		1.4	1.3	1.3	1.2	2
5		2.2	0.8	1.3	1.5	2.2
10		2.6	1	1.3	1.7	2.3
20		2.6	1.6	1.6	1.9	2.4

E

PHA-767491 (μM)

Doxorubicin (nM)

Fa	0	1	2	4	8	16
0	0	-0.2	-0.2	0.68	0.97	0.98
31	0.18	-0.1	0.01	0.73	0.97	0.98
63	0.43	0.15	-0	0.82	0.98	0.98
125	0.92	0.72	0.64	0.86	0.98	0.98
250	0.93	0.77	0.53	0.91	0.98	0.99
500	0.98	0.86	0.8	0.95	0.99	0.99

CI	0	1	2	4	8	16
0						
31		0	20	0.9	0.8	1.4
63		2.8	38	1	1	1.5
125		1.4	1.9	1.3	1	1.6
250		2.4	4	1.7	1	1.7
500		3.3	4.3	2.2	1	2

F

PHA-767491 (μM)

Bortezomib (nM)

Fa	0	1	2	4	8	16
0	0	0.02	0.24	0.74	0.94	0.94
2	0.22	0.2	0.34	0.8	0.94	0.93
4	0.47	0.39	0.4	0.84	0.93	0.94
8	0.68	0.54	0.53	0.91	0.95	0.95
16	0.83	0.69	0.78	0.96	0.97	0.97
32	0.98	0.94	0.96	0.99	0.99	0.99

CI	0	1	2	4	8	16
0						
2		1.5	1.4	0.8	0.8	1.7
4		1.5	1.8	0.9	1	1.7
8		1.8	2.1	0.9	1	1.7
16		2.3	1.9	0.8	1	1.6
32		1.5	1.2	0.8	0.9	1.3

Figure 4.15. Sequential combination analysis of PHA-767491 with drugs constituting standard of care. MM1S cells were treated with PHA-767491 and in combination with **A.** Melphalan **B.** Doxorubicin **C.** Bortezomib in a non-constant ratio three hours before PHA-767491 treatment. Cell viability was examined by CellTitre Glo 48 hours after drug treatment. Com-

bination Indices (blue circles) were calculated and plotted in relation to the fraction of cells affected (Fa) at any given experimental point. Raw Data is tabulated in **D**, **E** and **F**. The raw data reported in D relates to graph A, E to graph B, and F to graph C.

Figure 4.16

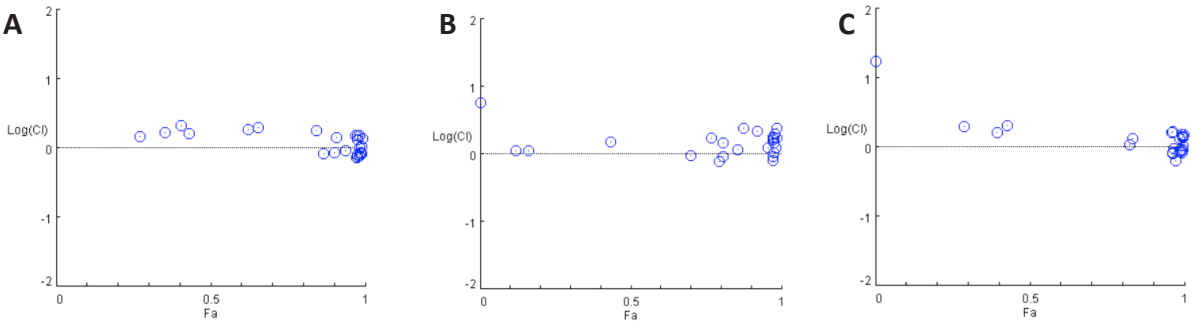

D

Melphalan (μM) \ PHA-767491 (μM)	0	0	1	2	4	8	16
Fa							
0	0	0	0.06	0.22	0.79	0.97	0.97
2	0.28	0.27	0.35	0.87	0.97	0.97	
4	0.53	0.43	0.4	0.9	0.98	0.97	
8	0.76	0.62	0.65	0.94	0.98	0.97	
16	0.89	0.84	0.91	0.98	0.98	0.98	
32	0.98	0.98	0.99	0.99	0.99	0.99	
CI							
0	0	1	2	4	8	16	
0							
2		1.5	1.7	0.8	0.7	1.3	
4		1.6	2	0.8	0.8	1.5	
8		1.9	2	0.9	0.7	1.5	
16		1.8	1.4	0.8	1	1.5	
32		0.9	0.8	0.8	1	1.4	

E

Doxorubicin (nM) \ PHA-767491 (μM)	0	0	1	2	4	8	16
Fa							
0	0	-0.1	0.01	0.72	0.97	0.97	
31	-0	-0	0.12	0.79	0.97	0.97	
63	0.24	0.16	-0.1	0.81	0.97	0.97	
125	0.91	0.7	0.43	0.85	0.98	0.98	
250	0.93	0.81	0.77	0.96	0.98	0.98	
500	0.96	0.87	0.92	0.97	0.99	0.99	
CI							
0	0	1	2	4	8	16	
0							
31		0	1.1	0.8	0.8	1.5	
63		1.1	5.8	0.9	0.9	1.6	
125		1	1.5	1	1	1.7	
250		1.5	1.7	1.2	1.3	2	
500		2.4	2.2	1.8	1.7	2.4	

F

Bortezomib (nM) \ PHA-767491 (μM)	0	0	1	2	4	8	16
Fa							
0	0	0.12	0.33	0.82	0.97	0.96	
1.3	0.08	0.81	0.29	0.82	0.96	0.96	
2.5	0.31	0.39	0.43	0.83	0.97	0.96	
5	0.96	0.97	0.96	0.97	0.99	0.99	
10	0.99	0.99	0.99	0.99	0.99	1	
20	0.99	0.99	0.99	1	1	1	
CI							
0	0	1	2	4	8	16	
0							
1.3		17	2	1	0.8	1.6	
2.5		1.6	2	1.3	1	1.7	
5		0.6	0.8	0.9	0.9	1.3	
10		0.8	0.9	0.9	0.9	1.1	
20		1.5	1.4	1.4	1.4	1.5	

Figure 4.16. Sequential combination analysis of PHA-767491 with drugs constituting standard of care. MM1S cells were treated with PHA-767491 and in combination with **A.** Melphalan **B.** Doxorubicin **C.** Bortezomib in a non-constant ratio three hours after PHA-767491 treatment. Cell viability was examined by CellTitre Glo 48 hours after drug treatment. Combination Indices (blue circles) were calculated and plotted in relation to the fraction of cells affected (Fa) at any given experimental point. Raw Data is tabulated in **D**, **E** and **F**. The raw data reported in D relates to graph A, E to graph B, and F to graph C.

In the first set of experiments, drugs were administered simultaneously. It was observed that almost all CIns calculated were either equal or very similar to 1 supporting an additive effect (Figure 4.14). Similarly, when the drugs were combined in a sequential manner with either melphalan, bortezomib or doxorubicin administered 3 hours before or after PHA-767491, the calculated CIn was still very close to 1 (Figures 4.15 and 4.16).

PHA-767491 therefore shows an additive effect with melphalan, bortezomib and doxorubicin.

4.5. CDC7/CDK9 inhibition and p38 MAP kinase in myeloma cells.

The p38 mitogen activated protein (p38 MAP) kinase is one member of the three families of kinase-sets that are modulated in response to different types of cellular stress in a cell-specific and context-dependent fashion (Wagner and Nebreda, 2009). Im *et al* demonstrated that CDC7 depletion induces apoptosis via an ATR dependent activation on p38 MAP kinase (Im, 2008). Ito *et al* (from the same group as Im, 2008) developed this further, demonstrating two different effects depending on TP53 mutational status (Ito et al., 2012a). The CDC7/CDK9 inhibitor was combined with a p38 MAP kinase inhibitor to assess it this could be also demonstrated in myeloma cells.

Inhibition of the p38MAP kinase does not prevent apoptosis but enhances the cytotoxic effects of PHA-767491 in a synergistic fashion

CDC7 depletion in Hela cells by *si*RNA has been shown to induce apoptosis via an ATR-dependent activation of the p38 MAP kinase. To assess if PHA-767491 depletion of CDC7 induces apoptosis in a similar way, PHA-767491 was combined with a selective p38 MAP kinase inhibitor. If CDC7 depletion with PHA-767491 induces apoptosis dependent on the p38 MAP kinase, such a combination would be expected to induce antagonism with a CIn greater than 1. To evaluate for such an effect, OCI-My5 myeloma cells were treated with each drug in a constant and non-constant combination ratio. After incubation, cell viability was assessed and data was then analysed with the Chou-Talalay median-dose-effect formula. CIn for each experimental combination point was calculated. SB202190 was added one hour prior to addition of PHA-767491 as published previously.

Figure 4.17

A

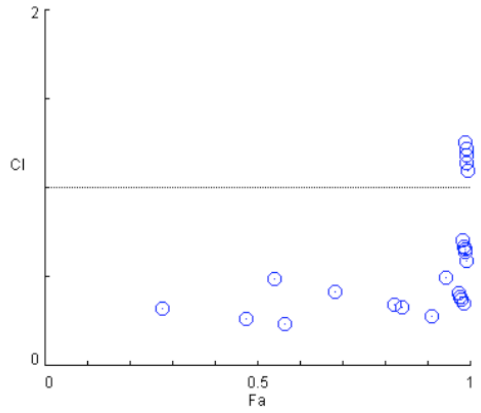

B

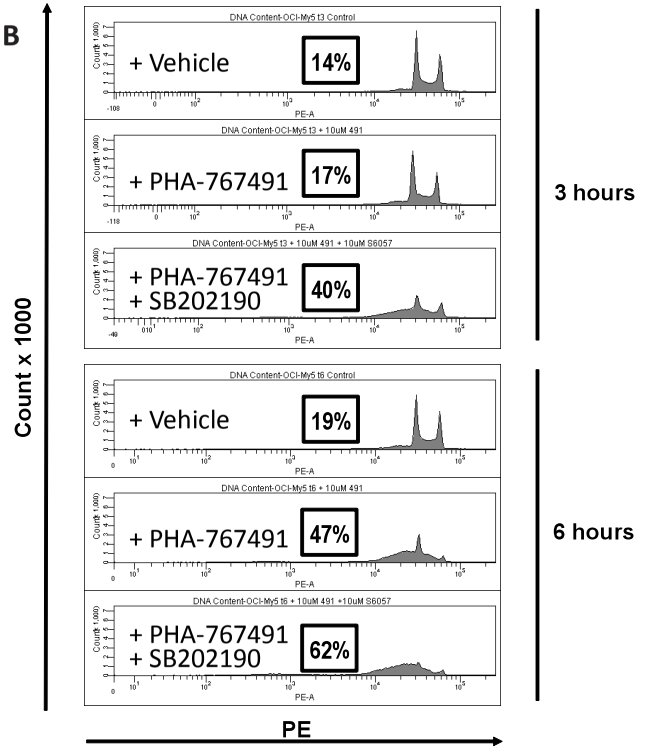

C

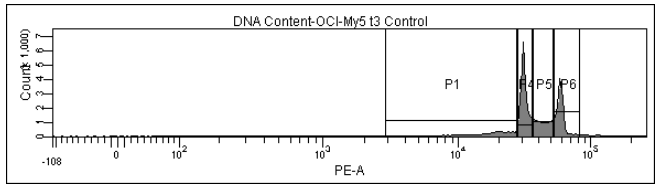

D

PHA-767491 µM

SB202190 µM

Fa

0	0	1	2	4	8	16
0	0.000	-0.146	0.217	0.764	0.941	0.990
1	0.10	0.000	0.541	0.944	0.984	0.990
2	-0.14	-0.028	0.682	0.973	0.987	0.992
4	-0.13	0.276	0.822	0.978	0.988	0.991
8	-0.02	0.473	0.841	0.981	0.989	0.993
16	0.16	0.564	0.912	0.985	0.992	0.994

CI

0	0	1	2	4	8	16
0						
1			0.488	0.500	0.700	1.300
2			0.420	0.400	0.670	1.200
4		0.330	0.340	0.380	0.660	1.200
8		0.260	0.330	0.370	0.640	1.100
16		0.240	0.280	0.350	0.600	1.000

Figure 4.17. PHA-767491 demonstrates potent synergism with the p38 MAP kinase inhibitor, SB202190. A. OCI-My5 myeloma cells were treated with PHA-767491 and SB202190 and in combination in a non-constant ratio in a sequential fashion. PHA-767491 was added one hour after SB202190 treatment. Cell viability was examined by CellTitre Glo 48 hours after drug treatment. Combination Indices (blue circles) were calculated and plotted in relation to the fraction of cells affected (Fa) at any given experimental point. **B.** OCI-My5 myeloma cells were incubated with 10µM PHA-767491 for the indicated time. Cells were fixed, stained with propidium iodide and analysed by flow cytometry for cell cycle profile. Less than 2N DNA content percentages are displayed in the boxes at individual time point profiles. **C.** Illustrates gates used for less than 2 N DNA content percentrages calculation. **D.** Raw data of graph A.

It was observed that all CIns calculated were less than one, showing potent synergism between the two compounds (Figure 4.17.A and D). This was contrary to the rescue phenotype that was expected. To assess the validity of this result further, OCI-My5 myeloma cells were pre-treated with 10 μM SB202190 for one hour prior to adding 10 μM PHA-767491. Additional controls with no treatment and individual PHA-767491 treatments were synchronously processed. Samples were taken and the percentage of cells in different phases of the cell cycle was assessed by measuring the DNA content of each cell by flow cytometry. After three and six hours of treatment, a massive accumulation of cells with less than 2N DNA content compared with controls was observed (Figure 4.17.B).

These results are consistent with the combination analysis findings that inhibition of the p38MAP kinase does not prevent apoptosis but enhances the cytotoxic effects of PHA-767491 in a synergistic fashion.

The synergism demonstrated with PHA-767491 and the p38 MAP kinase inhibitor is a cell-specific event not observed in HeLa cells

The p38 MAP kinase family demonstrates distinct balance and interplay with the Jun N-terminal kinase (JNK kinase) family in integrating proliferation, differentiation, survival and migration signals. This is achieved in a cell-context specific and cell-type specific manner. Apoptosis induced by ATR-dependent activation of p38 MAP kinase was observed in CDC7 depleted HeLa cells. To re-examine if this was observed in HeLa cells, in response to PHA-767491, HeLa cells were pre-treated with 10 μM SB202190 for one hour prior to adding 10 μM PHA-767491. Additional controls with no treatment and individual PHA-767491 and SB202190 treatments were simultaneously processed. Samples were taken and the DNA content of each cell was measured by flow cytometry.

Figure 4.18

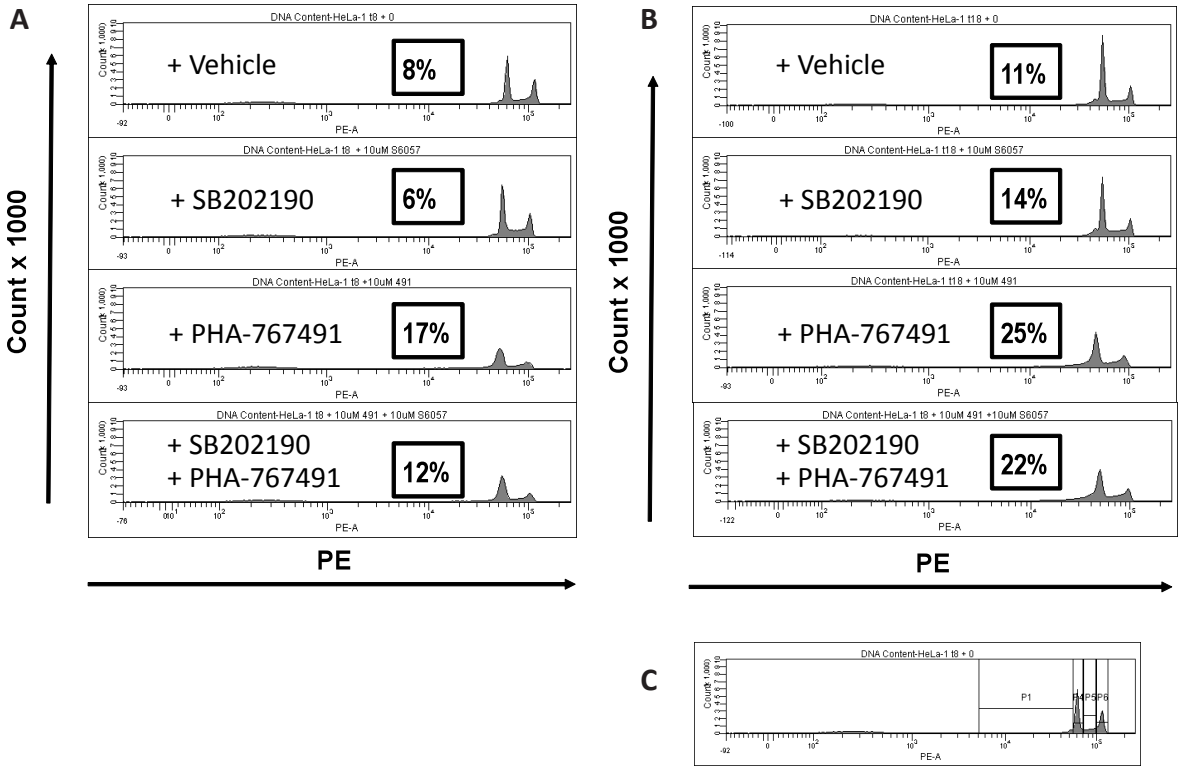

Figure 4.18. SB202190, the p38 MAP kinase inhibitor, does not induce potentiate PHA-767491 cell cytotoxicity in HeLa cells. HeLa cells were incubated with 10 µM PHA-767491 for the indicated time. **A.** Eight hours and **B.** Eighteen hours. Cells were fixed, stained with propidium iodide and analysed by flow cytometry for cell cycle profile. Less than 2N DNA content percentages are displayed in the boxes at individual time point profiles. **C.** Illustrates gates used for less than 2 N DNA content percentages calculation.

PHA-767491 treated cells displayed an accumulation of cells with less than 2N DNA content, consistent with induction of apoptosis (Figure 4.18.B). SB202190 and control profiles were almost identical at both eight and eighteen hours (Figure 4.18.B). The combination of SB202190 and PHA-767491 was almost identical to the profile of treatment with PHA-767491 on its own. There may be a subtle reduction of accumulated cells with less than 2N DNA content but overall this is not significant. These results support a cell-specific effect, relating to the role of the p38 MAP kinase in the context of CDC7 and CDK9 inhibition with PHA-767491. Alternatively, the p38 MAP kinase inhibitor may not have been functioning, as there was no positive control, to assess that it was active during this experiment.

The synergism demonstrated with PHA-767491 and the p38 MAP kinase inhibitor is a cell-specific event not observed in HeLa cells

Investigating the mechanism of synergy between PHA-767491 and the p38 MAP kinase inhibitor

KMS-18 myeloma cells were pre-incubated with 10 μM SB202190 and 10 μM SB203580, an alternative p38 MAP kinase inhibitor, for one hour prior to treating the same cells with 5 μM PHA-767491 for one, three, six and nine hours. Additional controls with no treatment and individual PHA-767491, SB202190 and SB203580 treatments were simultaneously processed as before. In addition, in order to assess if the p38 MAP kinase inhibitors were active, inhibition of phosphorylation of a downstream p38 MAP kinase target MK2 by doxorubicin was assessed at three hours.

Figure 4.19

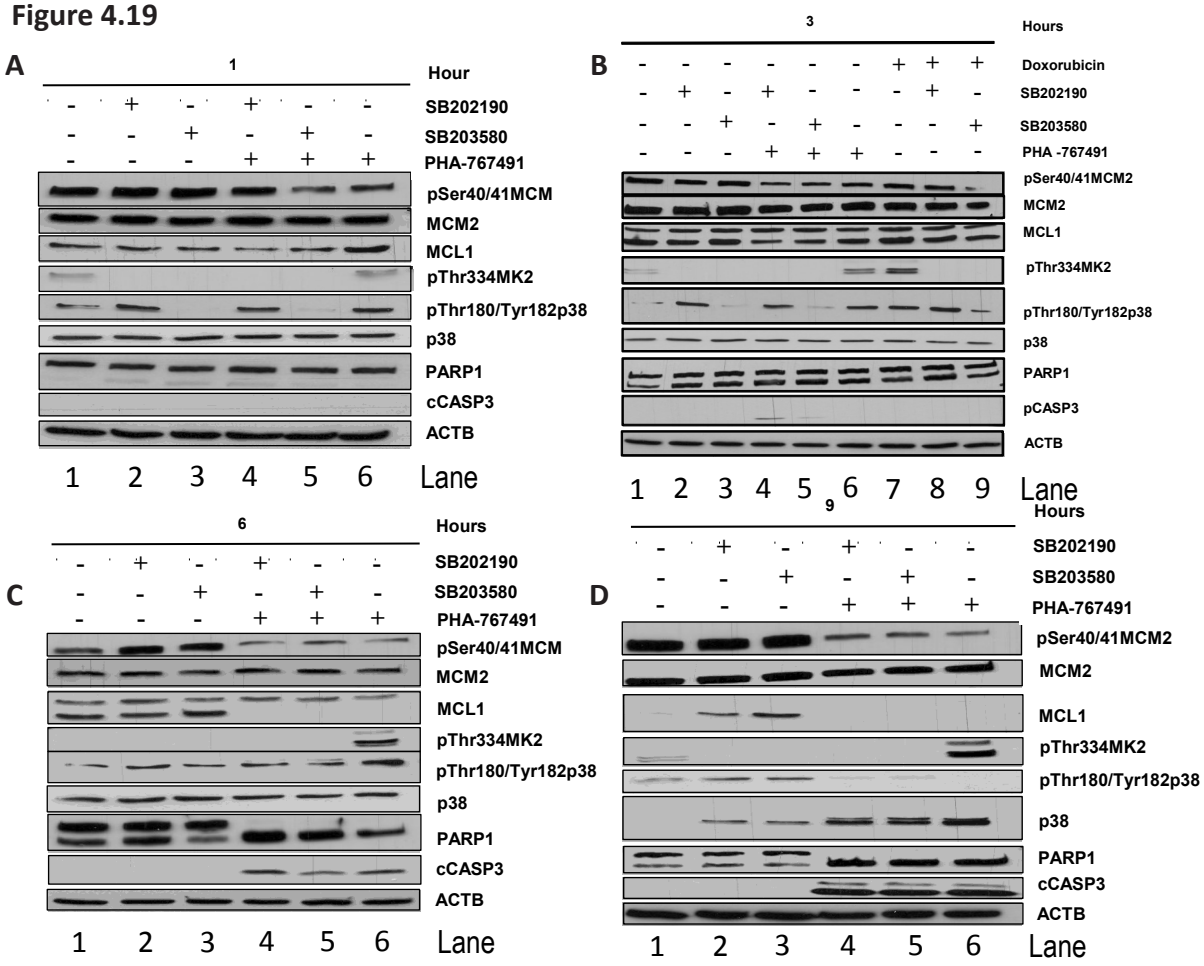

Figure 4.19. PHA-767491 in combination with p38 MAP kinase inhibitors induces more PARP1 cleavage than as a single agent. MK2, a downstream target of the p38 MAP kinase family is phosphorylated in response to PHA-767491 treatment. KMS-18 myeloma cells were incubated with 5 μM PHA-767491, 10 μM SB202190, 10 μM SB203580 and 500 nM doxorubicin for **A.** one, **B.** three, **C.** six and **D.** nine hour(s). In SB202190 and SB203580 treated samples, samples were pretreated with 10 μM of each drug for one hour. Protein extracts were prepared with TGN buffer and analysed by immunoblotting with the indicated antibodies. β-actin was used for loading control. Panel 1 indicates vehicle control. Panel 2 indicates treatment with SB202190. Panel 3 indicates treatment with SB203580. Panel 4 indicates with both PHA-767491 and SB202190. Panel 5 indicates treatment with both PHA-767491 and SB203580.

Panel 6 indicates treatment with PHA-767491 as a single agent. Panel 7 indicates treatment with Doxorubicin. Panel 8 indicates treatment with doxorubicin and SB202190. Panel 9 indicates treatment with doxorubicin and SB203580. Panel 7-9 are controls only visible in B.

Doxorubicin induces phosphorylation of MK2 at threonine 334 (Figure 4.19; B. Lane 7). SB202190 and SB203580 were active as doxorubicin induced phosphorylation of MK2 at threonine 334 by p38 was inhibited (Figure 4.19; B. Lane 8 and 9). PHA-767491 was also active as pSer40/41 phosphorylation was lost in a time-dependent manner (Figure 4.19; A, B, C and D. Lane 6). PARP1 and caspase 3 was cleaved and MCL1 was downregulated by six hours in both combinations of the two individual p38 MAPK inhibitors with PHA-767491 and with PHA-767491 on its own (Figure 4.19; C. Lane 3-6). There is a suggestion that there is more PARP1 cleavage when PHA-767491 is combined with both individual p38 MAP kinase inhibitors, especially noticeable at six hours (Figure 4.19; C. Lane 4 and 5). MCL1 also appears to be reduced at three hours with SB202190 single agent treatment (Figure 4.19; B. Lane 5). This may suggest an underlying aetiology of the proposed synergy of the two drugs. p38 remains unchanged but its phosphoryation at threonine180 and tyrosine182 was inhibited by SB202190 but not by SB203580 at one and three hours (Figure 4.19; A and B, Lane 2 and 3). This phosphorylation was restored at six and nine hours consistent with a known feedback loop between the p38 MAP kinase pathways (Figure 4.19; C and D, Lane 2 and 3). SB203580 does not inhibit this phosphorylation, as it acts downstream at the MK2 level. Interestingly, MK2 is noted to be phosphorylated after PHA-767491 treatment (Figure 4.19; A, B, C and D. Lane 6).

Overall, this result suggests that there may be more PARP1 cleavage with the combination, and that proposed synergy between SB202190 and PHA-767491 may be explained by SB202190 additionally reducing MCL1, further unbalancing the relative pro-apoptotic and anti-apoptotic equilibrium in myeloma cells. Since PHA-767491 induces MK2 phosphorylation in a time-dependent manner it is still surprising that the predicted rescue phenotype is not demonstrated, unless MK2 is not the dominant downstream target of this pathway in this cell-type or within the context of both CDC7 and CDK9 inhibition.

Increased apoptosis and the synergism of PHA-767491

As there was only a subtle difference in PARP1 cleavage levels (Figure 4.19; C. Lane 3-6) and sub-G1 accumulation of cells (Figure 4.17.B), it is hard to draw confident conclusions as to whether PHA-767491 maintains or has a conflicting phenotype to that observed with *si*RNA depletion of CDC7 in HeLa cells. In response to this, a further time course was completed but, in addition to harvesting protein for immunoblotting, combination drug analysis, cells were also prepared for Annexin V/PI staining.

Phosphatidylserine is exposed on cells undergoing apoptosis. Annexin V binds to phosphatidylserine and is used as a sensitive assay to quantify apoptosis in cells that expose phophatidylserine, measured by flow cytometry.

Protein samples harvested simultaneously were processed for immunoblotting.

Figure 4.20

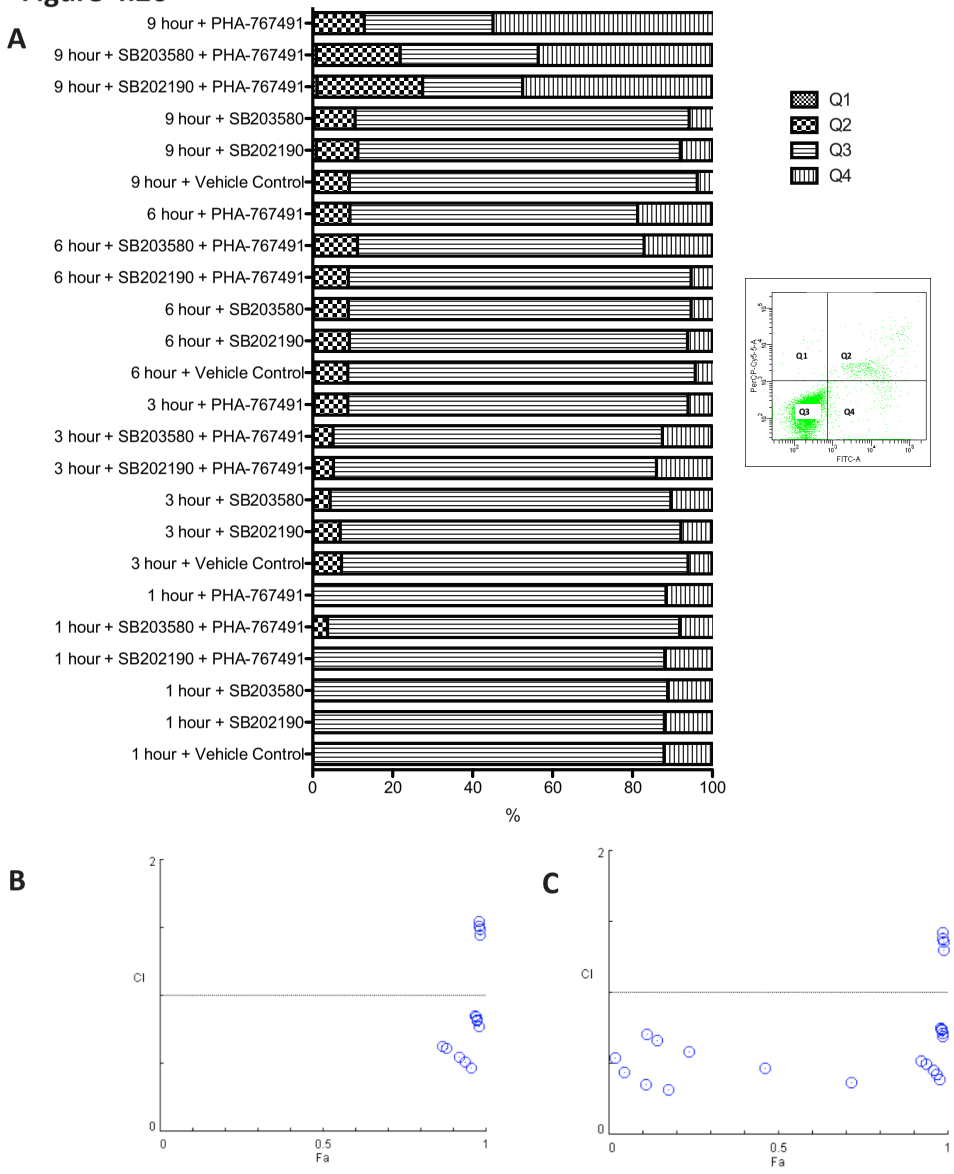

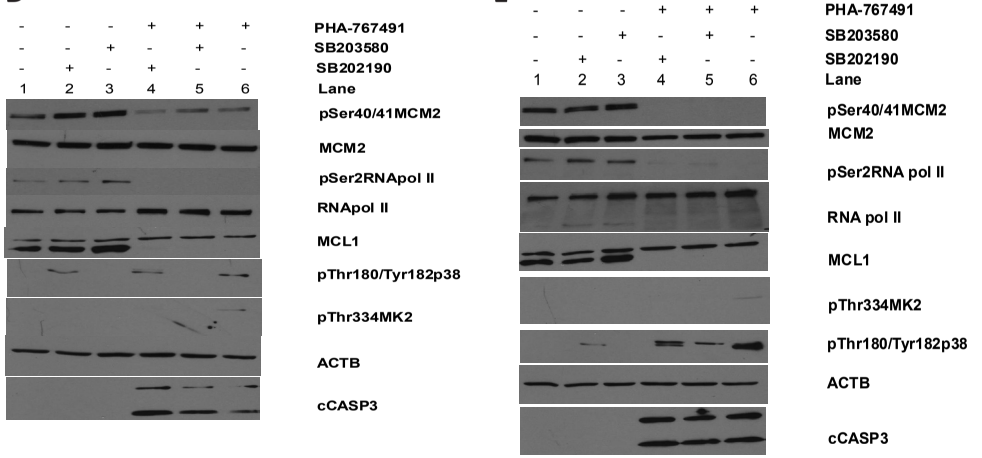

Figure 4.20. PHA-767491 demonstrates potent synergism with SB203580 and SB202190 and increased apoptosis in combination with both inhibitors relative to PHA-767491 alone. KMS-18 myeloma cells were incubated with 5 µM PHA-767491, 10 µM SB202190, 10 µM SB203580 and 500 nM doxorubicin for one, three, six and nine hour(s). In SB202190 and SB203580 treated samples, samples were pretreated with 10µM of each drug for one hour. A. KMS-18 cells were incubated with Annexin V and its buffer and immediately prior to flow cytometry analysis PI was added to each sample. Bar chart indicates percentage within each gated area as outlined by accompanying reference scatterplot. KMS-18 myeloma cells were treated with PHA-767491 and SB202190 B. and SB203580 C. separately in combination in a non-constant ratio in a sequential fashion. PHA-767491 was added one hour after SB202190/SB203580 treatment. Cell viability was examined by CellTitre Glo 48 hours after combined drug treatment. Combination Indices (blue circles) were calculated and plotted in relation to the fraction of cells affected (Fa) at any given experimental point. KMS-18 myeloma cells were incubated with 5 µM PHA-767491, 10 µM SB202190, 10 µM SB203580 for six D. and nine E. hour(s). In SB202190 and SB203580 treated samples, samples were pretreated with 10 µM of each drug for one hour. Protein extracts were prepared with TGN buffer and analysed by immunoblotting with the indicated antibodies. β-actin was used for loading control. Panel 1 indicates vehicle control. Panel 2 indicates treatment with SB202190. Panel 3 indicates treatment with SB203580. Panel 4 indicates with both PHA-767491 and SB202190. Panel 5 indicates treatment with both PHA-767491 and SB203580. Panel 6 indicates treatment with PHA-767491 as a single agent.

At six hours, both of the p38 inhibitors (SB203580 and SB202190) in combination with PHA-767491, induced more Annexin V positive apoptosis relative to PHA-767491 on its own (PHA-767491; 5.3%, SB202190+PHA-767491; 18% and SB203580+PHA-767491; 18.6%, Figure 4.20.A.). Figure 4.20.B and Figure 4.20.C represents the combination plots performed simultaneously to the Figure 4.20.A.

PHA-767491 treated in combination with SB203580 demonstrates that all CIn values are less than one, indicating potent synergism.

Protein analyses show a time dependent loss of pMCM2 (Figure 4.20.D-E. Lane 6), pSer2RNApol II (Figure 4.20.D-E. Lane 6) and MCL1 (Figure 4.20.D-E. Lane 6) with cleavage of caspase-3 (Figure 4.20.D-E. Lane 6), once again. In addition, as shown earlier, SB202190 induced phosphorylation of p38 at Thr180/Tyr182, which was not inhibited by PHA-767491 at either six or nine hours post treatment (Figure 4.20.D-E. Lane 2 and 4). PHA-767491 induced phosphorylation of MK2 at Thr334, maximal at nine hours post treatment (Figure 4.20.D-E. Lane 6). This phosphorylation at MK2 was inhibited when PHA-767491 was combined with either inhibitor (Figure 4.20.D-E. Lane 4 and 5). MK2 is the downstream effector kinase of the p38 MAPK G2M checkpoint response.

It was found that PHA-767491 demonstrates potent synergism with SB203580 and SB202190 and increased apoptosis in combination with both inhibitors relative to PHA-767491 alone.

In addition, protein immunoblots suggests that PHA-767491 is inducing the p38 MAPK checkpoint response. This result, discussed later, may suggest that if myeloma cells have a defective G2M checkpoint, under p38MAPK inhibition, may subsequently result in myeloma cells been pushed down a cell death pathway rather than stalling at G2M.

4.6. CDC7/CDK9 inhibition in the de-novo Vk*MYC mouse model.

The use of genetically engineered mouse models (GEMMs) of cancer is an approach that has shown significant promise, having been highlighted as a blueprint in advancing genetic targeted cancer therapy (Sellers, 2011). Singh *et al* used KRAS-driven GEMMs for non-small cell lung cancer (NSCLC) and pancreatic ductal adenocarcinoma, both of which model the multistage tumour progression from early to advanced disease (Singh et al., 2010). Importantly, the tumour evolves in an immunocompetent animal and apparently in the same microenvironment as the corresponding human tumours, and responds to drugs known to be effective in each disease state. Chen *et al* illustrated that this model paralleled the results of a synchronous trial involving a combination of a MEK inhibitor and standard of care in human subjects (Chen et al., 2012).

Similarly, in myeloma, the AID-dependent activation of the MYC transgene in the C57/BL mouse is a model that is increasingly used for pre-clinical validation of potential anti-myeloma, novel drugs (Chesi et al., 2008, Chesi et al., 2012). As such, this model was used in this thesis to validate the use of NMS-354 in myeloma.

PHA-767491 reduces MYC in an apoptotic and caspase-independent manner

Given the role MYC plays in the transgenic myeloma mouse model, the protein harvested from the BAX-BAK1 experiment (*cf.* Figure 4.3.A and B), where KMS-18 myeloma cells were pre-incubated with 50 μM Boc-D, a pan-caspase inhibitor for one hour prior to treating the same cells with 5 μM PHA-767491 for four and six hours and probed for MYC. In addition, a burkitt cell line, which has upregulation of MYC, was used as a positive control.

Figure 4.21

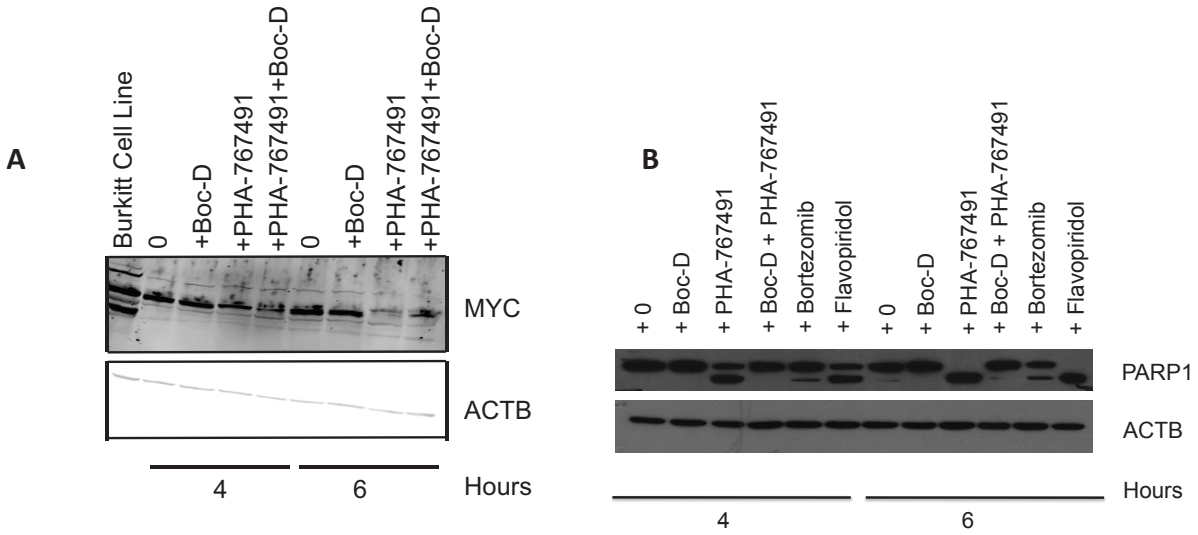

Figure 4.21. PHA-767491 reduces MYC in an apoptotic and caspase independent manner. KMS-18 myeloma cells were incubated with 5 µM PHA-767491 and vehicle control for four and six hours. In Boc-D treated samples, samples were pretreated with 50 µM Boc-D. Protein extracts were prepared with TGN buffer and analysed by immunoblotting for **A.** MYC. ACTB was included for loading control. **B.** Protein extracts were prepared and analysed by immunoblotting for PARP1 cleavage in order to demonstrate and control for Boc-D activity. A burkitt lymphoma line was used as an antibody control to indicate band pattern with MYC.

MYC showed a potent, time-dependent apoptosis and caspase-independent reduction within six hours of treatment with PHA-767-491 (Figure 4.21.A).

PHA-767491 therefore reduces MYC in an apoptotic and caspase-independent manner.

NMS-354 reduces Vk*MYC mice paraprotein by 20 %

To determine the response of Vk*MYC mice to NMS-354, mice with evidence of significant monoclonal Ig gammopathies (>20 g/L) were selected. In general a suitable mouse is aged between 40 and 60 weeks. A pilot study utilising three mice (B1899, B1436 and B1520) treated with 20 mg/kg of NMS-354 by oral gavage on alternate days for 21 days was completed. In the control group, animals were treated with the vehicle alone, using 0.5 % CMC, with the

same frequency as the treatment group. The baseline characteristics of the three mice had a similar genetic background, were similarly aged and were all male. This is illustrated in Table 4.2. Blood parameters, haemoglobin (Hb), white cell count (WBC), and platelet count (PLT) were recorded on a weekly basis.

Table 4.2

	B1457-B1899	B1520	B1436
Mouse Line	Vk.Myc11xBac7A	Vk.Myc11xBac6B	Vk.Myc11xBac6B
Age at Rx (Weeks)	69	60	79
Genotype	MYC+BAC-	MYC+BAC-	MYC+BAC-
Sex	Male	Male	Male
M-Protein			
# Spikes	2	3	3
Intensity	Medium	Medium	Medium
Weight (g) T0	36	35	39
Weight (g) T21	34.5	29	33.6
% Weight Loss	4	17	14

Table 4.2. NMS-354 Study Vk*MYC Mouse Characteristics. Table listing details of mouse line, age at treatment, genotype, sex, number of monoclonal paraprotein (M-spikes), the monoclonal band intensity, weight at day 0 and 21 and percentage weight loss. Rx indicates treatment.

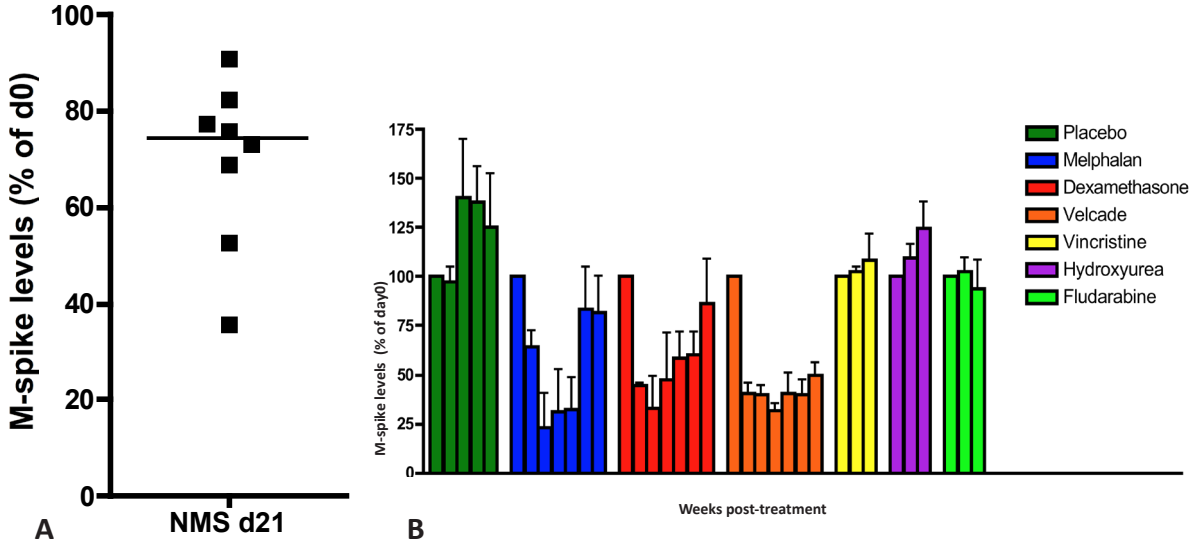

Figure 4.22

Figure 4.22. NMS-354 reduces Vk*MYC mice paraprotein by 20 %. A. The response of Vk*MYC mice treated on alternative days with 20 mg/kg NMS-354 after 21 days. Drug activity is quantified by measuring monoclonal-spike (M-spike), paraprotein levels at day 21 after treatment normalised to day 0. Each dot represents an individual M-spike. Two mice have three spikes and one has two spikes accounting for eight dots. The bar illustrates median M-spike at day 21 normalised to day 0. **B.** The response of Vk*MYC to three agents with known anti-myeloma activity - melphalan, dexamethasone, bortezomib (Velcade)- and to three agents known not to have anti-myeloma activity - vincristine, hydroxyurea and fludarabine. Drug activity is quantified by measuring M-spike on a weekly basis. Each histogram column represents a

weekly measurement.

The serum paraprotein level, M-spike, a surrogate of bone marrow plasmacytosis and thus tumour burden, was measured on a weekly basis. At best, there was an average of 20% reduction of total paraprotein at day 21 (Figure 4.22.A). This compares to 50-70% reduction in paraprotein spike with known anti-myeloma agents, melphalan, dexamethasone and bortezomib (Figure 4.22.B).

NMS-354 therefore reduces Vk*MYC mice paraprotein by 20%

Pharmacokinetic analysis illustrates sub-therapeutic level of NMS-354 in Vk*MYC de novo mouse model

To understand if the lack of efficacy *in vivo* was related to a suboptimal pharmacokinetic (PK) profile, two mice, a de-novo Vk*MYC (B1899) and transplanted Vk*MYC mouse (9354) were selected for PK profiling of NMS-354. Sample processing and data analysis were completed at Nerviano, Milan, Italy. The characteristics of each mouse are described in Table 4.3. Both mice were treated with 20 mg/kg NMS-354 orally by gavage. Both were bled before treatment, and 15, 30 minutes, 2 and 6 hours post treatment. A later time point at 24 hours post treatment was initially planned, but blood loss was not tolerated by either mouse.

Table 4.3

Name	Line	Age, Weeks.	Spike Intesity	Sex
B1899	VkMyc24	87	High	Male
9354	de novo	23	Low	Female

Table 4.3. NMS-354 Vk*MYC PK Study - Mouse Characteristics. Table listing details of mouse line, age at treatment, sex, and the monoclonal band intensity (M-spike).

Figure 4.23

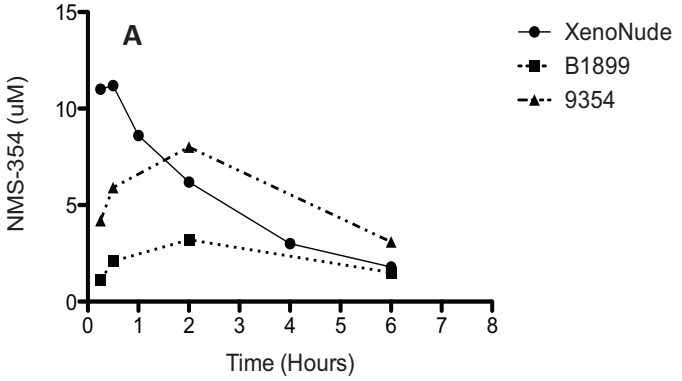

	AUC
XenoNude	29.13
Vk*MYC de novo	13.78
Vk*MYC Tx	33.89

Figure 4.23. NMS-354 Pharmokinetic Study in Vk*MYC models. B1899 a de-novo Vk*MYC mouse and 9354 a transplanted Vk*MYC mouse were treated with 20 mg/kg NMS-354 at time 0. Blood concentration of NMS-354 at 15, 30 minutes, 2 and 6 hours post treatment were measured and displayed. B. Area under curve (AUC) displayed as a table. Nude xenografted mice (XenoNude) results completed historically at Nerviano are included for the purpose of comparison.

A time course of mean plasma concentrations in nude xenografted mice are included for comparison with the de novo and transplant Vk*MYC myeloma mouse models. The xenograft experiment was historically completed at Nerviano, Milan, Italy. The mean plasma concentration in nude xenografted mice after 15 minutes is 11 µM. This compares with 4 µM and 1 µM in the de novo Vk*MYC and transplant Vk*MYC mice models respectively. Moreover, the maximum concentration achieved in the de novo Vk*MYC and transplant Vk*MYC were 8 µM and 5.9 µM respectively. The latest time point recorded in the Vk*MYC mice was six hours which illustrated clearance of the drug (Figure 4.23.A). The AUC calculated for the xenograft, de novo and transplant mouse was 29.13, 13.78 and 33.89 respectively resulting in a sub-therapeutic mean plasma concentration in the de novo mouse model (Figure 4.23.B).

Pharmacokinetic analysis illustrates sub-therapeutic level of NMS-354 in Vk*MYC de novo mouse model.

NMS-354 reduces Vk*MYC mice paraprotein by 80%

In an effort to optimise the NMS-354 PK profile in the de novo Vk*MYC model, the three original mice (B1899, B1436 and B1520) were treated with 20 mg/kg on a daily basis.

Figure 4.24

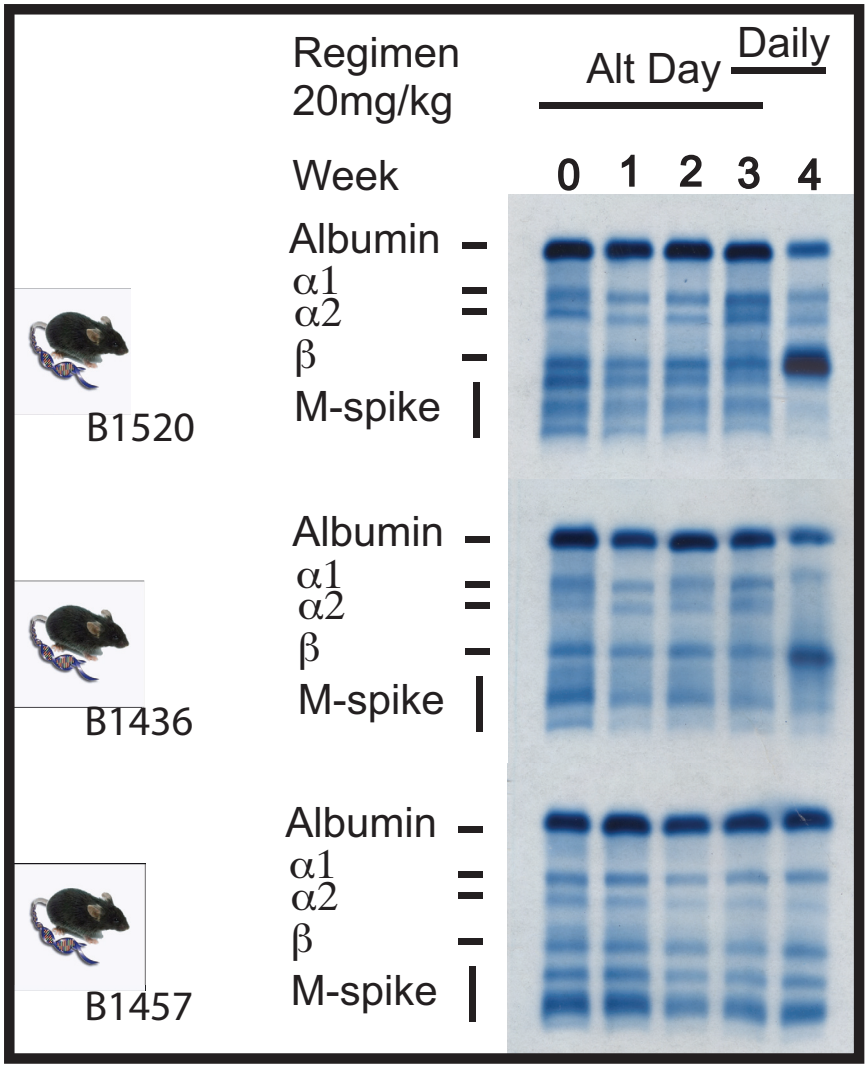

Figure 4.24. NMS-354 reduces Vk*MYC mice paraprotein by 80%. B1899, B1436 and B1520 mice were treated alternate days with 20 mg/kg NMS-354 week 0-3 and daily week 3-4. Weekly individual serum protein electrophoresis gels are illustrated.

This induced a dramatic reduction in the paraprotein within 7 days in two out of three of the mice (Figure 4.24). This however, was accompanied by increased toxicity in two animals with one animal dying (B1436) and the other clearly in extremis (B1520) necessitating euthanasia. The other mouse (B1899) illustrated a modest reduction of 10% of the paraprotein.

NMS-354 therefore reduces Vk*MYC mice paraprotein by 80%. However, the small sample size prevents any further extrapolation to larger populations.

DISCUSSION:

Pre-clinical validation of the CDC7/CDK9 inhibitor.

Myeloma Cell Lines

PHA-767491 is the first nanomolar, ATP-competitive, CDC7 small-molecule inhibitor that has been characterised as an anti-cancer agent in preclinical models (Montagnoli et al., 2008). An increasing number of alternative compounds that inhibit CDC7 are either in preclinical development or in the initial stages of clinical development (Montagnoli et al., 2008, Menichincheri et al., 2009, Sawa and Masai, 2009, Swords et al., 2007). Indeed, CDC7 inhibition appears to represent a new paradigm in cancer treatment given its attractive characteristics of inducing cell cycle arrest in normal primary fibroblast cells while inducing apoptosis in a TP53 independent manner in many different cancer cell lines (Montagnoli et al., 2004, Montagnoli et al., 2008). The underlying reason for this differential effect is yet to be understood, but is likely to be due to defects in the checkpoint pathways that control transition through the different phases of the cell cycle (Montagnoli et al., 2004) as well as loss of the equilibrium between pro-apoptotic and anti-apoptotic signals. Importantly, neither apoptosis in cancer cells nor cell cycle arrest in primary fibroblast cells are mediated by the activation of the canonical DNA-Damage-Response (DDR) pathways that are at the core of the cellular responses to traditional DNA targeting agents (Harper and Elledge, 2007).

Together with CDC7, PHA-767491 targets CDK9, and further drug development of the pyrrole compounds of which PHA-767491 was the lead compound, failed to separate these two activities (Menichincheri et al., 2009). This dual activity against CDC7 and CDK9 potentially increases the efficacy of the compound and broadens the spectrum of potential indications. Cancers that are dependent for survival on proteins with short half-lives such as MCL1, XIAP, are exceptionally susceptible to blocks in transcription which can rapidly influence cell-fate decisions (Sharma et al., 2006). Multiple lines of evidence suggest that haematologic malignancies are highly dependent on survival signaling proteins and disruption of the relative equilibrium of anti-apoptotic and pro-apoptotic proteins is sufficient to drive these cells into apoptosis (Wuilleme-Toumi et al., 2005,

MacCallum et al., 2005, Derenne et al., 2002, Wickremasinghe and Hoffbrand, 1999, Baliga and Kumar, 2002).

In this respect PHA-767491, by targeting both CDC7 and CDK9, causes a transient accumulation of cells traversing the S-phase of the cell cycle followed by apoptosis. Individually, CDC7 and CDK9 inhibition can drive cell death to different degrees depending on the cellular model in which it has been studied (Salerno et al., 2007, Cai et al., 2006, Silva et al., 2008).

Using myeloma cells, it was not possible to seperate the two inhibitory activities either in the time course or dose response experiments and therefore the relative contribution of CDC7 and CDK9 inhibition in driving cell death in this specific setting still needs to be determined. siRNA or shRNA would be an obvious method to evaluate the relative contribution of CDC7 and CDK9. Unfortunately, siRNA inhibition in the myeloma cell lines, despite much effort, was not successful. The stem cell experiments may point to a larger contribution of CDK9 but this would need to validated with knockdown experiments in future work.

It has been shown previously that MCL1 is a key survival factor in myeloma where its over-expression correlates with a poor prognosis (Wuilleme-Toumi et al., 2005, Gojo et al., 2002, Derenne et al., 2002, Beroukhim et al., 2010). The results of this study suggests that downregulation of MCL1, possibly mediated by CDK9 inhibition, could be a major determinant of cell-fate in this setting. Moreover, the mitochondrial gate way proteins, BAK1 and BAX appear to be instrumental in apoptosis induced by CDC7/CDK9 inhibition. Interestingly, BAK1 and BAX oligomerisation implies that cell death occurs largely through the intrinsic, mitochondial pathway.

Both the dual CDC7/CDK9 inhibitor, PHA-767491, and its bioavailable related compound, NMS-354, inhibit proliferation in a panel of myeloma cell lines which includes documented TP53 mutants and lines with resistance to dexamethasone, melphalan and doxorubicin. Furthermore,

PHA-767491 has the same effect on primary myeloma cells harvested from patients who have relapsed with progressive refractory disease. This suggests that the mechanisms which lead to chemoresistance to conventional therapy in myeloma may not affect the activity of a dual CDC7/CDK9 inhibitor. Essentially, this suggests that the activity of this drug class can be explored as second or third line therapy or in the relapsed/refractory setting in myeloma treatment.

The importance of the microenvironment in supporting myeloma growth has been demonstrated previously (Dalton et al., 2004, Mitsiades et al., 2004). In particular cytokines such as IL-6 and IGF-1 and direct interaction with stromal cells have previously been shown to confer drug resistance. These factors in the response to PHA-767491 were explored. It was found that IL-6, stromal derived CAM and paracrine stimulation do not protect myeloma cells against PHA-767491 while IGF-1 confers only moderate resistance. The differential effect of IL-6 and IGF-1 may be explained by their individual effects on proliferation and the relative equilibrium of pro-apoptotic and anti-apoptotic survival factors. IL-6 preferentially increases MCL1 whereas IGF-1 has been previously shown to reduce the pro-apoptotic BH3 only protein BCL2L11, which may counteract the MCL1 reduction, thereby increasing the apoptotic threshhold in myeloma cells (De Bruyne et al. 2010, Puthier et al., 1999).

As CDC7 inhibitors enter the clinic, the ability to devise rational combinations will become of utmost importance. It is clear from this work that PHA-767491 has an overall additive effect when combined with melphalan, bortezomib, and doxorubicin in an *in vitro* setting. Therefore, there is potential for this new drug class to be included in combination regimens

Myeloma Stem Cell Models

Highly clonogenic cancer stem cells (CSCs) have been identified in several human malignancies, including myeloma, and their combined resistance to chemotherapy and enhanced growth potential suggests that they may be responsible for disease relapse and progression (Matsui et al.,

2008, Matsui et al., 2004). The ability to target the CSC niche is an area of active research in most cancers. In particular, groups have focused on the developmental pathways, including Wnt, Notch and Hh.

Matsui *et al* found that myeloma CSC best resemble memory cells ($CD138^{neg}CD19^{+}CD27^{+}$) that give rise to differentiated $CD138^{+}$ plasma cells that are relatively resistant to agents used to treat myeloma. Other groups have challenged the validity of a true stem cell in myeloma. The lack of RAS mutations in memory cells suggests that myeloma cells originate from precursor B-cells (Rasmussen et al., 2010). Walker *et al* using a sequencing approach demonstrates that in certain translocations, a D_H-J_H rearrangement would suggest that the origin of the myeloma clone is pre-germinal B-cell and possibly at the pro-B cell progenitor cell level (Walker et al., 2013). Chaidos *et al* have demonstrated four distinct hierarchially organised phenotypically distinct populations defining myeloma (Chaidos et al., 2013). The pre-PC and PC characteristed by $CD19^{-}CD138^{-}$ and $CD19^{-}CD138^{+}$ retain an ability to convert phenotypically but also bidirectionally (Chaidos et al., 2013). Equally, this may suggest that 'stemness' may in fact relate more to the ability of the cell to adapt to a state of resistance. Sigal *et al* have, for example, demonstrated that protein expression is a stochastic process that leads to phenotypic variation among cells, particularly demonstrated when cells are under pressure (Sigal et al., 2006). This accounts for non-genetic heterogeneity which could potentially lead to clonal evolution (Brock et al., 2009). This alternative view of 'stemness' is supported by Chaidos *et al* work which illustrated that pre-PCs are up to 300 times more resistant than their PC counterparts (Chaidos et al., 2013)

In this thesis, it has been shown that both PHA-767491 and NMS-354 inhibited clonogenic growth across a range of myeloma cell lines where a stem cell niche has been previously described. In keeping with previously published data, NMS-354 was more potent than PHA-767491 in inhibiting clonogenic growth. Interestingly, RPMI-8226-S was less sensitive than the other two lines. RPMI-8226-S has an active Hegdgehog (Hh) pathway which may suggest that Hh may potentially

promote resistance to CDC7/CDK9 inhibition. Moreover, it is of note that IGF-1 can stimulate Hh-dependent GL1 transcription. This may link with the noted resistance in the IGF-1 stimulated myeloma cells discussed earlier. GLI transcriptional regulation is tissue specific; in keratinocytes FoxM1 is upregulated whereas in mesenchymal cells PDGFRA is upregulated. The regulation of Hh is controlled by the conservative negative kinase regulators, protein kinase A, casein kinases (CK1a and CK1e), and glycogen synthase kinases 3b (GSK3B) which co-operatively phosphorylate and inactivate GLI factors. Thus, loss of GSK3B may increase Hh GLI-dependent transcription, however this would require further, future, work to decipher this speculative effect.

NMS-354 also blocked clonogenic growth of $CD138^{neg}$ primary myeloma cells in three patients. Self-renewal was significantly inhibited with both treatments. This inhibition of self-renewal was not related to increased cell death or apoptosis in the treated groups as there was no significant differences in Annexin V and Annexin V/PI cells between control and treated groups. This is of significant interest as self-renewal is a key mechanism of resistance in cancer treatments. The ability of both CDC7/CDK9 inhibitors to block self-renewal is a welcomed phenomenon.

An increased population of $CD138^{neg}$ with high ALDH activity was noted in the treated group relative to the vehicle alone. This is counter-intuitive as if the compound had a direct effect on the stem cell population one would expect that the population of $CD138^{neg}$ would be reduced rather than increased. Moreover, one would expect that ALDH activity would also be reduced. The findings therefore suggest that CDC7/CDK9 inhibitors enrich for cells with a stem cell phenotype or indeed a cell with a resistant phenotype. The question follows as to why there is a block in self-renewal and clonogenic growth and yet an increase in cells with characteristics of stem cells? Is there a block in differenitation with CDC7/CDK9 inhibition?

Bai *et al*, working in Len Zon's lab at the Dana Faber Cancer Institute have published work that shows transcriptional elongation is critical in regulating cell fate and differentiation (Bai et al.,

2010). This was seen in haematopoeisis in the zebrafish developmental model but also in human $CD34^{+}$ cells. This work complements the observation that stem cells are already primed at transcription initiation and require activation of elongation for differentiation (Guenther et al., 2007). As discussed earlier, in section 1.3.1, RNA pol II elongation is largely carried out by the CDK9 kinase. On the other hand, Shi *et al* have illustrated that in a smooth muscle cellular model CDC7 regulates TGF-b induced cellular differentiation in a DBF4-independent and thus replication independent manner (Shi et al., 2012). Shi *et al* propose that CDC7 interacts with SMAD3 in order to induce differentiation.

In support of a similar effect in NMS-354 treated cells, in this study cells treated with NMS-354 demonstated increased polyadenylation of the HIST1H2BD gene, a surrogate of CDK9 inhibition. Moreover, there was no difference in pMCM2 staining between treated and control groups suggesting that CDC7 was not inhibited. Taken together, this suggests that CDK9 inhibition rather than CDC7 inhibiton is central to the block in self renewal and clonogenic growth.

In order to conclusively prove that NMS-354 has an effect on stem cells, it is necessary to complete sequential transplantion, or secondary transplantation in mouse models. Unfortunately the secondary transplant mouse work was incomplete as neither the control group or the treated group developed myeloma. Future work would importantly include re-examination of the secondary transplantation model used in validation of effects at a stem cell level.

In conclusion, this work supports the hypothesis that NMS-354 and PHA-767491 both have the ability to functionally block clonogenic growth and self renewal, both features of CSCs. In addition, CDK9 rather than CDC7 inhibition is key to explaining this block. The appearance of an increased population of $CD138^{neg}$ cells with high ALDH, but loss of clonogenic growth suggest that CDK9 is most likely blocking differentiation and thus influencing cell fate. A prolonged phase of block in differentiation may lead to terminal loss of stem cell self renewal and thus stem cell

maintenance.

p38 MAP kinase inhibition synergism with CDC7/CDK9 inhibition

p38 MAP kinase inhibition in combination with PHA-767491 demonstrates potent synergism. In comparison to other combinations assessed, SB202190 in combination with PHA-767491, was the most synergistic which has been assessed to date. Moreover, the synergism was noted in all cell lines tested – KMS-18, KMS-11 and OCI-My5. This potent synergism contrasts sharply with the findings of Im *et al* (Im and Lee, 2008). Their findings suggest that activation of apoptosis in CDC7-depleted cells was completely abolished in cells treated with either *si*RNA or an inhibitor of the p38 MAP kinase. This suggests that p38 MAP kinase activation was responsible for apoptotic cell death in CDC7 depleted cells. Thus, inhibition of p38 MAPK would be expected to rescue the cells from CDC7 inhibition. This discordance may be explained by the dual inhibition of CDC7 as well as CDK9 by PHA-767491. In addition, it is clear that the p38MAPK has different priorities in certain cell types. Im *et al* completed their work in the HeLa cell line. The potent synergism noted in myeloma cell lines was not observed in HeLa cells.

This synergism was also noted when directly measuring apoptosis. The synergism may be explained by further reduction in MCL1 with SB202190 alone but this was not a consistent finding. PHA-767491 persistently activated MK2 which was blocked in combination with both p38 MAPK inhibitors. CDC7/CDK9 inhibition has been already shown to induce DSB demonstrated by γ-H2AX staining, however, this was related to an apoptotic effect (Montagnoli et al., 2008). A TUNEL assay completed during this thesis but data not shown supports DSB formation in response to CDC7/CDK9 inhibition. This suggests that PHA-767491 may activate the p38MAPK checkpoint that may be required to promote repair. It is interesting to note that p38 MAP kinase localises to the nucleus in response to DSBs.

Gorska *et al* have shown previously that MK2 and its substrate HSP27 are essential for sustained

NFKB1 activation (Gorska et al., 2007). Keats *et al* have shown previously that myeloma cells 'lust' for NFKB1 (Keats et al., 2007). Here Keats *et al* illustrated primary myeloma cells and myeloma cell lines harbour mutations in genes encoding regulators and effectors of NFKB1 signaling and these mutations lead to chronic NFKB1 target gene expression which is required for the viability of myeloma cells. Gorska *et al* also illustrate that MK2 and HSP27 prevent nuclear retention of p38 MAPK by sequestering it in the cytosol, thus preventing MSK1 activity (Gorska et al., 2007). By reducing MSK1 activity, MK2 prevents p65 NFKB1 hyperphosphorylation and excessive IkBa transcription. Loss of IkBa transcription reduces export of NFKB1 from the nucleus (Gorska et al., 2007). Taken together, it can be stated that MK2 regulates the NFKB1 transcriptional output by switching the activation pattern from high level but short lasting to moderate level but long lasting. Loss of MK2 in myeloma cells may remove the 'tolerance' NFKB1 pathway shown to be essential to survival in myeloma cells. With this in mind future work should perform the combination study in KMS-28BM and KMS-28PE to ascertain if NFKB1 is the heart of why the combination is so synergistic. These cell lines, are an isogenic pair, that share identical genomes except for their difference in the presence (KMS-28BM) or absence (KMS-28PE) of BIRC2/3(formerly cIAP1/2), negative regulators of NFKB1. Their absence leads to constitutive NFKB1 activity. Thus, these two cell lines act as a screening tool to demonstrate a possible NFKB1-dependent effect, in particular if a difference in combinational indices between the two myeloma cells lines is noted. If this is the case, It will be important to postulate why p38 MAPK inhibitors have not shown much promise in clinical myeloma trials (Hideshima et al., 2003, Shannon, 2011). This may suggest that a particular combination may be necessary in the clinical scenario.

Ito *et al* have proposed that loss of CDC7 results in two separate outcomes depending on TP53 status (Ito et al., 2012a). TP53 mutants arrest in G2-phase, accumulate CCNB1 (CyclinB1), ultimately entering an aberrant M-phase due to the abnormal presence of CCNB1, followed by mitotic catastrophe or death. Blocking CCNB1 accumulation partially rescues the death phenotype. Cells without TP53 mutations do not accumulate CCNB1, but instead enter an aberrant S-phase.

KMS-11 has no measureable TP53 mRNA. OCI-MYC and KMS-18 have a functional TP53. Synergism is observed equally in TP53 mutants and non-mutants myeloma cells, although the sample number is too small to be statistically meaningful.

Nevertheless, this gives rise to an interesting hypothesis in that CDC7/CDK9 inhibition in combination with p38 MAPK inhibition may remove two important DDR pathways, namely ATR-CHK1 and ATR-MK2 leaving only ATM-CHK2 to respond. Malcolm Taylor's group have illustrated that ATM mutations are more common in myeloma patients relative to that expected in the general population. Moreover the C7181T mutation in myeloma patients with ATM has no functional ATM (Austen et al., 2008). Walker *et al* demonstrated that a single patient using single cell analyses had three different clones with only one shared mutation – ATM (Walker et al., 2012). As highlighted earlier**,** in chapter 3, ATM signaling is one of the top canonical pathways identified associated with the proliferation phenotype in myeloma. This may suggest that the G2/M checkpoint pathway is negligent or malfunctioning in myeloma. Pei *et al* demonstrated that H4K20 methylation increases locally upon the induction of DSB mediated by MMSET, ultimately recruiting 53BP1 (Pei et al.). This recruitment requires MDC1 and γ-H2AX and phosphorylation of MMSET by ATM at Ser102. Alternatively, the importance of the p38MAPK pathway in myeloma cells may relate to the fact that is a post-germinal B-cell that has undergone SHM and thus become dependent on such a pathway.

In conclusion, due to the heterogeneity of myeloma, the importance of combination therapies is clearly supported by the findings of this study. CDC7/CDK9 inhibition, in combination with p38MAPK inhibitors, illustrate potent synergism. The mechanism behind this is, however, is unclear but may relate to the importance of p38MAPK in maintaining its addiction to the NFKB1 pathway; it may also relate to irreparable DNA damage resulting in aberrant cell cycle release and or death.

Myeloma Mouse Model

The era of genetically engineered mouse models (GEMMs) has brought calculated progress in pre-clinical validation of anti-cancer treatments. This has been shown in NSCLC, pancreatic cancer and also myeloma. Moreover, Singh *et al* has shown that NCSLC GEMM was predictive of the overall outcome in the synchronously enrolled human trial (Singh et al., 2010). The use of mouse models however also comes with a word of caution, as, although the genetically modified mice are similar to human tumour states, they are not absolutely identical and often favour one particular pathway described in a particular tumour state.

In cell lines that express MYC, PHA-767491 categorically reduces protein levels of MYC in a time-dependent manner not influenced by apoptosis. This is not surprising as Delmore *et al* and Chaidos *et al* have shown that BET bromodomain inhibitors, in particular JQ1 and I-BET151, can potently reduce MYC dependent transcription in myeloma (Delmore et al., 2011, Chaidos et al., 2014). This is largely achieved, in fact, by inhibiting BRD4 regulation of CDK9 on RNA polymerase II. It is interesting to postulate if CDC7 inhibition could have similar importance as CDK9 as the Della-Favera B-cell developmental biology group at Columbia have shown that MYC can regulate DNA replication in a transcriptional independent manner (Dominguez-Sola et al., 2007).

Chesi *et al* have developed the myeloma GEMM, the Vk*MYC de-novo and syngenic transplant model which faithfully shares many features of human myeloma. At a genetic level it resembles TC1-like human myeloma where there is disruption of t(11;14) (Chesi et al., 2008). NMS-354 was tolerated in the wild-type C57/BL6 Vk*MYC background strain with no effect on weight or blood parameters. Vk*MYC de-novo myeloma mice receiving 20 mg/kg on alternate days illustrated only a minor reduction of serum paraprotein after 21 days treatment. The PK AUC in the *de novo* mouse model was suboptimal compared to previously tested mice. It is extremely difficult to perform PK studies in mice as in general they do not tolerate massive blood loss. This can impact on PK studies as blood may be shunted with systemic vasoconstriction to maintain the cardiac and

cerebral circulation in preference to other organs.

Taken together, the de novo transplant Vk*MYC mouse study served as a pilot study. With three mice within each group, definitive conclusions cannot be drawn, other than to say that this work indicates that future research with a larger sample size should be undertaken.

CHAPTER 5: CONCLUSION.

In chapter 3, CDC7 [DBF4-Dependent Kinase (DDK)] is documented to be expressed in non-malignant and malignant plasma cells. DBF4 is the main CDC7 regulator of plasma cells and its expression is observed across all seven UAMS groups. DBF4 mean expression was statistically different between MGUS, SMM, myeloma and HMCLs. Interestingly, DBF4 overexpression is not the result of a gain of function mutation within the DBF4 gene. DBF4 overexpression predicts an inferior OS and PFS in the UAMS dataset, but failed to reach independence to other genomic stratifiers on multivariate analysis. Myeloma cells dual stained with pSer40/41MCM2 and CD138, identifying plasma cells undergoing replication, were demonstrated to be the best statistical predictor of PCLI. This is an interesting finding as it suggests that an immunohistochemical stain can be used reproducibly in myeloma to predict a proliferation index. This parallels similar pathways that are used in DLBCL sub-classification currently. The Hans or Choi algorithim, consisting of three immunohistochemical stains are used as a surrogate to GEP based DLBCL classification of germinal centre (GC) and non-GC ([ABC- Activated B-cell]) DLBCL subtypes (Choi et al., 2009).

Section 3.3. contains an interesting finding. It confirms the importance of IL-6, TP53 and MYC in the proliferative phenotype in myeloma. Interestingly, it suggests that the most important canonical pathway potentially associated with the proliferation phenotype is the G2/M DNA checkpoint pathway. The additional role of ATM and PLK1 supports the probablity of a 'mitotic escape' which may ultimately perpetuate DNA damage. This prompts a different understanding of replication in myeloma. Historically, replication was thought to depend on Cyclin D expression with additional driver mutations such as RAS and MYC. This work suggests that, in fact, the potential driver is failure of the DDR G2/M pathway. This may also explain the finding in Vk*MYC mice where aurora kinase inhibition leads to an aggressive clonal expansion rather than therapeutic efficacy. Moreover, it provokes, perhaps, a reconsideration of the general approach of treating cells with a proliferative phenotype as having an S-phase problem. Interestingly, this reinforces the need to challenge cells with a combination approach, as already suggested with p38 MAPK inhibition and CDC7/CDK9 inhibition.

In chapter 4, the efficacy of CDC7 inhibition in myeloma pre-clinical bench-based models was evaluated. PHA-767491 and NMS-354 are two compounds characterised with specificities against both CDC7 and CDK9. Both compounds demonstrated efficacy in myeloma cell lines, primary patient samples and microenvironment cellular models within the μM range expected for ATP-competitive kinase inhibition. Both targets achieved inhibition in myeloma cells. Interestingly, BAX and BAK1, the two key 'mitochondrial gateway' pro-apoptotic mediators illustrated a preference for the intrinsic apoptotic pathway. MCL1, downstream of BAX and BAK1, as seen with flavopiridol, a pan-CDK inhibitor, is downregulated in a time dependent manner suggestive of a product of CDK9-related loss of RNA pol II mediated trascription.

It was impossible to separate the individual roles of CDC7 or CDK9, but one may equally question the clinical relevance of such a finding given that both will be inhibited within the patient. That said, it is unfortunate that siRNA experiments did not work, though these findings do support the less well-published finding that viral mediated transduction is essential for reliable and reproducible genetic knock-down in myeloma cell lines. Moreover, the viral mediated technology allows designs for conditional knockdown which are important in essential cell-cycle or indeed replication - dependent genes. Wu *et al* demonstrated that the new transcription activator-like effector nuclease (TALEN) is a suitable technology for genetic knockout in myeloma cell lines (Wu et al., 2014). This would be an interesting approach to knocking down CDC7, CDK9 or both. Alternatively, the use of XL-413 which is more selective CDC7 inhibitor than PHA-767491 across a panel of 77 human kinases is another option that could specify a direct role of CDC7 or other kinase (Hughes et al., 2012).

IGF-1 promoted a tendency to reistance to CDC7/CDK9 inhibition. Loss of the the pro-apoptotic BCL2 member, BBC3, may explain this but equally, an increase in free CDK9 released from the 7SK snRNA/HEMIM1 inactive pool may be an alternative explanation. CML lines are known to be relatively resistant to CDC7/CDK9 inhibition which may support the role of AKT1 mediated re-

sistance through the FOXO3, the forkhead family of transcription factors. This is speculative and will require further work to decipher the mechanism of resistance in IGF-1 treated myeloma cells.

Section 4.3 explored a controversial area of research but one which is, nonetheless, clearly important to study in order to eradicate a residual cancer niche be it a CSCs or a resistant subclone with phenotypic diversity. The results are undoubtedly puzzling to interpret. CDC7/CDK9 inhibition clearly blocks clonogenic growth and self renewal in cell lines with a CSC or 'self renewal' niche at doses that do not induce apoptosis. This is also observed in $CD138^{neg}$ primary myeloma cells. The difficulty, however, is that CDC7/CDK9 inhibition increases the potential CSC pool by ALDH and CD138 cellular staining. A secondary mouse transplant study is obviously necessary to demonstrate a true effect a the stem cell level.

This set of findings necessitates reviewing the literature which illustrates the huge importance of CDK9 in cellular differentation (Bai et al., 2013) but, equally, points to an evolving role for CDC7 (Shi et al., 2012). Guenther *et al* illustrated that genes associated with stemness are regulated at the post-initiation step of transcription (Guenther et al., 2007). Moreover, this would suggest a primary role of CDK9 in this process. This proposes that sustained block in differentiation of CSCs with CDK9 inhibition may ultimately lead to failure of CSC maintenance by loss of the capacity of self renewal. This is supported by the finding in the work conducted for the purpose of this thesis, that CDK9 but not CDC7 was inhibited at the doses tested.

PHA-767491 was shown to be potently synergistic with both p38 MAPK inhibitors. It is not surprising that CDC7/CDK9 inhibition activates MK2, possibly in response to DSBs. What is surprising, is that p38 MAPK does not rescue the cell from apoptosis as reported with Im *et al* with CDC7 depletion (Im and Lee, 2008). The loss of MK2 induction with combination treatment suggests an important mechanism of synergism. This may result in loss of tolerance to high NFKB1 levels but the fact that p38 MAPK inhibitors demonstrated no clinical efficacy in phase I trials poses

challenges for this hypothesis. Another potential possiblity is that myeloma cells have a negligent G2/M checkpoint. When challenged with both CDC7/CDK9 and p38 MAPK inhibition the myeloma cell escapes mitosis and subsequently enters an abortive S-phase. This is independent of TP53 status, contrary to Ito *et al's* work already discussed (Ito et al., 2012a). Indeed, the mechanism proposed by Ito *et al* may not apply to myeloma cells due to an inherent G2/M defect in the myeloma cell which was discussed earlier in chapter 3. In any case, this illustrates quite nicely that, in the pursuit of new myeloma treatments, a drug with little efficacy alone may nonetheless have potent synergism and thus theurapeutic rationale in combination. This is worth considering but does, unfortunately, require more mice per experimental arm, but is still achievable in future work if the Chou-Talalay combination method is followed.

The de novo mouse work is a logical extension of pre-clinical cellular based models. It examined the efficacy of CDC7/CDK9 inhibition in myeloma GEMMs, namely the Vk*MYC de-novo and syngenic transplant models. PHA-767491 potently reduces MYC expression in myeloma cell lines that express MYC, possibly similar to the BRD4 BET bromodomain inhibitors, whereas instead of inhibition of BRD4 recruitment of CDK9 to RNA pol II, CDK9 is inhibited directly by PHA-767491/NMS-354. However, the direct transcription-independent role of MYC in DNA replication can't be ignored. Despite this predicted efficacy based on the data from cell lines NMS-354 did not show efficacy below MTD in the Vk*MYC de novo myeloma mouse model. The PK data suggested suboptimal dosing with a poor AUC compared to other models used by Nerviano Medical Sciences. With increased doses there was demonstrable efficacy measured by reduction of M spike, but clear toxicity noted in animals. The BET bromodomain inhibitor study only documented the M-spike for 14 days and did not indicate any toxicity (Delmore et al., 2011). One important question to address is whether the Vk*MYC models accurately represents all heterogeneity within myeloma. Moreover, does the Vk*MYC models accurately represent the proliferative cohort of myeloma? The Vk*MYC de-novo model best resembles t(11;14) myeloma which has a generally good OS. The Vk*MYC transplant model is more proliferative but is it representative of the

proliferation escape seen throughout myeloma. This question has major implications for drug validation. On the otherhand, if the model is truly robust, a larger cohort needs to be completed with sufficient power to ascertain if CDC7/CDK9 inhibition is a valid drug for use in myeloma. Moreover, the tendency to resistance as observed with IGF-1 treatment and its link with MYC is interesting to explore. AKT1 can inhibit the pro-apoptotic activity of BAD, CASP9 and FAS, three proteins that are involved in apoptosis relating to MYC (Fearnhead et al., 1998, Janicke et al., 1996, Rohn et al., 1998). Again, the forkhead proteins, TP53, would be other possible links.

FUTURE PERSPECTIVES:

The role of CDC7/CDK9 inhibition as a therapeutic advance in myeloma remains unclear. The emergence of BRD4 targeting drugs, which arose from efforts to target MYC, suggested that CDK9 inhibition should have been more effective than was evident in this work. Another benefit of CDK9 inhibition is the potential block in the differentiation of stem cells. This is an extremely controversial area. This controversy, however, should not detract attention from the known existence of resistant populations of plasma cells, some of which may represent a true stem cell clone, which require directed therapy.

It is sobering to note the lesson learned from the lack of efficacy of lenalidomide in mice models. This highlights the lack of direct comparability between mice and humans. CDC7 and CDK9, however, are conserved essential proteins across species, including mice, and thus this does not explain the lack of efficacy of NMS-354 in the VK*MYC de novo mouse model. The Vk*MYC de novo myeloma mouse model does favour BCL2L1 (formerly BCL-xL) overexpression over MCL1 overexpression, which is different to that seen in human myeloma.

The separation of CDC7 and CDK9 function would be a clear prioritiy for future work. Knockdown of essential replication proteins can, however, be problematic. A conditional shRNA approach would be the obvious choice for future work. Rainey *et al* used the XL413 compound to separate CDC7 and CDK9 function as XL413 is a more specific CDC7 inhibitor than PHA-767491 (Rainey et al., 2013, Hughes et al., 2012).

The potent synergy between the p38 MAPK inhibitor, SB202190, and PHA-767491, possibly through its inhibition of MK2 demonstrates the power of novel combinations. It would be interesting to explore the effect of this combination on the NFKB1 pathway. A starting point, as mentioned previously, would be to assess for a differential effect in the KMS-28 myeloma cell line pair. If present this would suggest that MK2 may have an essential role in NFKB1 maintenance in

the myeloma cell. This would require further work, studying such effects at a protein level and once again with overexpression and knockdown experiments.

The need for implementing a more robust method of assessing the relative increase in proliferation in myeloma cells is clearly important for risk stratification but more importantly for targeting emerging treatments that specifically target the proliferative clone. The use of trephine-based material is clearly important so as to include patients with a patchy but significant plasmacytosis in the bone marrow. Dual staining of pMCM2/CD138 best predicts the gold standard PCLI. Its use could mirror similar work in DLBCL where immunohistochemical staining predicts important GEP-based classification used routinely in treatment decisions. That considered, recent work by Amin *et al* demonstrate that GEP alone is insufficient at predicting CR in myeloma (Amin et al., 2014).

Another exciting possibility is to correlate PCLI, or other measures of proliferation with the standardised uptake value calculated by PET imaging. The emergence of using low dose CT to comprehensively characterise lytic bone disease will soon be used in preference to skeletal surveys. Thus, PET/CT may become a modality to measure proliferation as well as lytic bone disease. That considered, there is clearly an emerging need to assess minimal residual disease (MRD) in myeloma patients. This clearly correlates with OS and PFS (Martinez-Lopez et al., 2014). The use of multi-parametric flow is leading the race but this is still dependent on sampling. I personally favour the emergency of WGS or WES or indeed the LymphoSIGHT chip for use in MRD as it will give the clinician access to competing drivers of resistance and clonal evolution as well as defining residual disease (Martinez-Lopez et al., 2014). The existence of circulating free DNA may be an intriguing resource to use, instead of a patient requiring a bone marrow aspirate.

The two dominant canonical pathways associated with patients with a proliferative phenotype demonstrate the importance of G2/M rather than considering the proliferation cohort in myeloma as an S-phase problem. The suggestion of a negligent G2/M pathway associated with prolifer-

ation in myeloma is intriguing. Building on this, the Cmap revealed some interesting possibilities that may arm the clinician in targeting the proliferative cohort in myeloma. This Cmap work is *in silico* work, that requires pre-clinical validation before proceeding to clinical use. This work also emphasise that treatment of myeloma is likely to require increased bioinformatics resources in the future management of myeloma patients at the bedside.

REFERENCES:

AGURA, E., NIESVIZKY, R., MATOUS, J. V., MUNSHI, N., HUSSEIN, M. A. & PARAMESWARAN, R. V. (2009) Dacetuzumab (SGN-40), lenalidomide, and weekly dexamethasone in relapsed or refractory multiple myeloma: multiple responses observed in a phase 1b study. *ASH Annu Meet Abstr,* 114, 2870.

AHMED, R. & GRAY, D. (1996) Immunological memory and protective immunity: understanding their relation. *Science,* 272**,** 54-60.

AKIYAMA, T., OHUCHI, T., SUMIDA, S., MATSUMOTO, K. & TOYOSHIMA, K. (1992) Phosphorylation of the retinoblastoma protein by cdk2. *Proc Natl Acad Sci U S A,* 89, 7900-4.

ALBERTS, D. S., DURIE, B. G. & SALMON, S. E. (1977) Treatment of multiple myeloma in remission with anticancer drugs having cell cycle specific characteristics. *Cancer Treat Rep,* 61, 381-8.

ALBIG, W. & DOENECKE, D. (1997) The human histone gene cluster at the D6S105 locus. *Hum Genet,* 101, 284-94.

ALBIG, W., KIOSCHIS, P., POUSTKA, A., MEERGANS, K. & DOENECKE, D. (1997) Human histone gene organization: nonregular arrangement within a large cluster. *Genomics,* 40, 314-22.

ALLINEN, M., HUUSKO, P., MANTYNIEMI, S., LAUNONEN, V. & WINQVIST, R. (2001) Mutation analysis of the CHK2 gene in families with hereditary breast cancer. Br J Cancer, 85, 209-12.

ALNEMRI, E. S., LIVINGSTON, D. J., NICHOLSON, D. W., SALVESEN, G., THORNBERRY, N. A., WONG, W. W. & YUAN, J. (1996) Human ICE/CED-3 protease nomenclature. *Cell,* 87, 171.

ALSAYED, Y., NGO, H., RUNNELS, J., LELEU, X., SINGHA, U. K., PITSILLIDES, C. M., SPENCER, J. A., KIMLINGER, T., GHOBRIAL, J. M., JIA, X., LU, G., TIMM, M., KUMAR, A., COTE, D., VEILLEUX, I., HEDIN, K. E., ROODMAN, G. D., WITZIG, T. E., KUNG, A. L., HIDESHIMA, T., ANDERSON, K. C., LIN, C. P. & GHOBRIAL, I. M. (2007) Mechanisms of regulation of CXCR4/SDF-1 (CXCL12)-dependent migration and homing in multiple myeloma. *Blood,* 109**,** 2708-17.

ALTEKRUSE SF, K. C., KRAPCHO M, NEYMAN N, AMINOU R, WALDRON W, RUHL J, HOWLADER N, TATLOVICH Z, CHO H, MARIOTTO A EISNER MP, LEWIS DR, CRONIN K, CHEN HS, FEUER EJ, STINCHCOMB DG, EDWARDS BD (2009) SEER Cancer Statistics Review, 1975 - 2007. IN INSTITUTE, N. C. (Ed. Bethesda, MD, National Cancer Institute.

AMIN, S. B., YIP, W. K., MINVIELLE, S., BROYL, A., LI, Y., HANLON, B., SWANSON, D., SHAH, P. K., MOREAU, P., VAN DER HOLT, B., VAN DUIN, M., MAGRANGEAS, F., PIETER SONNEVELD, P., ANDERSON, K. C., LI, C., AVET-LOISEAU, H. & MUNSHI, N. C. 2014. Gene expression profile alone is inadequate in predicting complete response in multiple myeloma. Leukemia, 28, 2229-34.

ANDERSON, K. C. & LUST, J. A. 1999. Role of cytokines in multiple myeloma. Semin Hematol, 36, 14-20.

ANGSTREICH, G. R., MATSUI, W., HUFF, C. A., VALA, M. S., BARBER, J., HAWKINS, A. L., GRIFFIN, C. A., SMITH, B. D. & JONES, R. J. (2005) Effects of imatinib and interferon on primitive chronic myeloid leukaemia progenitors. *Br J Haematol,* 130**,** 373-81.

APO-BRDU.

ATTAL, M., HAROUSSEAU, J. L., STOPPA, A. M., SOTTO, J. J., FUZIBET, J. G., ROSSI, J. F., CASASSUS, P., MAISONNEUVE, H., FACON, T., IFRAH, N., PAYEN, C. & BATAILLE, R. (1996) A prospective, randomized trial of autologous bone marrow transplantation and chemotherapy in multiple myeloma. Intergroupe Francais du Myelome. *N Engl J Med,* 335**,** 91-7.

ATTAL, M., LAUWERS-CANCES, V., MARIT, G., CAILLOT, D., MOREAU, P., FACON, T., STOPPA, A. M., HULIN, C., BENBOUBKER, L., GARDERET, L., DECAUX, O., LEYVRAZ, S., VEKEMANS, M. C., VOILLAT, L., MICHALLET, M., PEGOURIE, B., DUMONTET, C., ROUSSEL, M., LELEU, X., MATHIOT, C., PAYEN, C., AVET-LOISEAU, H. & HAROUSSEAU, J. L. (2012) Lenalidomide maintenance after stem-cell transplantation for multiple myeloma. *N Engl J Med,* 366**,** 1782-91.

AUSTEN, B., BARONE, G., REIMAN, A., BYRD, P. J., BAKER, C., STARCZYNSKI, J., NOBBS, M. C., MURPHY, R. P., ENRIGHT, H., CHAILA, E., QUINN, J., STANKOVIC, T., PRATT, G. & TAYLOR, A. M. (2008) Pathogenic ATM mutations occur rarely in a subset of multiple myeloma patients. *Br J Haematol,* 142, 925-33.

AZIMZADEH, J. & BORNENS, M. (2007) Structure and duplication of the centrosome. *J Cell Sci,* 120, 2139-42.

BAI, X., TROWBRIDGE, J. J., RILEY, E., LEE, J. A., DIBIASE, A., KAARTINEN, V. M., ORKIN, S. H. & ZON, L. I. (2013) TiF1-gamma plays an essential role in murine hematopoiesis and regulates transcriptional elongation of erythroid genes. *Dev Biol,* 373, 422-30.

BAKKUS, M. H., VAN RIET, I., DE GREEF, C., VAN CAMP, B. & THIELEMANS, K. (1995) The clonogenic precursor cell in multiple myeloma. *Leuk Lymphoma,* 18**,** 221-9.

BAKKUS, M. H., VAN RIET, I., VAN CAMP, B. & THIELEMANS, K. (1994) Evidence that the clonogenic cell in multiple myeloma originates from a pre-switched but somatically mutated B cell. *Br J Haematol,* 87**,** 68-74.

BALIGA, B. C. & KUMAR, S. (2002) Role of Bcl-2 family of proteins in malignancy. *Hematol Oncol,* 20, 63-74.

BARCZAK, A., RODRIGUEZ, M. W., HANSPERS, K., KOTH, L. L., TAI, Y. C., BOLSTAD, B. M., SPEED, T. P. & ERLE, D. J. (2003) Spotted long oligonucleotide arrays for human gene expression analysis. *Genome Res,* 13, 1775-85.

BARDIN, A. J., VISINTIN, R. & AMON, A. (2000) A mechanism for coupling exit from mitosis to partitioning of the nucleus. *Cell,* 102, 21-31.

BARLOGIE B, K. R., ANDERSON K, ET AL. (2003) Comparable survival in multiple my- eloma (MM) with high dose therapy (HDT) employing MEL 140 mg/m2 1 TBI 12 Gy autotransplants versus standard dose therapy with VBMCP and no benefit from interferon (IFN) maintenance: Results of Intergroup Trial S9321. *Blood,* 102**,** 42a.

BARLOGIE, B., VELASQUEZ, W. S., ALEXANIAN, R. & CABANILLAS, F. (1989) Etoposide, dexamethasone, cytarabine, and cisplatin in vincristine, doxorubicin, and dexamethasone-refractory myeloma. *J Clin Oncol,* 7, 1514-7.

BARLOW, J. H., FARYABI, R. B., CALLEN, E., WONG, N., MALHOWSKI, A., CHEN, H. T., GUTIERREZ-CRUZ, G., SUN, H. W., MCKINNON, P., WRIGHT, G., CASELLAS, R., ROBBIANI, D. F., STAUDT, L., FERNANDEZ-CAPETILLO, O. & NUSSENZWEIG, A. Identification of early replicating fragile sites that contribute to genome instability. *Cell,* 152, 620-32.

BARTEK, J. & LUKAS, J. (2007) DNA damage checkpoints: from initiation to recovery or adaptation. *Curr Opin Cell Biol,* 19, 238-45.

BATAILLE, R. & HAROUSSEAU, J. L. (1997) Multiple myeloma. *N Engl J Med,* 336**,** 1657-64.

BAZ, R., SHAIN, K., ALSINA, M., NARDELLI, L., NISHIHORI, T. & OCHOA, L. (2012) Oral weekly cyclophosphamide in combination with pomalidomide and dexamethasone for relapsed and refractory myeloma: report of the dose escalation cohort. *ASH Annu Meet Abstr,* 120, 4062.

BEACH, D., DURKACZ, B. & NURSE, P. (1982) Functionally homologous cell cycle control genes in budding and fission yeast. *Nature,* 300, 706-9.

BEDI, A., ZEHNBAUER, B. A., COLLECTOR, M. I., BARBER, J. P., ZICHA, M. S., SHARKIS, S. J. & JONES, R. J. (1993) BCR-ABL gene rearrangement and expression of primitive hematopoietic progenitors in chronic myeloid leukemia. *Blood,* 81**,** 2898-902.

BENNETT, J. M., SILBER, R., EZDINLI, E., LEVITT, M., OKEN, M., BAKEMEIER, R. F., BAILAR, J. C. & CARBONE, P. P. (1978) Phase II study of adriamycin and bleomycin in patients with multiple myeloma. *Cancer Treat Rep,* 62, 1367-9.

BERDEJA, J. G., HERNANDEZ-ILIZALITURRI, F., CHANAN-KHAN, A., PATEL, M., KELLY, K. R. & RUNNING, K. L. (2012) Phase I stud of lorvotuzumab mertansine (LM, IMGN901) in combination with lenalidomide and dexamethasone in patients with CD56-positive relapsed or

relapsed/refractor multiple myeloma. *ASH Annu Meet Abstr,* 120, 728.
BERENSON, J. R., VESCIO, R. A., HONG, C. H., CAO, J., KIM, A., LEE, C. C., SCHILLER, G., BERENSON, R. J. & LICHTENSTEIN, A. K. (1995) Multiple myeloma clones are derived from a cell late in B lymphoid development. *Curr Top Microbiol Immunol,* 194**,** 25-33.
BERGSAGEL, P. L., KUEHL, W. M., ZHAN, F., SAWYER, J., BARLOGIE, B. & SHAUGHNESSY, J., JR. (2005) Cyclin D dysregulation: an early and unifying pathogenic event in multiple myeloma. *Blood,* 106, 296-303.
BEROUKHIM, R., MERMEL, C. H., PORTER, D., WEI, G., RAYCHAUDHURI, S., DONOVAN, J., BARRETINA, J., BOEHM, J. S., DOBSON, J., URASHIMA, M., MC HENRY, K. T., PINCHBACK, R. M., LIGON, A. H., CHO, Y. J., HAERY, L., GREULICH, H., REICH, M., WINCKLER, W., LAWRENCE, M. S., WEIR, B. A., TANAKA, K. E., CHIANG, D. Y., BASS, A. J., LOO, A., HOFFMAN, C., PRENSNER, J., LIEFELD, T., GAO, Q., YECIES, D., SIGNORETTI, S., MAHER, E., KAYE, F. J., SASAKI, H., TEPPER, J. E., FLETCHER, J. A., TABERNERO, J., BASELGA, J., TSAO, M. S., DEMICHELIS, F., RUBIN, M. A., JANNE, P. A., DALY, M. J., NUCERA, C., LEVINE, R. L., EBERT, B. L., GABRIEL, S., RUSTGI, A. K., ANTONESCU, C. R., LADANYI, M., LETAI, A., GARRAWAY, L. A., LODA, M., BEER, D. G., TRUE, L. D., OKAMOTO, A., POMEROY, S. L., SINGER, S., GOLUB, T. R., LANDER, E. S., GETZ, G., SELLERS, W. R. & MEYERSON, M. (2010) The landscape of somatic copy-number alteration across human cancers. *Nature,* 463**,** 899-905.
BIEL, M., WASCHOLOWSKI, V. & GIANNIS, A. (2005) Epigenetics--an epicenter of gene regulation: histones and histone-modifying enzymes. *Angew Chem Int Ed Engl,* 44, 3186-216.
BILLADEAU, D., AHMANN, G., GREIPP, P. & VAN NESS, B. (1993) The bone marrow of multiple myeloma patients contains B cell populations at different stages of differentiation that are clonally related to the malignant plasma cell. *J Exp Med,* 178**,** 1023-31.
BISPING, G., WENNING, D., KROPFF, M., GUSTAVUS, D., MULLER-TIDOW, C., STELLJES, M., MUNZERT, G., HILBERG, F., ROTH, G. J., STEFANIC, M., VOLPERT, S., MESTERS, R. M., BERDEL, W. E. & KIENAST, J. (2009) Bortezomib, dexamethasone, and fibroblast growth factor receptor 3-specific tyrosine kinase inhibitor in t(4;14) myeloma. *Clin Cancer Res,* 15, 520-31.
BLADE J, S. A., RIBERA JM, ET AL. (2003) High-dose therapy autotransplantation/ intensification versus continued conventional chemotherapy in multiple my- eloma patients responding to initial chemotherapy. Definitive results from PETHEMA after a median follow-up of 66 months. *Blood,* 102, 42a.
BONNET, D. & DICK, J. E. (1997) Human acute myeloid leukemia is organized as a hierarchy that originates from a primitive hematopoietic cell. *Nat Med,* 3**,** 730-7.
BONNET, J., ALEXANIAN, R., SALMON, S., BOTTOMLEY, R., AMARE, M., HAUT, A. & DIXON, D. (1982) Vincristine, BCNU, doxorubicin, and prednisone (VBAP) combination in the treatment of relapsing or resistant multiple myeloma: a Southwest Oncology Group study. *Cancer Treat Rep,* 66, 1267-71.
BONNET, J. D., ALEXANIAN, R., SALMON, S. E., HAUT, A. & DIXON, D. O. (1984) Addition of cisplatin and bleomycin to vincristine-carmustine-doxorubicin-prednisone (VBAP) combination in the treatment of relapsing or resistant multiple myeloma: a Southwest Oncology Group study. *Cancer Treat Rep,* 68, 481-5.
BONTE, D., LINDVALL, C., LIU, H., DYKEMA, K., FURGE, K. & WEINREICH, M. (2008) Cdc7-Dbf4 kinase overexpression in multiple cancers and tumor cell lines is correlated with p53 inactivation. *Neoplasia,* 10, 920-31.
BORDE, V., GOLDMAN, A. S. & LICHTEN, M. (2000) Direct coupling between meiotic DNA replication and recombination initiation. *Science,* 290, 806-9.
BORK, P., HOFMANN, K., BUCHER, P., NEUWALD, A. F., ALTSCHUL, S. F. & KOONIN, E. V. (1997) A superfamily of conserved domains in DNA damage-responsive cell cycle checkpoint proteins. *FASEB J,* 11**,** 68-76.

BOUCHARD, V. J., ROULEAU, M. & POIRIER, G. G. (2003) PARP-1, a determinant of cell survival in response to DNA damage. *Exp Hematol,* 31, 446-54.
BOVIA, F., NABILI-TEHRANI, A. C., WERNER-FAVRE, C., BARNET, M., KINDLER, V. & ZUBLER, R. H. (1998) Quiescent memory B cells in human peripheral blood co-express bcl-2 and bcl-x(L) anti-apoptotic proteins at high levels. *Eur J Immunol,* 28, 4418-23.
BROCK, A., CHANG, H. & HUANG, S. (2009) Non-genetic heterogeneity--a mutation-independent driving force for the somatic evolution of tumours. *Nat Rev Genet,* 10, 336-42.
BRODSKY, R. A. & JONES, R. J. (2005) Aplastic anaemia. *Lancet,* 365, 1647-56.
BROWN, S. W. (1966) Heterochromatin. *Science,* 151, 417-25.
CAI, D., LATHAM, V. M., JR., ZHANG, X. & SHAPIRO, G. I. (2006) Combined depletion of cell cycle and transcriptional cyclin-dependent kinase activities induces apoptosis in cancer cells. *Cancer Res,* 66, 9270-80.
CALIMERI, T., BATTISTA, E., CONFORTI, F., NERI, P., DI MARTINO, M. T., ROSSI, M., FORESTA, U., PIRO, E., FERRARA, F., AMOROSI, A., BAHLIS, N., ANDERSON, K. C., MUNSHI, N., TAGLIAFERRI, P., CAUSA, F. & TASSONE, P. (2011) A unique three-dimensional SCID-polymeric scaffold (SCID-synth-hu) model for in vivo expansion of human primary multiple myeloma cells. *Leukemia,* 25**,** 707-11.
CAO, J., VESCIO, R. A., HONG, C. H., KIM, A., LICHTENSTEIN, A. K. & BERENSON, J. R. (1995) Identification of malignant cells in multiple myeloma bone marrow with immunoglobulin VH gene probes by fluorescent in situ hybridization and flow cytometry. *J Clin Invest,* 95**,** 964-72.
CARRASCO, D. R., TONON, G., HUANG, Y., ZHANG, Y., SINHA, R., FENG, B., STEWART, J. P., ZHAN, F., KHATRY, D., PROTOPOPOVA, M., PROTOPOPOV, A., SUKHDEO, K., HANAMURA, I., STEPHENS, O., BARLOGIE, B., ANDERSON, K. C., CHIN, L., SHAUGHNESSY, J. D., JR., BRENNAN, C. & DEPINHO, R. A. (2006) High-resolution genomic profiles define distinct clinicopathogenetic subgroups of multiple myeloma patients. *Cancer Cell,* 9**,** 313-25.
CASTEDO, M., PERFETTINI, J. L., ROUMIER, T. & KROEMER, G. (2002) Cyclin-dependent kinase-1: linking apoptosis to cell cycle and mitotic catastrophe. *Cell Death Differ,* 9, 1287-93.
CASUCCI, M., NICOLIS DI ROBILANT, B., FALCONE, L., CAMISA, B., NORELLI, M., GENOVESE, P., GENTNER, B., GULLOTTA, F., PONZONI, M., BERNARDI, M., MARCATTI, M., SAUDEMONT, A., BORDIGNON, C., SAVOLDO, B., CICERI, F., NALDINI, L., DOTTI, G., BONINI, C. & BONDANZA, A. CD44v6-targeted T cells mediate potent antitumor effects against acute myeloid leukemia and multiple myeloma. *Blood,* 122**,** 3461-72.
CAVO, M., TACCHETTI, P., PATRIARCA, F., PETRUCCI, M. T., PANTANI, L., GALLI, M., DI RAIMONDO, F., CRIPPA, C., ZAMAGNI, E., PALUMBO, A., OFFIDANI, M., CORRADINI, P., NARNI, F., SPADANO, A., PESCOSTA, N., DELILIERS, G. L., LEDDA, A., CELLINI, C., CARAVITA, T., TOSI, P. & BACCARANI, M. (2010) Bortezomib with thalidomide plus dexamethasone compared with thalidomide plus dexamethasone as induction therapy before, and consolidation therapy after, double autologous stem-cell transplantation in newly diagnosed multiple myeloma: a randomised phase 3 study. *Lancet,* 376**,** 2075-85.
CEULEMANS, H. & BOLLEN, M. (2004) Functional diversity of protein phosphatase-1, a cellular economizer and reset button. *Physiol Rev,* 84, 1-39.
CHAIDOS, A., BARNES, C. P., COWAN, G., MAY, P. C., MELO, V., HATJIHARISSI, E., PAPAIOANNOU, M., HARRINGTON, H., DOOLITTLE, H., TERPOS, E., DIMOPOULOS, M., ABDALLA, S., YARRANTON, H., NARESH, K., FORONI, L., REID, A., RAHEMTULLA, A., STUMPF, M., ROBERTS, I. & KARADIMITRIS, A. (2013) Clinical drug resistance linked to interconvertible phenotypic and functional states of tumor-propagating cells in multiple myeloma. *Blood,* 121**,** 318-28.
CHAIDOS, A., CAPUTO, V., GOUVEDENOU, K., LIU, B., MARIGO, I., CHAUDHRY, M. S., ROTOLO, A., TOUGH, D. F., SMITHERS, N. N., BASSIL, A. K., CHAPMAN, T. D., HARKER, N. R., BAR-

BASH, O., TUMMINO, P., AL-MAHDI, N., HAYNES, A. C., CUTLER, L., LE, B., RAHEMTULLA, A., ROBERTS, I., KLEIJNEN, M., WITHERINGTON, J. J., PARR, N. J., PRINJHA, R. K. & KARA-DIMITRIS, A. (2014) Potent antimyeloma activity of the novel bromodomain inhibitors I-BET151 and I-BET762. *Blood,* 123**,** 697-705.

CHAPMAN, M. A., LAWRENCE, M. S., KEATS, J. J., CIBULSKIS, K., SOUGNEZ, C., SCHINZEL, A. C., HARVIEW, C. L., BRUNET, J. P., AHMANN, G. J., ADLI, M., ANDERSON, K. C., ARDLIE, K. G., AUCLAIR, D., BAKER, A., BERGSAGEL, P. L., BERNSTEIN, B. E., DRIER, Y., FONSECA, R., GABRIEL, S. B., HOFMEISTER, C. C., JAGANNATH, S., JAKUBOWIAK, A. J., KRISHNAN, A., LEVY, J., LIEFELD, T., LONIAL, S., MAHAN, S., MFUKO, B., MONTI, S., PERKINS, L. M., ONOFRIO, R., PUGH, T. J., RAJKUMAR, S. V., RAMOS, A. H., SIEGEL, D. S., SIVACHENKO, A., STEWART, A. K., TRUDEL, S., VIJ, R., VOET, D., WINCKLER, W., ZIMMERMAN, T., CARPTEN, J., TRENT, J., HAHN, W. C., GARRAWAY, L. A., MEYERSON, M., LANDER, E. S., GETZ, G. & GOLUB, T. R. (2011) Initial genome sequencing and analysis of multiple myeloma. *Nature,* 471**,** 467-72.

CHAN, L. Y. & AMON, A. (2009) The protein phosphatase 2A functions in the spindle position checkpoint by regulating the checkpoint kinase Kin4. *Genes Dev,* 23, 1639-49.

CHAO, S. H. & PRICE, D. H. (2001) Flavopiridol inactivates P-TEFb and blocks most RNA polymerase II transcription in vivo. *J Biol Chem,* 276, 31793-9.

CHAUHAN, D., RAY, A., VIKTORSSON, K., SPIRA, J., PABA-PRADA, C., MUNSHI, N., RICHARDSON, P., LEWENSOHN, R. & ANDERSON, K. C. (2013) In vitro and in vivo antitumor activity of a novel alkylating agent, melphalan-flufenamide, against multiple myeloma cells. *Clin Cancer Res,* 19, 3019-31.

CHEN, R., YANG, Z. & ZHOU, Q. (2004) Phosphorylated positive transcription elongation factor b (P-TEFb) is tagged for inhibition through association with 7SK snRNA. *J Biol Chem,* 279, 4153-60.

CHEN, Z., CHENG, K., WALTON, Z., WANG, Y., EBI, H., SHIMAMURA, T., LIU, Y., TUPPER, T., OUYANG, J., LI, J., GAO, P., WOO, M. S., XU, C., YANAGITA, M., ALTABEF, A., WANG, S., LEE, C., NAKADA, Y., PENA, C. G., SUN, Y., FRANCHETTI, Y., YAO, C., SAUR, A., CAMERON, M. D., NISHINO, M., HAYES, D. N., WILKERSON, M. D., ROBERTS, P. J., LEE, C. B., BARDEESY, N., BUTANEY, M., CHIRIEAC, L. R., COSTA, D. B., JACKMAN, D., SHARPLESS, N. E., CASTRILLON, D. H., DEMETRI, G. D., JANNE, P. A., PANDOLFI, P. P., CANTLEY, L. C., KUNG, A. L., ENGELMAN, J. A. & WONG, K. K. (2012) A murine lung cancer co-clinical trial identifies genetic modifiers of therapeutic response. *Nature,* 483**,** 613-7.

CHEN, Z., ORLOWSKI, R. Z., WANG, M., KWAK, L. & MCCARTY, N. (2014) Osteoblastic niche supports the growth of quiescent multiple myeloma cells. *Blood,* 123**,** 2204-8.

CHENG, L., COLLYER, T. & HARDY, C. F. (1999) Cell cycle regulation of DNA replication initiator factor Dbf4p. *Mol Cell Biol,* 19**,** 4270-8

CHESI, M., MATTHEWS, G. M., GARBITT, V. M., PALMER, S. E., SHORTT, J., LEFEBURE, M., STEWART, A. K., JOHNSTONE, R. W. & BERGSAGEL, P. L. (2012) Drug response in a genetically engineered mouse model of multiple myeloma is predictive of clinical efficacy. *Blood,* 120, 376-85.

CHESI, M., ROBBIANI, D. F., SEBAG, M., CHNG, W. J., AFFER, M., TIEDEMANN, R., VALDEZ, R., PALMER, S. E., HAAS, S. S., STEWART, A. K., FONSECA, R., KREMER, R., CATTORETTI, G. & BERGSAGEL, P. L. (2008) AID-dependent activation of a MYC transgene induces multiple myeloma in a conditional mouse model of post-germinal center malignancies. *Cancer Cell,* 13**,** 167-80.

CHILD, J. A., MORGAN, G. J., DAVIES, F. E., OWEN, R. G., BELL, S. E., HAWKINS, K., BROWN, J., DRAYSON, M. T. & SELBY, P. J. (2003) High-dose chemotherapy with hematopoietic stem-cell rescue for multiple myeloma. *N Engl J Med,* 348**,** 1875-83.

CHNG, W. J., KUMAR, S., VANWIER, S., AHMANN, G., PRICE-TROSKA, T., HENDERSON, K., CHUNG,

T. H., KIM, S., MULLIGAN, G., BRYANT, B., CARPTEN, J., GERTZ, M., RAJKUMAR, S. V., LACY, M., DISPENZIERI, A., KYLE, R., GREIPP, P., BERGSAGEL, P. L. & FONSECA, R. (2007) Molecular dissection of hyperdiploid multiple myeloma by gene expression profiling. *Cancer Res,* 67, 2982-9.

CHO, W. H., LEE, Y. J., KONG, S. I., HURWITZ, J. & LEE, J. K. (2006) CDC7 kinase phosphorylates serine residues adjacent to acidic amino acids in the minichromosome maintenance 2 protein. *Proc Natl Acad Sci U S A,* 103, 11521-6.

CHOI, W. W., WEISENBURGER, D. D., GREINER, T. C., PIRIS, M. A., BANHAM, A. H., DELABIE, J., BRAZIEL, R. M., GENG, H., IQBAL, J., LENZ, G., VOSE, J. M., HANS, C. P., FU, K., SMITH, L. M., LI, M., LIU, Z., GASCOYNE, R. D., ROSENWALD, A., OTT, G., RIMSZA, L. M., CAMPO, E., JAFFE, E. S., JAYE, D. L., STAUDT, L. M. & CHAN, W. C. (2009) A new immunostain algorithm classifies diffuse large B-cell lymphoma into molecular subtypes with high accuracy. *Clin Cancer Res,* 15, 5494-502.

CHOU, T. C. (2008) Preclinical versus clinical drug combination studies. *Leuk Lymphoma,* 49, 2059-80.

CHRISTMANN, J. L. & DAHMUS, M. E. (1981) Monoclonal antibody specific for calf thymus RNA polymerases IIO and IIA. *J Biol Chem,* 256**,** 11798-803.

CHRISTOFFERSON, D. E. & YUAN, J. Necroptosis as an alternative form of programmed cell death. *Curr Opin Cell Biol,* 22, 263-8.

CHU, V. T., FROHLICH, A., STEINHAUSER, G., SCHEEL, T., ROCH, T., FILLATREAU, S., LEE, J. J., LOHNING, M. & BEREK, C. 2011. Eosinophils are required for the maintenance of plasma cells in the bone marrow. Nat Immunol, 12, 151-9.

CLAPPERTON, J. A., MANKE, I. A., LOWERY, D. M., HO, T., HAIRE, L. F., YAFFE, M. B. & SMERDON, S. J. (2004) Structure and mechanism of BRCA1 BRCT domain recognition of phosphorylated BACH1 with implications for cancer. *Nat Struct Mol Biol,* 11**,** 512-8.

CLAUDIO, J. O., ZHAN, F., ZHUANG, L., KHAJA, R., ZHU, Y. X., SIVANANTHAN, K., TRUDEL, S., MASIH-KHAN, E., FONSECA, R., BERGSAGEL, P. L., SCHERER, S. W., SHAUGHNESSY, J. & STEWART, A. K. 2007. Expression and mutation status of candidate kinases in multiple myeloma. Leukemia, 21, 1124-7.

CLAYTON, H., TITLEY, I. & VIVANCO, M. (2004) Growth and differentiation of progenitor/stem cells derived from the human mammary gland. *Exp Cell Res,* 297**,** 444-60.

COOK, G., MARINAKI, P., FARRELL, E., PEARSON, C., ALCORN, M. J., SHARP, R. A., TANSEY, P. J. & FRANKLIN, I. M. (1997) Peripheral blood progenitor cell mobilisation in patients with multiple myeloma following oral idarubicin and dexamethasone (Z-Dex) induction therapy. *Leukemia,* 11 Suppl 5, S35-40.

CULOTTI, J. & HARTWELL, L. H. (1971) Genetic control of the cell division cycle in yeast. 3. Seven genes controlling nuclear division. *Exp Cell Res,* 67, 389-401.

D'SA, S., YONG, K., KYRIAKOU, C., BHATTACHARYA, S., PEGGS, K. S., FOULKES, B., WATTS, M. J., INGS, S. J., ARDESHNA, K. M., GOLDSTONE, A. H. & WILLIAMS, C. D. (2004) Etoposide, methylprednisolone, cytarabine and cisplatin successfully cytoreduces resistant myeloma patients and mobilizes them for transplant without adverse effects. *Br J Haematol,* 125, 756-65.

DALTON, W. & ANDERSON, K. C. (2006) Synopsis of a roundtable on validating novel therapeutics for multiple myeloma. *Clin Cancer Res,* 12**,** 6603-10.

DALTON, W. S., HAZLEHURST, L., SHAIN, K., LANDOWSKI, T. & ALSINA, M. (2004) Targeting the bone marrow microenvironment in hematologic malignancies. *Semin Hematol,* 41, 1-5.

DAMIANO, J. S. & DALTON, W. S. (2000) Integrin-mediated drug resistance in multiple myeloma. *Leuk Lymphoma,* 38**,** 71-81.

DE BRUYNE, E., BOS, T. J., SCHUIT, F., VAN VALCKENBORGH, E., MENU, E., THORREZ, L., ATADJA, P., JERNBERG-WIKLUND, H. & VANDERKERKEN, K. (2010) IGF-1 suppresses Bim expres-

sion in multiple myeloma via epigenetic and posttranslational mechanisms. *Blood,* 115, 2430-40.

DECAUX, O., LODE, L., MAGRANGEAS, F., CHARBONNEL, C., GOURAUD, W., JEZEQUEL, P., ATTAL, M., HAROUSSEAU, J. L., MOREAU, P., BATAILLE, R., CAMPION, L., AVET-LOISEAU, H. & MINVIELLE, S. (2008) Prediction of survival in multiple myeloma based on gene expression profiles reveals cell cycle and chromosomal instability signatures in high-risk patients and hyperdiploid signatures in low-risk patients: a study of the Intergroupe Francophone du Myelome. *J Clin Oncol,* 26**,** 4798-805.

DECLERCQ, W., VANDEN BERGHE, T. & VANDENABEELE, P. (2009) RIP kinases at the crossroads of cell death and survival. *Cell,* 138, 229-32.

DELMORE, J. E., ISSA, G. C., LEMIEUX, M. E., RAHL, P. B., SHI, J., JACOBS, H. M., KASTRITIS, E., GILPATRICK, T., PARANAL, R. M., QI, J., CHESI, M., SCHINZEL, A. C., MCKEOWN, M. R., HEFFERNAN, T. P., VAKOC, C. R., BERGSAGEL, P. L., GHOBRIAL, I. M., RICHARDSON, P. G., YOUNG, R. A., HAHN, W. C., ANDERSON, K. C., KUNG, A. L., BRADNER, J. E. & MITSIADES, C. S. (2011) BET bromodomain inhibition as a therapeutic strategy to target c-Myc. *Cell,* 146, 904-17.

DEPAMPHILIS, M. L. (2006) *DNA replication and human disease,* Cold Spring Harbor, N.Y., Cold Spring Harbor Laboratory Press.

DEPHOURE, N., ZHOU, C., VILLEN, J., BEAUSOLEIL, S. A., BAKALARSKI, C. E., ELLEDGE, S. J. & GYGI, S. P. (2008) A quantitative atlas of mitotic phosphorylation. *Proc Natl Acad Sci U S A,* 105, 10762-7.

DERENNE, S., MONIA, B., DEAN, N. M., TAYLOR, J. K., RAPP, M. J., HAROUSSEAU, J. L., BATAILLE, R. & AMIOT, M. (2002) Antisense strategy shows that Mcl-1 rather than Bcl-2 or Bcl-x(L) is an essential survival protein of human myeloma cells. *Blood,* 100, 194-9.

DESHPANDE, A. M. & NEWLON, C. S. (1996) DNA replication fork pause sites dependent on transcription. *Science,* 272, 1030-3.

DHODAPKAR, M. V., SEXTON, R., WAHEED, S., USMANI, S., PAPANIKOLAOU, X., NAIR, B., PETTY, N., SHAUGHNESSY, J. D., JR., HOERING, A., CROWLEY, J., ORLOWSKI, R. Z. & BARLOGIE, B. (2014) Clinical, genomic, and imaging predictors of myeloma progression from asymptomatic monoclonal gammopathies (SWOG S0120). *Blood,* 123**,** 78-85.

DIFFLEY, J. F., COCKER, J. H., DOWELL, S. J., HARWOOD, J. & ROWLEY, A. (1995) Stepwise assembly of initiation complexes at budding yeast replication origins during the cell cycle. *J Cell Sci Suppl,* 19, 67-72.

DIGNAM, J. D., LEBOVITZ, R. M. & ROEDER, R. G. (1983) Accurate transcription initiation by RNA polymerase II in a soluble extract from isolated mammalian nuclei. *Nucleic Acids Res,* 11, 1475-89.

DIMITROVA, D. S. & GILBERT, D. M. (2000) Temporally coordinated assembly and disassembly of replication factories in the absence of DNA synthesis. *Nat Cell Biol,* 2, 686-94.

DIMOPOULOS, M., ET AL. (2011) Vantage 088: Vorinostat in Combination with Bortezomib in Patients with Relapsed/Refractory Multiple Myeloma: Results of a Global, Randomized Phase 3 Trial. *ASH Annu Meet Abstr*.

DISPENZIERI, A., GERTZ, M. A., LACY, M. Q., GEYER, S. M., FITCH, T. R., FENTON, R. G., FONSECA, R., ISHAM, C. R., ZIESMER, S. C., ERLICHMAN, C. & BIBLE, K. C. (2006) Flavopiridol in patients with relapsed or refractory multiple myeloma: a phase 2 trial with clinical and pharmacodynamic end-points. *Haematologica,* 91, 390-3.

DISPENZIERI, A., RAJKUMAR, S. V., GERTZ, M. A., FONSECA, R., LACY, M. Q., BERGSAGEL, P. L., KYLE, R. A., GREIPP, P. R., WITZIG, T. E., REEDER, C. B., LUST, J. A., RUSSELL, S. J., HAYMAN, S. R., ROY, V., KUMAR, S., ZELDENRUST, S. R., DALTON, R. J. & STEWART, A. K. (2007) Treatment of newly diagnosed multiple myeloma based on Mayo Stratification of Myeloma and Risk-adapted Therapy (mSMART): consensus statement. *Mayo Clin Proc,* 82**,**

323-41.
DIZDAR, O., BARISTA, I., KALYONCU, U., KARADAG, O., HASCELIK, G., CILA, A., PINAR, A., CELIK, I., KARS, A. & TEKUZMAN, G. (2007) Biochemical markers of bone turnover in diagnosis of myeloma bone disease. *Am J Hematol,* 82**,** 185-91.
DOMINGUEZ-SOLA, D., YING, C. Y., GRANDORI, C., RUGGIERO, L., CHEN, B., LI, M., GALLOWAY, D. A., GU, W., GAUTIER, J. & DALLA-FAVERA, R. (2007) Non-transcriptional control of DNA replication by c-Myc. *Nature,* 448, 445-51.
DORNER, T. & RADBRUCH, A. (2005) Selecting B cells and plasma cells to memory. *J Exp Med,* 201**,** 497-9.
DREWINKO, B., ALEXANIAN, R., BOYER, H., BARLOGIE, B. & RUBINOW, S. I. (1981) The growth fraction of human myeloma cells. *Blood,* 57**,** 333-8.
DURIE, B. G., HAROUSSEAU, J. L., MIGUEL, J. S., BLADE, J., BARLOGIE, B., ANDERSON, K., GERTZ, M., DIMOPOULOS, M., WESTIN, J., SONNEVELD, P., LUDWIG, H., GAHRTON, G., BEKSAC, M., CROWLEY, J., BELCH, A., BOCCADARO, M., CAVO, M., TURESSON, I., JOSHUA, D., VESOLE, D., KYLE, R., ALEXANIAN, R., TRICOT, G., ATTAL, M., MERLINI, G., POWLES, R., RICHARDSON, P., SHIMIZU, K., TOSI, P., MORGAN, G. & RAJKUMAR, S. V. (2006) International uniform response criteria for multiple myeloma. *Leukemia,* 20**,** 1467-73.
DURIE, B. G. & SALMON, S. E. (1975) A clinical staging system for multiple myeloma. Correlation of measured myeloma cell mass with presenting clinical features, response to treatment, and survival. *Cancer,* 36, 842-54.
DURKIN, S. G., ARLT, M. F., HOWLETT, N. G. & GLOVER, T. W. (2006) Depletion of CHK1, but not CHK2, induces chromosomal instability and breaks at common fragile sites. *Oncogene,* 25, 4381-8.
EARNSHAW, W. C., MARTINS, L. M. & KAUFMANN, S. H. (1999) Mammalian caspases: structure, activation, substrates, and functions during apoptosis. *Annu Rev Biochem,* 68, 383-424.
EBERHARDY, S. R. & FARNHAM, P. J. (2001) c-Myc mediates activation of the cad promoter via a post-RNA polymerase II recruitment mechanism. *J Biol Chem,* 276, 48562-71.
EDELSTEIN, M. B., CROWLEY, J. J., VALERIOTE, F. A., BONNET, J. D., CARDEN, J. O., KHANNA, R. C., SALMON, S. E. & UNGERLEIDER, J. S. (1990) A-phase II study of intravenous 6-thioguanine (NSC-752) in multiple myeloma. A Southwest Oncology Group study. *Invest New Drugs,* 8 Suppl 1, S83-6.
EGAN, J. B., SHI, C. X., TEMBE, W., CHRISTOFORIDES, A., KURDOGLU, A., SINARI, S., MIDDHA, S., ASMANN, Y., SCHMIDT, J., BRAGGIO, E., KEATS, J. J., FONSECA, R., BERGSAGEL, P. L., CRAIG, D. W., CARPTEN, J. D. & STEWART, A. K. (2012) Whole-genome sequencing of multiple myeloma from diagnosis to plasma cell leukemia reveals genomic initiating events, evolution, and clonal tides. *Blood,* 120**,** 1060-6.
ELY, S., DI LIBERTO, M., NIESVIZKY, R., BAUGHN, L. B., CHO, H. J., HATADA, E. N., KNOWLES, D. M., LANE, J. & CHEN-KIANG, S. (2005) Mutually exclusive cyclin-dependent kinase 4/cyclin D1 and cyclin-dependent kinase 6/cyclin D2 pairing inactivates retinoblastoma protein and promotes cell cycle dysregulation in multiple myeloma. *Cancer Res,* 65**,** 11345-53.
ENDL, E. & GERDES, J. (2000) The Ki-67 protein: fascinating forms and an unknown function. *Exp Cell Res,* 257, 231-7.
ESKELINEN, E. L. (2008) New insights into the mechanisms of macroautophagy in mammalian cells. *Int Rev Cell Mol Biol,* 266, 207-47.
EVANS, T., ROSENTHAL, E. T., YOUNGBLOM, J., DISTEL, D. & HUNT, T. (1983) Cyclin: a protein specified by maternal mRNA in sea urchin eggs that is destroyed at each cleavage division. *Cell,* 33, 389-96.
FACON, T., RICHARDSON, P. G., JAGANNATH, S., MOREAU, J., JAKUBOWIAK, A. & RAAB, M. S. (2012) Phase I/II study of elotuzumab plus lenalidomide/dexamethasone in relpased/refractory multiple myeloma: updated phase II results adn phase I/II long term safety.

Haematologica, 2013, Abstract 228.
FACON, T., MARY, J. Y., HULIN, C., BENBOUBKER, L., ATTAL, M., PEGOURIE, B., RENAUD, M., HAROUSSEAU, J. L., GUILLERM, G., CHALETEIX, C., DIB, M., VOILLAT, L., MAISONNEUVE, H., TRONCY, J., DORVAUX, V., MONCONDUIT, M., MARTIN, C., CASASSUS, P., JAUBERT, J., JARDEL, H., DOYEN, C., KOLB, B., ANGLARET, B., GROSBOIS, B., YAKOUB-AGHA, I., MATHIOT, C. & AVET-LOISEAU, H. (2007) Melphalan and prednisone plus thalidomide versus melphalan and prednisone alone or reduced-intensity autologous stem cell transplantation in elderly patients with multiple myeloma (IFM 99-06): a randomised trial. *Lancet,* 370**,** 1209-18.
FACON T, M. J., HAROUSSEAU JL, ET AL. (1996) Front-line or rescue autologous bone marrow transplantation (ABMT) following a first course of high dose melphalan (HDM) in multiple myeloma (MM). Preliminary results of a pro- spective randomized trial (CIAM) protocol. *Blood,* 88**,** 685a.
FALSCHLEHNER, C., GANTEN, T. M., KOSCHNY, R., SCHAEFER, U. & WALCZAK, H. (2009) TRAIL and other TRAIL receptor agonists as novel cancer therapeutics. *Adv Exp Med Biol,* 647, 195-206.
FAUL, T., STAIB, C., NANDA, I., SCHMID, M. & GRUMMT, F. (1999) Identification and characterization of mouse homologue to yeast Cdc7 protein and chromosomal localization of the cognate mouse gene Cdc7l. *Chromosoma,* 108**,** 26-31.
FEARNHEAD, H. O., RODRIGUEZ, J., GOVEK, E. E., GUO, W., KOBAYASHI, R., HANNON, G. & LAZEBNIK, Y. A. (1998) Oncogene-dependent apoptosis is mediated by caspase-9. *Proc Natl Acad Sci U S A,* 95, 13664-9.
FEARON, D. T., MANDERS, P. & WAGNER, S. D. (2001) Arrested differentiation, the self-renewing memory lymphocyte, and vaccination. *Science,* 293, 248-50.
FENK, R., SCHNEIDER, P., KROPFF, M., HUENERLITUERKOGLU, A. N., STEIDL, U., AUL, C., HILDEBRANDT, B., HAAS, R., HEYLL, A. & KOBBE, G. (2005) High-dose idarubicin, cyclophosphamide and melphalan as conditioning for autologous stem cell transplantation increases treatment-related mortality in patients with multiple myeloma: results of a randomised study. *Br J Haematol,* 130, 588-94.
FERMAND, J. P., RAVAUD, P., CHEVRET, S., DIVINE, M., LEBLOND, V., BELANGER, C., MACRO, M., PERTUISET, E., DREYFUS, F., MARIETTE, X., BOCCACIO, C. & BROUET, J. C. (1998) High-dose therapy and autologous peripheral blood stem cell transplantation in multiple myeloma: up-front or rescue treatment? Results of a multicenter sequential randomized clinical trial. *Blood,* 92**,** 3131-6.
FERREIRA, M. F., SANTOCANALE, C., DRURY, L. S. & DIFFLEY, J. F. (2000) Dbf4p, an essential S phase-promoting factor, is targeted for degradation by the anaphase-promoting complex. *Mol Cell Biol,* 20, 242-8.
FIEN, K. & HURWITZ, J. (2006) Fission yeast Mcm10p contains primase activity. *J Biol Chem,* 281, 22248-60.
FITZGERALD-HAYES, M., CLARKE, L. & CARBON, J. (1982) Nucleotide sequence comparisons and functional analysis of yeast centromere DNAs. *Cell,* 29, 235-44.
FRANCIS, L. I., RANDELL, J. C., TAKARA, T. J., UCHIMA, L. & BELL, S. P. (2009) Incorporation into the prereplicative complex activates the Mcm2-7 helicase for Cdc7-Dbf4 phosphorylation. *Genes Dev,* 23, 643-54.
FRIGYESI, I., ADOLFSSON, J., ALI, M., CHRISTOPHERSEN, M. K., JOHNSSON, E., TURESSON, I., GULLBERG, U., HANSSON, M. & NILSSON, B. Robust isolation of malignant plasma cells in multiple myeloma. *Blood,* 123**,** 1336-40.
FU, T. J., PENG, J., LEE, G., PRICE, D. H. & FLORES, O. (1999) Cyclin K functions as a CDK9 regulatory subunit and participates in RNA polymerase II transcription. *J Biol Chem,* 274**,** 34527-30.

FUJINAGA, K., IRWIN, D., HUANG, Y., TAUBE, R., KUROSU, T. & PETERLIN, B. M. (2004) Dynamics of human immunodeficiency virus transcription: P-TEFb phosphorylates RD and dissociates negative effectors from the transactivation response element. *Mol Cell Biol,* 24**,** 787-95.

FULLGRABE, J., HAJJI, N. & JOSEPH, B. Cracking the death code: apoptosis-related histone modifications. *Cell Death Differ,* 17, 1238-43.

GABRIELSE, C., MILLER, C. T., MCCONNELL, K. H., DEWARD, A., FOX, C. A. & WEINREICH, M. (2006) A Dbf4p BRCA1 C-terminal-like domain required for the response to replication fork arrest in budding yeast. *Genetics,* 173**,** 541-55.

GARRIGA, J., SEGURA, E., MAYOL, X., GRUBMEYER, C. & GRANA, X. (1996) Phosphorylation site specificity of the CDC2-related kinase PITALRE. *Biochem J,* 320 (Pt 3)**,** 983-9.

GAZITT, Y., SHAUGHNESSY, P. & ROTHENBERG, M. L. (2006) A phase II trial with gemcitabine and paclitaxel for the treatment of refractory and relapsed multiple myeloma patients. *Oncol Rep,* 16, 877-84.

GERTZ, M. A., LACY, M. Q., DISPENZIERI, A., GREIPP, P. R., LITZOW, M. R., HENDERSON, K. J., VAN WIER, S. A., AHMANN, G. J. & FONSECA, R. (2005) Clinical implications of t(11;14)(q13;q32), t(4;14)(p16.3;q32), and -17p13 in myeloma patients treated with high-dose therapy. *Blood,* 106**,** 2837-40.

GEYMONAT, M., SPANOS, A., WALKER, P. A., JOHNSTON, L. H. & SEDGWICK, S. G. (2003) In vitro regulation of budding yeast Bfa1/Bub2 GAP activity by Cdc5. *J Biol Chem,* 278, 14591-4.

GHOBRIAL, I. M., LAUBACH, J., ARMAND, P., BOSWELL, E., HANLON, C. & CHUMA, S. (2013) Phase 1 study of TH-302, an investigational hypoxia-targeted drug, and dexamethasone in patients with relapsed/refractory multiple myeloma. *ASCO Meet Abstr,* 31(15_suppl), 8602.

GIACINTI, C., BAGELLA, L., PURI, P. L., GIORDANO, A. & SIMONE, C. (2006) MyoD recruits the cdk9/cyclin T2 complex on myogenic-genes regulatory regions. *J Cell Physiol,* 206**,** 807-13.

GIACINTI, C., MUSARO, A., DE FALCO, G., JOURDAN, I., MOLINARO, M., BAGELLA, L., SIMONE, C. & GIORDANO, A. (2008) Cdk9-55: a new player in muscle regeneration. *J Cell Physiol,* 216**,** 576-82.

GIMOTTY, P. A., GUERRY, D., MING, M. E., ELENITSAS, R., XU, X., CZERNIECKI, B., SPITZ, F., SCHUCHTER, L. & ELDER, D. (2004) Thin primary cutaneous malignant melanoma: a prognostic tree for 10-year metastasis is more accurate than American Joint Committee on Cancer staging. *J Clin Oncol,* 22**,** 3668-76.

GIMOTTY, P. A., VAN BELLE, P., ELDER, D. E., MURRY, T., MONTONE, K. T., XU, X., HOTZ, S., RAINES, S., MING, M. E., WAHL, P. & GUERRY, D. (2005) Biologic and prognostic significance of dermal Ki67 expression, mitoses, and tumorigenicity in thin invasive cutaneous melanoma. *J Clin Oncol,* 23**,** 8048-56.

GLASMACHER, A., GOLDSCHMIDT, H., MEZGER, J., HAFERLACH, T., SCHMIDT-WOLF, I. G. & GIESELER, F. (2004) Oral idarubicin, dexamethasone and vincristine in the treatment of multiple myeloma: final analysis of a phase II trial. *Haematologica,* 89, 371-3.

GLASMACHER, A., HAFERLACH, T., GORSCHLUTER, M., MEZGER, J., MAINTZ, C., CLEMENS, M. R., KO, Y., HAHN, C., UBELACKER, R., KLEINSCHMIDT, R. & GIESELER, F. (1997) Oral idarubicin, dexamethasone and vincristine (VID) in the treatment of multiple myeloma. *Leukemia,* 11 Suppl 5, S22-6.

GOJO, I., ZHANG, B. & FENTON, R. G. (2002) The cyclin-dependent kinase inhibitor flavopiridol induces apoptosis in multiple myeloma cells through transcriptional repression and down-regulation of Mcl-1. *Clin Cancer Res,* 8, 3527-38.

GONZALEZ, M. A., TACHIBANA, K. E., LASKEY, R. A. & COLEMAN, N. (2005) Control of DNA replication and its potential clinical exploitation. *Nat Rev Cancer,* 5**,** 135-41.

GOODELL, M. A. (2002) Multipotential stem cells and 'side population' cells. *Cytotherapy,* 4**,** 507-8.

GOODELL, M. A., BROSE, K., PARADIS, G., CONNER, A. S. & MULLIGAN, R. C. (1996) Isolation and functional properties of murine hematopoietic stem cells that are replicating in vivo. *J Exp Med,* 183**,** 1797-806.

GOODRICH, J. A. & TJIAN, R. (1994) Transcription factors IIE and IIH and ATP hydrolysis direct promoter clearance by RNA polymerase II. *Cell,* 77, 145-56.

GORGOULIS, V. G., VASSILIOU, L. V., KARAKAIDOS, P., ZACHARATOS, P., KOTSINAS, A., LILOGLOU, T., VENERE, M., DITULLIO, R. A., JR., KASTRINAKIS, N. G., LEVY, B., KLETSAS, D., YONETA, A., HERLYN, M., KITTAS, C. & HALAZONETIS, T. D. (2005) Activation of the DNA damage checkpoint and genomic instability in human precancerous lesions. *Nature,* 434, 907-13.

GORSKA, M. M., LIANG, Q., STAFFORD, S. J., GOPLEN, N., DHARAJIYA, N., GUO, L., SUR, S., GAESTEL, M. & ALAM, R. (2007) MK2 controls the level of negative feedback in the NF-kappaB pathway and is essential for vascular permeability and airway inflammation. *J Exp Med,* 204, 1637-52.

GOULD, K. L. & NURSE, P. (1989) Tyrosine phosphorylation of the fission yeast cdc2+ protein kinase regulates entry into mitosis. *Nature,* 342, 39-45.

GRANA, X., DE LUCA, A., SANG, N., FU, Y., CLAUDIO, P. P., ROSENBLATT, J., MORGAN, D. O. & GIORDANO, A. (1994) PITALRE, a nuclear CDC2-related protein kinase that phosphorylates the retinoblastoma protein in vitro. *Proc Natl Acad Sci U S A,* 91**,** 3834-8.

GREIPP, P. R., LUST, J. A., O'FALLON, W. M., KATZMANN, J. A., WITZIG, T. E. & KYLE, R. A. (1993) Plasma cell labeling index and beta 2-microglobulin predict survival independent of thymidine kinase and C-reactive protein in multiple myeloma. *Blood,* 81, 3382-7.

GREIPP, P. R., SAN MIGUEL, J., DURIE, B. G., CROWLEY, J. J., BARLOGIE, B., BLADE, J., BOCCADORO, M., CHILD, J. A., AVET-LOISEAU, H., KYLE, R. A., LAHUERTA, J. J., LUDWIG, H., MORGAN, G., POWLES, R., SHIMIZU, K., SHUSTIK, C., SONNEVELD, P., TOSI, P., TURESSON, I. & WESTIN, J. 2005. International staging system for multiple myeloma. J Clin Oncol, 23, 3412-20.

GROTH, A. (2009) Replicating chromatin: a tale of histones. *Biochem Cell Biol,* 87, 51-63.

GROTH, A., RAY-GALLET, D., QUIVY, J. P., LUKAS, J., BARTEK, J. & ALMOUZNI, G. (2005) Human Asf1 regulates the flow of S phase histones during replicational stress. *Mol Cell,* 17, 301-11.

GROTH, A., ROCHA, W., VERREAULT, A. & ALMOUZNI, G. (2007) Chromatin challenges during DNA replication and repair. *Cell,* 128, 721-33.

GUENTHER, M. G., LEVINE, S. S., BOYER, L. A., JAENISCH, R. & YOUNG, R. A. (2007) A chromatin landmark and transcription initiation at most promoters in human cells. *Cell,* 130, 77-88.

GUNJAN, A., PAIK, J. & VERREAULT, A. (2005) Regulation of histone synthesis and nucleosome assembly. *Biochimie,* 87, 625-35.

HAASE, S. B., WINEY, M. & REED, S. I. (2001) Multi-step control of spindle pole body duplication by cyclin-dependent kinase. *Nat Cell Biol,* 3, 38-42.

HAMBURGER, A. & SALMON, S. E. (1977a) Primary bioassay of human myeloma stem cells. *J Clin Invest,* 60**,** 846-54.

HAMBURGER, A. W. & SALMON, S. E. (1977b) Primary bioassay of human tumor stem cells. *Science,* 197**,** 461-3.

HAMPSEY, M. & REINBERG, D. (1999) RNA polymerase II as a control panel for multiple coactivator complexes. *Curr Opin Genet Dev,* 9, 132-9.

HAN, J., ZHOU, H., LI, Z., XU, R. M. & ZHANG, Z. (2007) The Rtt109-Vps75 histone acetyltransferase complex acetylates non-nucleosomal histone H3. *J Biol Chem,* 282, 14158-64.

HANAMURA, I., HUANG, Y., ZHAN, F., BARLOGIE, B. & SHAUGHNESSY, J. (2006) Prognostic value of cyclin D2 mRNA expression in newly diagnosed multiple myeloma treated with high-dose chemotherapy and tandem autologous stem cell transplantations. *Leukemia,* 20, 1288-90.

HARADA, H., NAKAGAWA, H., TAKAOKA, M., LEE, J., HERLYN, M., DIEHL, J. A. & RUSTGI, A. K. (2008) Cleavage of MCM2 licensing protein fosters senescence in human keratinocytes. *Cell Cycle,* 7, 3534-8.

HARDY, C. F., DRYGA, O., SEEMATTER, S., PAHL, P. M. & SCLAFANI, R. A. (1997) mcm5/cdc46-bob1 bypasses the requirement for the S phase activator Cdc7p. *Proc Natl Acad Sci U S A,* 94, 3151-5.

HARKINS, V., GABRIELSE, C., HASTE, L. & WEINREICH, M. (2009) Budding yeast Dbf4 sequences required for Cdc7 kinase activation and identification of a functional relationship between the Dbf4 and Rev1 BRCT domains. *Genetics,* 183**,** 1269-82.

HAROUSSEAU, J. L., ATTAL, M., AVET-LOISEAU, H., MARIT, G., CAILLOT, D., MOHTY, M., LENAIN, P., HULIN, C., FACON, T., CASASSUS, P., MICHALLET, M., MAISONNEUVE, H., BENBOUBKER, L., MALOISEL, F., PETILLON, M. O., WEBB, I., MATHIOT, C. & MOREAU, P. (2010) Bortezomib plus dexamethasone is superior to vincristine plus doxorubicin plus dexamethasone as induction treatment prior to autologous stem-cell transplantation in newly diagnosed multiple myeloma: results of the IFM 2005-01 phase III trial. *J Clin Oncol,* 28**,** 4621-9.

HARPER, J. W. & ELLEDGE, S. J. (2007) The DNA damage response: ten years after. *Mol Cell,* 28, 739-45.

HARTIGAN, J. A., KLEINER, B. (1981) Mosaics for Contingency Tables. *Computer Science and Statistics: Proceedings of the 13th Symposium on the Interface,* ed. W. F. Eddy, New York: Springer Verlag, 268-273.

HARTWELL, L. H., CULOTTI, J., PRINGLE, J. R. & REID, B. J. (1974) Genetic control of the cell division cycle in yeast. *Science,* 183, 46-51.

HARTWELL, L. H., CULOTTI, J. & REID, B. (1970) Genetic control of the cell-division cycle in yeast. I. Detection of mutants. *Proc Natl Acad Sci U S A,* 66, 352-9.

HARTWELL, L. H., MORTIMER, R. K., CULOTTI, J. & CULOTTI, M. (1973) Genetic Control of the Cell Division Cycle in Yeast: V. Genetic Analysis of cdc Mutants. *Genetics,* 74, 267-86.

HARTWELL, L. H. & UNGER, M. W. (1977) Unequal division in Saccharomyces cerevisiae and its implications for the control of cell division. *J Cell Biol,* 75, 422-35.

HAYTER, A. J. (1984) A Proof of the Conjecture that the Tukey-Kramer Multiple Comparisons Procedure is Conservative. *Ann Statist,* 12, 61-75.

HAZLEHURST, L. A., DAMIANO, J. S., BUYUKSAL, I., PLEDGER, W. J. & DALTON, W. S. (2000) Adhesion to fibronectin via beta1 integrins regulates p27kip1 levels and contributes to cell adhesion mediated drug resistance (CAM-DR). *Oncogene,* 19**,** 4319-27.

HE, N., JAHCHAN, N. S., HONG, E., LI, Q., BAYFIELD, M. A., MARAIA, R. J., LUO, K. & ZHOU, Q. (2008) A La-related protein modulates 7SK snRNP integrity to suppress P-TEFb-dependent transcriptional elongation and tumorigenesis. *Mol Cell,* 29**,** 588-99.

HE, C. & KLIONSKY, D. J. (2009) Regulation mechanisms and signaling pathways of autophagy. *Annu Rev Genet,* 43, 67-93.

HE, N., PEZDA, A. C. & ZHOU, Q. (2006) Modulation of a P-TEFb functional equilibrium for the global control of cell growth and differentiation. *Mol Cell Biol,* 26, 7068-76.

HEMMATI, H. D., NAKANO, I., LAZAREFF, J. A., MASTERMAN-SMITH, M., GESCHWIND, D. H., BRONNER-FRASER, M. & KORNBLUM, H. I. (2003) Cancerous stem cells can arise from pediatric brain tumors. *Proc Natl Acad Sci U S A,* 100**,** 15178-83.

HERRICK, J. & BENSIMON, A. (1999) Single molecule analysis of DNA replication. *Biochimie,* 81**,** 859-71.

HERRICK, J., JUN, S., BECHHOEFER, J. & BENSIMON, A. (2002) Kinetic model of DNA replication in eukaryotic organisms. *J Mol Biol,* 320**,** 741-50.

HESS, G. F., DRONG, R. F., WEILAND, K. L., SLIGHTOM, J. L., SCLAFANI, R. A. & HOLLINGSWORTH, R. E. (1998) A human homolog of the yeast CDC7 gene is overexpressed in some tumors and transformed cell lines. *Gene,* 211, 133-40.

HEUER, T. S. (2008) Discovery of Selective CDK9 Small Molecule Inhibitors: CDK9 inhibition in tumor cells is associated with inhibition of proliferation and induction of apoptosis. EORTC.
HEYLL, A., SOHNGEN, D., KOBBE, G., SCHNEIDER, P., BAUSER, U., THIELE, K. P., WEHMEIER, A., SUDHOFF, T., QUENZEL, E. M., RIETH, C., WERNET, P., FISCHER, J., FRICK, M. & AUL, C. (1997) Idarubicin, melphalan and cyclophosphamide: an intensified high-dose regimen for the treatment of myeloma patients. *Leukemia,* 11 Suppl 5, S32-4.
HIDESHIMA, T., AKIYAMA, M., HAYASHI, T., RICHARDSON, P., SCHLOSSMAN, R., CHAUHAN, D. & ANDERSON, K. C. (2003) Targeting p38 MAPK inhibits multiple myeloma cell growth in the bone marrow milieu. *Blood,* 101, 703-5.
HIDESHIMA, T., CHAUHAN, D., HAYASHI, T., PODAR, K., AKIYAMA, M., GUPTA, D., RICHARDSON, P., MUNSHI, N. & ANDERSON, K. C. (2002) The biological sequelae of stromal cell-derived factor-1alpha in multiple myeloma. *Mol Cancer Ther,* 1**,** 539-44.
HIDESHIMA, T., CHAUHAN, D., SCHLOSSMAN, R., RICHARDSON, P. & ANDERSON, K. C. (2001) The role of tumor necrosis factor alpha in the pathophysiology of human multiple myeloma: therapeutic applications. *Oncogene,* 20**,** 4519-27.
HILGER, J. D., BERENSON, J. R., KLEIN, L. M., BESSUDO, A., ROSEN, P. & ESHAGHIAN, S. (2013) A phase I/II study (NCT01541332) of pomalidomide (POM), Dexamethasone (DEX) and pegylated liposomaldoxorubicin (PLD) for patients with relapsed/refractory multiple myeloma. *ASCO Meet Abstr,* 31(15_suppl), 8589.
HIRSCHMANN-JAX, C., FOSTER, A. E., WULF, G. G., NUCHTERN, J. G., JAX, T. W., GOBEL, U., GOODELL, M. A. & BRENNER, M. K. (2004) A distinct "side population" of cells with high drug efflux capacity in human tumor cells. *Proc Natl Acad Sci U S A,* 101**,** 14228-33.
HJORTH, M., HELLQUIST, L., HOLMBERG, E., MAGNUSSON, B., RODJER, S. & WESTIN, J. (1993) Initial versus deferred melphalan-prednisone therapy for asymptomatic multiple myeloma stage I--a randomized study. Myeloma Group of Western Sweden. Eur J Haematol, 50, 95-102.
HOLLINGSWORTH, R. E., JR. & SCLAFANI, R. A. (1990) DNA metabolism gene CDC7 from yeast encodes a serine (threonine) protein kinase. *Proc Natl Acad Sci U S A,* 87**,** 6272-6.
HOLT, P. R., MOSS, S. F., KAPETANAKIS, A. M., PETROTOS, A. & WANG, S. (1997) Is Ki-67 a better proliferative marker in the colon than proliferating cell nuclear antigen? *Cancer Epidemiol Biomarkers Prev,* 6**,** 131-5.
HOSE, D., REME, T., HIELSCHER, T., MOREAUX, J., MESSNER, T., SECKINGER, A., BENNER, A., SHAUGHNESSY, J. D., JR., BARLOGIE, B., ZHOU, Y., HILLENGASS, J., BERTSCH, U., NEBEN, K., MOHLER, T., ROSSI, J. F., JAUCH, A., KLEIN, B. & GOLDSCHMIDT, H. (2011) Proliferation is a central independent prognostic factor and target for personalized and risk-adapted treatment in multiple myeloma. *Haematologica,* 96, 87-95.
HOWARD, S. C., JONES, D. P. & PUI, C. H. The tumor lysis syndrome. *N Engl J Med,* 364, 1844-54.
HOYT, M. A., TOTIS, L. & ROBERTS, B. T. (1991) S. cerevisiae genes required for cell cycle arrest in response to loss of microtubule function. *Cell,* 66, 507-17.
HU, F., WANG, Y., LIU, D., LI, Y., QIN, J. & ELLEDGE, S. J. (2001) Regulation of the Bub2/Bfa1 GAP complex by Cdc5 and cell cycle checkpoints. *Cell,* 107**,** 655-65.
HUBSCHER, U., MAGA, G. & SPADARI, S. (2002) Eukaryotic DNA polymerases. *Annu Rev Biochem,* 71, 133-63.
HUGHES, S., ELUSTONDO, F., DI FONZO, A., LEROUX, F. G., WONG, A. C., SNIJDERS, A. P., MATTHEWS, S. J. & CHEREPANOV, P. (2012) Crystal structure of human CDC7 kinase in complex with its activator DBF4. Nat Struct Mol Biol, 19, 1101-7.
HULIN, C., FACON, T., RODON, P., PEGOURIE, B., BENBOUBKER, L., DOYEN, C., DIB, M., GUILLERM, G., SALLES, B., ESCHARD, J. P., LENAIN, P., CASASSUS, P., AZAIS, I., DECAUX, O., GARDERET, L., MATHIOT, C., FONTAN, J., LAFON, I., VIRION, J. M. & MOREAU, P. (2009) Efficacy of melphalan and prednisone plus thalidomide in patients older than 75 years

with newly diagnosed multiple myeloma: IFM 01/01 trial. *J Clin Oncol,* 27**,** 3664-70.
HURD, P. J., BANNISTER, A. J., HALLS, K., DAWSON, M. A., VERMEULEN, M., OLSEN, J. V., ISMAIL, H., SOMERS, J., MANN, M., OWEN-HUGHES, T., GOUT, I. & KOUZARIDES, T. (2009) Phosphorylation of histone H3 Thr-45 is linked to apoptosis. *J Biol Chem,* 284, 16575-83.
IM, J. S. & LEE, J. K. (2008) ATR-dependent activation of p38 MAP kinase is responsible for apoptotic cell death in cells depleted of Cdc7. *J Biol Chem,* 283, 25171-7.
INGVARSSON, S., SIGBJORNSDOTTIR, B. I., HUIPING, C., HAFSTEINSDOTTIR, S. H., RAGNARSSON, G., BARKARDOTTIR, R. B., ARASON, A., EGILSSON, V. & BERGTHORSSON, J. T. (2002) Mutation analysis of the CHK2 gene in breast carcinoma and other cancers. Breast Cancer Res, 4, R4.
ISHIKAWA, F. (2006) Cellular senescence as a stress response. *Cornea,* 25, S3-6.
ITO, S., ISHII, A., KAKUSHO, N., TANIYAMA, C., YAMAZAKI, S., FUKATSU, R., SAKAUE-SAWANO, A., MIYAWAKI, A. & MASAI, H. (2012a) Mechanism of cancer cell death induced by depletion of an essential replication regulator. *PLoS One,* 7, e36372.
ITO, R., TAKAHASHI, T., KATANO, I. & ITO, M. (2012b) Current advances in humanized mouse models. Cell Mol Immunol, 9, 208-14.
IVANOV, D., KWAK, Y. T., GUO, J. & GAYNOR, R. B. (2000) Domains in the SPT5 protein that modulate its transcriptional regulatory properties. *Mol Cell Biol,* 20**,** 2970-83.
JACAMO, R., CHEN, Y., WANG, Z., MA, W., ZHANG, M., SPAETH, E. L., WANG, Y., BATTULA, V. L., MAK, P. Y., SCHALLMOSER, K., RUVOLO, P., SCHOBER, W. D., SHPALL, E. J., NGUYEN, M. H., STRUNK, D., BUESO-RAMOS, C. E., KONOPLEV, S., DAVIS, R. E., KONOPLEVA, M. & ANDREEFF, M. Reciprocal leukemia-stroma VCAM-1/VLA-4-dependent activation of NF-kappaB mediates chemoresistance. *Blood,* 123**,** 2691-702.
JACKSON, A. L., PAHL, P. M., HARRISON, K., ROSAMOND, J. & SCLAFANI, R. A. (1993) Cell cycle regulation of the yeast Cdc7 protein kinase by association with the Dbf4 protein. *Mol Cell Biol,* 13**,** 2899-908.
JACOBUS S, C. N., SIEGEL D, ET AL. (2010) Outcome of elderly patients 70 years and older with newly diagnosed myeloma in the ECOG randomized trial of lenalidomide/high-dose dexamethasone (RD) versus lenalidomide/ low-dose dexamethasone (Rd). *Haematologica,* 95, 149.
JAGANNATH, S., VIJ, R., STEWART, A. K., TRUDEL, S., JAKUBOWIAK, A. J., REIMAN, T., SOMLO, G., BAHLIS, N., LONIAL, S., KUNKEL, L. A., WONG, A., ORLOWSKI, R. Z. & SIEGEL, D. S. (2012) An open-label single-arm pilot phase II study (PX-171-003-A0) of low-dose, single-agent carfilzomib in patients with relapsed and refractory multiple myeloma. *Clin Lymphoma Myeloma Leuk,* 12**,** 310-8.
JAKOB, C., STERZ, J., ZAVRSKI, I., HEIDER, U., KLEEBERG, L., FLEISSNER, C., KAISER, M. & SEZER, O. (2006) Angiogenesis in multiple myeloma. *Eur J Cancer,* 42**,** 1581-90.
JAKUBOWIAK, A. J., BENSON, D. M., BENSINGER, W., SIEGEL, D. S., ZIMMERMAN, T. M., MOHR-BACHER, A., RICHARDSON, P. G., AFAR, D. E., SINGHAL, A. K. & ANDERSON, K. C. (2012a) Phase I trial of anti-CS1 monoclonal antibody elotuzumab in combination with bortezomib in the treatment of relapsed/refractory multiple myeloma. *J Clin Oncol,* 30, 1960-5.
JAKUBOWIAK, A. J., RICHARDSON, P. G., ZIMMERMAN, T., ALSINA, M., KAUFMAN, J. L., KANDARPA, M., KRAFTSON, S., ROSS, C. W., HARVEY, C., HIDESHIMA, T., SPORTELLI, P., PORADOSU, E., GARDNER, L., GIUSTI, K. & ANDERSON, K. C. (2012b) Perifosine plus lenalidomide and dexamethasone in relapsed and relapsed/refractory multiple myeloma: a Phase I Multiple Myeloma Research Consortium study. *Br J Haematol,* 158, 472-80.
JANICKE, R. U., LIN, X. Y., LEE, F. H. & PORTER, A. G. (1996) Cyclin D3 sensitizes tumor cells to tumor necrosis factor-induced, c-Myc-dependent apoptosis. *Mol Cell Biol,* 16, 5245-53.
JANSSENS, V., LONGIN, S. & GORIS, J. (2008) PP2A holoenzyme assembly: in cauda venenum (the sting is in the tail). *Trends Biochem Sci,* 33, 113-21.

JARES, P., LUCIANI, M. G. & BLOW, J. J. (2004) A Xenopus Dbf4 homolog is required for Cdc7 chromatin binding and DNA replication. *BMC Mol Biol,* 5, 5.

JASPERSEN, S. L. & WINEY, M. (2004) The budding yeast spindle pole body: structure, duplication, and function. *Annu Rev Cell Dev Biol,* 20, 1-28.

JEANMOUGIN, F., WURTZ, J. M., LE DOUARIN, B., CHAMBON, P. & LOSSON, R. (1997) The bromodomain revisited. *Trends Biochem Sci,* 22, 151-3.

JEGO, G., BATAILLE, R. & PELLAT-DECEUNYNCK, C. (2001) Interleukin-6 is a growth factor for nonmalignant human plasmablasts. *Blood,* 97**,** 1817-22.

JEGO, G., ROBILLARD, N., PUTHIER, D., AMIOT, M., ACCARD, F., PINEAU, D., HAROUSSEAU, J. L., BATAILLE, R. & PELLAT-DECEUNYNCK, C. (1999) Reactive plasmacytoses are expansions of plasmablasts retaining the capacity to differentiate into plasma cells. *Blood,* 94**,** 701-12.

JEMAL, A., BRAY, F., CENTER, M. M., FERLAY, J., WARD, E. & FORMAN, D. (2011) Global cancer statistics. *CA Cancer J Clin,* 61**,** 69-90.

JEMAL, A., SIEGEL, R., XU, J. & WARD, E. (2010) Cancer statistics, 2010. *CA Cancer J Clin,* 60**,** 277-300.

JERONIMO, C., FORGET, D., BOUCHARD, A., LI, Q., CHUA, G., POITRAS, C., THERIEN, C., BERGERON, D., BOURASSA, S., GREENBLATT, J., CHABOT, B., POIRIER, G. G., HUGHES, T. R., BLANCHETTE, M., PRICE, D. H. & COULOMBE, B. (2007) Systematic analysis of the protein interaction network for the human transcription machinery reveals the identity of the 7SK capping enzyme. *Mol Cell,* 27**,** 262-74.

JIANG, W. & HUNTER, T. (1997) Identification and characterization of a human protein kinase related to budding yeast Cdc7p. *Proc Natl Acad Sci U S A,* 94**,** 14320-5.

JIANG, W., MCDONALD, D., HOPE, T. J. & HUNTER, T. (1999) Mammalian Cdc7-Dbf4 protein kinase complex is essential for initiation of DNA replication. *EMBO J,* 18**,** 5703-13.

JIANG, Y. (2006) Regulation of the cell cycle by protein phosphatase 2A in Saccharomyces cerevisiae. *Microbiol Mol Biol Rev,* 70, 440-9.

JOHNSON, R. T. & RAO, P. N. (1970) Mammalian cell fusion: induction of premature chromosome condensation in interphase nuclei. *Nature,* 226, 717-22.

JOHNSTON, L. H. & THOMAS, A. P. (1982) A further two mutants defective in initiation of the S phase in the yeast Saccharomyces cerevisiae. *Mol Gen Genet,* 186, 445-8.

JONES, R. J., BARBER, J. P., VALA, M. S., COLLECTOR, M. I., KAUFMANN, S. H., LUDEMAN, S. M., COLVIN, O. M. & HILTON, J. (1995) Assessment of aldehyde dehydrogenase in viable cells. *Blood,* 85, 2742-6.

KARIN, M. & GALLAGHER, E. (2009) TNFR signaling: ubiquitin-conjugated TRAFfic signals control stop-and-go for MAPK signaling complexes. *Immunol Rev,* 228, 225-40.

KASHYAP, S., GANGULY, K., BARDHAN, G. & MAJUMDAR, G. (1999) Low dose oral idarubicin in combination with cyclophosphamide and dexamethasone (CID) for management of melphalan-prednisolone (MP) resistant myeloma. *Leuk Lymphoma,* 33, 407-8.

KASTAN, M. B., SCHLAFFER, E., RUSSO, J. E., COLVIN, O. M., CIVIN, C. I. & HILTON, J. (1990) Direct demonstration of elevated aldehyde dehydrogenase in human hematopoietic progenitor cells. *Blood,* 75, 1947-50.

KATZMANN, J. A., DISPENZIERI, A., KYLE, R. A., SNYDER, M. R., PLEVAK, M. F., LARSON, D. R., ABRAHAM, R. S., LUST, J. A., MELTON, L. J., 3RD & RAJKUMAR, S. V. (2006) Elimination of the need for urine studies in the screening algorithm for monoclonal gammopathies by using serum immunofixation and free light chain assays. *Mayo Clin Proc,* 81, 1575-8.

KEATS, J. J., FONSECA, R., CHESI, M., SCHOP, R., BAKER, A., CHNG, W. J., VAN WIER, S., TIEDEMANN, R., SHI, C. X., SEBAG, M., BRAGGIO, E., HENRY, T., ZHU, Y. X., FOGLE, H., PRICE-TROSKA, T., AHMANN, G., MANCINI, C., BRENTS, L. A., KUMAR, S., GREIPP, P., DISPENZIERI, A., BRYANT, B., MULLIGAN, G., BRUHN, L., BARRETT, M., VALDEZ, R., TRENT, J., STEWART, A. K., CARPTEN, J. & BERGSAGEL, P. L. (2007) Promiscuous mutations activate

the noncanonical NF-kappaB pathway in multiple myeloma. *Cancer Cell,* 12, 131-44.
KERK, D., TEMPLETON, G. & MOORHEAD, G. B. (2008) Evolutionary radiation pattern of novel protein phosphatases revealed by analysis of protein data from the completely sequenced genomes of humans, green algae, and higher plants. *Plant Physiol,* 146, 351-67.
KIHARA, M., NAKAI, W., ASANO, S., SUZUKI, A., KITADA, K., KAWASAKI, Y., JOHNSTON, L. H. & SUGINO, A. (2000) Characterization of the yeast Cdc7p/Dbf4p complex purified from insect cells. Its protein kinase activity is regulated by Rad53p. *J Biol Chem,* 275**,** 35051-62.
KIM, J., DENU, R. A., DOLLAR, B. A., ESCALANTE, L. E., KUETHER, J. P., CALLANDER, N. S., ASIMAKOPOULOS, F. & HEMATTI, P. 2012. Macrophages and mesenchymal stromal cells support survival and proliferation of multiple myeloma cells. Br J Haematol, 158, 336-46.
KIM, J. M., KAKUSHO, N., YAMADA, M., KANOH, Y., TAKEMOTO, N. & MASAI, H. (2008) Cdc7 kinase mediates Claspin phosphorylation in DNA replication checkpoint. *Oncogene,* 27**,** 3475-82.
KIM, J. M., NAKAO, K., NAKAMURA, K., SAITO, I., KATSUKI, M., ARAI, K. & MASAI, H. (2002) Inactivation of Cdc7 kinase in mouse ES cells results in S-phase arrest and p53-dependent cell death. *EMBO J,* 21, 2168-79.
KIM, S. H., LIN, D. P., MATSUMOTO, S., KITAZONO, A. & MATSUMOTO, T. (1998) Fission yeast Slp1: an effector of the Mad2-dependent spindle checkpoint. *Science,* 279**,** 1045-7
KITADA, K., JOHNSTON, L. H., SUGINO, T. & SUGINO, A. (1992) Temperature-sensitive cdc7 mutations of Saccharomyces cerevisiae are suppressed by the DBF4 gene, which is required for the G1/S cell cycle transition. *Genetics,* 131, 21-9.
KLEIN, B., ZHANG, X. G., LU, Z. Y. & BATAILLE, R. 1995. Interleukin-6 in human multiple myeloma. Blood, 85, 863-72.
KNEISSL, M., PUTTER, V., SZALAY, A. A. & GRUMMT, F. (2003) Interaction and assembly of murine pre-replicative complex proteins in yeast and mouse cells. *J Mol Biol,* 327**,** 111-28.
KONDO, T., SETOGUCHI, T. & TAGA, T. (2004) Persistence of a small subpopulation of cancer stem-like cells in the C6 glioma cell line. *Proc Natl Acad Sci U S A,* 101**,** 781-6.
KOONIN, E. V., ALTSCHUL, S. F. & BORK, P. (1996) BRCA1 protein products ... Functional motifs. *Nat Genet,* 13**,** 266-8.
KORBEL, J. O. & CAMPBELL, P. J. Criteria for inference of chromothripsis in cancer genomes. *Cell,* 152, 1226-36.
KORDE, N., KRISTINSSON, S. Y. & LANDGREN, O. (2011) Monoclonal gammopathy of undetermined significance (MGUS) and smoldering multiple myeloma (SMM): novel biological insights and development of early treatment strategies. Blood, 117, 5573-81.
KRAMER, C. Y. (1956) Extensions of multiple range tests to group means with unequal numbers of replications. *Biometrics,* 12, 307-310.
KRONKE, J., UDESHI, N. D., NARLA, A., GRAUMAN, P., HURST, S. N., MCCONKEY, M., SVINKINA, T., HECKL, D., COMER, E., LI, X., CIARLO, C., HARTMAN, E., MUNSHI, N., SCHENONE, M., SCHREIBER, S. L., CARR, S. A. & EBERT, B. L. (2014) Lenalidomide causes selective degradation of IKZF1 and IKZF3 in multiple myeloma cells. *Science,* 343, 301-5.
KRUEGER, B. J., JERONIMO, C., ROY, B. B., BOUCHARD, A., BARRANDON, C., BYERS, S. A., SEARCEY, C. E., COOPER, J. J., BENSAUDE, O., COHEN, E. A., COULOMBE, B. & PRICE, D. H. (2008) LARP7 is a stable component of the 7SK snRNP while P-TEFb, HEXIM1 and hnRNP A1 are reversibly associated. *Nucleic Acids Res,* 36**,** 2219-29.
KUKREJA, A., HUTCHINSON, A., DHODAPKAR, K., MAZUMDER, A., VESOLE, D., ANGITAPALLI, R., JAGANNATH, S. & DHODAPKAR, M. V. 2006. Enhancement of clonogenicity of human multiple myeloma by dendritic cells. J Exp Med, 203, 1859-65.
KUMAGAI, H., SATO, N., YAMADA, M., MAHONY, D., SEGHEZZI, W., LEES, E., ARAI, K. & MASAI, H. (1999) A novel growth- and cell cycle-regulated protein, ASK, activates human Cdc7-related kinase and is essential for G1/S transition in mammalian cells. *Mol Cell Biol,* 19**,**

5083-95.
KUMAR, A., LOUGHRAN, T., ALSINA, M., DURIE, B. G. & DJULBEGOVIC, B. (2003) Management of multiple myeloma: a systematic review and critical appraisal of published studies. *Lancet Oncol,* 4**,** 293-304.
KUMAR S, B. J., CROWLEY J, ET AL. (2010a) Outcome of patients with myeloma relapsing after IMiD and bortezomib therapy: A multicenter study from the International Myeloma Foundation Working Group. *Haematologica,* 95, 151.
KUMAR S, B. J., NIESVIZKY R, ET AL. (2012) A Phase 1/2 Study of Weekly MLN9708, an Investigational Oral Proteasome Inhibitor, in Combination with Lenalidomide and Dexamethasone in Patients with Previously Untreated Multiple Myeloma (MM). *ASH Annu Meet Abstr*.
KUMAR S, F. I., RICHARDSON PG, ET AL. (2010b) Novel three- and four-drug combi- nation regimens of bortezomib, dexamethasone, cyclophosphamide, and lenalidomide, for previously untreated multiple myeloma: Results From the Multi-Center, Randomized, Phase 2 EVOLUTION Study. *ASH Annu Meet Abstr,* 116, 621.
KUMAR, S. K., BENSINGER, W. I., ZIMMERMAN, T. M., REEDER, C. B., BERENSON, J. R., BERG, D., HUI, A. M., GUPTA, N., DI BACCO, A., YU, J., SHOU, Y. & NIESVIZKY, R. (2014) Phase 1 study of weekly dosing with the investigational oral proteasome inhibitor ixazomib in relapsed/refractory multiple myeloma. Blood, 124, 1047-55.
KUMAR, S. K., MIKHAEL, J. R., BUADI, F. K., DINGLI, D., DISPENZIERI, A., FONSECA, R., GERTZ, M. A., GREIPP, P. R., HAYMAN, S. R., KYLE, R. A., LACY, M. Q., LUST, J. A., REEDER, C. B., ROY, V., RUSSELL, S. J., SHORT, K. E., STEWART, A. K., WITZIG, T. E., ZELDENRUST, S. R., DALTON, R. J., RAJKUMAR, S. V. & BERGSAGEL, P. L. (2009) Management of newly diagnosed symptomatic multiple myeloma: updated Mayo Stratification of Myeloma and Risk-Adapted Therapy (mSMART) consensus guidelines. *Mayo Clin Proc,* 84**,** 1095-110.
KUMAR, S. K., THERNEAU, T. M., GERTZ, M. A., LACY, M. Q., DISPENZIERI, A., RAJKUMAR, S. V., FONSECA, R., WITZIG, T. E., LUST, J. A., LARSON, D. R., KYLE, R. A. & GREIPP, P. R. (2004) Clinical course of patients with relapsed multiple myeloma. *Mayo Clin Proc,* 79, 867-74.
KUNKEL, L. A., VESCIO, R., CAO, J., HONG, C. H., KIM, A., SCHILLER, G. J., LICHTENSTEIN, A. K. & BERENSON, J. R. (1995) Analysis of multiple myeloma third complementarity-determining regions reveals characteristics of prenatal B cells. *Ann N Y Acad Sci,* 764**,** 519-22.
KYLE, R. A. & RAJKUMAR, S. V. (2009) Criteria for diagnosis, staging, risk stratification and response assessment of multiple myeloma. *Leukemia,* 23, 3-9.
KYLE, R. A., THERNEAU, T. M., RAJKUMAR, S. V., LARSON, D. R., PLEVAK, M. F., OFFORD, J. R., DISPENZIERI, A., KATZMANN, J. A. & MELTON, L. J., 3RD (2006) Prevalence of monoclonal gammopathy of undetermined significance. *N Engl J Med,* 354**,** 1362-9.
KYLE, R. A., GERTZ, M. A., WITZIG, T. E., LUST, J. A., LACY, M. Q., DISPENZIERI, A., FONSECA, R., RAJKUMAR, S. V., OFFORD, J. R., LARSON, D. R., PLEVAK, M. E., THERNEAU, T. M. & GREIPP, P. R. (2003) Review of 1027 patients with newly diagnosed multiple myeloma. *Mayo Clin Proc,* 78**,** 21-33.
KYLE, R. A., THERNEAU, T. M., RAJKUMAR, S. V., LARSON, D. R., PLEVAK, M. F. & MELTON, L. J., 3RD (2004) Incidence of multiple myeloma in Olmsted County, Minnesota: Trend over 6 decades. *Cancer,* 101, 2667-74.
KYLE, R. A., THERNEAU, T. M., RAJKUMAR, S. V., OFFORD, J. R., LARSON, D. R., PLEVAK, M. F. & MELTON, L. J., 3RD (2002) A long-term study of prognosis in monoclonal gammopathy of undetermined significance. *N Engl J Med,* 346**,** 564-9.
LACY, M. Q., HAYMAN, S. R., GERTZ, M. A., DISPENZIERI, A., BUADI, F., KUMAR, S., GREIPP, P. R., LUST, J. A., RUSSELL, S. J., DINGLI, D., KYLE, R. A., FONSECA, R., BERGSAGEL, P. L., ROY, V., MIKHAEL, J. R., STEWART, A. K., LAUMANN, K., ALLRED, J. B., MANDREKAR, S. J. & RAJKUMAR, S. V. (2009) Pomalidomide (CC4047) plus low-dose dexamethasone as therapy for relapsed multiple myeloma. *J Clin Oncol,* 27**,** 5008-14.

LAI, E. C. (2004) Notch signaling: control of cell communication and cell fate. *Development,* 131, 965-73.

LAMB, J. (2007) The Connectivity Map: a new tool for biomedical research. *Nat Rev Cancer,* 7, 54-60.

LAMB, J., CRAWFORD, E. D., PECK, D., MODELL, J. W., BLAT, I. C., WROBEL, M. J., LERNER, J., BRUNET, J. P., SUBRAMANIAN, A., ROSS, K. N., REICH, M., HIERONYMUS, H., WEI, G., ARMSTRONG, S. A., HAGGARTY, S. J., CLEMONS, P. A., WEI, R., CARR, S. A., LANDER, E. S. & GOLUB, T. R. (2006) The Connectivity Map: using gene-expression signatures to connect small molecules, genes, and disease. *Science,* 313, 1929-35.

LANDGREN, O. & WEISS, B. M. (2009) Patterns of monoclonal gammopathy of undetermined significance and multiple myeloma in various ethnic/racial groups: support for genetic factors in pathogenesis. *Leukemia,* 23, 1691-7.

LANDIS, G. & TOWER, J. (1999) The Drosophila chiffon gene is required for chorion gene amplification, and is related to the yeast Dbf4 regulator of DNA replication and cell cycle. *Development,* 126**,** 4281-93.

LANDOWSKI, T. H., OLASHAW, N. E., AGRAWAL, D. & DALTON, W. S. (2003) Cell adhesion-mediated drug resistance (CAM-DR) is associated with activation of NF-kappa B (RelB/p50) in myeloma cells. *Oncogene,* 22**,** 2417-21.

LANZAVECCHIA, A. & SALLUSTO, F. (2002) Progressive differentiation and selection of the fittest in the immune response. *Nat Rev Immunol,* 2, 982-7.

LARNER, J. M., LEE, H., LITTLE, R. D., DIJKWEL, P. A., SCHILDKRAUT, C. L. & HAMLIN, J. L. (1999) Radiation down-regulates replication origin activity throughout the S phase in mammalian cells. *Nucleic Acids Res,* 27, 803-9.

LAROCCA, A., MONTEFUSCO, V., BRINGHEN, S., ROSSI, D., CRIPPA, C., MINA, R., GALLI, M., MARCATTI, M., LA VERDE, G., GIULIANI, N., MAGAROTTO, V., GUGLIELMELLI, T., ROTA-SCALABRINI, D., OMEDE, P., SANTAGOSTINO, A., BALDI, I., CARELLA, A. M., BOCCADORO, M., CORRADINI, P. & PALUMBO, A. (2013) Pomalidomide, cyclophosphamide, and prednisone for relapsed/refractory multiple myeloma: a multicenter phase 1/2 open-label study. *Blood,* 122**,** 2799-806.

LAPIDOT, T., SIRARD, C., VORMOOR, J., MURDOCH, B., HOANG, T., CACERES-CORTES, J., MINDEN, M., PATERSON, B., CALIGIURI, M. A. & DICK, J. E. (1994) A cell initiating human acute myeloid leukaemia after transplantation into SCID mice. *Nature,* 367**,** 645-8.

LAYBOURN, P. J. & DAHMUS, M. E. (1989) Transcription-dependent structural changes in the C-terminal domain of mammalian RNA polymerase subunit IIa/o. *J Biol Chem,* 264**,** 6693-8.

LENDVAI, N., HILDEN, P., DEVLIN, S., LANDAU, H., HASSOUN, H., LESOKHIN, A. M., TSAKOS, I., REDLING, K., KOEHNE, G., CHUNG, D. J., SCHAFFER, W. L. & GIRALT, S. A. (2014) A phase 2 single-center study of carfilzomib 56 mg/m2 with or without low-dose dexamethasone in relapsed multiple myeloma. Blood, 124, 899-906.

LEE, S. E., FRENZ, L. M., WELLS, N. J., JOHNSON, A. L. & JOHNSTON, L. H. (2001) Order of function of the budding-yeast mitotic exit-network proteins Tem1, Cdc15, Mob1, Dbf2, and Cdc5. *Curr Biol,* 11, 784-8.

LENNOX, R. W. & COHEN, L. H. (1983) The histone H1 complements of dividing and nondividing cells of the mouse. *J Biol Chem,* 258, 262-8.

LEVINE, A. J. (1997) p53, the cellular gatekeeper for growth and division. *Cell,* 88, 323-31.

LEW, D. J. & BURKE, D. J. (2003) The spindle assembly and spindle position checkpoints. *Annu Rev Genet,* 37, 251-82.

LI, C., HEIDT, D. G., DALERBA, P., BURANT, C. F., ZHANG, L., ADSAY, V., WICHA, M., CLARKE, M. F. & SIMEONE, D. M. 2007. Identification of pancreatic cancer stem cells. Cancer Res, 67, 1030-7.

LI, C. J., VASSILEV, A. & DEPAMPHILIS, M. L. (2004) Role for Cdk1 (Cdc2)/cyclin A in preventing the

mammalian origin recognition complex's largest subunit (Orc1) from binding to chromatin during mitosis. *Mol Cell Biol,* 24, 5875-86.
LI, L. Y., LUO, X. & WANG, X. (2001) Endonuclease G is an apoptotic DNase when released from mitochondria. *Nature,* 412, 95-9.
LIANG, J. & FANTES, P. (2007) The Schizosaccharomyces pombe Cdc7 protein kinase required for septum formation is a client protein of Cdc37. *Eukaryot Cell,* 6, 1089-96.
LIU, H. & HERRMANN, C. H. 2005. Differential localization and expression of the Cdk9 42k and 55k isoforms. J Cell Physiol, 203, 251-60.
LIU, H., HERRMANN, C. H., CHIANG, K., SUNG, T. L., MOON, S. H., DONEHOWER, L. A. & RICE, A. P. 2010. 55K isoform of CDK9 associates with Ku70 and is involved in DNA repair. Biochem Biophys Res Commun, 397, 245-50.
LIU, X., SHI, S., LAM, F., PEPPER, C., FISCHER, P. M. & WANG, S. (2012) CDKI-71, a novel CDK9 inhibitor, is preferentially cytotoxic to cancer cells compared to flavopiridol. *Int J Cancer,* 130**,** 1216-26.
LONIAL, S., VIJ, R., HAROUSSEAU, J. L., FACON, T., MOREAU, P., MAZUMDER, A., KAUFMAN, J. L., LELEU, X., TSAO, L. C., WESTLAND, C., SINGHAL, A. K. & JAGANNATH, S. (2012) Elotuzumab in combination with lenalidomide and low-dose dexamethasone in relapsed or refractory multiple myeloma. *J Clin Oncol,* 30, 1953-9.
LU, G., MIDDLETON, R. E., SUN, H., NANIONG, M., OTT, C. J., MITSIADES, C. S., WONG, K. K., BRADNER, J. E. & KAELIN, W. G., JR. (2014) The myeloma drug lenalidomide promotes the cereblon-dependent destruction of Ikaros proteins. *Science,* 343, 305-9.
MACCALLUM, D. E., MELVILLE, J., FRAME, S., WATT, K., ANDERSON, S., GIANELLA-BORRADORI, A., LANE, D. P. & GREEN, S. R. (2005) Seliciclib (CYC202, R-Roscovitine) induces cell death in multiple myeloma cells by inhibition of RNA polymerase II-dependent transcription and down-regulation of Mcl-1. *Cancer Res,* 65, 5399-407.
MADINE, M. A., SWIETLIK, M., PELIZON, C., ROMANOWSKI, P., MILLS, A. D. & LASKEY, R. A. (2000) The roles of the MCM, ORC, and Cdc6 proteins in determining the replication competence of chromatin in quiescent cells. *J Struct Biol,* 129**,** 198-210.
MARK, T. M., BOYER, A., ROSSI, A. C., SHAH, M., PEARSE, R. N. & ZAFAR, F. (2012) ClaPD (clarithromycin, pomalidomide, dexamethasone) therapy in relapsed or refractory multiple myeloma. *ASH Annu Meet Abstr,* 120, 77.
MARKS, P. A., RICHON, V. M., KIYOKAWA, H. & RIFKIND, R. A. (1994) Inducing differentiation of transformed cells with hybrid polar compounds: a cell cycle-dependent process. *Proc Natl Acad Sci U S A,* 91, 10251-4.
MARSHALL, N. F., PENG, J., XIE, Z. & PRICE, D. H. (1996) Control of RNA polymerase II elongation potential by a novel carboxyl-terminal domain kinase. *J Biol Chem,* 271**,** 27176-83.
MARSHALL, N. F. & PRICE, D. H. (1995) Purification of P-TEFb, a transcription factor required for the transition into productive elongation. *J Biol Chem,* 270**,** 12335-8.
MARTINEZ-LOPEZ, J., LAHUERTA, J. J., PEPIN, F., GONZALEZ, M., BARRIO, S., AYALA, R., PUIG, N., MONTALBAN, M. A., PAIVA, B., WENG, L., JIMENEZ, C., SOPENA, M., MOORHEAD, M., CEDENA, T., RAPADO, I., MATEOS, M. V., ROSINOL, L., ORIOL, A., BLANCHARD, M. J., MARTINEZ, R., BLADE, J., SAN MIGUEL, J., FAHAM, M. & GARCIA-SANZ, R. (2014) Prognostic value of deep sequencing method for minimal residual disease detection in multiple myeloma. Blood, 123, 3073-9.
MARZLUFF, W. F., WAGNER, E. J. & DURONIO, R. J. (2008) Metabolism and regulation of canonical histone mRNAs: life without a poly(A) tail. *Nat Rev Genet,* 9, 843-54.
MASAI, H. & ARAI, K. (2000) Dbf4 motifs: conserved motifs in activation subunits for Cdc7 kinases essential for S-phase. *Biochem Biophys Res Commun,* 275, 228-32.
MASAI, H., MATSUI, E., YOU, Z., ISHIMI, Y., TAMAI, K. & ARAI, K. (2000) Human Cdc7-related kinase complex. In vitro phosphorylation of MCM by concerted actions of Cdks and Cdc7 and that

of a criticial threonine residue of Cdc7 bY Cdks. *J Biol Chem,* 275, 29042-52.
MASAI, H., MIYAKE, T. & ARAI, K. (1995) hsk1+, a Schizosaccharomyces pombe gene related to Saccharomyces cerevisiae CDC7, is required for chromosomal replication. *EMBO J,* 14**,** 3094-104.
MASUI, Y. & MARKERT, C. L. (1971) Cytoplasmic control of nuclear behavior during meiotic maturation of frog oocytes. *J Exp Zool,* 177, 129-45.
MASUMOTO, H., HAWKE, D., KOBAYASHI, R. & VERREAULT, A. (2005) A role for cell-cycle-regulated histone H3 lysine 56 acetylation in the DNA damage response. *Nature,* 436, 294-8.
MATOS, J., LIPP, J. J., BOGDANOVA, A., GUILLOT, S., OKAZ, E., JUNQUEIRA, M., SHEVCHENKO, A. & ZACHARIAE, W. (2008) Dbf4-dependent CDC7 kinase links DNA replication to the segregation of homologous chromosomes in meiosis I. *Cell,* 135**,** 662-78.
MATSUI, W., HUFF, C. A., WANG, Q., MALEHORN, M. T., BARBER, J., TANHEHCO, Y., SMITH, B. D., CIVIN, C. I. & JONES, R. J. (2004) Characterization of clonogenic multiple myeloma cells. *Blood,* 103, 2332-6.
MATSUI, W., WANG, Q., BARBER, J. P., BRENNAN, S., SMITH, B. D., BORRELLO, I., MCNIECE, I., LIN, L., AMBINDER, R. F., PEACOCK, C., WATKINS, D. N., HUFF, C. A. & JONES, R. J. (2008) Clonogenic multiple myeloma progenitors, stem cell properties, and drug resistance. *Cancer Res,* 68, 190-7.
MATSUMOTO, S., OGINO, K., NOGUCHI, E., RUSSELL, P. & MASAI, H. (2005) Hsk1-Dfp1/Him1, the Cdc7-Dbf4 kinase in Schizosaccharomyces pombe, associates with Swi1, a component of the replication fork protection complex. *J Biol Chem,* 280**,** 42536-42.
MATTHEWS, L. A., DUONG, A., PRASAD, A. A., DUNCKER, B. P. & GUARNE, A. (2009) Crystallization and preliminary X-ray diffraction analysis of motif N from Saccharomyces cerevisiae Dbf4. *Acta Crystallogr Sect F Struct Biol Cryst Commun,* 65, 890-4.
MCCARTHY PL, O. K., ANDERSON KC, ET AL. (2010) Phase III intergroup study of lenalidomide versus placebo maintenance therapy following single autolo- gous stem cell transplant (ASCT) for multiple myeloma (MM): CALGB 100104. *J Clin Oncol,* 28**,** 15s.
MCHEYZER-WILLIAMS, L. J. & MCHEYZER-WILLIAMS, M. G. (2005) Antigen-specific memory B cell development. *Annu Rev Immunol,* 23**,** 487-513.
MENICHINCHERI, M., BARGIOTTI, A., BERTHELSEN, J., BERTRAND, J. A., BOSSI, R., CIAVOLELLA, A., CIRLA, A., CRISTIANI, C., CROCI, V., D'ALESSIO, R., FASOLINI, M., FIORENTINI, F., FORTE, B., ISACCHI, A., MARTINA, K., MOLINARI, A., MONTAGNOLI, A., ORSINI, P., ORZI, F., PESENTI, E., PEZZETTA, D., PILLAN, A., POGGESI, I., ROLETTO, F., SCOLARO, A., TATO, M., TIBOLLA, M., VALSASINA, B., VARASI, M., VOLPI, D., SANTOCANALE, C. & VANOTTI, E. (2009) First Cdc7 kinase inhibitors: pyrrolopyridinones as potent and orally active antitumor agents. 2. Lead discovery. *J Med Chem,* 52, 293-307.
MENSSEN, R., NEUTZNER, A. & SEUFERT, W. (2001) Asymmetric spindle pole localization of yeast Cdc15 kinase links mitotic exit and cytokinesis. *Curr Biol,* 11, 345-50.
MENU, E., GARCIA, J., HUANG, X., DI LIBERTO, M., TOOGOOD, P. L., CHEN, I., VANDERKERKEN, K. & CHEN-KIANG, S. (2008) A novel therapeutic combination using PD 0332991 and bortezomib: study in the 5T33MM myeloma model. *Cancer Res,* 68**,** 5519-23.
MICHAELIS, C., CIOSK, R. & NASMYTH, K. (1997) Cohesins: chromosomal proteins that prevent premature separation of sister chromatids. *Cell,* 91, 35-45.
MIELE, L., GOLDE, T. & OSBORNE, B. (2006) Notch signaling in cancer. *Curr Mol Med,* 6, 905-18.
MIKHAEL, J. R., DINGLI, D., ROY, V., REEDER, C. B., BUADI, F. K., HAYMAN, S. R., DISPENZIERI, A., FONSECA, R., SHER, T., KYLE, R. A., LIN, Y., RUSSELL, S. J., KUMAR, S., BERGSAGEL, P. L., ZELDENRUST, S. R., LEUNG, N., DRAKE, M. T., KAPOOR, P., ANSELL, S. M., WITZIG, T. E., LUST, J. A., DALTON, R. J., GERTZ, M. A., STEWART, K., RAJKUMAR, S. V., CHANAN-KHAN, A. & LACY, M. Q. (2013) Management of Newly Diagnosed Symptomatic Multiple Myeloma: Updated Mayo Stratification of Myeloma and Risk-Adapted Therapy (mSMART)

Consensus Guidelines 2013. *Mayo Clin Proc,* 88**,** 360-76.
MILLER ME, C. F. (2001) Cyclin specificity: How many wheels do you need on a unicycle? *J Cell Sci,* 114, 1811-20.
MITSIADES, C. S., MITSIADES, N. S., BRONSON, R. T., CHAUHAN, D., MUNSHI, N., TREON, S. P., MAXWELL, C. A., PILARSKI, L., HIDESHIMA, T., HOFFMAN, R. M. & ANDERSON, K. C. (2003) Fluorescence imaging of multiple myeloma cells in a clinically relevant SCID/NOD in vivo model: biologic and clinical implications. *Cancer Res,* 63**,** 6689-96.
MITSIADES, C. S., MITSIADES, N. S., MCMULLAN, C. J., POULAKI, V., SHRINGARPURE, R., AKIYAMA, M., HIDESHIMA, T., CHAUHAN, D., JOSEPH, M., LIBERMANN, T. A., GARCIA-ECHEVERRIA, C., PEARSON, M. A., HOFMANN, F., ANDERSON, K. C. & KUNG, A. L. (2004) Inhibition of the insulin-like growth factor receptor-1 tyrosine kinase activity as a therapeutic strategy for multiple myeloma, other hematologic malignancies, and solid tumors. *Cancer Cell,* 5, 221-30.
MITSIADES, N., MITSIADES, C. S., POULAKI, V., CHAUHAN, D., FANOURAKIS, G., GU, X., BAILEY, C., JOSEPH, M., LIBERMANN, T. A., TREON, S. P., MUNSHI, N. C., RICHARDSON, P. G., HIDESHIMA, T. & ANDERSON, K. C. (2002) Molecular sequelae of proteasome inhibition in human multiple myeloma cells. Proc Natl Acad Sci U S A, 99, 14374-9.
MITSIADES, C. S., MITSIADES, N., POULAKI, V., SCHLOSSMAN, R., AKIYAMA, M., CHAUHAN, D., HIDESHIMA, T., TREON, S. P., MUNSHI, N. C., RICHARDSON, P. G. & ANDERSON, K. C. (2002) Activation of NF-kappaB and upregulation of intracellular anti-apoptotic proteins via the IGF-1/Akt signaling in human multiple myeloma cells: therapeutic implications. *Oncogene,* 21**,** 5673-83.
MONTAGNOLI, A., BOSOTTI, R., VILLA, F., RIALLAND, M., BROTHERTON, D., MERCURIO, C., BERTHELSEN, J. & SANTOCANALE, C. (2002) Drf1, a novel regulatory subunit for human Cdc7 kinase. *EMBO J,* 21**,** 3171-81.
MONTAGNOLI, A., TENCA, P., SOLA, F., CARPANI, D., BROTHERTON, D., ALBANESE, C. & SANTOCANALE, C. (2004) Cdc7 inhibition reveals a p53-dependent replication checkpoint that is defective in cancer cells. *Cancer Res,* 64, 7110-6.
MONTAGNOLI, A., VALSASINA, B., BROTHERTON, D., TROIANI, S., RAINOLDI, S., TENCA, P., MOLINARI, A. & SANTOCANALE, C. (2006) Identification of Mcm2 phosphorylation sites by S-phase-regulating kinases. *J Biol Chem,* 281, 10281-90.
MONTAGNOLI, A. S., C. VALSASINA, B. MENICHINCHERI, M. CIAVOLELLA, A. CROCI, V. FIORENTINI, F. CATTONI, M. SOLA, F. PATTON, V. RAINOLDI, S. ALBANESSE, C. GALVANI, A. PESENTI, E. ISACCHI, A. VANOTTI, E. MOLL, J. (2008) A new potent and orally available class of Cdc7 inhibitors with anti-tumor activity. *AACR*.
MOREAU, P., AVET-LOISEAU, H., FACON, T., ATTAL, M., TIAB, M., HULIN, C., DOYEN, C., GARDERET, L., RANDRIAMALALA, E., ARAUJO, C., LEPEU, G., MARIT, G., CAILLOT, D., ESCOFFRE, M., LIOURE, B., BENBOUBKER, L., PEGOURIE, B., KOLB, B., STOPPA, A. M., FUZIBET, J. G., DECAUX, O., DIB, M., BERTHOU, C., CHALETEIX, C., SEBBAN, C., TRAULLE, C., FONTAN, J., WETTERWALD, M., LENAIN, P., MATHIOT, C. & HAROUSSEAU, J. L. (2011) Bortezomib plus dexamethasone versus reduced-dose bortezomib, thalidomide plus dexamethasone as induction treatment before autologous stem cell transplantation in newly diagnosed multiple myeloma. *Blood,* 118**,** 5752-8; quiz 5982.
MOREAU, P., PYLYPENKO, H., GROSICKI, S., KARAMANESHT, I., LELEU, X., GRISHUNINA, M., REKHTMAN, G., MASLIAK, Z., ROBAK, T., SHUBINA, A., ARNULF, B., KROPFF, M., CAVET, J., ESSELTINE, D. L., FENG, H., GIRGIS, S., VAN DE VELDE, H., DERAEDT, W. & HAROUSSEAU, J. L. (2011) Subcutaneous versus intravenous administration of bortezomib in patients with relapsed multiple myeloma: a randomised, phase 3, non-inferiority study. *Lancet Oncol,* 12**,** 431-40.
MOREAUX, J., LEGOUFFE, E., JOURDAN, E., QUITTET, P., REME, T., LUGAGNE, C., MOINE, P., ROS-

SI, J. F., KLEIN, B. & TARTE, K. (2004) BAFF and APRIL protect myeloma cells from apoptosis induced by interleukin 6 deprivation and dexamethasone. *Blood,* 103**,** 3148-57.

MORRISON, S. J. & WEISSMAN, I. L. (1994) The long-term repopulating subset of hematopoietic stem cells is deterministic and isolatable by phenotype. *Immunity,* 1**,** 661-73.

MULLIGAN, G., LICHTER, D. I., DI BACCO, A., BLAKEMORE, S. J., BERGER, A., KOENIG, E., BERNARD, H., TREPICCHIO, W., LI, B., NEUWIRTH, R., CHATTOPADHYAY, N., BOLEN, J. B., DORNER, A. J., VAN DE VELDE, H., RICCI, D., JAGANNATH, S., BERENSON, J. R., RICHARDSON, P. G., STADTMAUER, E. A., ORLOWSKI, R. Z., LONIAL, S., ANDERSON, K. C., SONNEVELD, P., SAN MIGUEL, J. F., ESSELTINE, D. L. & SCHU, M. Mutation of NRAS but not KRAS significantly reduces myeloma sensitivity to single-agent bortezomib therapy. *Blood,* 123**,** 632-9.

MUSACCHIO, A. & SALMON, E. D. (2007) The spindle-assembly checkpoint in space and time. *Nat Rev Mol Cell Biol,* 8, 379-93.

MUSAHL, C., HOLTHOFF, H. P., LESCH, R. & KNIPPERS, R. (1998) Stability of the replicative Mcm3 protein in proliferating and differentiating human cells. *Exp Cell Res,* 241**,** 260-4.

MUZIO, M., STOCKWELL, B. R., STENNICKE, H. R., SALVESEN, G. S. & DIXIT, V. M. (1998) An induced proximity model for caspase-8 activation. *J Biol Chem,* 273, 2926-30.

NAM, D. K., LEE, S., ZHOU, G., CAO, X., WANG, C., CLARK, T., CHEN, J., ROWLEY, J. D. & WANG, S. M. (2002) Oligo(dT) primer generates a high frequency of truncated cDNAs through internal poly(A) priming during reverse transcription. *Proc Natl Acad Sci U S A,* 99, 6152-6.

NATONI, A., MURILLO, L. S., KLISZCZAK, A. E., CATHERWOOD, M. A., MONTAGNOLI, A., SAMALI, A., O'DWYER, M. & SANTOCANALE, C. Mechanisms of action of a dual Cdc7/Cdk9 kinase inhibitor against quiescent and proliferating CLL cells. *Mol Cancer Ther,* 10, 1624-34.

NEOPTOLEMOS, J. P., OATES, G. D., NEWBOLD, K. M., ROBSON, A. M., MCCONKEY, C. & POWELL, J. (1995) Cyclin/proliferation cell nuclear antigen immunohistochemistry does not improve the prognostic power of Dukes' or Jass' classifications for colorectal cancer. *Br J Surg,* 82**,** 184-7.

NEUGEBAUER, K. M. (2002) On the importance of being co-transcriptional. *J Cell Sci,* 115, 3865-71.

NIESVIZKY, R., MARTIN, T. G., 3RD, BENSINGER, W. I., ALSINA, M., SIEGEL, D. S., KUNKEL, L. A., WONG, A. F., LEE, S., ORLOWSKI, R. Z. & WANG, M. Phase Ib Dose-Escalation Study (PX-171-006) of Carfilzomib, Lenalidomide, and Low-Dose Dexamethasone in Relapsed or Progressive Multiple Myeloma. *Clin Cancer Res,* 19**,** 2248-56.

NIIDA, A., HIROKO, T., KASAI, M., FURUKAWA, Y., NAKAMURA, Y., SUZUKI, Y., SUGANO, S. & AKIYAMA, T. (2004) DKK1, a negative regulator of Wnt signaling, is a target of the beta-catenin/TCF pathway. *Oncogene,* 23**,** 8520-6.

NISHIHARA, K., SHOMORI, K., FUJIOKA, S., TOKUYASU, N., INABA, A., OSAKI, M., OGAWA, T. & ITO, H. (2008) Minichromosome maintenance protein 7 in colorectal cancer: implication of prognostic significance. *Int J Oncol,* 33**,** 245-51.

NOLL, J. E., WILLIAMS, S. A., PURTON, L. E. & ZANNETTINO, A. C. 2012. Tug of war in the haematopoietic stem cell niche: do myeloma plasma cells compete for the HSC niche? Blood Cancer J, 2, e91.

NOUGAREDE, R., DELLA SETA, F., ZARZOV, P. & SCHWOB, E. (2000) Hierarchy of S-phase-promoting factors: yeast Dbf4-Cdc7 kinase requires prior S-phase cyclin-dependent kinase activation. *Mol Cell Biol,* 20**,** 3795-806.

NYBERG, K. A., MICHELSON, R. J., PUTNAM, C. W. & WEINERT, T. A. (2002) Toward maintaining the genome: DNA damage and replication checkpoints. *Annu Rev Genet,* 36, 617-56.

O'BRIEN, C. A., POLLETT, A., GALLINGER, S. & DICK, J. E. 2007. A human colon cancer cell capable of initiating tumour growth in immunodeficient mice. Nature, 445, 106-10.

OBERMANN, E. C., WENT, P., ZIMPFER, A., TZANKOV, A., WILD, P. J., STOEHR, R., PILERI, S. A. &

DIRNHOFER, S. (2005) Expression of minichromosome maintenance protein 2 as a marker for proliferation and prognosis in diffuse large B-cell lymphoma: a tissue microarray and clinico-pathological analysis. *BMC Cancer,* 5, 162.

OCIO, E. M., RICHARDSON, P. G., RAJKUMAR, S. V., PALUMBO, A., MATEOS, M. V., ORLOWSKI, R., KUMAR, S., USMANI, S., ROODMAN, D., NIESVIZKY, R., EINSELE, H., ANDERSON, K. C., DIMOPOULOS, M. A., AVET-LOISEAU, H., MELLQVIST, U. H., TURESSON, I., MERLINI, G., SCHOTS, R., MCCARTHY, P., BERGSAGEL, L., CHIM, C. S., LAHUERTA, J. J., SHAH, J., REIMAN, A., MIKHAEL, J., ZWEEGMAN, S., LONIAL, S., COMENZO, R., CHNG, W. J., MOREAU, P., SONNEVELD, P., LUDWIG, H., DURIE, B. G. & MIGUEL, J. F. (2014) New drugs and novel mechanisms of action in multiple myeloma in 2013: a report from the International Myeloma Working Group (IMWG). *Leukemia,* 28, 525-42.

OFFIDANI, M., MELE, A., CORVATTA, L., MARCONI, M., MALERBA, L., OLIVIERI, A., RUPOLI, S., ALESIANI, F. & LEONI, P. (2002) Gemcitabine alone or combined with cisplatin in relapsed or refractory multiple myeloma. *Leuk Lymphoma,* 43, 1273-9.

OGAWA, M., NISHIURA, T., ORITANI, K., YOSHIDA, H., YOSHIMURA, M., OKAJIMA, Y., ISHIKAWA, J., HASHIMOTO, K., MATSUMURA, I., TOMIYAMA, Y. & MATSUZAWA, Y. 2000. Cytokines prevent dexamethasone-induced apoptosis via the activation of mitogen-activated protein kinase and phosphatidylinositol 3-kinase pathways in a new multiple myeloma cell line. Cancer Res, 60, 4262-9.

OGINO, K., TAKEDA, T., MATSUI, E., IIYAMA, H., TANIYAMA, C., ARAI, K. & MASAI, H. (2001) Bipartite binding of a kinase activator activates Cdc7-related kinase essential for S phase. *J Biol Chem,* 276**,** 31376-87.

OSHIRO, G., OWENS, J. C., SHELLMAN, Y., SCLAFANI, R. A. & LI, J. J. (1999) Cell cycle control of Cdc7p kinase activity through regulation of Dbf4p stability. *Mol Cell Biol,* 19**,** 4888-96.

OKAMURA, H., YOSHIDA, K., AMORIM, B. R. & HANEJI, T. (2008) Histone H1.2 is translocated to mitochondria and associates with Bak in bleomycin-induced apoptotic cells. *J Cell Biochem,* 103, 1488-96.

ORLOWSKI, R. Z., NAGLER, A., SONNEVELD, P., BLADE, J., HAJEK, R., SPENCER, A., SAN MIGUEL, J., ROBAK, T., DMOSZYNSKA, A., HORVATH, N., SPICKA, I., SUTHERLAND, H. J., SUVOROV, A. N., ZHUANG, S. H., PAREKH, T., XIU, L., YUAN, Z., RACKOFF, W. & HAROUSSEAU, J. L. (2007) Randomized phase III study of pegylated liposomal doxorubicin plus bortezomib compared with bortezomib alone in relapsed or refractory multiple myeloma: combination therapy improves time to progression. *J Clin Oncol,* 25, 3892-901.

PAIVA, B., CHANDIA, M., VIDRIALES, M. B., COLADO, E., CABALLERO-VELAZQUEZ, T., ESCALANTE, F., GARCIA DE COCA, A., MONTES, M. C., GARCIA-SANZ, R., OCIO, E. M., MATEOS, M. V. & SAN MIGUEL, J. F. Multiparameter flow cytometry for staging of solitary bone plasmacytoma: new criteria for risk of progression to myeloma. *Blood*.

PALUMBO, A., BRINGHEN, S., CARAVITA, T., MERLA, E., CAPPARELLA, V., CALLEA, V., CANGIALOSI, C., GRASSO, M., ROSSINI, F., GALLI, M., CATALANO, L., ZAMAGNI, E., PETRUCCI, M. T., DE STEFANO, V., CECCARELLI, M., AMBROSINI, M. T., AVONTO, I., FALCO, P., CICCONE, G., LIBERATI, A. M., MUSTO, P. & BOCCADORO, M. (2006) Oral melphalan and prednisone chemotherapy plus thalidomide compared with melphalan and prednisone alone in elderly patients with multiple myeloma: randomised controlled trial. *Lancet,* 367**,** 825-31.

PALUMBO A, D. M., DELFORGE M, ET AL. (2009) A Phase III study to deter- mine the efficacy and safety of lenalidomide in combination with melphalan and prednisone (MPR) in elderly patients with newly diagnosed multiple my-eloma. *ASH Annu Meet Abstr 2009,* 114, 613.

PAPE, T., MEKA, H., CHEN, S., VICENTINI, G., VAN HEEL, M. & ONESTI, S. (2003) Hexameric ring structure of the full-length archaeal MCM protein complex. *EMBO Rep,* 4, 1079-83.

PARKER, L. L. & PIWNICA-WORMS, H. (1992) Inactivation of the p34cdc2-cyclin B complex by the human WEE1 tyrosine kinase. *Science,* 257, 1955-7.

PATTERSON, M., SCLAFANI, R. A., FANGMAN, W. L. & ROSAMOND, J. (1986) Molecular characterization of cell cycle gene CDC7 from Saccharomyces cerevisiae. *Mol Cell Biol,* 6**,** 1590-8.

PEACOCK, C. D., WANG, Q., GESELL, G. S., CORCORAN-SCHWARTZ, I. M., JONES, E., KIM, J., DEVEREUX, W. L., RHODES, J. T., HUFF, C. A., BEACHY, P. A., WATKINS, D. N. & MATSUI, W. (2007) Hedgehog signaling maintains a tumor stem cell compartment in multiple myeloma. *Proc Natl Acad Sci U S A,* 104, 4048-53.

PEI, H., ZHANG, L., LUO, K., QIN, Y., CHESI, M., FEI, F., BERGSAGEL, P. L., WANG, L., YOU, Z. & LOU, Z. MMSET regulates histone H4K20 methylation and 53BP1 accumulation at DNA damage sites. *Nature,* 470, 124-8.

PELIZON, C., D'ADDA DI FAGAGNA, F., FARRACE, L. & LASKEY, R. A. (2002) Human replication protein Cdc6 is selectively cleaved by caspase 3 during apoptosis. *EMBO Rep,* 3, 780-4.

PELLICIOLI, A. Novel insights on Cdc5 and checkpoint adaptation come from meiotic cells. *Cell Cycle,* 9, 1461-2.

PELLICIOLI, A., LEE, S. E., LUCCA, C., FOIANI, M. & HABER, J. E. (2001) Regulation of Saccharomyces Rad53 checkpoint kinase during adaptation from DNA damage-induced G2/M arrest. *Mol Cell,* 7, 293-300.

PENG, J., ZHU, Y., MILTON, J. T. & PRICE, D. H. (1998) Identification of multiple cyclin subunits of human P-TEFb. *Genes Dev,* 12**,** 755-62.

PENTZ, E. I. (1969) Adaptation of the Rimini-Schryver reaction for the measurement of allantoin in urine to the autoanalyzer: allantoin and taurine excretion following neutron irradiation. *Anal Biochem,* 27, 333-42.

PEREIRA, G., HOFKEN, T., GRINDLAY, J., MANSON, C. & SCHIEBEL, E. (2000) The Bub2p spindle checkpoint links nuclear migration with mitotic exit. *Mol Cell,* 6, 1-10.

PETERLIN, B. M. & PRICE, D. H. (2006) Controlling the elongation phase of transcription with P-TEFb. *Mol Cell,* 23**,** 297-305.

PINSKY, B. A., KUNG, C., SHOKAT, K. M. & BIGGINS, S. (2006) The Ipl1-Aurora protein kinase activates the spindle checkpoint by creating unattached kinetochores. *Nat Cell Biol,* 8, 78-83.

PIRNGRUBER, J., SHCHEBET, A. & JOHNSEN, S. A. (2009a) Insights into the function of the human P-TEFb component CDK9 in the regulation of chromatin modifications and co-transcriptional mRNA processing. *Cell Cycle,* 8, 3636-42.

PIRNGRUBER, J., SHCHEBET, A., SCHREIBER, L., SHEMA, E., MINSKY, N., CHAPMAN, R. D., EICK, D., AYLON, Y., OREN, M. & JOHNSEN, S. A. (2009b) CDK9 directs H2B monoubiquitination and controls replication-dependent histone mRNA 3'-end processing. *EMBO Rep,* 10, 894-900.

PODAR, K., TAI, Y. T., LIN, B. K., NARSIMHAN, R. P., SATTLER, M., KIJIMA, T., SALGIA, R., GUPTA, D., CHAUHAN, D. & ANDERSON, K. C. (2002) Vascular endothelial growth factor-induced migration of multiple myeloma cells is associated with beta 1 integrin- and phosphatidylinositol 3-kinase-dependent PKC alpha activation. *J Biol Chem,* 277**,** 7875-81.

PUTHIER, D., BATAILLE, R. & AMIOT, M. (1999) IL-6 up-regulates mcl-1 in human myeloma cells through JAK / STAT rather than ras / MAP kinase pathway. *Eur J Immunol,* 29, 3945-50.

PRINCE, M. E. & AILLES, L. E. 2008. Cancer stem cells in head and neck squamous cell cancer. J Clin Oncol, 26, 2871-5.

RAINEY, M. D., HARHEN, B., WANG, G. N., MURPHY, P. V. & SANTOCANALE, C. (2014) Cdc7-dependent and -independent phosphorylation of Claspin in the induction of the DNA replication checkpoint. Cell Cycle, 12, 1560-8.

RAJAGOPALAN, H. & LENGAUER, C. (2004) Aneuploidy and cancer. *Nature,* 432, 338-41.

RAJE, N., KUMAR, S., HIDESHIMA, T., ROCCARO, A., ISHITSUKA, K., YASUI, H., SHIRAISHI, N., CHAUHAN, D., MUNSHI, N. C., GREEN, S. R. & ANDERSON, K. C. (2005) Seliciclib (CYC202 or R-roscovitine), a small-molecule cyclin-dependent kinase inhibitor, mediates activity via down-regulation of Mcl-1 in multiple myeloma. *Blood,* 106, 1042-7.

RAJE, N., FABER, E. A., RICHARDSON, P. A., SCHILLER, G. J., HOHL, R. J. & COHEN, A. D. (2012a) Phase I study of tabalumab, a human anti-BAFF antibody adn bortezomib in patients with previously-treated multiple myeloma. *ASH Annu Meet Abstr,* 120, 447.

RAJE, N., HARI, P. N., VOGL, D. T., JAGANNATH, S., ORLOWSKI, R. & SUPKO, J. G. (2012b) Rocilinostat (ACY-1215), a selective HDAC6 inhibitor, alone or in combination with bortezomib in multiple myeloma: preliminary results from the first-in-humans phase I/II study. *ASH Annu Meet Abstr,* 120, 4061.

RAJKUMAR, S. V. (2013) Treatment of multiple myeloma. *Nat Rev Clin Oncol,* 8**,** 479-91.

RAJKUMAR, S. V., GAHRTON, G. & BERGSAGEL, P. L. (2011) Approach to the treatment of multiple myeloma: a clash of philosophies. *Blood,* 118**,** 3205-11.

RAMIREZ, J. M., OCIO, E. M., SAN MIGUEL, J. F. & PANDIELLA, A. (2007) Pemetrexed acts as an antimyeloma agent by provoking cell cycle blockade and apoptosis. *Leukemia,* 21, 797-804.

RANDALL, T. D. & WEISSMAN, I. L. (1997) Phenotypic and functional changes induced at the clonal level in hematopoietic stem cells after 5-fluorouracil treatment. *Blood,* 89**,** 3596-606.

RASMUSSEN, T., HAABER, J., DAHL, I. M., KNUDSEN, L. M., KERNDRUP, G. B., LODAHL, M., JOHNSEN, H. E. & KUEHL, M. (2010) Identification of translocation products but not K-RAS mutations in memory B cells from patients with multiple myeloma. *Haematologica,* 95, 1730-7.

REENA, R. M., MASTURA, M., SITI-AISHAH, M. A., MUNIRAH, M. A., NORLIA, A., NAQIYAH, I., ROHAIZAK, M. & SHARIFAH, N. A. (2008) Minichromosome maintenance protein 2 is a reliable proliferative marker in breast carcinoma. *Ann Diagn Pathol,* 12**,** 340-3.

REMUS, D., BEURON, F., TOLUN, G., GRIFFITH, J. D., MORRIS, E. P. & DIFFLEY, J. F. (2009) Concerted loading of Mcm2-7 double hexamers around DNA during DNA replication origin licensing. *Cell,* 139**,** 719-30.

RICHARDSON P, E. A. (2011) Phase 1 Clinical Evaluation of Twice-Weekly Marizomib (NPI-0052), a Novel Proteasome Inhibitor, in Patients with Relapsed/Refractory Multiple Myeloma (MM). *ASH Annu Meet Abstr*.

RICHARDSON P, E. A. (2012) PANORAMA 2: Panobinostat Combined with Bortezomib and Dexamethasone in Patients with Relapsed and Bortezomib-Refractory Multiple Myeloma. *ASH Annu Meet Abstr*.

RICHARDSON, P. G., HOFMEISTER, C. C., SIEGEL, D. S., LONIAL, S., LAUBACH, J. & EFEBERA, Y. (2013a) MM-005: a phase I trial of pomalidomide, bortezomib, and low-dose dexamethasone (PVD) in relapsed and/or refractory multiple myeloma. *ASCO Meet Abstr,* 31 (15_suppl), 8584.

RICHARDSON, P. G., SIEGEL, D., BAZ, R., KELLEY, S. L., MUNSHI, N. C., LAUBACH, J., SULLIVAN, D., ALSINA, M., SCHLOSSMAN, R., GHOBRIAL, I. M., DOSS, D., LOUGHNEY, N., MCBRIDE, L., BILOTTI, E., ANAND, P., NARDELLI, L., WEAR, S., LARKINS, G., CHEN, M., ZAKI, M. H., JACQUES, C. & ANDERSON, K. C. (2013b) Phase 1 study of pomalidomide MTD, safety, and efficacy in patients with refractory multiple myeloma who have received lenalidomide and bortezomib. *Blood,* 121, 1961-7.

RICHARDSON, P. G., JAGANNATH, S., MOREAU, P., JAKUBOWIAK, A., RAAB, M. S. & FACON, T. (2012) A phase 2 study of elotuzumab (Elo) in combination with lenalidomide and low dose dexamethasone (Ld) in patients with relapsed/refractory multiple myeloma: updated results. *ASH Annu Meet Abstr,* 120, 202.

RICHARDSON, P. G., WOLF, J., JAKUBOWIAK, A., ZONDER, J., LONIAL, S., IRWIN, D., DENSMORE, J., KRISHNAN, A., RAJE, N., BAR, M., MARTIN, T., SCHLOSSMAN, R., GHOBRIAL, I. M., MUNSHI, N., LAUBACH, J., ALLERTON, J., HIDESHIMA, T., COLSON, K., PORADOSU, E., GARDNER, L., SPORTELLI, P. & ANDERSON, K. C. (2011) Perifosine plus bortezomib and dexamethasone in patients with relapsed/refractory multiple myeloma previously treated with bortezomib: results of a multicenter phase I/II trial. *J Clin Oncol,* 29, 4243-9.

ROBERTSON (2008) Identification of XL413, a Selective Cdc7 Kinase Inhibitor Which Induces Cell Cycle Arrest and Exhibits Potent Antitumor Activity. *20th EORTC-NCI-AACR Annual Meeting.* Geneva, Switzerland.

RODRIGUEZ GOMEZ, M., TALKE, Y., GOEBEL, N., HERMANN, F., REICH, B. & MACK, M. 2010. Basophils support the survival of plasma cells in mice. J Immunol, 185, 7180-5.

ROHN, J. L., HUEBER, A. O., MCCARTHY, N. J., LYON, D., NAVARRO, P., BURGERING, B. M. & EVAN, G. I. (1998) The opposing roles of the Akt and c-Myc signalling pathways in survival from CD95-mediated apoptosis. *Oncogene,* 17, 2811-8.

ROODMAN, G. D. (2009) Pathogenesis of myeloma bone disease. *Leukemia,* 23**,** 435-41.

ROSSI, J. F., MANGES, R. F., SUTHERLAND, H. J., JAGANNATH, S., VOORHEES, P. & SONNEVELD, P. (2008) Preliminary results of CNTO 328, an anti-interleukin-6 monoclonal antibody, in combination with bortezomib in the treatment of of relapsed or refractory multiple myeloma. *ASH Annu Meet Abstr,* 112, 867.

RUSSELL, P. & NURSE, P. (1986) cdc25+ functions as an inducer in the mitotic control of fission yeast. *Cell,* 45, 145-53.

SALERNO, D., HASHAM, M. G., MARSHALL, R., GARRIGA, J., TSYGANKOV, A. Y. & GRANA, X. (2007) Direct inhibition of CDK9 blocks HIV-1 replication without preventing T-cell activation in primary human peripheral blood lymphocytes. *Gene,* 405, 65-78.

SAMEJIMA, K., SVINGEN, P. A., BASI, G. S., KOTTKE, T., MESNER, P. W., JR., STEWART, L., DURRIEU, F., POIRIER, G. G., ALNEMRI, E. S., CHAMPOUX, J. J., KAUFMANN, S. H. & EARNSHAW, W. C. (1999) Caspase-mediated cleavage of DNA topoisomerase I at unconventional sites during apoptosis. *J Biol Chem,* 274, 4335-40.

SAN MIGUEL, J. F., SCHLAG, R., KHUAGEVA, N. K., DIMOPOULOS, M. A., SHPILBERG, O., KROPFF, M., SPICKA, I., PETRUCCI, M. T., PALUMBO, A., SAMOILOVA, O. S., DMOSZYNSKA, A., ABDULKADYROV, K. M., SCHOTS, R., JIANG, B., MATEOS, M. V., ANDERSON, K. C., ESSELTINE, D. L., LIU, K., CAKANA, A., VAN DE VELDE, H. & RICHARDSON, P. G. (2008) Bortezomib plus melphalan and prednisone for initial treatment of multiple myeloma. *N Engl J Med,* 359**,** 906-17.

SATO, N., ARAI, K. & MASAI, H. (1997) Human and Xenopus cDNAs encoding budding yeast Cdc7-related kinases: in vitro phosphorylation of MCM subunits by a putative human homologue of Cdc7. *EMBO J,* 16**,** 4340-51.

SAWA, M. & MASAI, H. (2009) Drug design with Cdc7 kinase: a potential novel cancer therapy target. *Drug Des Devel Ther,* 2, 255-64.

SCHOTT, E. J. & HOYT, M. A. (1998) Dominant alleles of Saccharomyces cerevisiae CDC20 reveal its role in promoting anaphase. *Genetics,* 148, 599-610.

SCHWACHA, A. & BELL, S. P. (2001) Interactions between two catalytically distinct MCM subgroups are essential for coordinated ATP hydrolysis and DNA replication. *Mol Cell,* 8, 1093-104.

SCLAFANI, R. A. (2000) Cdc7p-Dbf4p becomes famous in the cell cycle. *J Cell Sci,* 113 (Pt 12), 2111-7.

SCLAFANI, R. A. & HOLZEN, T. M. (2007) Cell cycle regulation of DNA replication. *Annu Rev Genet,* 41, 237-80.

SEARS, R. C. & NEVINS, J. R. (2002) Signaling networks that link cell proliferation and cell fate. *J Biol Chem,* 277, 11617-20.

SELLERS, W. R. (2011) A blueprint for advancing genetics-based cancer therapy. *Cell,* 147**,** 26-31.

SEMPLE, J. W. & DUNCKER, B. P. (2004) ORC-associated replication factors as biomarkers for cancer. *Biotechnol Adv,* 22**,** 621-31.

SHAFER, C. M., LINDVALL, M., BELLAMACINA, C., GESNER, T. G., YABANNAVAR, A., JIA, W., LIN, S. & WALTER, A. (2008) 4-(1H-indazol-5-yl)-6-phenylpyrimidin-2(1H)-one analogs as potent CDC7 inhibitors. *Bioorg Med Chem Lett,* 18**,** 4482-5.

SHAH, J. J., STADTMAUER, E. A., ABONOUR, R., COHEN, A. D., BENSINGER, W. L. & GASPARETTO,

C. (2012a) A multi-center phase I/II trial of carfilzomib and pomalidomide with dexamethasone (Car-Pom-d) in patients with relapsed/refractory multiple myeloma. *ASH Annu Meet Abstr,* 120, 4082.

SHAH, J. J., ZONDER, J., COHEN, A., BENSINGER, W., KAUFMAN, J. L. & ORLOWSKI, R. (2012b) The novel KSP inhibitor ARRY-520, i sactive both with and without low dose dexamethasone in patients with multiple myeloma refractory to bortezomib and lenalidomide: results from a phase 2 study. *ASH Annu Meet Abstr,* 120, 449.

SHANNON, L., WINSKI, D., ANDERSON, K., LITWILER, M., MUNSON, P., WINKLER, J. (2011) Effects of ARRY-797, a potent small molecule p38 MAPK inhibitor, on in vivo xeno - graft tumor growth, alone and in combination with cytotoxic agents. *ASH Annu Meet Abstr*.

SHARMA, S. V., FISCHBACH, M. A., HABER, D. A. & SETTLEMAN, J. (2006) "Oncogenic shock": explaining oncogene addiction through differential signal attenuation. *Clin Cancer Res,* 12, 4392s-4395s.

SHAUGHNESSY, J. D., JR., ZHAN, F., BURINGTON, B. E., HUANG, Y., COLLA, S., HANAMURA, I., STEWART, J. P., KORDSMEIER, B., RANDOLPH, C., WILLIAMS, D. R., XIAO, Y., XU, H., EPSTEIN, J., ANAISSIE, E., KRISHNA, S. G., COTTLER-FOX, M., HOLLMIG, K., MOHIUDDIN, A., PINEDA-ROMAN, M., TRICOT, G., VAN RHEE, F., SAWYER, J., ALSAYED, Y., WALKER, R., ZANGARI, M., CROWLEY, J. & BARLOGIE, B. (2007) A validated gene expression model of high-risk multiple myeloma is defined by deregulated expression of genes mapping to chromosome 1. *Blood,* 109**,** 2276-84.

SHI, N., XIE, W. B. & CHEN, S. Y. (2012) Cell division cycle 7 is a novel regulator of transforming growth factor-beta-induced smooth muscle cell differentiation. *J Biol Chem,* 287, 6860-7.

SHORE, S. M., BYERS, S. A., MAURY, W. & PRICE, D. H. (2003) Identification of a novel isoform of Cdk9. *Gene,* 307, 175-82.

SHOU, W., AZZAM, R., CHEN, S. L., HUDDLESTON, M. J., BASKERVILLE, C., CHARBONNEAU, H., ANNAN, R. S., CARR, S. A. & DESHAIES, R. J. (2002) Cdc5 influences phosphorylation of Net1 and disassembly of the RENT complex. *BMC Mol Biol,* 3, 3.

SHULTZ, L. D., ISHIKAWA, F. & GREINER, D. L. (2007) Humanized mice in translational biomedical research. *Nat Rev Immunol,* 7**,** 118-30.

SIEGEL, R., NAISHADHAM, D. & JEMAL, A. (2012a) Cancer statistics, 2012. *CA Cancer J Clin,* 62**,** 10-29.

SIEGEL, D. S., MARTIN, T., WANG, M., VIJ, R., JAKUBOWIAK, A. J., LONIAL, S., TRUDEL, S., KUKRETI, V., BAHLIS, N., ALSINA, M., CHANAN-KHAN, A., BUADI, F., REU, F. J., SOMLO, G., ZONDER, J., SONG, K., STEWART, A. K., STADTMAUER, E., KUNKEL, L., WEAR, S., WONG, A. F., ORLOWSKI, R. Z. & JAGANNATH, S. (2012b) A phase 2 study of single-agent carfilzomib (PX-171-003-A1) in patients with relapsed and refractory multiple myeloma. *Blood,* 120**,** 2817-25.

SIGAL, A., MILO, R., COHEN, A., GEVA-ZATORSKY, N., KLEIN, Y., LIRON, Y., ROSENFELD, N., DANON, T., PERZOV, N. & ALON, U. (2006) Variability and memory of protein levels in human cells. *Nature,* 444, 643-6.

SILVA, M. T., DO VALE, A. & DOS SANTOS, N. M. (2008) Secondary necrosis in multicellular animals: an outcome of apoptosis with pathogenic implications. *Apoptosis,* 13, 463-82.

SILVESTRIS, F., LOMBARDI, L., DE MATTEO, M., BRUNO, A. & DAMMACCO, F. (2007) Myeloma bone disease: pathogenetic mechanisms and clinical assessment. *Leuk Res,* 31**,** 129-38.

SINGH, M., LIMA, A., MOLINA, R., HAMILTON, P., CLERMONT, A. C., DEVASTHALI, V., THOMPSON, J. D., CHENG, J. H., BOU RESLAN, H., HO, C. C., CAO, T. C., LEE, C. V., NANNINI, M. A., FUH, G., CARANO, R. A., KOEPPEN, H., YU, R. X., FORREST, W. F., PLOWMAN, G. D. & JOHNSON, L. (2010) Assessing therapeutic responses in Kras mutant cancers using genetically engineered mouse models. *Nat Biotechnol,* 28**,** 585-93.

SINGH, S. K., CLARKE, I. D., TERASAKI, M., BONN, V. E., HAWKINS, C., SQUIRE, J. & DIRKS, P. B.

(2003) Identification of a cancer stem cell in human brain tumors. *Cancer Res,* 63**,** 5821-8.

SINGH, S. K., HAWKINS, C., CLARKE, I. D., SQUIRE, J. A., BAYANI, J., HIDE, T., HENKELMAN, R. M., CUSIMANO, M. D. & DIRKS, P. B. (2004) Identification of human brain tumour initiating cells. *Nature,* 432**,** 396-401.

SONNEVELD P, S.-W. I., VAN DER HOLT B, ET AL (2010) HOVON-65/GMMG-HD4 randomized phase III trial comparing bortezomib, doxorubicin, dexametha- sone (PAD) vs VAD followed by high-dose melphalan (HDM) and mainte- nance with bortezomib or thalidomide in patients with newly diagnosed multi- ple myeloma (MM). *ASH Annu Meet Abstr,* 116, 40.

SPECTOR, D. L. (1993) Macromolecular domains within the cell nucleus. *Annu Rev Cell Biol,* 9, 265-315.

SPENCER, A., YOON, S. S., HARRISON, S. J., MORRIS, S. R., SMITH, D. A., BRIGANDI, R. A., GAUVIN, J., KUMAR, R., OPALINSKA, J. B. & CHEN, C. (2014) Novel AKT inhibitor afuresertib shows favorable safety, pharmacokinetics, and clinical activity in multiple myeloma: Phase 1 study results. Blood.

SRIVASTAVA, G., RANA, V., LACY, M. Q., BUADI, F. K., HAYMAN, S. R., DISPENZIERI, A., GERTZ, M. A., DINGLI, D., ZELDENRUST, S., RUSSELL, S., MCCURDY, A., KAPOOR, P., KYLE, R., RAJKUMAR, S. V. & KUMAR, S. (2013) Long-term outcome with lenalidomide and dexamethasone therapy for newly diagnosed multiple myeloma. Leukemia, 27, 2062-6.

STEENSMA, D. P., GERTZ, M. A., GREIPP, P. R., KYLE, R. A., LACY, M. Q., LUST, J. A., OFFORD, J. R., PLEVAK, M. F., THERNEAU, T. M. & WITZIG, T. E. (2001) A high bone marrow plasma cell labeling index in stable plateau-phase multiple myeloma is a marker for early disease progression and death. *Blood,* 97, 2522-3.

STEPHENS, P. J., GREENMAN, C. D., FU, B., YANG, F., BIGNELL, G. R., MUDIE, L. J., PLEASANCE, E. D., LAU, K. W., BEARE, D., STEBBINGS, L. A., MCLAREN, S., LIN, M. L., MCBRIDE, D. J., VARELA, I., NIK-ZAINAL, S., LEROY, C., JIA, M., MENZIES, A., BUTLER, A. P., TEAGUE, J. W., QUAIL, M. A., BURTON, J., SWERDLOW, H., CARTER, N. P., MORSBERGER, L. A., IACOBUZIO-DONAHUE, C., FOLLOWS, G. A., GREEN, A. R., FLANAGAN, A. M., STRATTON, M. R., FUTREAL, P. A. & CAMPBELL, P. J. (2011) Massive genomic rearrangement acquired in a single catastrophic event during cancer development. *Cell,* 144, 27-40.

STIER, S., CHENG, T., DOMBKOWSKI, D., CARLESSO, N. & SCADDEN, D. T. (2002) Notch1 activation increases hematopoietic stem cell self-renewal in vivo and favors lymphoid over myeloid lineage outcome. *Blood,* 99, 2369-78.

STOEBER, K., TLSTY, T. D., HAPPERFIELD, L., THOMAS, G. A., ROMANOV, S., BOBROW, L., WILLIAMS, E. D. & WILLIAMS, G. H. (2001) DNA replication licensing and human cell proliferation. *J Cell Sci,* 114, 2027-41.

STRAHL, B. D. & ALLIS, C. D. (2000) The language of covalent histone modifications. *Nature,* 403, 41-5.

SWORDS, R., MAHALINGAM, D., O'DWYER, M., SANTOCANALE, C., KELLY, K., CAREW, J. & GILES, F. Cdc7 kinase - a new target for drug development. *Eur J Cancer,* 46, 33-40.

SZYDLOWSKA, K. & TYMIANSKI, M. Calcium, ischemia and excitotoxicity. *Cell Calcium,* 47, 122-9.

TAATJES, D. J., MARR, M. T. & TJIAN, R. (2004) Regulatory diversity among metazoan co-activator complexes. *Nat Rev Mol Cell Biol,* 5, 403-10.

TAI, Y. T., LI, X. F., BREITKREUTZ, I., SONG, W., NERI, P., CATLEY, L., PODAR, K., HIDESHIMA, T., CHAUHAN, D., RAJE, N., SCHLOSSMAN, R., RICHARDSON, P., MUNSHI, N. C. & ANDERSON, K. C. (2006) Role of B-cell-activating factor in adhesion and growth of human multiple myeloma cells in the bone marrow microenvironment. *Cancer Res,* 66**,** 6675-82.

TAIPALE, J. & BEACHY, P. A. (2001) The Hedgehog and Wnt signalling pathways in cancer. *Nature,* 411, 349-54.

TAIT, S. W. & GREEN, D. R. Mitochondria and cell death: outer membrane permeabilization and

beyond. *Nat Rev Mol Cell Biol,* 11, 621-32.
TAKEDA, T., OGINO, K., TATEBAYASHI, K., IKEDA, H., ARAI, K. & MASAI, H. (2001) Regulation of initiation of S phase, replication checkpoint signaling, and maintenance of mitotic chromosome structures during S phase by Hsk1 kinase in the fission yeast. *Mol Biol Cell,* 12**,** 1257-74.
TANAKA, T., KNAPP, D. & NASMYTH, K. (1997) Loading of an Mcm protein onto DNA replication origins is regulated by Cdc6p and CDKs. *Cell,* 90, 649-60.
TANNO, T., LIM, Y., WANG, Q., CHESI, M., BERGSAGEL, P. L., MATTHEWS, G., JOHNSTONE, R. W., GHOSH, N., BORRELLO, I., HUFF, C. A. & MATSUI, W. (2013) Growth differentiating factor 15 enhances the tumor-initiating and self-renewal potential of multiple myeloma cells. *Blood,* 123**,** 725-33.
TENCA, P., BROTHERTON, D., MONTAGNOLI, A., RAINOLDI, S., ALBANESE, C. & SANTOCANALE, C. (2007) Cdc7 is an active kinase in human cancer cells undergoing replication stress. *J Biol Chem,* 282**,** 208-15.
THIEDE, B., DIMMLER, C., SIEJAK, F. & RUDEL, T. (2001) Predominant identification of RNA-binding proteins in Fas-induced apoptosis by proteome analysis. *J Biol Chem,* 276, 26044-50.
TIAN, Z., D'ARCY, P., WANG, X., RAY, A., TAI, Y. T., HU, Y., CARRASCO, R. D., RICHARDSON, P., LINDER, S., CHAUHAN, D. & ANDERSON, K. C. A novel small molecule inhibitor of deubiquitylating enzyme USP14 and UCHL5 induces apoptosis in multiple myeloma and overcomes bortezomib resistance. *Blood,* 123**,** 706-16.
TIAN, E., ZHAN, F., WALKER, R., RASMUSSEN, E., MA, Y., BARLOGIE, B. & SHAUGHNESSY, J. D., JR. (2003) The role of the Wnt-signaling antagonist DKK1 in the development of osteolytic lesions in multiple myeloma. *N Engl J Med,* 349**,** 2483-94.
TIEDEMANN, R. E., ZHU, Y. X., SCHMIDT, J., YIN, H., SHI, C. X., QUE, Q., BASU, G., AZORSA, D., PERKINS, L. M., BRAGGIO, E., FONSECA, R., BERGSAGEL, P. L., MOUSSES, S. & STEWART, A. K. 2010. Kinome-wide RNAi studies in human multiple myeloma identify vulnerable kinase targets, including a lymphoid-restricted kinase, GRK6. Blood, 115, 1594-604.
TOCZYSKI, D. P., GALGOCZY, D. J. & HARTWELL, L. H. (1997) CDC5 and CKII control adaptation to the yeast DNA damage checkpoint. *Cell,* 90, 1097-106.
TONG, W. G., CHEN, R., PLUNKETT, W., SIEGEL, D., SINHA, R., HARVEY, R. D., BADROS, A. Z., POPPLEWELL, L., COUTRE, S., FOX, J. A., MAHADOCON, K., CHEN, T., KEGLEY, P., HOCH, U. & WIERDA, W. G. (2010) Phase I and pharmacologic study of SNS-032, a potent and selective Cdk2, 7, and 9 inhibitor, in patients with advanced chronic lymphocytic leukemia and multiple myeloma. *J Clin Oncol,* 28, 3015-22.
TURESSON, I., KOVALCHIK, S. A., PFEIFFER, R. M., KRISTINSSON, S. Y., GOLDIN, L. R., DRAYSON, M. T. & LANDGREN, O. (2014) Monoclonal gammopathy of undetermined significance and risk of lymphoid and myeloid malignancies: 728 cases followed up to 30 years in Sweden. *Blood,* 123**,** 338-45.
UBERSAX, J. A., WOODBURY, E. L., QUANG, P. N., PARAZ, M., BLETHROW, J. D., SHAH, K., SHOKAT, K. M. & MORGAN, D. O. (2003) Targets of the cyclin-dependent kinase Cdk1. *Nature,* 425, 859-64.
UHLMANN, F., LOTTSPEICH, F. & NASMYTH, K. (1999) Sister-chromatid separation at anaphase onset is promoted by cleavage of the cohesin subunit Scc1. *Nature,* 400, 37-42.
VARNUM-FINNEY, B., BRASHEM-STEIN, C. & BERNSTEIN, I. D. (2003) Combined effects of Notch signaling and cytokines induce a multiple log increase in precursors with lymphoid and myeloid reconstituting ability. *Blood,* 101, 1784-9.
VENEZIA, T. A., MERCHANT, A. A., RAMOS, C. A., WHITEHOUSE, N. L., YOUNG, A. S., SHAW, C. A. & GOODELL, M. A. (2004) Molecular signatures of proliferation and quiescence in hematopoietic stem cells. *PLoS Biol,* 2**,** e301.
VESCIO, R. A., CAO, J., HONG, C. H., LEE, J. C., WU, C. H., DER DANIELIAN, M., WU, V., NEWMAN,

R., LICHTENSTEIN, A. K. & BERENSON, J. R. (1995) Myeloma Ig heavy chain V region sequences reveal prior antigenic selection and marked somatic mutation but no intraclonal diversity. *J Immunol,* 155**,** 2487-97.

VESOLE, D. H. (2003) Transplantation for multiple myeloma: who, when, how often? Patient selection and goals. *Blood,* 102**,** 3471-2.

VIGNALI, M. & WORKMAN, J. L. (1998) Location and function of linker histones. *Nat Struct Biol,* 5, 1025-8.

VISINTIN, R., STEGMEIER, F. & AMON, A. (2003) The role of the polo kinase Cdc5 in controlling Cdc14 localization. *Mol Biol Cell,* 14, 4486-98.

VIJ, R., SIEGEL, D. S., JAGANNATH, S., JAKUBOWIAK, A. J., STEWART, A. K., MCDONAGH, K., BAHLIS, N., BELCH, A., KUNKEL, L. A., WEAR, S., WONG, A. F. & WANG, M. (2012a) An open-label, single-arm, phase 2 study of single-agent carfilzomib in patients with relapsed and/or refractory multiple myeloma who have been previously treated with bortezomib. *Br J Haematol,* 158**,** 739-48.

VIJ, R., WANG, M., KAUFMAN, J. L., LONIAL, S., JAKUBOWIAK, A. J., STEWART, A. K., KUKRETI, V., JAGANNATH, S., MCDONAGH, K. T., ALSINA, M., BAHLIS, N. J., REU, F. J., GABRAIL, N. Y., BELCH, A., MATOUS, J. V., LEE, P., ROSEN, P., SEBAG, M., VESOLE, D. H., KUNKEL, L. A., WEAR, S. M., WONG, A. F., ORLOWSKI, R. Z. & SIEGEL, D. S. (2012b) An open-label, single-arm, phase 2 (PX-171-004) study of single-agent carfilzomib in bortezomib-naive patients with relapsed and/or refractory multiple myeloma. *Blood,* 119**,** 5661-70.

WAAGE, A., GIMSING, P., FAYERS, P., ABILDGAARD, N., AHLBERG, L., BJORKSTRAND, B., CARLSON, K., DAHL, I. M., FORSBERG, K., GULBRANDSEN, N., HAUKAS, E., HJERTNER, O., HJORTH, M., KARLSSON, T., KNUDSEN, L. M., NIELSEN, J. L., LINDER, O., MELLQVIST, U. H., NESTHUS, I., ROLKE, J., STRANDBERG, M., SORBO, J. H., WISLOFF, F., JULIUSSON, G. & TURESSON, I. (2010) Melphalan and prednisone plus thalidomide or placebo in elderly patients with multiple myeloma. *Blood,* 116**,** 1405-12.

WAGNER, E. F. & NEBREDA, A. R. (2009) Signal integration by JNK and p38 MAPK pathways in cancer development. *Nat Rev Cancer,* 9, 537-49.

WALKER, B. A., WARDELL, C. P., CHIECCHIO, L., SMITH, E. M., BOYD, K. D., NERI, A., DAVIES, F. E., ROSS, F. M. & MORGAN, G. J. (2011) Aberrant global methylation patterns affect the molecular pathogenesis and prognosis of multiple myeloma. *Blood,* 117, 553-62.

WALKER, B. A., WARDELL, C. P., MELCHOR, L., HULKKI, S., POTTER, N. E., JOHNSON, D. C., FENWICK, K., KOZAREWA, I., GONZALEZ, D., LORD, C. J., ASHWORTH, A., DAVIES, F. E. & MORGAN, G. J. (2012) Intraclonal heterogeneity and distinct molecular mechanisms characterize the development of t(4;14) and t(11;14) myeloma. *Blood,* 120, 1077-86.

WALKER, B. A., WARDELL, C. P., JOHNSON, D. C., KAISER, M. F., BEGUM, D. B., DAHIR, N. B., ROSS, F. M., DAVIES, F. E., GONZALEZ, D. & MORGAN, G. J. (2013) Characterization of IGH locus breakpoints in multiple myeloma indicates a subset of translocations appear to occur in pregerminal center B cells. *Blood,* 121, 3413-9.

WALKER, B. A., WARDELL, C. P., MELCHOR, L., BRIOLI, A., JOHNSON, D. C., KAISER, M. F., MIRABELLA, F., LOPEZ-CORRAL, L., HUMPHRAY, S., MURRAY, L., ROSS, M., BENTLEY, D., GUTIERREZ, N. C., GARCIA-SANZ, R., SAN MIGUEL, J., DAVIES, F. E., GONZALEZ, D. & MORGAN, G. J. (2014) Intraclonal heterogeneity is a critical early event in the development of myeloma and precedes the development of clinical symptoms. *Leukemia,* 28, 384-90.

WALKER, B. A., WARDELL, C. P., BRIOLI, A., BOYLE, E., KAISER, M. F., BEGUM, D. B., DAHIR, N. B., JOHNSON, D. C., ROSS, F. M., DAVIES, F. E. & MORGAN, G. J. (2014) Translocations at 8q24 juxtapose MYC with genes that harbor superenhancers resulting in overexpression and poor prognosis in myeloma patients. *Blood Cancer J,* 4, e191.

WALLACH, D., VARFOLOMEEV, E. E., MALININ, N. L., GOLTSEV, Y. V., KOVALENKO, A. V. & BOLDIN, M. P. (1999) Tumor necrosis factor receptor and Fas signaling mechanisms. *Annu Rev Im-*

munol, 17, 331-67.
WANG, M., MARTIN, T., BENSINGER, W., ALSINA, M., SIEGEL, D. S., KAVALERCHIK, E., HUANG, M., ORLOWSKI, R. Z. & NIESVIZKY, R. Phase 2 dose-expansion study (PX-171-006) of carfilzomib, lenalidomide, and low-dose dexamethasone in relapsed or progressive multiple myeloma. *Blood,* 122**,** 3122-8.
WANSINK, D. G., MANDERS, E. E., VAN DER KRAAN, I., ATEN, J. A., VAN DRIEL, R. & DE JONG, L. (1994) RNA polymerase II transcription is concentrated outside replication domains throughout S-phase. *J Cell Sci,* 107 (Pt 6), 1449-56.
WEI, M. C., LINDSTEN, T., MOOTHA, V. K., WEILER, S., GROSS, A., ASHIYA, M., THOMPSON, C. B. & KORSMEYER, S. J. (2000) tBID, a membrane-targeted death ligand, oligomerizes BAK to release cytochrome c. *Genes Dev,* 14, 2060-71.
WEI, P., GARBER, M. E., FANG, S. M., FISCHER, W. H. & JONES, K. A. (1998) A novel CDK9-associated C-type cyclin interacts directly with HIV-1 Tat and mediates its high-affinity, loop-specific binding to TAR RNA. *Cell,* 92**,** 451-62.
WEICK, J. K., CROWLEY, J. J., HUSSEIN, M. A., MOORE, D. F. & BARLOGIE, B. (2002) The evaluation of gemcitabine in resistant or relapsing multiple myeloma, phase II: a Southwest Oncology Group study. *Invest New Drugs,* 20, 117-21.
WEINREICH, M. & STILLMAN, B. (1999) Cdc7p-Dbf4p kinase binds to chromatin during S phase and is regulated by both the APC and the RAD53 checkpoint pathway. *EMBO J,* 18**,** 5334-46.
WEST, M. L. & CORDEN, J. L. (1995) Construction and analysis of yeast RNA polymerase II CTD deletion and substitution mutations. *Genetics,* 140, 1223-33.
WICKREMASINGHE, R. G. & HOFFBRAND, A. V. (1999) Biochemical and genetic control of apoptosis: relevance to normal hematopoiesis and hematological malignancies. *Blood,* 93, 3587-600.
WINTER, O., MOSER, K., MOHR, E., ZOTOS, D., KAMINSKI, H., SZYSKA, M., ROTH, K., WONG, D. M., DAME, C., TARLINTON, D. M., SCHULZE, H., MACLENNAN, I. C. & MANZ, R. A. 2010. Megakaryocytes constitute a functional component of a plasma cell niche in the bone marrow. Blood, 116, 1867-75.
WIJERMANS, P., SCHAAFSMA, M., TERMORSHUIZEN, F., AMMERLAAN, R., WITTEBOL, S., SINNIGE, H., ZWEEGMAN, S., VAN MARWIJK KOOY, M., VAN DER GRIEND, R., LOKHORST, H. & SONNEVELD, P. (2010) Phase III study of the value of thalidomide added to melphalan plus prednisone in elderly patients with newly diagnosed multiple myeloma: the HOVON 49 Study. *J Clin Oncol,* 28**,** 3160-6.
WU, X., BLACKBURN, P. R., TSCHUMPER, R. C., EKKER, S. C. & JELINEK, D. F. (2014) TALEN-mediated genetic tailoring as a tool to analyze the function of acquired mutations in multiple myeloma cells. *Blood Cancer J,* 4, e210.
WU, X. & LEE, H. (2002) Human Dbf4/ASK promoter is activated through the Sp1 and MluI cell-cycle box (MCB) transcription elements. *Oncogene,* 21**,** 7786-96.
WIJDENES, J., VOOIJS, W. C., CLEMENT, C., POST, J., MORARD, F., VITA, N., LAURENT, P., SUN, R. X., KLEIN, B. & DORE, J. M. (1996) A plasmocyte selective monoclonal antibody (B-B4) recognizes syndecan-1. *Br J Haematol,* 94, 318-23.
WUILLEME-TOUMI, S., ROBILLARD, N., GOMEZ, P., MOREAU, P., LE GOUILL, S., AVET-LOISEAU, H., HAROUSSEAU, J. L., AMIOT, M. & BATAILLE, R. (2005) Mcl-1 is overexpressed in multiple myeloma and associated with relapse and shorter survival. *Leukemia,* 19, 1248-52.
WONG, D., WINTER, O., HARTIG, C., SIEBELS, S., SZYSKA, M., TIBURZY, B., MENG, L., KULKARNI, U., FAHNRICH, A., BOMMERT, K., BARGOU, R., BEREK, C., CHU, V. T., BOGEN, B., JUNDT, F. & MANZ, R. A. 2014. Eosinophils and megakaryocytes support the early growth of murine MOPC315 myeloma cells in their bone marrow niches. PLoS One, 9, e109018.
WONG, T. W., KITA, H., HANSON, C. A., WALTERS, D. K., ARENDT, B. K. & JELINEK, D. F. 2013. In-

duction of malignant plasma cell proliferation by eosinophils. PLoS One, 8, e70554.
WOOD, C. D., THORNTON, T. M., SABIO, G., DAVIS, R. A. & RINCON, M. (2009) Nuclear localization of p38 MAPK in response to DNA damage. *Int J Biol Sci,* 5, 428-37.
WUILLEME-TOUMI, S., ROBILLARD, N., GOMEZ, P., MOREAU, P., LE GOUILL, S., AVET-LOISEAU, H., HAROUSSEAU, J. L., AMIOT, M. & BATAILLE, R. (2005) Mcl-1 is overexpressed in multiple myeloma and associated with relapse and shorter survival. *Leukemia,* 19, 1248-52.
YATA, K. & YACCOBY, S. (2004) The SCID-rab model: a novel in vivo system for primary human myeloma demonstrating growth of CD138-expressing malignant cells. *Leukemia,* 18, 1891-7.
YOO, H. Y., KUMAGAI, A., SHEVCHENKO, A. & DUNPHY, W. G. (2004) Adaptation of a DNA replication checkpoint response depends upon inactivation of Claspin by the Polo-like kinase. *Cell,* 117, 575-88.
YOON, H. J. & CAMPBELL, J. L. (1991) The CDC7 protein of Saccharomyces cerevisiae is a phosphoprotein that contains protein kinase activity. *Proc Natl Acad Sci U S A,* 88**,** 3574-8.
YOON, H. J., LOO, S. & CAMPBELL, J. L. (1993) Regulation of Saccharomyces cerevisiae CDC7 function during the cell cycle. *Mol Biol Cell,* 4**,** 195-208.
ZACHARIAE, W. & NASMYTH, K. (1999) Whose end is destruction: cell division and the anaphase-promoting complex. *Genes Dev,* 13, 2039-58.
ZHAN, F., BARLOGIE, B., ARZOUMANIAN, V., HUANG, Y., WILLIAMS, D. R., HOLLMIG, K., PINEDA-ROMAN, M., TRICOT, G., VAN RHEE, F., ZANGARI, M., DHODAPKAR, M. & SHAUGHNESSY, J. D., JR. (2007) Gene-expression signature of benign monoclonal gammopathy evident in multiple myeloma is linked to good prognosis. *Blood,* 109, 1692-700.
ZHAN, F., HUANG, Y., COLLA, S., STEWART, J. P., HANAMURA, I., GUPTA, S., EPSTEIN, J., YACCOBY, S., SAWYER, J., BURINGTON, B., ANAISSIE, E., HOLLMIG, K., PINEDA-ROMAN, M., TRICOT, G., VAN RHEE, F., WALKER, R., ZANGARI, M., CROWLEY, J., BARLOGIE, B. & SHAUGHNESSY, J. D., JR. (2006) The molecular classification of multiple myeloma. *Blood,* 108**,** 2020-8.
ZHAO, C., TOVAR, C., YIN, X., XU, Q., TODOROV, I. T., VASSILEV, L. T. & CHEN, L. (2008) Synthesis and evaluation of pyrido-thieno-pyrimidines as potent and selective Cdc7 kinase inhibitors. *Bioorg Med Chem Lett*.
ZHOU, B. B. & ELLEDGE, S. J. (2000) The DNA damage response: putting checkpoints in perspective. *Nature,* 408, 433-9.
ZHOU, Q. & YIK, J. H. (2006) The Yin and Yang of P-TEFb regulation: implications for human immunodeficiency virus gene expression and global control of cell growth and differentiation. *Microbiol Mol Biol Rev,* 70, 646-59.
ZHU, Y. X., TIEDEMANN, R., SHI, C. X., YIN, H., SCHMIDT, J. E., BRUINS, L. A., KEATS, J. J., BRAGGIO, E., SEREDUK, C., MOUSSES, S. & STEWART, A. K. (2011) RNAi screen of the druggable genome identifies modulators of proteasome inhibitor sensitivity in myeloma including CDK5. *Blood,* 117, 3847-57.
ZOU, L. & STILLMAN, B. (2000) Assembly of a complex containing Cdc45p, replication protein A, and Mcm2p at replication origins controlled by S-phase cyclin-dependent kinases and Cdc7p-Dbf4p kinase. *Mol Cell Biol,* 20**,** 3086-96.

APPENDIX I

Genetic Nomenclature

This thesis uses the genetic nomenclature as directed by the HUGO Gene Nomenclature Committee (HGNC) and related committees as directed by HGNC.

Detailed information of individual committee guidelines are found at the following sites:

Human – HUGO Gene Nomenclature Committee

http://www.genenames.org/

Murine – Mouse Genome Informatics;

http://www.informatics.jax.org/mgihome/nomen/

Yeast – Saccharomyces Genome Database

http://www.yeastgenome.org/help/community/gene-registry

Fission Yeast – PomBase

http://www.pombase.org/

Xenopus – Xenbase

http://www.xenbase.org/gene/static/geneNomenclature.jsp

Zebrafish – ZFIN

https://wiki.zfin.org/display/general/ZFIN+Zebrafish+Nomenclature+Guidelines

Vertebrates

Both genes and their products are written in uppercase. There is no use of italics as per HGNC guidelines. Thus, CDC7 gene and CDC7 protein. The corresponding mRNA would be referred to as the CDC7 mRNA.

Budding Yeast

Names of wild type genes and dominant mutations are uppercase. Names of recessive mutations are lowercase. To specify a particular mutation in a gene the gene number is followed by the al-

lele number. Gene deletions are lower case and preceded by D. Gene products are indicated by uppercase first letter and the p suffix. +, -, ts, D refer to wild-type, recessive mutant, temperature sensitive mutant and dominant mutant respectively.

Fission Yeast

All genes are lowercase, regardless if wildtype or mutant and italicised. The conventions for wild-type, dominance, temperature sensitivity, gene deletions, and specific allele mutants are applied as for budding yeast.

Xenopus

All gene and RNA names are lowercase italics i.e. *cdc7*. Protein symbols are first letter capital and not italics Cdc7. The conventions for wild-type, dominance, temperature sensitivity, gene deletions, and specific allele mutants are applied as before.

Bacteria

Gene designations are followed by an uppercase letter instead of a number as used in budding yeast. The conventions for wild-type, dominant mutants, gene deletions are applied as before.

Species Abbreviations

Cat	FELCA
Chicken	CHICK
Chimp	PANTR
Dog	CANFA
Fruit Fly	DROME
Human	HUMAN
Mouse	Mouse
Worm	CAEEL

Yeast	YEAST
Fission Yeast	SCHPO
Zebrafish	DANRE
Rabbit	RABIT

APPENDIX II

Probeset ID	Gene Symbol	p-value(PI Cat (1= High Risk: > 10.33))
222608_s_at	ANLN	1.60E-18
208079_s_at	AURKA	1.16E-16
228729_at	CCNB1	3.24E-16
218663_at	NCAPG	1.51E-15
222740_at	ATAD2	3.69E-15
218542_at	CEP55	1.70E-14
204444_at	KIF11	1.91E-14
209642_at	BUB1	1.94E-14
222848_at	CENPK	5.00E-14
204962_s_at	CENPA	8.90E-14
226936_at	CENPW	1.06E-13
226980_at	DEPDC1B	1.30E-13
222958_s_at	DEPDC1	1.56E-13
225655_at	UHRF1	3.40E-13
230165_at	SGOL2	4.34E-13
209891_at	SPC25	5.90E-13
223381_at	NUF2	6.45E-13
213007_at	FANCI	7.01E-13
228273_at	---	7.85E-13
203214_x_at	CDK1	1.20E-12
203213_at	CDK1	2.05E-12
204162_at	NDC80	2.07E-12
206102_at	GINS1	2.77E-12
207165_at	HMMR	2.90E-12
218355_at	KIF4A	4.33E-12
1554696_s_at	TYMS	4.38E-12
200783_s_at	STMN1	4.92E-12
202705_at	CCNB2	4.97E-12
203358_s_at	EZH2	7.06E-12
204033_at	TRIP13	7.52E-12
214710_s_at	CCNB1	1.26E-11
218883_s_at	MLF1IP	1.34E-11
222077_s_at	RACGAP1	2.01E-11
204822_at	TTK	2.02E-11
202954_at	UBE2C	2.30E-11
219918_s_at	ASPM	3.33E-11
202589_at	TYMS	4.21E-11
219493_at	SHCBP1	4.73E-11
203554_x_at	PTTG1	5.29E-11
203755_at	BUB1B	5.53E-11
222680_s_at	DTL	6.12E-11
204825_at	MELK	6.54E-11
204641_at	NEK2	6.60E-11
1554768_a_at	MAD2L1	6.71E-11
210052_s_at	TPX2	6.88E-11
218585_s_at	DTL	9.90E-11
203362_s_at	MAD2L1	1.12E-10

201291_s_at	TOP2A	1.16E-10
213226_at	CCNA2	1.85E-10
228323_at	CASC5	1.91E-10
202107_s_at	MCM2	2.22E-10
205393_s_at	CHEK1	2.75E-10
219588_s_at	NCAPG2	2.97E-10
204026_s_at	ZWINT	5.11E-10
205394_at	CHEK1	6.85E-10
227212_s_at	PHF19	7.75E-10
201292_at	TOP2A	8.13E-10
213599_at	OIP5	1.11E-9
212533_at	WEE1	1.12E-9
203432_at	TMPO	1.56E-9
219148_at	PBK	1.72E-9
210559_s_at	CDK1	1.89E-9
222036_s_at	MCM4	2.43E-9
201890_at	RRM2	3.05E-9
204146_at	RAD51AP1	3.42E-9
1555758_a_at	CDKN3	3.79E-9
219787_s_at	ECT2	6.83E-9
209714_s_at	CDKN3	6.84E-9
218039_at	NUSAP1	7.84E-9
218009_s_at	PRC1	1.19E-8
222606_at	ZWILCH	1.30E-8
225834_at	FAM72A /// FAM72B /// FAM72C /// FAM72D	1.53E-8
218350_s_at	GMNN	1.64E-8
228597_at	C21orf45	2.35E-8
231772_x_at	CENPH	2.35E-8
219978_s_at	NUSAP1	2.68E-8
202503_s_at	KIAA0101	3.82E-8
201897_s_at	CKS1B	7.76E-8
229551_x_at	ZNF367	2.67E-7
203967_at	CDC6	6.34E-7
208808_s_at	HMGB2	6.73E-7
203968_s_at	CDC6	8.59E-7
227350_at	HELLS	9.32E-7
204170_s_at	CKS2	1.85E-6
206632_s_at	APOBEC3B	3.82E-6
201202_at	PCNA	3.83E-6
202345_s_at	FABP5	4.60E-6
203560_at	GGH	7.72E-6
212281_s_at	TMEM97	0.000
204159_at	CDKN2C	0.004